

ESCUELA SUPERIOR POLITÉCNICA DEL LITORAL

Facultad de Ingeniería Marítima y Ciencias del Mar

“Modelling of tsunamigenic scenarios using NamiDance for selected areas along the coast of Northern Adriatic Sea”

CAPSTONE PROJECT REPORT

Prior to receiving the degree of:

Ingeniero Oceanográfico

&

Ingeniera Oceanográfica

Presented by:

Rafael Dario González Muñoz

&

Stephanie Melanie Salvatierra Viteri

GUAYAQUIL - ECUADOR

Year: 2020

DEDICATORIA

Dedico mi trabajo a toda mi familia en especial,a mis padres Julio González O. & Toya Muñoz R. por su apoyo incondicional ante todo, con ideales y una voluntad inquebrantable. A mi hermano por su apoyo constante, consejos y guía en cada momento en este largo camino. Ellos me han enseñado el valor gratificante del esfuerzo, la perseverancia y sacrificio siempre con humildad y responsabilidad.

Rafael Dario González Muñoz

Mi proyecto va dirigido a mis Padres José Salvatierra y Vilma Viteri por enseñarme ser perseverante y creer en mí incondicionalmente. A mi hermano Ronald Salvatierra que hasta el último día que estuvo conmigo en la tierra y ahora desde el cielo me enseñó siempre luchar por mis ideales y metas con optimismo, a mi hermana Sylvia Salvatierra, por siempre ser mi maestra, mi ejemplo de mujer y cuidar de mí. Y finalmente se lo dedico a mi abuelita María Delgado por ser la guardiana de mis luchas y sueños.

Stephanie Melanie Salvatierra Viteri

AGRADECIMIENTOS

Agradecemos principalmente a Dios, quien nos dio la fuerza para superar los obstáculos en nuestra carrera universitaria.

Nuestro más sincero agradecimiento a nuestras familias por su abnegación e incondicionalidad.

Nuestra gratitud a los doctores Milton Plasencia, Antonella Peresan y Chiara Scaini de National Institute of Oceanography and Applied Geophysics-OGS, Italia que nos brindó toda la ayuda posible desde principio a fin con información necesaria. Al Dr Hany Hassan de National Research Institute of Astronomy and Geophysics-NRIAG, Egypt quien nos supervisó en todo el trayecto de modelación. A nuestra Decana María del Pilar Cornejo, Coordinador de Oceanografía Jonathan Cedeño, a nuestros tutores MSc Ivan Saltos y Dr. Carlos Martillo y todos los profesores de nuestra carrera que nos apoyaron incondicionalmente

En especial a nuestros amigos:

De parte de Rafael a Yomaira M, Elvis E. por su constante apoyo y recomendaciones

De parte de Stephanie a Gabriela T., Alejandro L. y Agustín G. por brindar su respaldo y acompañamiento incondicional.en todo el proceso universitario.

EXPRESS STATEMENT

"The responsibility and authorship of the degree work corresponds exclusively to us; and we give our consent so that ESPOL can make public communication of this work with the goal to promote the consult diffusion and public use of the intellectual production"

Rafael Dario
González Muñoz

Stephanie Melanie
Salvatierra Viteri

EVALUATION COURT

Luis Miguel Altamirano Perez

EVALUATOR TEACHER

Iván Marcelo Saltos Andrade

ACADEMIC ADVISOR

RESUMEN

Los tsunamis significativos en el norte del Adriático son extremadamente raros y sólo se han registrado unos pocos sucesos históricos en la literatura, con posibles fuentes localizadas principalmente a lo largo de las partes central y sur de las costas del Adriático. Recientemente, se ha establecido un sistema de alerta de tsunamis para toda la zona del Mediterráneo, incluido el Mar Adriático. Sin embargo, sigue faltando una descripción detallada del impacto potencial de dichas olas en las zonas costeras, especialmente las urbanas. El objetivo de esta tesis es modelar el peligro asociado a posibles tsunamis, generados por terremotos relativamente lejanos (es decir, con epicentros situados a unos cientos de kilómetros de distancia, y tiempos de llegada de horas), para las zonas urbanas situadas a lo largo de las costas del norte del Adriático. La modelización de los tsunamis se realiza con el programa informático NamiDance, que permite tener en cuenta las propiedades de las fuentes sísmicas, la batimetría variable y los efectos no lineales en la propagación de las olas. Los escenarios de peligro a escala urbana para ciudades seleccionadas (por ejemplo, Trieste) se desarrollan considerando diferentes fuentes potenciales de tsunamis de origen tectónico, situadas en el centro y el sur del Mar Adriático. Las fuentes se definen de acuerdo con la literatura disponible, que incluye catálogos de tsunamis históricos y modelos a gran escala existentes. Se utiliza la información sobre la morfología de las áreas de estudio (es decir, batimetría, topografía) disponible en la OGS, junto con datos adicionales recuperados en línea y de la literatura. Se modeliza un conjunto de escenarios de tsunami, considerando posibles fuentes relacionadas con eventos históricos, así como eventos extremadamente grandes aún no observados; se realizan pruebas paramétricas, para aumentar las magnitudes de los terremotos del escenario (es decir, el tamaño de la fuente), a fin de tener en cuenta la variabilidad de la fuente sísmica. Se calculan estimaciones preliminares de peligro de tsunami, que pueden permitir el desarrollo de escenarios de inundación, para ciudades seleccionadas, a saber, Trieste, Monfalcone, Lignano y Grado, en función de la disponibilidad de datos y de la relevancia del lugar. En consecuencia, se obtiene un conjunto preliminar de parámetros y mapas relacionados con los tsunamis, entre los que se incluyen: el run-up máximo en los lugares seleccionados; la hora de llegada de la primera ola a lo largo de la costa; las series temporales de las fluctuaciones del nivel del agua en los lugares seleccionados (mareogramas); los mapas de propagación de los tsunamis; las distribuciones de la hora de llegada del oleaje máximo a lo largo de la costa.

Palabras Clave: propagación de ondas de tsunami, fuente tsunamigénicas, peligro de tsunami, escenarios de tsunami

ABSTRACT

Significant tsunamis in Northern Adriatic are extremely rare and only a few historical events were reported in the literature, with possible sources mostly located along with central and southern parts of the Adriatic coasts. Recently, an alert tsunami system has been established for the whole Mediterranean area, including the Adriatic Sea. However, a detailed description of the potential impact of such waves on coastal areas, particularly urban ones, is still missing.

The scope of this thesis is to model the hazard associated with possible tsunamis, generated by relatively distant earthquakes (i.e., with epicentres located at few hundred kilometres distance, and arrival times of hours), for urban areas located along the Northern Adriatic coasts. Tsunami modelling is performed by the NamiDance software, which allows accounting for seismic source properties, variable bathymetry, and non-linear effects in waves propagation. Urban scale hazard scenarios for selected cities are developed considering different potential tsunamigenic sources of tectonic origin, located in the Central and Southern Adriatic Sea. Sources are defined according to available literature, which includes catalogues of a historical tsunami and existing large-scale models. Information about the morphology of the study areas (i.e., bathymetry, topography) available at OGS is used, along with additional data retrieved online and from literature.

A set of tsunami scenarios is modelled, considering possible sources related to historical events, as well as extremely large events not yet observed; parametric tests are performed, for increasing scenario earthquakes magnitudes (i.e. source size), to account for seismic source variability. Preliminary tsunami hazard estimates, which may allow developing inundation scenarios, are computed for selected cities, namely Trieste, Monfalcone, Lignano and Grado, depending on data availability and on the relevance of the site. Accordingly, a preliminary set of tsunami-related parameters and maps are obtained, including maximum runup at the selected sites; arrival time of the first wave along the coast; time series of water level fluctuations at selected locations (mareograms); tsunami propagation maps; distributions of the arrival time of the maximum swell along the coast.

Keywords: *tsunami waves propagation, tsunamigenic source, tsunami hazard, tsunami scenarios*

CONTENTS

RESUMEN	I
ABSTRACT	II
ABBREVIATIONS.....	VI
SIMBOLOGY.....	VII
FIGURES INDEX.....	VIII
TABLE INDEX	XI
MAPS INDEX	XII
CHAPTER 1	1
1 INTRODUCTION	1
1.1 Literature review	1
1.2 Description of the problem	1
1.3 Objectives.....	3
1.3.1 General objective	3
1.3.2 Specific objectives.....	3
1.4 Theoretical framework	4
1.4.1 Site information	4
1.4.2 Seismicity and Tectonics of the Adriatic Sea	6
1.4.3 Tsunami	19
CHAPTER 2	26
2 METHODOLOGY	26
2.1 Model set-up.....	27
2.1.1 Bathymetry and topography	27
2.1.2 Virtual Tide-Gauges	29
2.1.3 Friction Coefficient	29
2.2 Calibration: Tsunamigenic earthquakes.....	30
2.2.1 Define Seismic Scenario	30

2.3	Software Simulation.....	39
2.4	Zoning Validation.....	40
2.4.1	Zoning Feedback	40
CHAPTER 3	42
3	RESULTS AND DISCUSSION.....	42
3.1	Ancona – Italy.....	43
3.1.1	Wave Amplitudes (Water Height)	44
3.1.2	Runup	46
3.1.3	Tsunami Wave Velocity.....	47
3.1.4	Arrival Time of First Wave	48
3.2	Split – Croatia.....	49
3.2.1	Wave Amplitudes (Water Height)	50
3.2.2	Runup	52
3.2.3	Tsunami Wave Velocity.....	53
3.2.4	Arrival Time of First Wave	54
3.3	Offshore Montenegro.....	55
3.3.1	Wave Amplitudes (Water Height)	56
3.3.2	Runup	58
3.3.3	Tsunami Wave Velocity.....	59
3.3.4	Arrival Time of First Wave	60
3.4	Time series histories in the zone of interest	61
3.5	Validation.....	65
3.6	Overview of results	67
3.7	Flood effects.....	68
CHAPTER 4	73
4	CONCLUSIONS AND RECOMMENDATIONS	73

4.1	Conclusions	73
4.2	Recommendations.....	75
5	BIBLIOGRAPHY	76
	APPENDIX	80
6	appendix A.....	81
7	APPENDIX B	104
8	Appendix C	107
8.1	Empirical relationships Well & Coppersmith.....	107
9	Appendix d.....	111
9.1	Ancona maps	111
9.2	Split Maps.....	116
9.3	Montenegro Maps.....	121
10	Appendix E	126
10.1	Ancona - Maximum Amplitude History	126
10.2	Montenegro - Maximum Amplitude History	130

ABBREVIATIONS

ANSS	Advanced National Seismic System of USGS
ASCI	American Standard Code for Information Interchange
CEM	Coastal Engineering Manual
COPERNICUS	European Union's Earth Observation Programme
DEM	Digital elevation model
ESPOL	Escuela Superior Politécnica del Litoral
ESRI	Environmental Systems Research Institute
GEBCO	General Bathymetric Chart of the Oceans
GIS	Geographic Information System
GPS	Global Positioning System
INGV	Istituto Nazionale di Geofisica e Vulcanologia
METU	Middle East Technical University
NOAA	National Center for Environment Information
QGIS	Quantum GIS
SPM	Shore Protection Manual
TRASNFER	Tsunami Risk And Strategies For The European Region
UNESCO	United Nations Educational, Scientific and Cultural Organization
USGS	United States Geological Survey
W&C	Well & Coppersmith

SIMBOLOGY

min	Minute
Hr	Hour
Mw	Magnitude
Km	Kilometer
m	Meter
Ts	Trieste
Mn	Monfalcone
Lg	Lignano
Gr	Grado
Strian	Geological Units Of Measurement
°	Degrees
grd	Gride
dat	Data File
L	Surface Rupture Length.
W	Subsurface Rupture Width
D	Maximum Displacement
θ	Strike
λ	Rake
δ	Dip
h	Focal Depth
MSL	Mean Sea Level
H	Wave Height
a _{max}	Maximum Amplitude
m/s	Meter per Seconddo

FIGURES INDEX

Figure 1.1: Regional Map, zoom to north-east Adriatic Sea and cities of interest. (Author`s, 2020)	4
Figure 1.2: Bathymetry and Topography of the area of influence indicating the area of interest. (GEBCO, 2020).....	6
Figure 1.3 Structure of a Normal Fault. (INPRES, 2013).....	8
Figure 1.4 Structure of a Reverse Fault. (INPRES, 2013).....	8
Figure 1.5 Structure of a Reverse Fault. (INPRES, 2013).....	9
Figure 1.6 Tectonic motion vectors on the Adria Plate. (Altiner et al., 2006)	10
Figure 1.7: Geology structure of the Adriatic Sea region. (de Leeuw et al., 2012)....	11
Figure 1.8: The 3D view of the geological formations in the study area. (Author`s, 2020)	13
Figure 1.9: Tectonic zones developed. (Tiberti, Basili, et al., 2008)	14
Figure 1.10: Tectonic zoning developed by (Paulatto et al., 2007b)	15
Figure 1.11 Graphic Description of Fault Parameters.	19
Figure 1.12 Schematic of tsunami parameters. (UC, 2019).	20
Figure 2.1: Diagram of the methodological process. (Author`s, 2020).	26
Figure 2.2: Local/Global domains of bathymetry data in city of interest.(Author`s, 2020)	27
Figure 2.3 View GeoTtif and Grid files for each large and small dominions	28
Figure 2.4:Historical Tsunamigenic Events Records. (Author`s, 2020).	30
Figure 2.5: Normal Distribution Probability of the magnitude in the Adriatic Sea.(Author`s, 2020)	32
Figure 2.6: Most Probable Scenario Zoning Process. (Author`s, 2020).....	33
Figure 2.7: Probabilistic Zoning Map of the Adriatic Sea. (Author`s, 2020)	34
Figure 2.8: Tectonic Composition in the Adriatic Sea Zoning. (Author`s, 2020)	36
Figure 2.9: Empirical correlations between magnitude with break length and break width. (Author`s, 2020)	37
Figure 2.10: Main Data Input Screen of NAMIDANCE/NAMIDANCE. (Author`s, 2020)	39
Figure 2.11: Tsunamigenic Source Tectonic Zoning. (Author`s, 2020)	40
Figure 3.1: Seismic source of the Ancona scenario. (Author`s, 2021).....	43

Figure 3.2 Maximum coastal amplitude in the middle domain. (Author`s, 2021)	44
Figure 3.3: The 2D profiles of maximum tsunami amplitude from the coastline to the perpendicular flooded to urban zone. (Author`s, 2020).	45
Figure 3.4: Runup at the selected sites. (Author`s, 2021)	46
Figure 3.5 Maximum instantaneous tsunami wave speed in the medium study domain.(Author`s, 2020)	47
Figure 3.6: Tsunami travel time in minutes for the Ancona scenario.	48
Figure 3.7 Seismic source of the Split Scenario. (Author`s, 2021)	49
Figure 3.8: Maximum coastal amplitude in the middle domain. (Author`s, 2021)	50
Figure 3.9: The 2D profiles of the maximum tsunami amplitude, perpendicular trace from the coastline to the flooded urban area. (Author`s, 2020)	51
Figure 3.10: Runup at the selected sites. (Author`s, 2020)	52
Figure 3.11: Maximum instantaneous tsunami wave speed in the medium study domain. (Author`s, 2020)	53
Figure 3.12: Tsunami travel time in minutes for the Split scenario.	54
Figure 3.13: Seismic source of the Montenegro Scenario. (Author`s, 2020)	55
Figure 3.14: Maximum coastal amplitude in the middle domain. (Author`s, 2021)	56
Figure 3.15: The 2d profiles of maximum tsunami amplitude from the coastline to the perpendicular flooded to urban zone. (Author`s, 2020)	57
Figure 3.16: Runup at the selected sites. (Author`s, 2020)	58
Figure 3.17: Maximum instantaneous tsunami wave speed in the medium study domain. (Author`s, 2020)	59
Figure 3.18: Tsunami travel time in minutes for the Montenegro scenario. (Author`s, 2020)	60
Figure 3.19: Maximum amplitude with respect to the transfer time according to the generated Monfalcone gauges. (Author`s, 2020)	61
Figure 3.20: Maximum amplitude for the transfer time according to the generated Lignano gauges. (Author`s, 2020)	62
Figure 3.21: Maximum amplitude for the transfer time according to the generated Grado gauges. (Author`s, 2020)	63
Figure 3.22: Maximum amplitude for the transfer time according to the generated Trieste gauges. (Author`s, 2020)	64
Figure 3.23: Maximum recorded height according to (Tiberti, Lorito, et al., 2008) ..	65

Figure 3.24 Flooding of Trieste Commercial Port. (Author`s, 2020)	68
Figure 3.25 Flooding of Trieste Commercial Port south zone and nearby urban area. (Author`s, 2020)	69
Figure 3.26 Flooding on the beach extension of Lignano. (Author`s, 2020)	70
Figure 3.27 Oblique view flooding on Lignano beach extension. (Author`s, 2020)	70
Figure 3.28 Affected area in the city Grado. (Author`s, 2020)	71
Figure 3.29 Monfalcone affected area. (Author`s, 2020)	72

TABLE INDEX

Table 1.1 Computational models for the simulation of a tsunami. (NTHMP, 2017) ...	21
Table 1.2 Technical specifications of NAMIDANCE computer model. (Zaytsev et al., 2019).....	24
Table 1.3 Output File of the NAMIDANCE computer model.(Survey, 2012b)	25
Table 2.1: Values of the Manning roughness coefficient according to sea-bottom. ...	29
Table 2.2: Catalogs of reported tsunami events. (Author`s, 2020).	31
Table 2.3: Statistical results by zone. (Author`s, 2020)	34
Table 2.4: Regressions Empirics of Rupture Length, Rupture Width, Displacement.(Author`s, 2020)	35
Table 2.5: Empirical Failure Parameters Per Established Zone. (Author`s, 2020)....	38
Table 2.6: Model Setup of Simulation Scenarios.(Author`s, 2020)	39
Table 2.7: Fault Parameters for Selected Zones.(Author`s, 2020)	41
Table 3.1 Different fault parameters for the Ancona area according to their magnitude.(Author`s, 2020)	43
Table 3.2 Different fault parameters for the Split area according to their magnitude. (Author`s, 2020)	49
Table 3.3: Different fault parameters for the Montenegro area according to their magnitude, (Author`s, 2020)	55
Table 3.4 Error limits allowable for model validation/verification based on OAR-PMEL-135 Standard, (Kurnia, 2017)	65
Table 3.5 : Root mean square error of Hmax, (Author`s, 2020)	66
Table 3.6: Summary of simulation results (Author`s, 2020).....	67

MAPS INDEX

Appendix A 6.1: Data from Tsunamigenic Event Logs of the Institute of Volcanology and Geophysics of Italy(DISS Catalogue).....	81
Appendix A 6.2 Data from Tsunamigenic Event Logs of the Institute of Volcanology and Geophysics of Italy (CFT5Med Catalogue)	82
Appendix A 6.3 Data from tsunamigenic event records published in Paulatto's work in 2007.	86
Appendix A 6.4 Data from tsunamigenic event records published in Pasarie's work in 2012	86
Appendix A 6.5 Data from Tsunamigenic Event Logs of California University (Northern	87
Appendix B 7.1: Probabilistic Zoning Map of the Adriatic Sea. (Author`s, 2020)	104
Appendix B 7.2: Tectonic Composition in the Adriatic Sea Zoning. (Author`s, 2020)	105
Appendix B 7.3: Tsunamigenic Source Tectonic Zoning. (Author`s, 2020)	106
Appendix C 8.1 Zone 1: Croatia Coast, (Author`s, 2020)	107
Appendix C 8.2 Zone 2: Albanide, (Author`s, 2020)	107
Appendix C 8.3 Zone 3: Offshore Ancona.....	108
Appendix C 8.4 Zone 4: Kefallonia, (Author`s, 2020)	108
Appendix C 8.5 Zone 5: Gargano Promontory, (Author`s, 2020).....	109
Appendix C 8.6 Zone 6: Apulia, (Author`s, 2020).....	109
Appendix C 8.7: Zone 7: Jabuka Island. (Author`s, 2020).....	110
Appendix D 9.1.1: : Maximum coastal amplitude in the middle domain during simulation. (Author`s, 2020)	111
Appendix D 9.1.2: The maximum depth of flow on land during the simulation. (Author`s, 2020)	112
Appendix D 9.1.3: Maximum instantaneous tsunami wave speed in the medium study domain during the simulation. (Author`s, 2020)	113
Appendix D 9.1.4: Tsunami travel time in minutes for the Ancona scenario. (Author`s, 2020)	114
Appendix D 9.1.5: Maximum number of Froude in relation to the maximum level of amplitude m (sea elevation).(Author`s, 2020)	115

Appendix D 9.1.1: Maximum coastal amplitude in the middle domain during simulation. (Author`s, 2020)	116
Appendix D 9.2.2: Maximum instantaneous tsunami wave speed in the medium study domain during the simulation. (Author`s, 2020)	117
Appendix D 9.2.3: The maximum depth of flow on land during the simulation. (Author`s, 2020)	118
Appendix D 9.2.4: Tsunami travel time in minutes for the Split scenario. (Author`s, 2020)	119
Appendix D 9.2.5: Maximum number of Froude in relation to the maximum level of amplitude m (sea elevation). (Author`s, 2020)	120
Appendix D 9.2.1: Maximum coastal amplitude in the middle domain during simulation. (Author`s, 2020)	121
Appendix D 9.3.2: The maximum depth of flow on land during the simulation. (Author`s, 2020)	122
Appendix D 9.3.3: Maximum instantaneous tsunami wave speed in the medium study domain during the simulation. (Author`s, 2020)	123
Appendix D 9.3.4: Tsunami travel time in minutes for the Montenegro scenario. (Author`s, 2020)	124
Appendix D 9.3.5: Maximum number of Froude in relation to the maximum level of amplitude m (sea elevation) . (Author`s, 2020)	125
Appendix E 10.1.1 History of maximum sea level amplitude in relation to propagation time.	127
Appendix E 10.1.2: History of maximum sea level amplitude in relation to propagation time.Ancona-Grado. (Author`s, 2020)	128
Appendix E 10.1.3 :History of maximum sea level amplitude in relation to propagation time.Ancona-Lignano. (Author`s, 2020)	129
Appendix E 10.2.1:History of maximum sea level amplitude in relation to propagation time. Monfalcone - Lignano. (Author`s, 2020)	130
Appendix E 10.2.2: History of maximum sea level amplitude in relation to propagation time.Montenegro - Trieste. (Author`s, 2020)	131
Appendix E 10.2.3: History of maximum sea level amplitude in relation to propagation time. Montenegro - Grado. (Author`s, 2020)	132

Appendix E 10.2.4: History of maximum sea level amplitude in relation to propagation time. Montenegro - Lignano. (Author`s, 2020) 133

CHAPTER 1

1 INTRODUCTION

1.1 Literature review

Although tsunamigenic earthquake events are not so frequent in the Adriatic Sea, compared to the Pacific and Indian oceans and the Mediterranean Sea, nevertheless their impacts along the coastline could be considerable. In 2007, a detailed investigation of earthquake tsunami in the central Adriatic Sea was released (Maramai et al., 2007). This work provided an updated tsunami catalogue that affected the region in the last century; also, it determined the potential events that generate a tsunami by showing the great uncertainties in the locations of the hypocenters, as well as in the estimations of the magnitudes of the seismic events (Maramai et al., 2007). Similarly, (Pasarić et al., 2012b) have detected 27 tsunamigenic events that happened in the last 600 years, 18 of them distributed on the east side: 10 are unreliable, 6 are reliable and another 2 in the updated list are omitted because they are assigned meteorological origin in the GITEC catalogue (*Euro-Mediterranean Tsunami Catalogue*, n.d.) On the other hand, on the west side of the Adriatic 9 events were recorded

1.2 Description of the problem

There is limited or scarce information that could indicate the possible impacts that an earthquake-tsunami could pose to cities located along the north-east Adriatic Sea coastline, specifically in the localities of Trieste, Monfalcone, Grado, and Lignano (Pasarić et al., 2012b). The main seismogenic source that could generate a large tsunami is located hundreds of kilometres (approximately) away from the area of interest. However, very little is known about how it could propagate along the Adriatic Sea, the arrival times of the waves and the level of impact.

Due to this lack of information on the height, a tsunami wave may reach, with what speed it may produce drag forces, and what is the level of impact on the coasts, is of paramount importance in the northern Adriatic Sea region, in the selected cities of Trieste, Monfalcone di Grado and Lignano in particular. Therefore, tsunami modelling is a promising tool that may help to generate possible scenarios, from the collected historical

seismic and topo-bathymetric data, to assess their possible impacts in the areas of interest.

Establishing the possible impacts of a tsunami in coastal communities is of essential importance and this value is increased by the fact that these cities are relevant and of thriving development, which makes them more vulnerable to these events, this is the case of the four study cities, the significant of which is Trieste, one of the most important port cities in the Adriatic Sea basin, because of this it is an important centre and a point of confluence of different ethnicities and cultures for centuries. Its port makes it a strategic site for trade and tourism and its economy is based on these aspects, in addition to its high historical relevance. Monfalcone is an industrial midpoint, with several ship and aircraft shipyards, a center ground of textile production and chemical manufacturing, as well as being an important point of production of refined petroleum products, which makes it a strategic center of industrial production in Italy and the province of Gorizia. To the west are the cities of Grado and Monfalcone both cities with a high tourist impact for its variety of resorts and beaches, in addition to several marinas located inside the lagoon of Grado makes it a center of high demographic movement and besides being an area with a high degree of vulnerability due to its direct location to the Adriatic Sea basin. Finally, the city of Lignano is a primary touristic site, which during summertime reaches a population of several hundred thousand people.

Knowing how a tsunami reaches the coasts of these important cities, along with the possibility to estimate how much damage it can cause, will allow establishing emergency plans to be prepared for this hazard, an aspect that has been largely overlooked so far, due to the limited information available for these areas.

1.3 Objectives

1.3.1 General objective

Modelling tsunamigenic earthquake scenarios located at far distance in the Adriatic Sea from the area of interest and study their potential.

1.3.2 Specific objectives

- Analyze the historical data of tectonic tsunamis in the northern Adriatic Sea for the identification of possible tsunamigenic sources.
- Compute different tsunamigenic earthquake scenarios based on numerical simulation code of NamiDance and provide tsunami hazard parameters of interest that can be used for risk assessment for the area of interest (wave arrival time, change of velocities, effects and run-up).
- Generate of final maps and illustrations of the necessary tsunami parameters (wave arrival time, change of velocities).

1.4 Theoretical framework

1.4.1 Site information

1.4.1.1 Adriatic Sea

The elongated landlocked basin located in the northernmost part of the Mediterranean Sea $45^{\circ}47'N$ with an area of 138600 km^2 and the volume of 15000 km^3 . Its shape is close to a rectangle of 800 km long and 200 km wide.



**Figure 1.1: Regional Map, zoom to north-east Adriatic Sea and cities of interest.
(Author's, 2020)**

Receives a large amount of fresh water because it is surrounded by a considerable number of rivers, with an average annual inflow of 5700 m³/s, predominantly 28% Po River as well as the 22% Albanian group of rivers, however for this last one its circulation is weaker than the first river since it is a very narrow area. Regarding its bathymetry, northwest corresponds to shallow waters increasing slowly to the south, with the Middle Adriatic reaching a depth of 270 m, drastically. There is a peak locating the Patagrusa Sill trench rising to 170 m and afterwards there is, again, depression of 1200 m that occupy the southern Adriatic trench. Finally, Otranto Sill of 780 m is formed as the bottom rises to separate the Adriatic Sea from the Ionian Sea. This element is transversally and longitudinally asymmetrical for two reasons, because of its morphology and orography: the west coastline is relatively soft, smooth, and regular without islands and the Apennine Mountains are distant from the coast. In contrast to the west coastline, the east has many islands, and its bottom is very irregular, with a mountain range of important heights, the Dinaric Alps. Consequently, the water dynamics of the two sides are very different (Cushman-Roisin et al., 2001b; Plan et al., 1994).

Northern Adriatic

The bathymetry of the northwest shows shallow water bathymetry of depth generally less than 30 m along the entire coast of Trieste and Venice (Figure 1.2). A study of the coastal front of north Adriatic was carried out under the Alpex-Medalpex experiment during 1982-1983. It indicated that the coastal front changes its position rather significantly. It seems that the bora (NE wind) has a strong impact on the dynamics of the area (Cushman-Roisin et al., 2001a). Due to its local conditions, its temperature fluctuates around 25 °C. In this work, tsunami hazard for four north-east Adriatic's cities is evaluated "Areas of interest": Trieste, Monfalcone, Grado and Lignano (Figure 1.1)

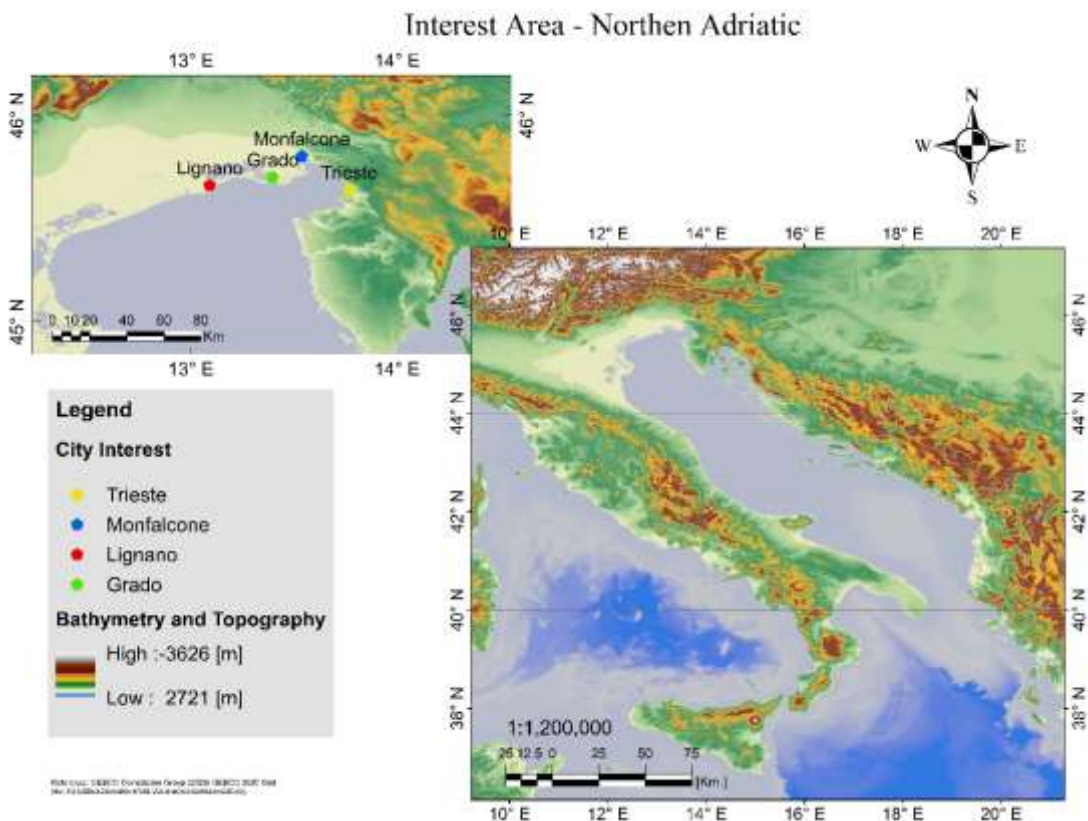


Figure 1.2: Bathymetry and Topography of the area of influence indicating the area of interest. (GEBCO, 2020)¹

1.4.2 Seismicity and Tectonics of the Adriatic Sea

Earthquakes are an abrupt tectonic movement due to the energy accumulated by tectonic forces throughout geological time. They occur along with different types of geological or tectonic faults, which are ruptures in the earth's crust. At the instant of rupture, the energy released produces relative movements that move in the form of waves of blocks on the crust (Iglesias Cerdeira, 2015).

For an earthquake to be considered a tsunamigenic event, the crustal rupture must have a vertical component, originating at the seafloor and disturbing the water column due to deformation and displacement of the crust. Producing the effective transfer of the movement over the water column generating a tsunami wave that can propagate (Iglesias Cerdeira, 2015).

¹GEBCO is a global terrain model for the ocean and land structured on a gridded bathymetric dataset. Available for public download or access through Web Map Services access. <https://download.gebco.net/>

NOAA National Center for Environment Information database (*NCEI Hazard Tsunami Search*) records a global distribution of tsunamigenic earthquakes is 70% Pacific Ocean, 15% Mediterranean Sea, 9% the Caribbean Sea and the Atlantic Ocean and 6% Indian Ocean. According to the data collected from these global sources, about 76% of the tsunamis worldwide are earthquakes.

General tectonics and active faults

Plate tectonics are portions of the Earth's crust that move independently. Plate boundaries are locations where plates are in interaction with each other's (Iglesias Cerdeira, 2015)

Inside the domain of each of the limits, a distinction is made in terms of their behaviour between:

- **Divergent boundaries**

They move in opposite directions to their position creating a rift.

- **Convergent boundaries**

They move towards each other's, generating collision or subduction zones.

- **Transforming boundaries or faults**

They are produced by displacement in a parallel direction between plates producing shearing.

Faults in geology is a discontinuity accompanied with displacement produced by a fracture or fracture zone where the tectonic force overcomes the elemental strength of the crust, this is caused by movements in different directions as vertical, horizontal or oblique to the plane (INPRES, 2013).

The sudden fracture of a fault generates disturbances in the earth's surface, which can be evidenced and traced in topographic maps of the terrain after the event, called fault scarp, these traces are to understand the behaviour of the faults and thus to be able to subdivide them by kinematics.

- **Normal Fault (Dip-Slip)**

These are generated by tensile forces in the horizontal direction, produced by the forces induced on the rock and which are perpendicular to the fault plane which is about the azimuthal north which is called the surface rupture line (Figure 1.3). The constituent elements of this type of fault structure are the roof, the section of the block above the central axis of the fault plane, and the lower section of the fault plane, which is called the floor. Particularly these faults present an inclination angle of the fault plane of 30° with the vertical (INPRES, 2013).

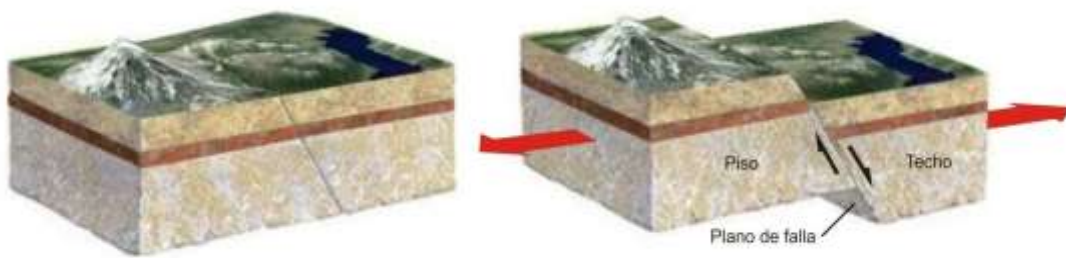


Figure 1.3 Structure of a Normal Fault. (INPRES, 2013).

- **Reverse Fault (Dip-Slip)**

Generated by movement with horizontal compressional forces (Figure 1.4) and with a typical fault plane with an oblique direction of 30 degrees to the horizon, but these tend to have faults with a direction of 45 degrees called thrusting. These faults are characterized by reverse movement to normal faults where the roof moves along the horizontal line of action and the floor deepens (INPRES, 2013).

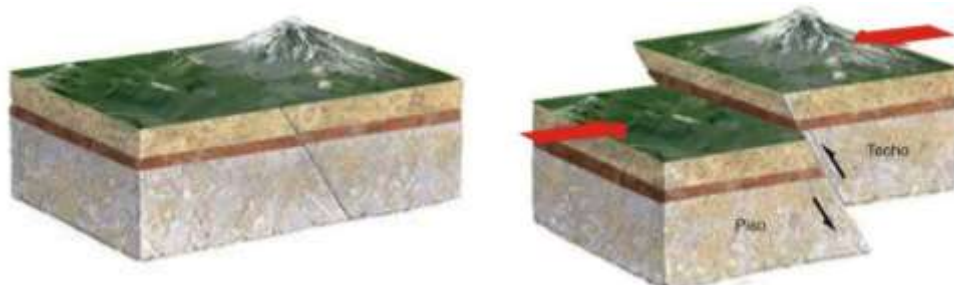


Figure 1.4 Structure of a Reverse Fault. (INPRES, 2013)

- **Strike Fault.**

Also called Transforming Faults, they develop along vertical planes with continuous lateral movements along the cracks (Quimiz et al., 2019). They are characterized by relative movements of the blocks in the same plan in a right lateral or dextral manner and left lateral or sinistral movements as shown Figure 1.5. (INPRES, 2013).

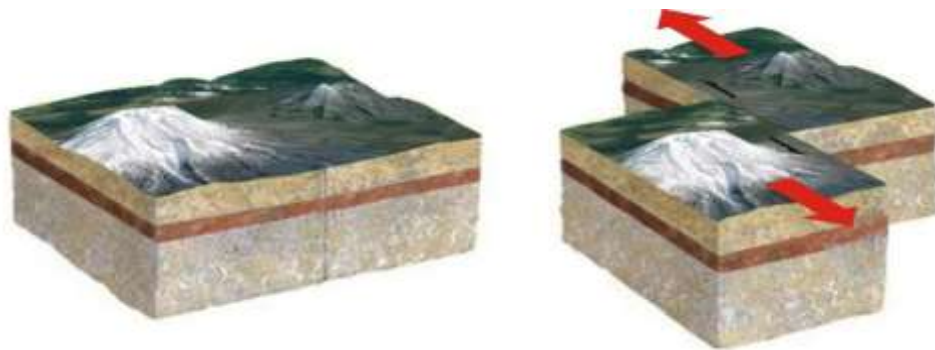


Figure 1.5 Structure of a Reverse Fault. (INPRES, 2013).

The Adriatic Sea is a basin stretching from northwest to southeast and bounded by a chain of active tectonic zones and slip faults. These zones are characterized by their potential for generation of earthquakes of considerable magnitude. Throughout history, earthquakes in Adriatic are known to generate direct and indirect impacts for the coastal populations i.e. ground motion and tsunamis. Undoubtedly, the generation and severity of tsunami events generally depend on their locations and magnitude, and fault geometry and kinematics, which makes the Adriatic Sea classified as a potential tsunami zone.

Historically recorded earthquakes in the Adriatic Sea date back to the 16th century with events of a maximum magnitude of 7 Mw (Pasarić et al., 2012b) and a shallow water depth (Paulatto et al., 2007b). The tectonic configuration of the area of influence, which includes the entire length of the Adriatic Sea and its western and eastern littoral coasts, shared between Italy, Slovenia, Croatia, Bosnia and Herzegovina and Serbia and Montenegro, is positioned on the Adria microplate. The movement of the Adriatic microplate is of main relevance to determine the relationship of its boundaries with the African and Eurasian tectonic plates and to contrast the compression and deformation of the crust over a large area of central Europe.

Data collected by the Advanced National Seismic System (Survey, 2012a) demonstrated that Adria's features have been constrained by the collision of the African plate generating the subduction of the Eurasian plate. Consequently, the Adria microplate can be divided into three different deformation zones denoted by zonal location as north, central and south (Palano, 2015). To the north-east of Adria, it moves with an average of 5 mm/year and the section to the south-west of Slovenia moves in the range of 3 to 7 mm/year in an east-northeast direction. In the south of the Adria plate, it shifts by 4 to 5 mm/year in a west-east direction (Figure 1.6). In the Centre of Adria the largest movements are evident in the area between Dinarides and Gargano, which are between 8 and 10 mm/year (Altiner et al., 2006).

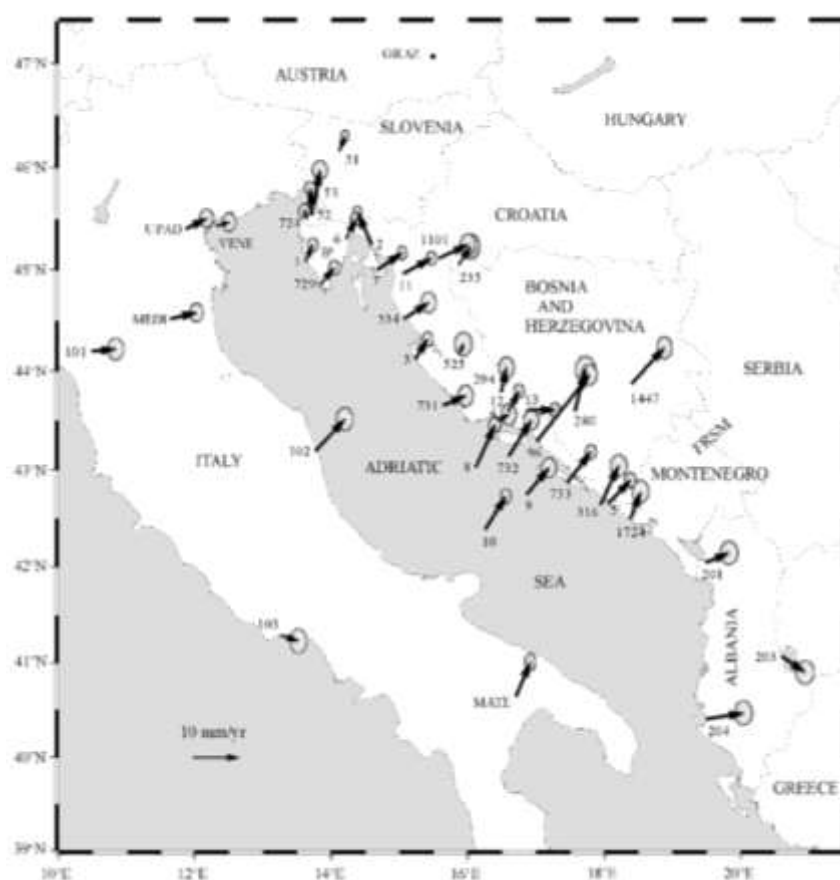


Figure 1.6 Tectonic motion vectors on the Adria Plate. (Altiner et al., 2006).

These displacements determined in the work of Altiner et al. (2006), plus the already known movements of the African continental plate, make it possible to contrast the level of understanding at the contact limits where the Adria microplate and the African-Eurasian plate are located. The plate convergence zones give rise to the formation of the

predominant mountain ranges in this area, such as the Alps in the north, the Apennines throughout the Italian peninsula and the Dinarides in the eastern Adriatic Sea.

Seismogenic zones of relatively high seismic activity are mainly located along the western side of the Adriatic, due to the presence of several tectonic faults are located offshore in the central Adriatic section between Gargano and central Dinarides can be delineated. For instance, earthquakes with higher frequency and intensity such as those of higher to magnitude 7 in the central Adriatic Sea margin, along the Montenegro portion of the Dinaride-Albanide chain, and the southern end of the Kefallonia-Lefkada chain, which are structures with a high tsunamigenic potential (Necmioglu & Ozel, 2014)

The study area is characterized by interplate subduction faults and normal and reverse tectonic faults, which are the result of the horizontal tension generated by the earth's crust in the direction induced by the subduction of the plate.

According to the work of Tiberti et al., (2008), the Adria plate boundary has 4 main tectonic domains distributed along its entire contour, namely in the following way and are shown at (Figure 1.7):

- Apennines
- Apulia
- Kefallonia-Lefkada
- Dinarides, Albanides and Hellenides

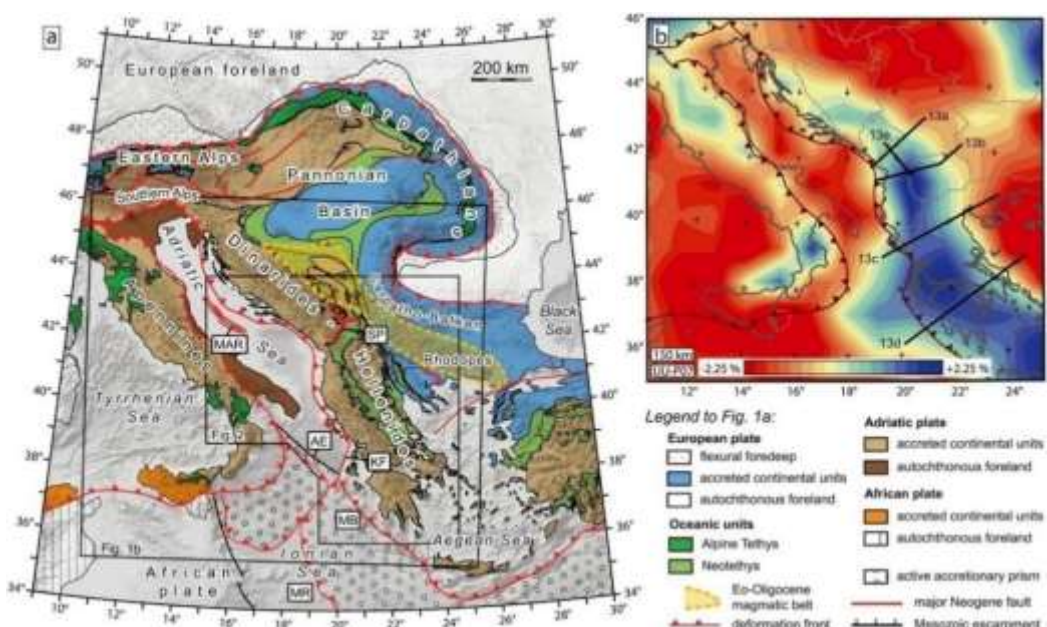


Figure 1.7: Geology structure of the Adriatic Sea region. (de Leeuw et al., 2012)

Apennines

Extends along the eastern edge of the Adriatic Sea, crossing Italy from the north to the south (750 km long), and whose historical earthquake-prone zone. From the coast from the Gargano promontory to the south (Paulatto et al., 2007b)

Apulia

Typical fault line extension in the southern part of the Italian peninsula on the coast of Bari bounded by 400 km to the north and 500 km to the south (Ozer Sozdinler et al., 2019).

Kefallonia-Lefkada

The Kafellonia Fault runs along the southern coast of Albania to Greece, due to its geographical conditions located in the narrowest part of the Adriatic Sea, maximizing the impact generated by a tectonic event or subsequent tsunami due to the amplification effect and the bathymetric conditions (Tiberti, Lorito, et al., 2008).

Dinarides, Albanides and Hellenides

A geological belt of formations formed because of the subduction of the Adriatic microplate beneath the northward-thrusting continental plate of Europe extending on the eastern edge of the Adriatic Sea from the Alps in the north to southern Serbia and Montenegro (Figure 1.8).

The compressional strain along the geological chain determined by GPS (Global Positional System) data shows an approximate rate of 30 nanostrain²/yr over the entire extent of the rock formation (Hollenstein et al., 2003). The dynamics of the central Dinarides zone show evidence of a relatively large dipping fault with oblique dextral slip motion on the edge of the North Adriatic dipping plane. Different characteristics are shown in the southern section where west-dipping thrust fault types are shown, which preserve the equilibrium generated at the other end of the Adria microplate. The record of relative

² Unit of estimation of value with respect to time of tectonic deformation for a tectonic plate.

displacement velocities of each of the faults varies between 3 to 10 mm/year subdivided into 3 sections:

- Dinarides (Slovenia): 4 – 5 mm / year North-East
- Albanides (Montenegro): 8 – 10 mm / year North-East
- Hellenides (Albania): 5 – 7 mm /year North-East

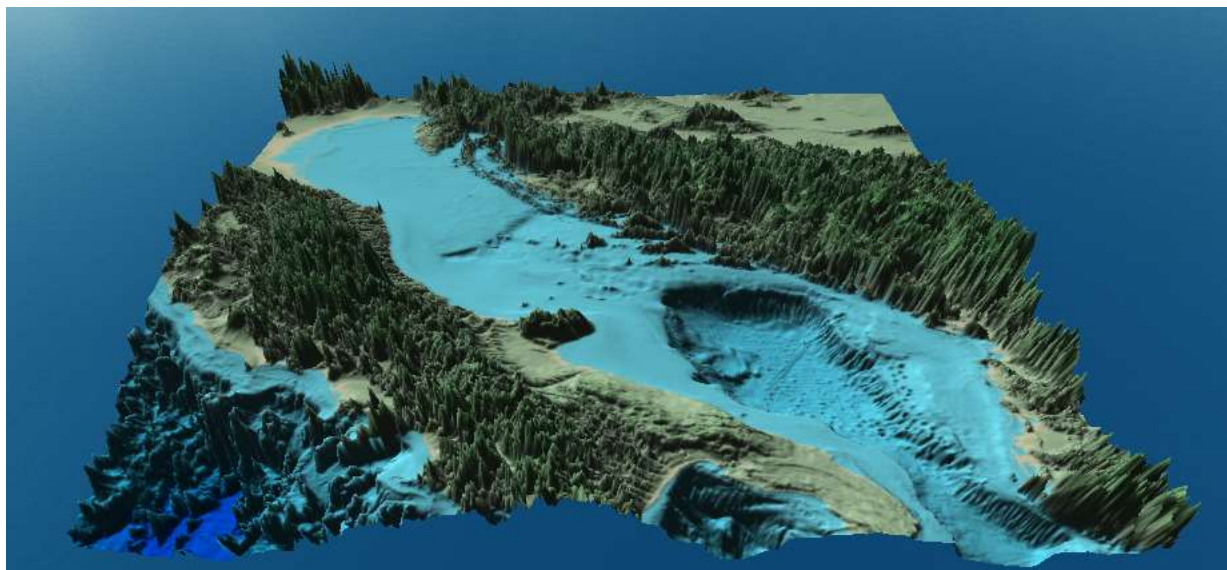


Figure 1.8: The 3D view of the geological formations in the study area. (Author's, 2020)

According to Lorito et al., (2008), the determination of a tectonic zonation is governed by initial aspects such as the conditions of each of the faults that cross these zones, based on kinematic, geological, and dynamic parameters of the geological faults. In such a way that a complex of grouped faults can be established, determined by their physical geometrical and kinematic parameters throughout the basin from north to south on the Adria microplate, which is:

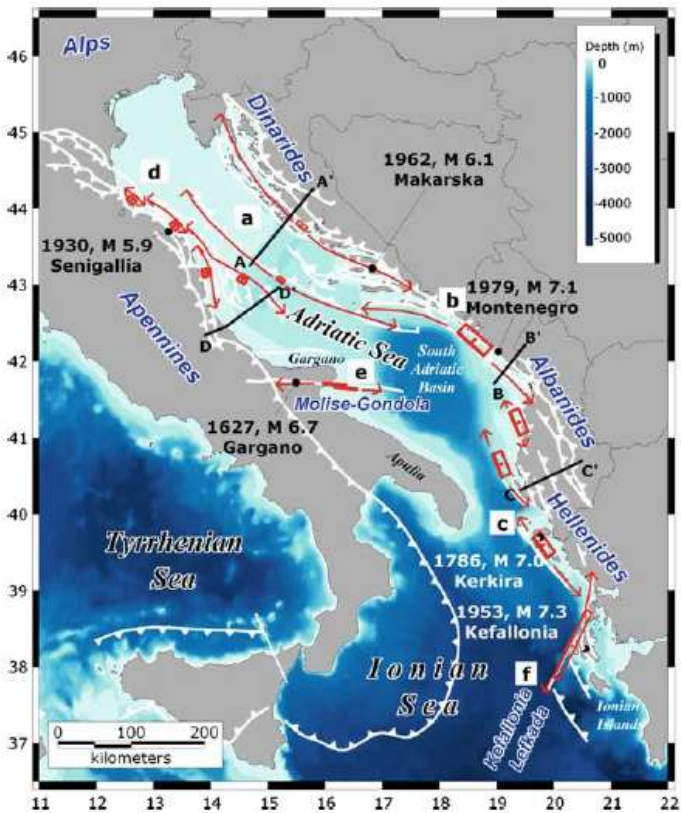


Figure 1.9: Tectonic zones developed. (Tiberti, Basili, et al., 2008)

Seismogenic and or tsunamigenic zones delineated by Tiberti et al. (2008) shown in Figure 1.9 are:

- Zone a: Coastal Croatia
- Zone a1: Offshore Croatia
- Zone b: Montenegro
- Zone c: Albania-N Greece
- Zone d: Northern Apennines
- Zone e: Apulia
- Zone f: Kefallonia-Lefkada

According to Paulatto et al., (2007a), the focal mechanisms are grouped by the considerations of the historical records and thus establish a common fault zone between them. With this information, the fault parameters were standardized by zone and a maximum potential event value was assigned (Figure 1.10). The epicenter of each zone is established at the geographic location of the maximum historical record.

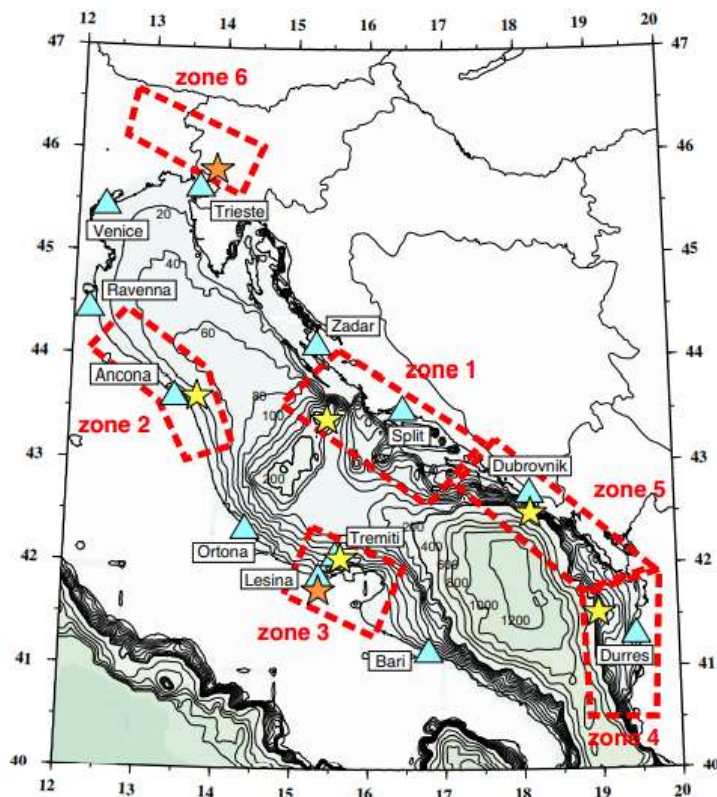


Figure 1.10: Tectonic zoning developed by (Paulatto et al., 2007b)

Seismogenic/ tsunamigenic zones developed of (Paulatto et al., 2007b) are:

- Zone 1: Eastern Central Adriatic Sea and the coast of Croatia.
- Zone 2: Eastern Italian Coastal.
- Zone 3a: Gargano peninsula, offshore source.
- Zone 3b: Gargano peninsula, inland source.
- Zone 4: Northern Albanian Coast.
- Zone 5: Southern Croatia, Bosnia, Herzegovina, and Montenegro.
- Zone 6: Julia and Friuli.

Tsunamigenic zone named Coastal Croatia by Tiberti et al. (2008) or Eastern Central Adriatic Sea and the coast of Croatia by Paulatto et al. (2007b) comprises two faults located respectively on the coastal edge and offshore Croatia with focal points of 10 to 25 km depth, whose seismicity is governed by the subduction of the Adriatic plate under the continuity of the Dinarides zone plate.

Offshore Croatia (Tiberti, Lorito, et al., 2008) or Eastern Italian Coastal tsunamigenic earthquake source (Paulatto et al., 2007b). Comprising the central-eastern coast of Italy at the edge of the Adriatic Sea from Ravenna to San Benedetto, characterized by a passive subduction process of the Adriatic plate beneath the Northern Apennines geological formation.

Montenegro source zone (Tiberti, Lorito, et al., 2008) bounded between the area from Hvar Island to Bosnia Herzegovina, extending along the coast of Montenegro in its large domain. This zone shows a relatively high potential for tsunami generation due to subduction features beneath Dinarides with typical strike-slip and strike-slip faults.

Albania-N Greece (Tiberti, Lorito, et al., 2008) or Northern Albanian Coast (Paulatto et al., 2007b) zone established by a rift fault e between the European plate and the Apulian platform, with slight variations of strike-slip faults extending from northeast to southwest. Apulia (Tiberti, Lorito, et al., 2008) or Gargano peninsula, offshore and Gargano peninsula, inland source (Paulatto et al., 2007b). Geographical protrusion characteristic of a bay, with inter-plate faulting predominant on the coastal edge of Italy, plus small geological rift faults with dextral movement in its offshore domain.

1.4.2.1 Source model in Tsunami modelling

Okada Theory

Okada (1985), has established a numerical simulation to calculate seabed deformation with empirical expressions for the shear-type failure plane with homogeneous elastic displacements and stresses with point focal points.

Okada coseismic elastic deformation of seafloor proposed a uniform displacement over a rectangular portion as finite elements, with assumptions of a stationary system with a depth below the water column which allows distinguishing a transfer of the seafloor deformation to the surface. The limitation of this methodology is the deficiency in the variation of bottom conditions due to irregularities, however, it is most commonly used to approximate historically proven tsunamigenic events (Clawpack, 2009).

The source definition is summarized in a mathematical expression described below:

$$\text{Strike-Slip} = \frac{1}{F} \mu U_1 \Delta \sum \left[-\left(\frac{\partial u_i^1}{\partial \xi_2} + \frac{\partial u_i^2}{\partial \xi_1} \right) \sin \delta + \left(\frac{\partial u_i^1}{\partial \xi_3} + \frac{\partial u_i^3}{\partial \xi_1} \right) \cos \delta \right] \quad (1.1)$$

Equations for a Strike Fault. Source. (Okada, 1985)

$$\text{Dip-Slip} = \frac{1}{F} \mu U_1 \Delta \sum \left[\left(\frac{\partial u_i^1}{\partial \xi_2} + \frac{\partial u_i^2}{\partial \xi_1} \right) \cos 2\delta + \left(\frac{\partial u_i^1}{\partial \xi_3} + \frac{\partial u_i^3}{\partial \xi_1} \right) \sin 2\delta \right] \quad (1.2)$$

Equations for a Dip Fault. Source. (Okada, 1985)

Fault parameters

The SATREPS Tsunami Project (2016), defines the following parameters necessary to be able to size a seismic source.

- **Length, (L) and Fault Width, (W)** - Geometric dimensions of the fault plane to establish its intensity magnitudes. These parameters can be established by a scaling law (e.g. Wells & Coppersmith, 1994) (Figure 1.11).

$$\log(L) = -3.02 + 0.69(M_w) \quad (1.3)$$

An empirical relationship between fault length and magnitude.
(Wells & Coppersmith, 1994)

$$\log(W) = 2.44 + 0.59(M_w) \quad (1.4)$$

An empirical relationship between width of fault and magnitude.
(Wells & Coppersmith. (1994))

- **Focal depth (h)** - The average vertical distance measured from the point of origin to the seabed surface by estimating a horizontal plane.
- **Strike (θ)** - The azimuthal strike angle of the fault plane measured from the origin to geographic north, ranging from 0° to 360° .
- **Rake (λ)** - The angle between the relative position of the fault floor block and the fault roof under ideal conditions of repose in the horizontal plane of repose.
- **Dip (δ)** - Geological feature defined as the angle of subduction of the fault plane.
- **Vertical displacement (D)** - Relative displacement, in the direction defined by the slip angle, between the upper and lower blocks of the fault, measured in the fault plane.

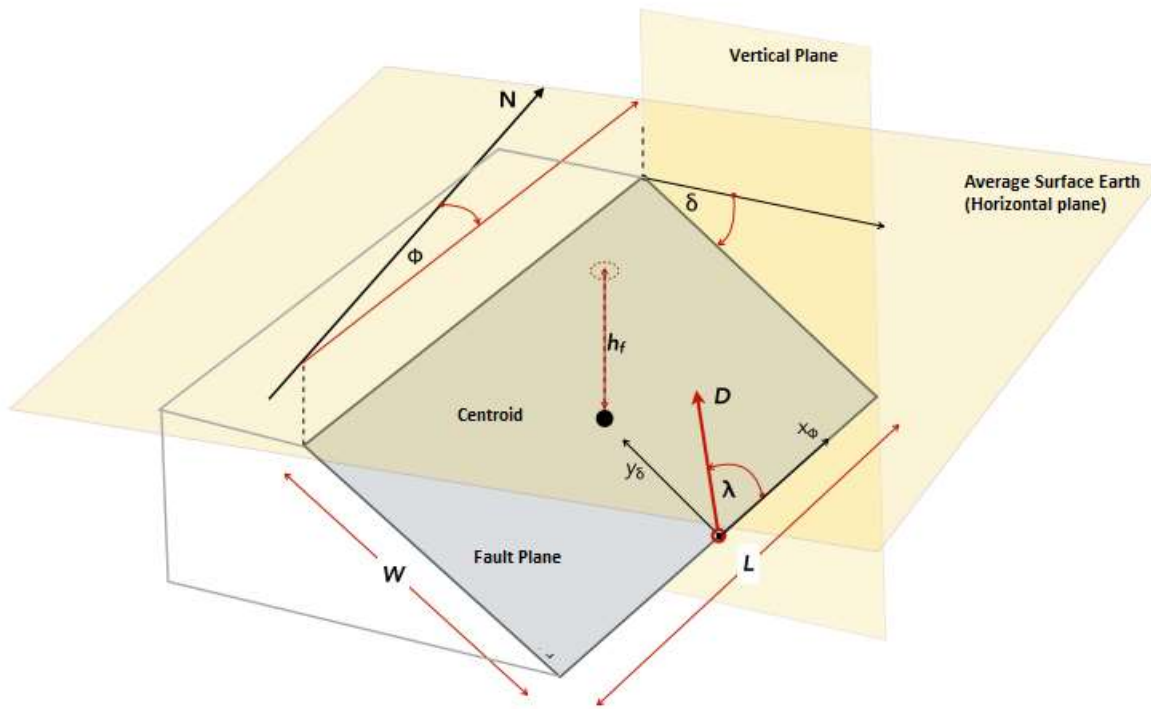


**Figure 1.11 Graphic Description of Fault Parameters.
(SATREPS Tsunami Project, 2016)**

1.4.3 Tsunami

Tsunamis originated from the Japanese term "harbour wave" (Survey, 2012b), are one of the most devastating and dangerous fluctuations or disturbances of the sea, it is an extremely long wave, its period is long, it travels in shallow water and its wavelength grows rapidly as it reaches the coast (CERC, 1984). Disturbances are mainly generated by volcanic eruptions, earthquakes, meteorites, or landslides. The hydrodynamic parameters that determine the level of damage of a tsunami are the tsunami wave height which is taken as a reference from the still water sea level at the point of the disturbance; the run-up height measured from sea level to the maximum vertical height that the wave reaches on land and finally the inundation distance, which is a horizontal measure of the tsunami trajectory entering the land. Tsunami dynamics has 3 phases: generation, propagation, and inundation (Figure 1.12). Tsunami waves have small wave heights and long wavelengths up to hundreds of kilometres long, at the coast. As the waves move towards the coast, they undergo changes depending on the bathymetry of the coast; their celerity is considerably reduced and they become significantly higher (Velioglu et al., 2016).

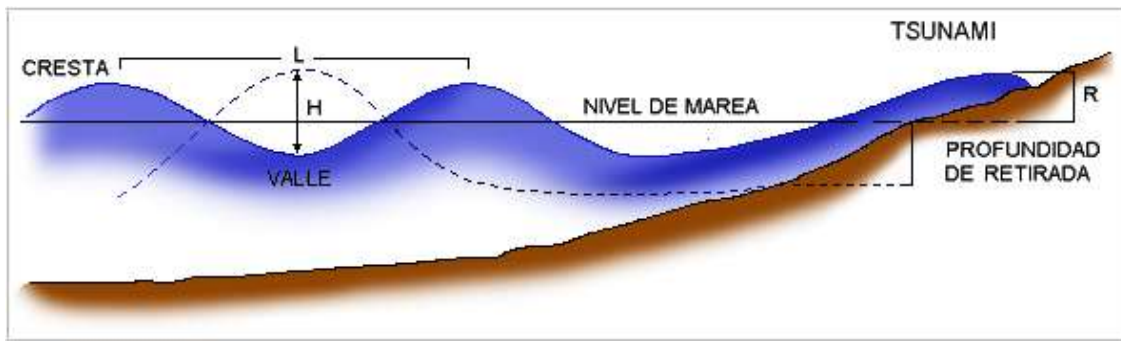


Figure 1.12 Schematic of tsunami parameters. (UC, 2019).

Generally, tsunami wave is composed of peaks and trough, i.e. positive and negative respectively, if the first wave to arrive is a peak, the breaking wave is massive, and the inundation will be sudden. On the other hand, if it is valley trough, the shoreline will recede abruptly, and the inundation will happen after a bit longer time. Generally, tsunami wave height depends on the vertical displacement, focal depth, water depth of the offshore or near-shore earthquake (Survey, 2012b). Also, at a near distance to the fault, the wave height depends on the details of the source rupture process. The final stage of tsunami is uncertain due to its trajectory because it depends on the topography of the area, the collapse of buildings or houses in its path and the accumulation of debris (Dias & Dutykh, 2007).

1.4.3.1 Numeric Model

Numerical models help to solve various engineering problems, being developed based on numerical methods techniques of temporal and spatial discretization that computational is automated according to the algorithm that has implemented the developer, currently the interfaces, the debugging of the files as the time have improved, the most used methods are finite-difference and hydrodynamic modelling with fewer inputs to process (Table 1.1).

Table 1.1 Computational models for the simulation of a tsunami. (NTHMP, 2017)

Model Name	Equations Solved [Spatial Dimensions]	Numerical Approach	Numerical Treatment of Convection Terms	Numerical Accuracy of Other Gradient Terms	Numerical Treatment of Time Integration
ALASKA GI-T	Nonlinear Shallow Water (NSW) [2D]	FD	Upwind (1st-order accurate)	Centered (2nd-order accurate)	Semi-implicit (1st-order accurate)
NAMIDANCE	Nonlinear Shallow Water (NSW) [2D]	FD	Upwind (1st-order accurate)	Centered (2nd-order accurate)	Explicit (2nd-order accurate)
MOST	Nonlinear Shallow Water (NSW) [2D]	FD	Centered (2nd-order accurate)	Centered (2nd-order accurate)	Explicit (1st-order accurate)
Cliffs	Nonlinear Shallow Water (NSW) [2D]	FD	Centered (2nd-order accurate)	Centered (2nd-order accurate)	Explicit (1st-order accurate)
GeoClaw	Nonlinear Shallow Water (NSW) [2D]	FV	Limiter-based (1st-order near shocks, 2nd-order when smooth)	Centered (2nd-order accurate)	Explicit (2nd-order accurate)
GeoClaw - AECOM	Nonlinear Shallow Water (NSW) [2D]	FV	Limiter-based (1st-order near shocks, 2nd-order when smooth)	Centered (2nd-order accurate)	Explicit (2nd-order accurate)
Tsunami-HySEA	Nonlinear Shallow Water (NSW) [2D]	FV	Limiter-based (2nd-order near shocks, 3rd-order when smooth)	Centered (2nd-order accurate)	Explicit (3rd-order accurate)
COULWAVE	Highly Nonlinear Boussinesq-type [2D]	FV	Limiter-based (2nd-order near shocks, 4th-order when smooth)	Centered (4th-order accurate)	Semi-implicit (4th-order accurate)
FUNWAVE-TVD	Highly Nonlinear Boussinesq-type [2D]	FV / FD	Limiter-based (2nd-order near shocks, 5th-order when smooth)	Centered (4th-order accurate)	Explicit (3rd-order accurate)
BOSZ	Weakly Nonlinear Boussinesq-type [2D]	FV	Limiter-based (2nd-order near shocks, 5th-order when smooth)	Centered (5th-order accurate)	Explicit (2nd-order accurate)
NEOWAVE	One-Layer, Non-Hydrostatic [2D]	FD	Upwind (1st-order near shocks, 2nd-order when smooth)	Centered (2nd-order accurate)	Semi-implicit (2nd-order accurate)
TSUNAMI3D	Navier-Stokes [3D]	FD	Upwind (1st-order accurate)	Centered (2nd-order accurate)	Explicit (2nd-order accurate)
SCHISM	Navier-Stokes, Hydrostatic [3D]	FE / FV	Limiter-based (1st-order near shocks, 2nd-order when smooth)	Centered (2nd-order accurate)	Semi-implicit (2nd-order accurate)

Tsunami waves are estimated from shallow water models describing their propagation using the long-wave theory of linear models, when approaching the coast this theory is not appropriate to use due to its non-linear conditions, the non-linear equations with friction effect on the bottom are considered.

Different computational models are used for various case studies and adapt the solitary wave theory such as FLOW 3D and NamiDance. Due to the first wave arrives at the coast and its bathymetric conditions.

$$C = \sqrt{g(H + d)} \quad (1.5)$$

Approximate lone wave speed. (CERC, 1984)

$$E = \frac{8}{3\sqrt{3}} \rho g H^{\frac{3}{2}} d^{\frac{3}{2}} \quad (1.6)$$

Energy on a solitary wave. (CERC, 1984)

NAMIDANCE for Tsunami Modeling

NAMIDANCE is a numerical computational model developed by Middle East Technical University (METU) in Turkey and Laboratory of spatial Research Bureau for automation of Marine Research, Far Eastern Branch Academy of Sciences in Russia. NAMIDANCE is a tool that develops tsunami model simulations using historical records for model accuracy and then a projection of an idealized scenario event recommended by the United Nations Educational, Scientific and Cultural Organizational (IOC UNESCO). This software performs long-wave modelling and uses the finite-difference method to solve non-linear long-wave shallow-depth equations, initially dominated by the Navier-Stokes equations and finely adapted to the domains in shallow-water equations. Its assumptions are approximated due to the depreciation of the vertical motion of the particles, eliminating the pressure distribution and the vertical acceleration to adapt it to a hydrostatic model. (Velioglu Sogut & Yalciner, 2019). The model has been applied as

a research model in a series of experiments on different case studies of events that have occurred over the last 15 years, respectively.

It uses the C++ programming language and is based on the TUNAMI-N2 and TUNAMI-N3 processes. These are developed under the framework of the UNESCO Tsunami Inundation Model Exchange Programme. They are based on the linear long-wave theory of shallow-water and land run-up with constant grids, second-order finite-difference equations. The seismic sources are structured by an epicentre located below a focal depth and with uniform background domain to estimate the distribution of the disturbance as a mechanism according to OKADA (1985) for tsunamis of seismic origin. NamiDance is finally described by discretized equations using dynamic and kinematic conditions.

- **Cartesian Coordinates**

$$\frac{\delta\eta}{\delta t} + \frac{\delta M}{\delta x} + \frac{\delta N}{\delta y} = 0 \quad (1.7)$$

$$\frac{\delta M}{\delta t} + \frac{\delta}{\delta x} \left(\frac{M^2}{D} \right) + \frac{\delta}{\delta y} \left(\frac{MN}{D} \right) + gD \frac{\delta\eta}{\delta x} + \frac{n^2}{D^{\frac{7}{3}}} M \sqrt{M^2 + N^2} = 0 \quad (1.8)$$

- **Spherical Coordinates:**

$$+ \frac{1}{R\cos\phi} \left[\frac{\delta M}{\delta\lambda} + \frac{\delta(N\cos\phi)}{\delta\phi} \right] = 0 \quad (1.9)$$

$$\frac{\delta M}{\delta t} + \frac{1}{R\cos\phi} \frac{\delta}{\delta\lambda} \left(\frac{M^2}{D} \right) + \frac{1}{R} \frac{\delta}{\delta\phi} \left(\frac{MN}{D} \right) + \frac{gD}{R\cos\phi} \frac{\delta\eta}{\delta\lambda} + \frac{\tau_x}{\rho} = 0 \quad (1.10)$$

$$\frac{\delta N}{\delta t} + \frac{1}{R\cos\phi} \frac{\delta}{\delta\lambda} \left(\frac{MN}{D} \right) + \frac{1}{R} \frac{\delta}{\delta\phi} \left(\frac{N^2}{D} \right) + \frac{gD}{R} \frac{\delta\eta}{\delta\phi} + \frac{\tau_y}{\rho} = 0 \quad (1.11)$$

Source: (Survey, 2012a)

The Equation (1.9) to (1.11) in terms of dispersion taken from the Boussinesq model called dispersive nonlinear surface equations. Seismic or large magnitude conditions are negligible for these spherical equations. (Survey, 2012a).

NAMIDANCE operates through a structured rectangular grid to solve equations for the initial conditions to determine the distribution of maximum and minimum water surface elevations. The behaviour of the wave approaching the coastal margin is evaluated in two variables velocities, wave directions, currents, momentum fluxes and their relative directions (Tables 1.2, 1.3). In the coastal zone, it allows the determination of the flood level, the maximum overland flow, flow depths, the Froude number, and the Rousse number in the domain (Tables 1.2, 1.3). Unlike TUNAMI-N2, NAMIDANCE could create the initial wave using both the rupture parameters of an earthquake and the user-defined shapes of the initial water surface disturbance.

Table 1.2 Technical specifications of NAMIDANCE computer model. (Zaytsev et al., 2019).

Variables	Specifications
Equations	Non-Linear Shallow Water
Mesh	Rectangular Structured Grids
Friction	Conditions Variable by Background Material
Source	Rectangular Seismic Source.
Domains	Bathymetries and topographies of different resolution and portions of the area of study, nested between them.
File Types	Grid, Ascii, NECDF, Grig Binary
Time	Seconds, Milliseconds, Minutes

Table 1.3 Output File of the NAMIDANCE computer model.(Survey, 2012b)

Output files	Specifications
Run-up	Flooding (depending on the resolution of the grid)
Time of arrival	Estimated time of arrival of the wave to the coast.
Source	Characteristics of the break and surface distribution.
Propagation	Propagation of the tsunami with respect to the instant of time interval.
Speeds	Distribution of current velocities with respect to the instant of time interval.
Flows	Distribution of discharge flows with respect to the instant of time interval.
Time	seconds, milliseconds, minutes
3D Animation	Tsunami propagation animation.
Time History	History of sea-level rise fluctuations, speeds, flows with respect to simulation time.

CHAPTER 2

2 METHODOLOGY

The methodology is based on the design thinking concept of the engineering design process by the Society of Naval Architects and Marine Engineers (SNAME) and The Graduate School Of Natural And Applied Sciences Of Middle East Technical University. (IEEE, 2020). The following diagram flow (Figure 2.1) shows the methodology used, which is divided into 4 phases: 1st define the problem and the need of the case study, 2nd setup of the model (processing the respective input files for the simulation), 3rd calibration and validation and finally the result.

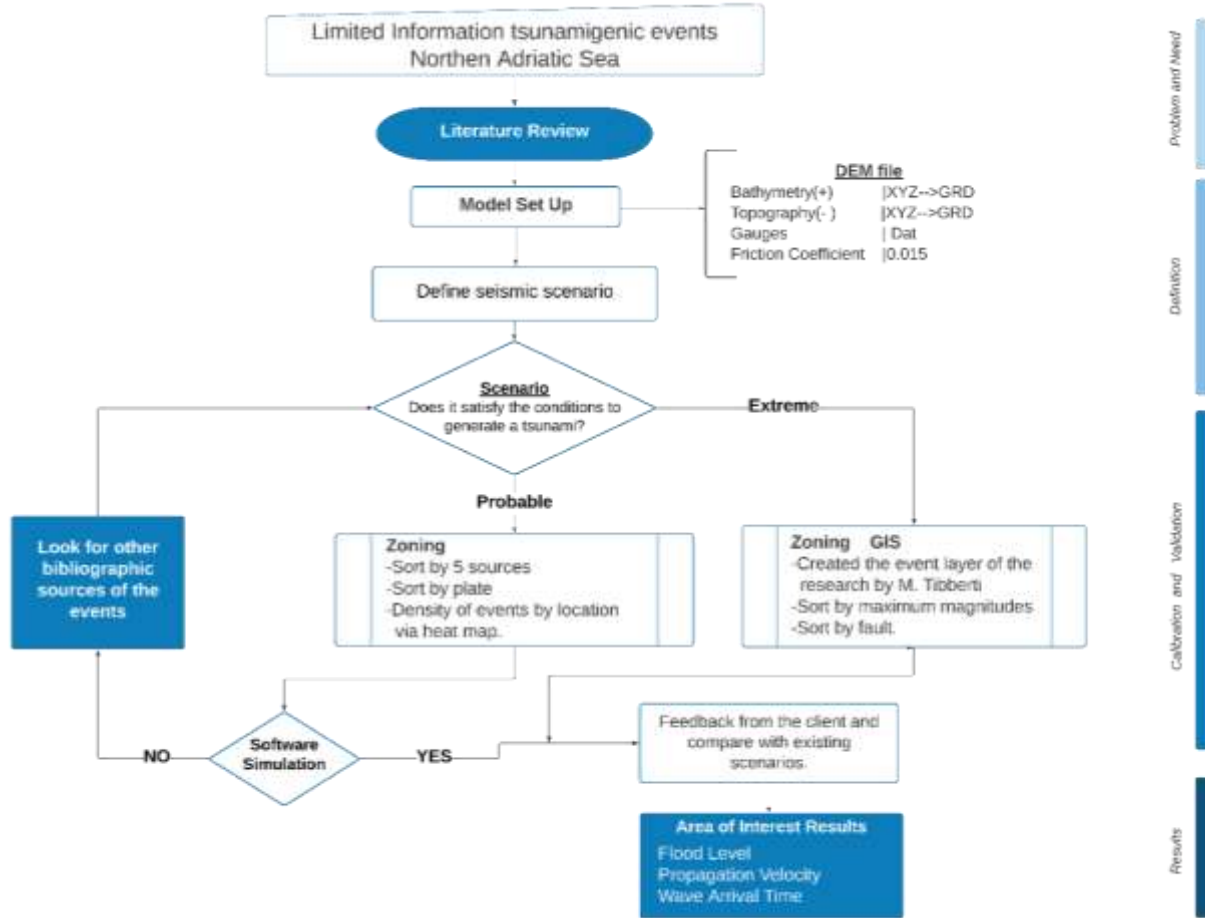


Figure 2.1: Diagram of the methodological process. (Author's, 2020).

2.1 Model set-up

2.1.1 Bathymetry and topography

The DEM data required by NAMIDANCE for the simulation process must be previously prepared in different programs, to establish the necessary input file in grid format (Figure 2.1). Bathymetry and topography data are one of the indispensable inputs, reliant on the effects that can be required, and depending on the resolution of the GeoTiff files. The data was obtained based on (GEBCO, 2020) grid, the version of the global bathymetric product published by the General Bathymetric Chart of the Oceans for the extended domains of 250 m grid resolution (Figure 2.2).

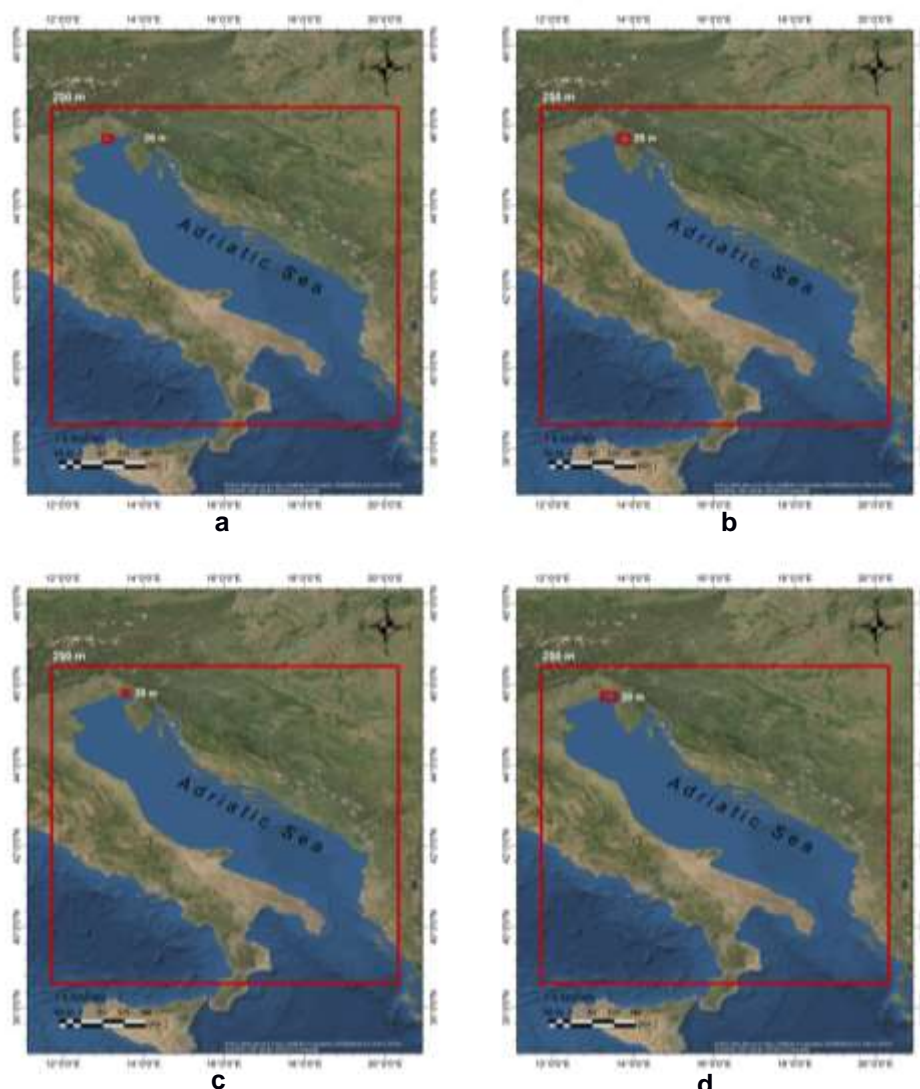
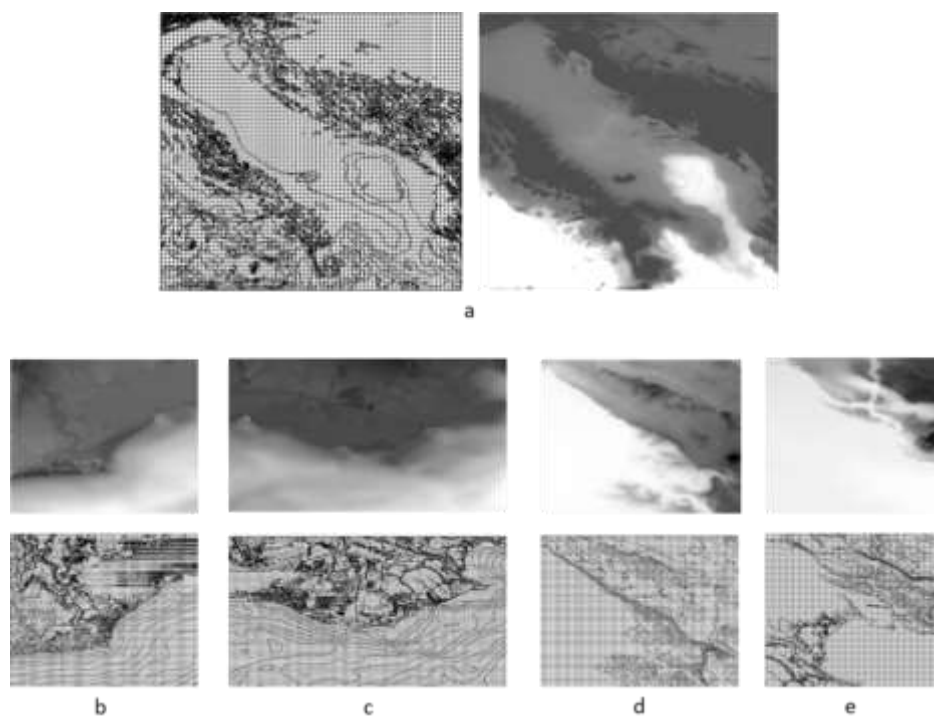


Figure 2.2: Local/Global domains of bathymetry data in city of interest.(Author's, 2020)

The chosen regions are located in the northern Adriatic Sea region and their geographical position is described as follows: a.- Trieste, b.- Monfalcone, c.- Lignano and d.- Grado.

The bathymetry data of 50 m resolution for the local domains of each of the cities of interest were obtained from the work of (Trobèc et al., 2018), while a 15 m resolution topography was extracted (GEBCO, 2020) and then joined in QGIS environmental (Figure 2.2). The DEM files in "GeoTiff" format were processed to convert them into the required grid format. To do that, they were exported in "xyz" format to be imported into Golden Surfer software which processes them as rectangular grid files with z-dimensional values for each grid point. Once exported in Golden Surfer they are exported in "Grid Surfer 6 Binary Grid" format (Figure 2.3). As shown in Figure 2.3, two domains were used in the simulation large domain grid of 400 m resolution and small domain of 250 m resolution resolutions for the coastline of the area of interest a. Adriatic, b. Lignano, c. Grado d. Trieste, e. Monfalcone.



**Figure 2.3 View GeoTtif and Grid files for each large and small dominions.
(Author's, 2020)**

The domains used in each of the simulations are described in two detailed global and local subgroups for each city: a.- Adriatic Sea, b.-Grado, c.- Lignano and d.- Trieste.

2.1.2 Virtual Tide-Gauges

A set of virtual gauges is placed to monitor the evolution of the tsunami through time, at the tide-gauge location the time series of change in still water height over time or named marigram are given (Hassan et al., 2020). The location of the Gauges is chosen to be 10 m water depth. Each area (Trieste, Lignano, Monfalcone and Grado di Coastal) have about between 10 and 15 gauges, which allowed to see the variation in wave height as a function of time, velocity, Froud number and inundation.

2.1.3 Friction Coefficient

The choice of Manning's value will affect the inundation thus the severity of tsunami impacts because it represents the value of the soil friction applied to the fluid (Hassan et al., 2020).

**Table 2.1: Values of the Manning roughness coefficient according to sea-bottom.
(Imamura et al., 2006) &(Survey, 2012a)**

Bed Material	Coefficient
Neat cement, smooth metal	0.010
Rubble masonry	0.017
Smooth Earth	0.018
Natural channels in good condition	0.025
Natural channels with stones/weeds/etc.	0.035
Natural channels in condition	0.060

The case study 2011 Tōhoku Tsunami in Hilo Harbor, Hawaii conducted by the NamiDance software developer determined that the effect of coefficient varies between 0 to 0.015, where it is most denoted in the maximum and minimum values of the velocity and surface height time series. Therefore, the value used in this case is 0.015, recommended by the developer.

2.2 Calibration: Tsunamigenic earthquakes

2.2.1 Define Seismic Scenario

Tsunamigenic sources were obtained from monographs, published papers and official website alert platforms (Figure 2.4).

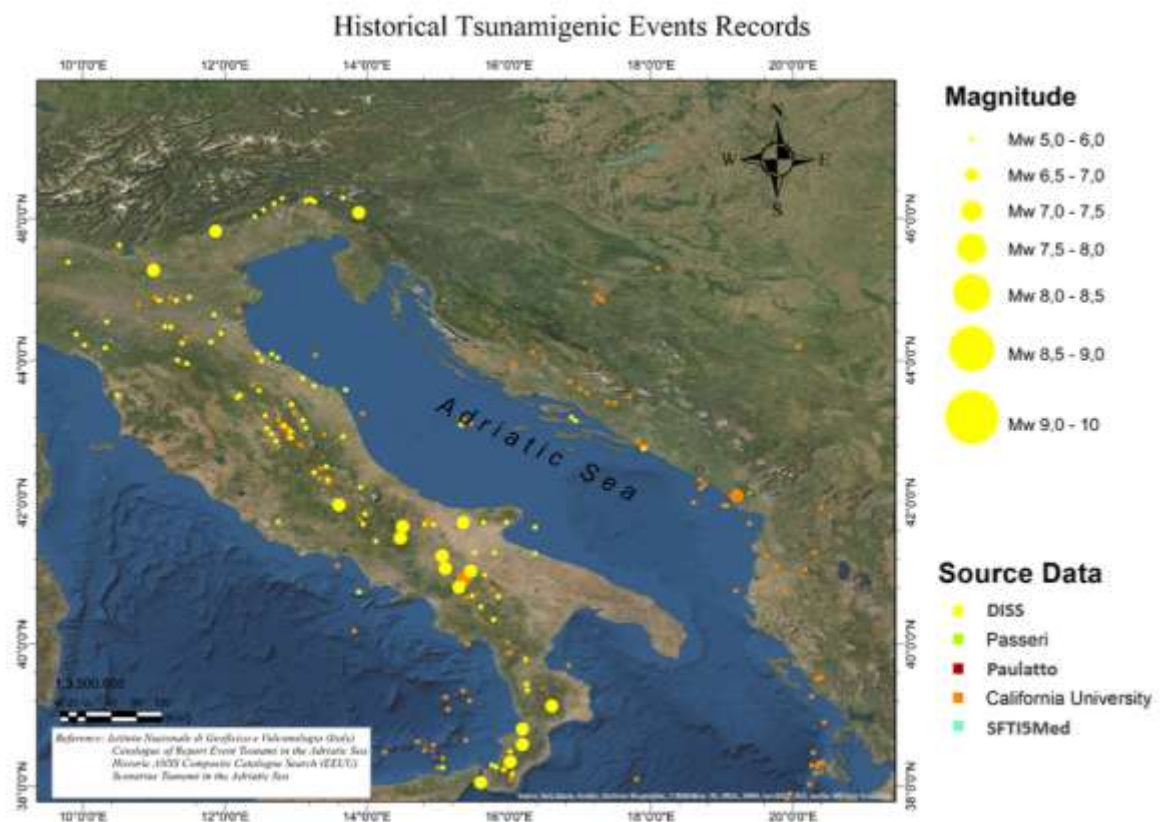


Figure 2.4:Historical Tsunamigenic Events Records. (Author`s, 2020).

In the published works of (Pasarić et al., 2012a) about 27 tsunamigenic earthquakes were reported from 1511 to 1979. Compared to the work of (Paulatto et al., 2007b), 50 tsunamis were reported for the same time and 62 in total in the time from 58 BC to 1979. Both papers are developed and constructed based on several catalogues of earthquakes, but a large difference in the number of tsunamigenic earthquakes is recognized, this calls for the careful selection of the catalogue upon which any hazard assessment should be accomplished.

Table 2.2: Catalogs of reported tsunami events. (Author's, 2020).

Reference	Source	Year of publication	
AM	Ambrasseys	1962	
CF	Caputo and Faila	1984	
BC	Bedosti and Caputo	1986	Tsunamigenic events
PA	Papadopoulos	2001	
ITC	Italian Tsunami Catalogue	2004	
TMC	Soloviev	2000	
CFT	Catalogo dei Forti Terremoti	2000	
NT4.1	NT4.1 Catalogue	1998	Seismic events
CO	Copernicus Catalogue	1996,2000	

DISS and CFT5Med are catalogues developed by the Istituto Nazionale di Geofisica e Vulcanologia-INGV. These catalogues contain the strong earthquakes that struck Italy from 461 BC to 1997. California University (Northern California Earthquake Data Center), this is a global catalogue of ANSS (Advanced National Seismic System) belonging to the USGS (United States Geological Survey).

The methodological process developed for the definition of tsunamigenic scenarios is developed in several phases among different areas: geological structures, number of recurrent events by zones and limited geographical sections for each historical epicenter. A zoning process was structured to limit the areas with favourable conditions along the Adriatic Sea basin, as strategic points with a high probability of generating possible epicenters because of tectonic movements.

These points will be determined considering several variables such as historical event records, occurrence, geological conditions (fault length, fault width, focal point, etc.). The conditions in each of the zoning phases detailed below were contrasted by different bibliographic sources to obtain an optimal probability to choose the most appropriate scenario required.

2.2.1.1 Phase 1: Recurrence

A probabilistic normal distribution of the dataset was globally performed using the MATLAB programming tool, for all the sources mentioned in 2.2.1 Historical Tsunamigenic events. The Magnitude of 4.68 Mw shows a higher probability in the Adriatic Sea (Figure 2.5 and Figure 2.6).

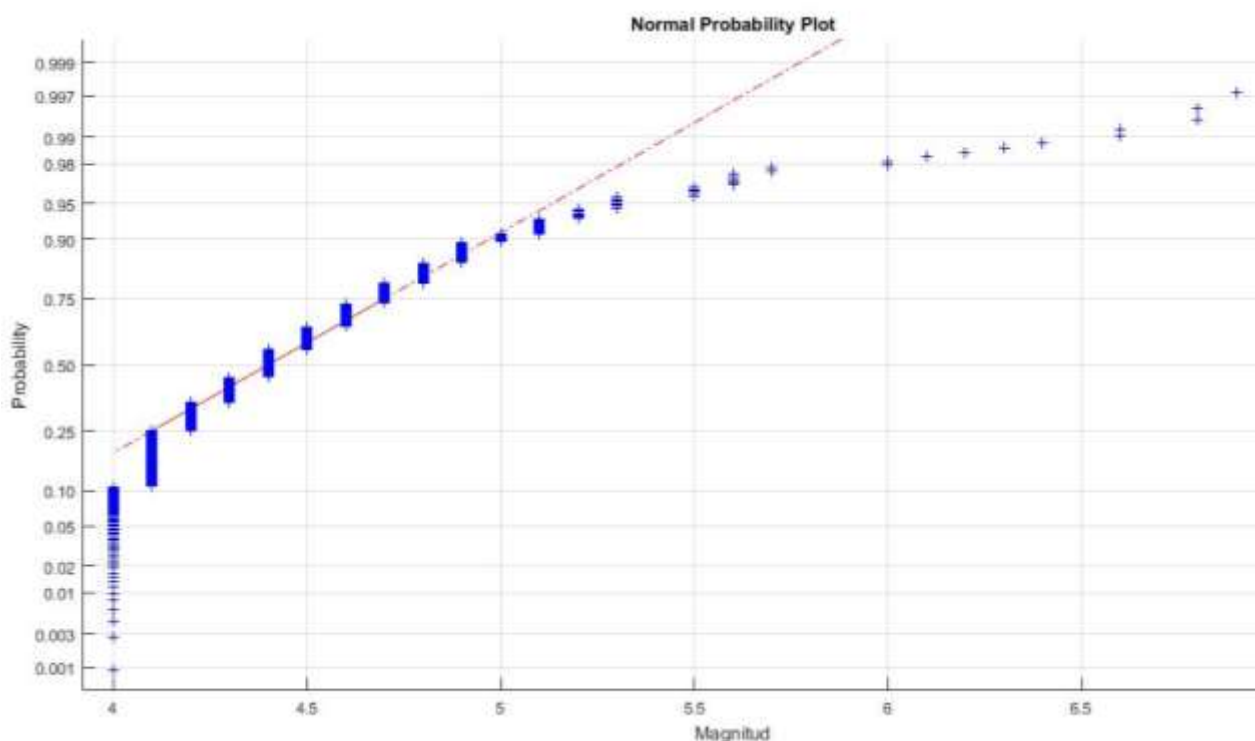


Figure 2.5: Normal Distribution Probability of the magnitude in the Adriatic Sea.(Author`s, 2020)

In this work, tsunamigenic earthquake zones as far as 400 km from the area of interest of maximum magnitude $Mw \geq 6.0$ were selected for tsunami hazard analysis. Also, a worst-case scenario with proper reliability happens in these zones was listed and considered as a scenario to be modelled hereinafter. The second filter, sorting the data by catalogue and the third filter was distributed by tectonic plate Aegean, Eurasia and Africa.

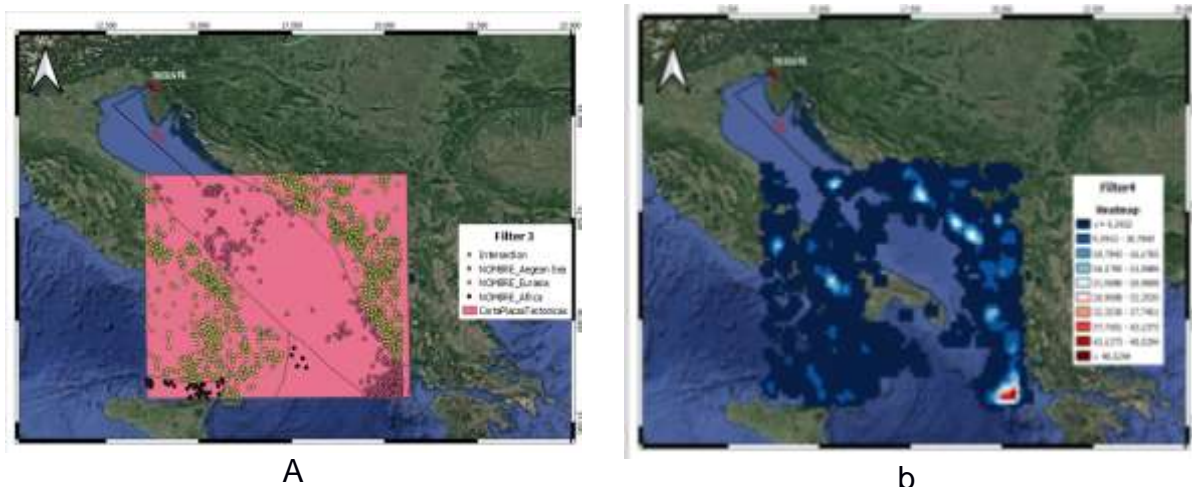


Figure 2.6: Most Probable Scenario Zoning Process. (Author's, 2020)

The last filter will help determine which potential locations are most concentrated through the Heatmap tool. Figure 2.6 (a), the colour scale indicates the redder the higher the concentration and the darker the blue the higher the recurrence of a seismic event at the site. As a result of this process, the zoning of the most probable scenario is obtained as shown in Figure 2.6 (b), highlighting the zone of interest or the wave arrival zone in the northern Adriatic Sea and from there the 400km distance to the zoning. To check that our clustering is correct, the QGIS nearest neighbour tool is used to confirm that the model is properly distributed.

The average observed distance is 0, the clustered events are close to each other, the nearest neighbour index is 0 as it is less than 1 meaning that there is a concentration in specific areas and finally the Z-Score -47.6350 this value is less than -2.56, therefore rejecting the randomness hypothesis.

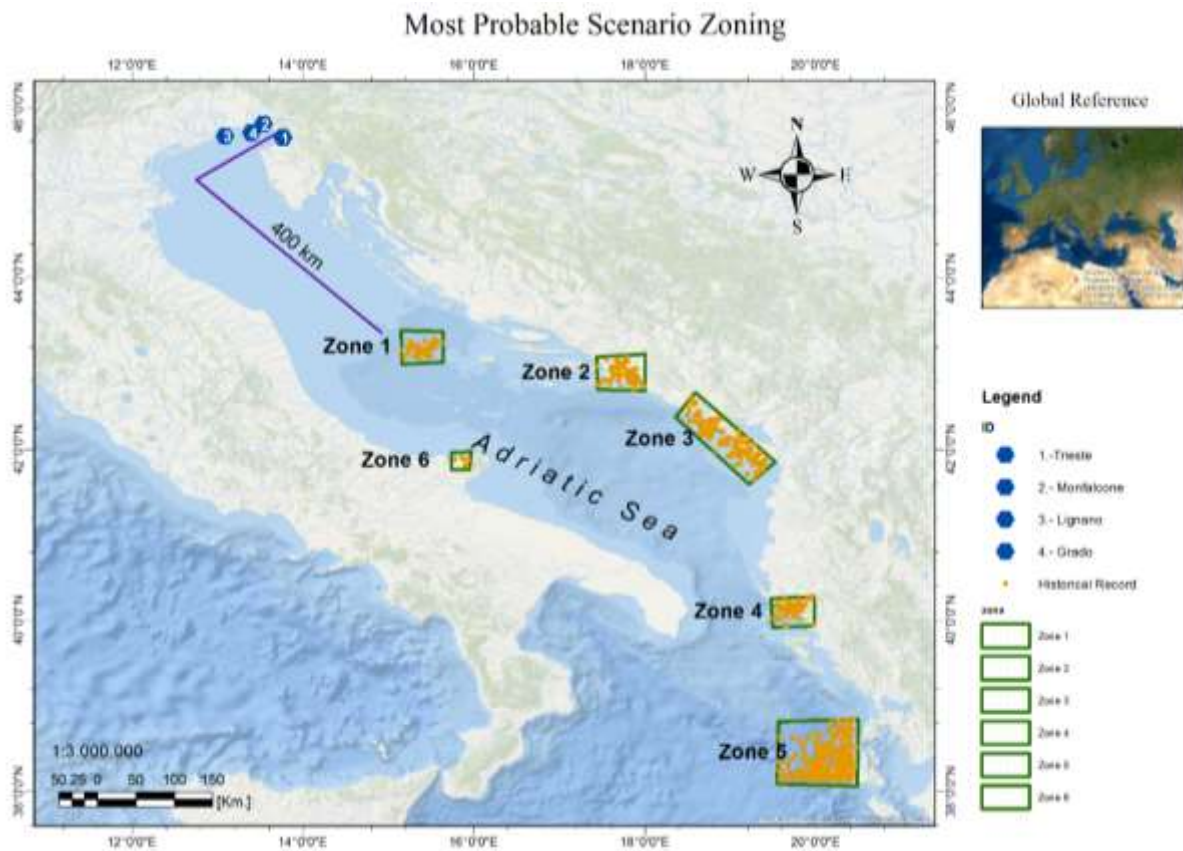


Figure 2.7: Probabilistic Zoning Map of the Adriatic Sea. (Author`s, 2020)

Table 2.3: Statistical results by zone. (Author`s, 2020)

Zone	Count	Unique	Min	Max	Range	Sum	Mean	Median	Stddev
Zone 1	46	12	4	5,5	1,5	201,1	4,37	4,2	0,396541
Zone 2	68	14	4	6	2	301,5	4,43	4,3	0,442124
Zone 3	140	21	4	6,9	2,9	642	4,58	4,5	0,520603
Zone 4	51	12	4	5,2	1,2	225,5	4,42	4,3	0,294601
Zone 5	309	18	4	6,4	2,4	1351	4,37	4,3	0,359663
Zone 6	6	6	4,3	6,3	2	29,4	4,9	4,6	0,690411

Carried out with the Quantum GIS statistical tool by category (QGIS)

The zoning comprises of 6 zones, Zone 1 comprises offshore Bosnia called Hvar Island with an average magnitude of 4.37, Zone 2 the city of Dubrovnik in Bosnia with 4.43 Mw, Zone 3 the country of Montenegro in Kotor with 4.58 Mw, Zone 4 and 5 Albania with 4.42 and 4.37 respectively and Zone 6 the city of Garganico in the region of Apulia with 4.9 Mw average being the highest of all the zones according to Table 2.3

2.2.1.2 Phase 2: Worst-Case Scenario

The zoning was developed by grouping geological structures to estimate the parameters of a tsunamigenic event of maximum possible magnitude by considering the characteristics of each of the faults in the domain to determine a potential future seismic event (Stirling et al., 1998). Establish the failure parameters as a generalised value for each focal point using the empirical relation of (Wells & Coppersmith, 1994) which relates the earthquake magnitude on the Richter scale to the length, width, and other fault rupture parameters. Empirical relationships (Wells & Coppersmith, 1994) was estimated from 421 earthquake records worldwide from different types of rupture sources such as shallow-focus (focal points above 40 km), displacement and continental interplate subduction compiled in their 1994 study.

Table 2.4: Regressions Empirics of Rupture Length, Rupture Width, Displacement.(Author's, 2020)

Equation	Number of Events	Coefficient		Standard Deviation	Correlation Coefficient	Magnitude Range	Length /Width Range (km)
		a	b				
$M = a + b * \log(L)$	77	5.08(0.10)	1.16(0.07)	0.28	0.89	5.2 to 8.1	1.3 to 432
$\log(L) = a + b * M$	77	3.22(0.27)	0.69(0.04)	0.22	0.89	5.2 to 8.1	1.3 to 432
$M = a + b * \log(W)$	167	4.38(0.06)	1.49(0.04)	0.26	0.94	4.8 to 8.1	1.1 to 350
$\log(W) = a + b * M$	167	2.44(0.11)	0.59(0.02)	0.16	0.94	4.8 to 8.2	1.1 to 350
$M = a + b * \log(D)$	80	6.69(0.04)	0.74(0.07)	0.4	0.78	5.2 to 8.1	0.01 to 14.6
$\log(D) = a + b * M$	80	5.46(0.51)	0.82(0.08)	0.42	0.78	5.2 to 8.1	0.01 to 14.6

L. - surface rupture length (km), W. -subsurface rupture width (km), D.-maximum displacement (m). Source: (Wells & Coppersmith, 1994).

The Adriatic Sea region is dominated by subduction faults between plates and strike-slip faults, so the empirical relationships will be applied in a globalised form of faults. Therefore, the empirical relationships used in this process relate all faults with a percentage of proximity varying between 0.89% and 0.94% compared to the results of historical records. The zonation by geologic structure was initially based on the historical records to establish the maximum event per region, thus estimating the geologic complex to which it belongs and establishing a predominant fault range for each region.

The Database of Individual Seismogenic Sources (DISS) which is provided in an interactive geo-spatial map that able the user to visualize and download the data of interest. Also, it provides information on different tectonic compositions; these have different numbers of faults and therefore in different zones there will be more information as shown in Figure 2.8.

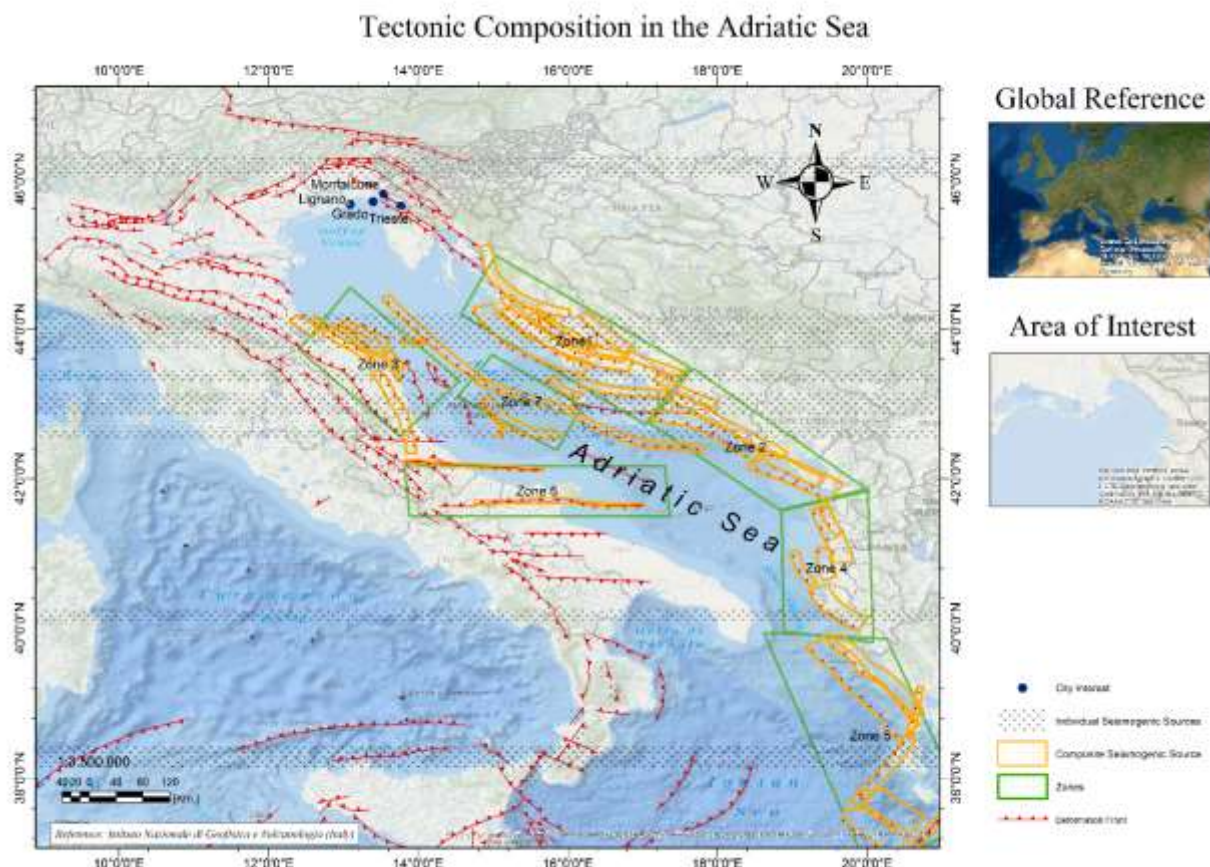


Figure 2.8: Tectonic Composition in the Adriatic Sea Zoning. (Author's, 2020)

The geological faults are described in DISS database by strike, rake, dip and displacement in a shapefile format. Moreover, the empirical source scaling relationship of W&C to estimate the rest of the parameters needed to characterize the tsunamigenic source model:

- Fault width
- Fault Length
- Fault vertical displacement

The values needed above are set by the behaviour trend in each established zone and projecting to a probable maximum event of magnitude between 7 to 7.5 Mw. The focal depth value was standardized due to the conditions of the entire Adriatic Sea which ranges from 5 to 12 km depth therefore, a standard value of 10 km was established. It is presented in Figure 2.9: Empirical correlations between magnitude with break length and break width. (Author`s, 2020) Figure 2.9 the ratio estimates for zone 1 - (Coastal-Croatia), the other study zones can be reviewed in Annexes B.

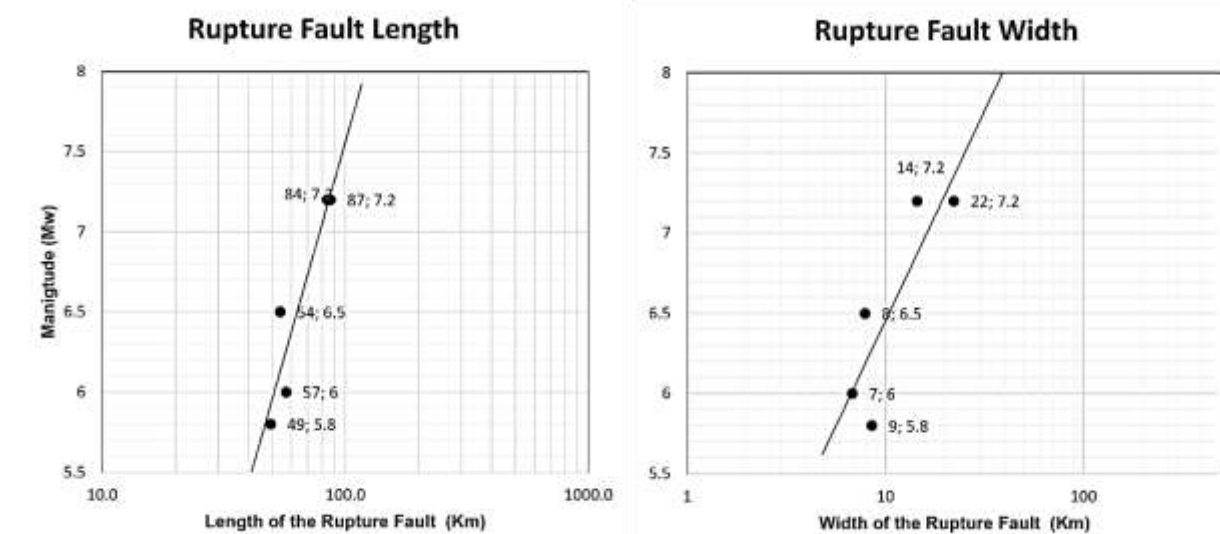


Figure 2.9: Empirical correlations between magnitude with break length and break width. (Author`s, 2020)

Table 2.5: Empirical Failure Parameters Per Established Zone. (Author`s, 2020)

Zones		Lon	Lat	L (Km)	W (Km)	D	Slip (m)	Strike (°)	Dip (°)	Rake (°)	Depth (Km)
zone 1	Coastal-Croatia	16.076	43.847	120	34	1	0.6	312	40	110	10
zone 2	Montenegro	18.425	42.426	75	50	2	2.5	312	35	82	10
zone 3	Albania-N	19.619	40.71	36.2	16	1	2	337	35	96	10
zone 4	Ancona	20.131	38.36	100	34	1	0.6	140	30	90	10
zone 5	Apulia	15.356	43.059	34	15	1	0.9	275	80	173	10
zone 6	Kefallonia-Lefkada	15.847	41.88	110	18	3	2	27	60	162	10
zone 7	Jabuka	13.061	43.863	22	19.6	2	2	269	42	70	10

Lon. - longitude, Lat.- latitude L. - rupture length (km), W. - rupture width (km), D.-maximum displacement (m).

2.3 Software Simulation

NAMIDANCE presents a very attractive and user-friendly graphical interface, with detailed sectioned windows for data entry, input display and visual rendering options.

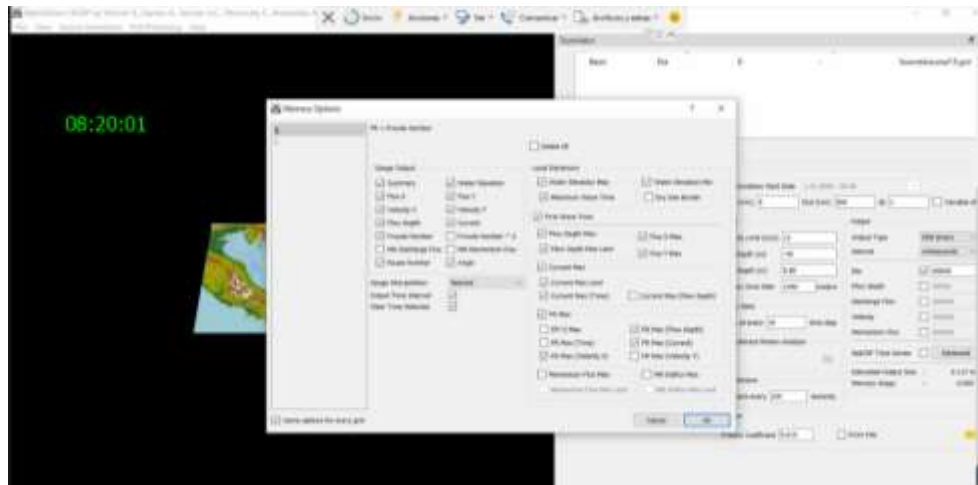


Figure 2.10: Main Data Input Screen of NAMIDANCE. (Author's, 2020)

Summary of the simulation setup parameters for each variable and parameter used in the simulation process of the 3 scenarios are described in Table 2.6

Table 2.6: Model Setup of Simulation Scenarios.(Author's, 2020)

Inputs	Variable	Description
Time	Start	0
	End	500 s
Gauges	Store every	10 s
	Autosave every	100 s
Friction	Friction Coefficient	0.015
Output	Output Type	GRD Binary
	Interval	milliseconds
Gauge Output	Flux x	m ³ /s/m
	Flux y	m ³ /s/m
	Velocity x	m/s
	Velocity y	m/s
	Flow Depth	m
	Current	m/s
	Time History	min

2.4 Zoning Validation

2.4.1 Zoning Feedback

Following discussions with the client on the zoning of the most probable scenario and the zoning of the maximum credible future scenario according to the conditions proposed at the start of the work, it was determined that the conditions were not sufficient due to the distance of the epicenter from the area of interest.

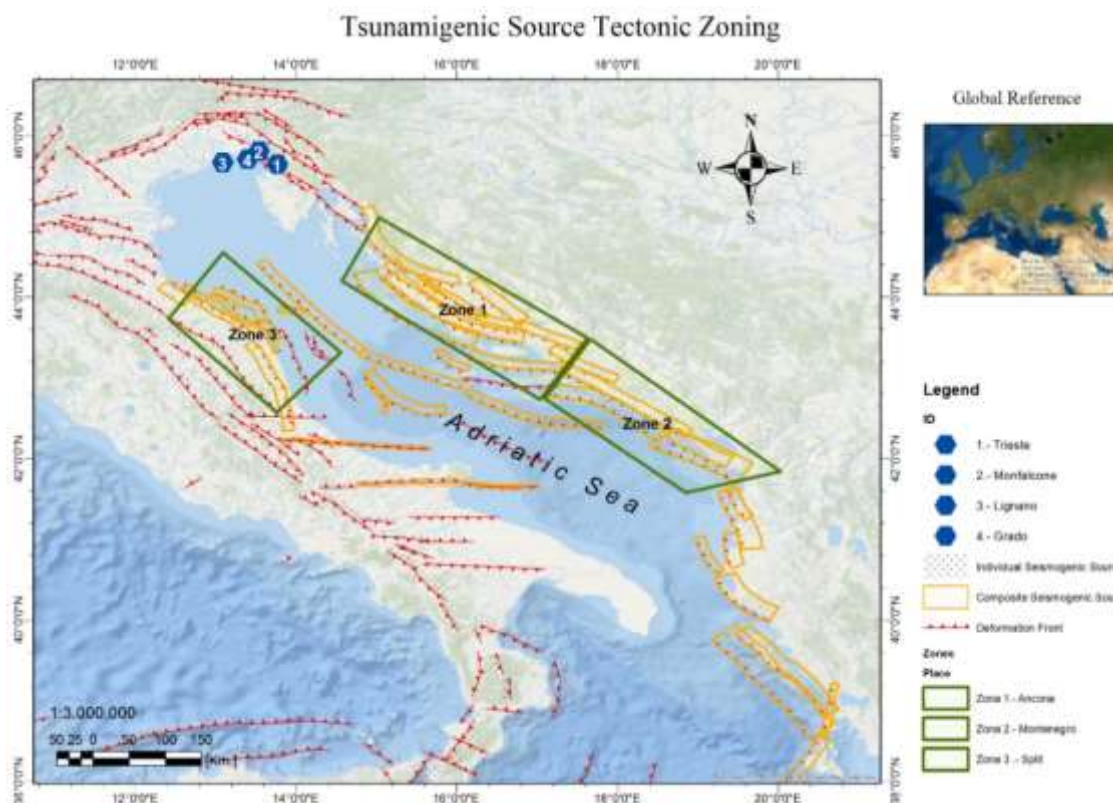


Figure 2.11: Tsunamigenic Source Tectonic Zoning. (Author's, 2020)

The zoning validated with the client was used to determine the failure parameters necessary for the creation of tsunamigenic scenarios, these were compared with the zonings previously performed for phase 1 and phase 2 of this work in addition to the research of (Tiberti, Basili, et al., 2008).

Table 2.7: Fault Parameters for Selected Zones.(Author`s, 2020)

	Zone	Lon (X) °E	Lat (Y) °N	Mag (Mw)	L (Km)	W (Km)	D (m)	Focal Depth (Km)	Strike (Km)	Dip (Km)	Rake (Km)
Zoning	Ancona	13.55	43.65	7.50	124	34	2.2	10	90	140	30
Literature Review				6.10	12	8	1	2.5	90	140	30
Zoning	Split	15.21	43.20	7.50	124	34	2.2	10	110	312	40
Literature Review				6.10	16	7	1	1.00	110	312	40
Zoning	Montenegro	18.10	42.30	7.50	124	34	2.2	10	82	312	35
Literature Review				7.20	50	20	1	1.00	82	312	35

In each seismogenic zone, a seismic source scenario was considered which is the maximum possible earthquake of 7.5 Mw as suggested by (Paulatto et al., 2007a), in total 3 scenarios were developed and used for tsunami hazard assessment.

CHAPTER 3

3 RESULTS AND DISCUSSION

Before the analysis of tsunami modelling results for the area of interest, it would be important to communicate different specifications on how hazard parameters can vary and under what conditions they change in their way toward the coast. Tsunami's physics are strictly related to the water depth where they move and therefore suffer constant alterations in their speed and direction of propagation, due to the characteristics of the seabed. Tsunami speed is directly proportional to water depth in which it moves, while its height is inversely proportional to water depth., This effect of deceleration and acceleration is evident in the energy transferred by the waves, which can be concentrated or deconcentrated, making the energy increase (CERC, 1984).

The proposed scenarios are structured with sources located between 200 to 800 km which are categorized as regional to basin-wide tsunamis, but due to the geographical formation of the development basin, the time of arrival to the coast obtained in the calibration process was around 250 min for the closest source (Ancona) and 440 min for the farthest source (Montenegro), categorizing it as a tsunami of distant characteristics which should exceed 3 hours of travel about 180 min.

In each model scenario, particular topographic characteristics are evidenced on the coastal edge, with essential relevance in two of the four cities of interest studied. These cities are Lignano and Grado, which are of great tourist importance for the province of Gorizia, according to the contrast of the topographic level in these cities that extend in their entirety along a coast whose average elevation is in the range of 1 to 2 meters. A different case of the remaining cities such as Monfalcone whose maximum bathymetric level is on average 5 meters and Trieste which is in a mountainous region, so it tends to increase topographic level rapidly from the coastal edge to 2 kilometres inland.

The simulations carried out were established with an equal time range for each scenario to establish more accurate and statistical comparisons.

3.1 Ancona – Italy

The maximum scenario proposed in Ancona eastern region of the Italian peninsula with dextral rifting geological characteristics allows estimating the maximum sea-level rise generated by a tsunami generated by an earthquake Mw. 7.5 and an epicentre with coordinates 43.65° N and 13.55° similar to the epicentre of the maximum historical record of the region with an earthquake magnitude of Mw 6. To 10.

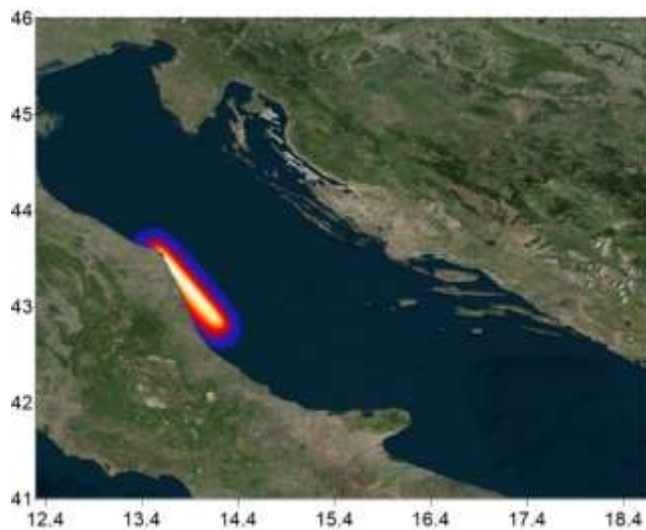


Figure 3.1: Seismic source of the Ancona scenario. (Author's, 2021)

Table 3.1 Different fault parameters for the Ancona area according to their magnitude.(Author's, 2020)

Zone	ANCONA (Northern Apennines)		(Tiberti, 2008)
Mw	7.50	7.00	6.10
L	124	57	12
W	34	20	8
DISPL MAX (m)	2.2	1.5	
FOCAL DEPTH	10	10	2.5
SLIP-RAKE	90	90	90
STRIKE	140	140	140
DIP-DELTA	30	30	30

3.1.1 Wave Amplitudes (Water Height)

The maximum wave height map for the area of interest because of Ancona scenario is $0.38 \pm \text{MSL}$ m. The max computed wave height near the shoreline of Lignano and Grado being the highest in their upper limit of 0.38 m and 0.29 m $\pm \text{MSL}$, respectively (Figure 3.2).

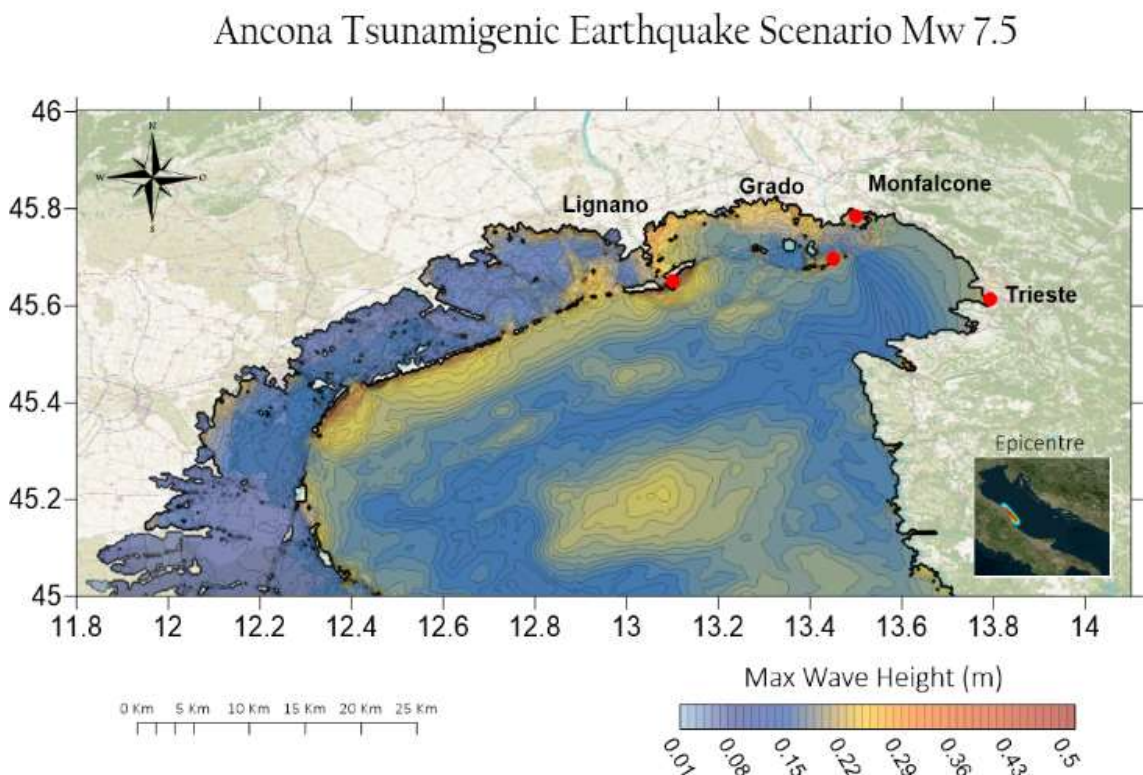


Figure 3.2 Maximum coastal amplitude in the middle domain. (Author's, 2021)

Tsunami wave height due to Ancona scenario in the northern Adriatic Sea (Figure 3.3) was shown where the maximum amplitude at 40 kilometres out to sea on the coast of the Ravenna region and which shows a radius of 20 km where values of 0.30m and then decrease as it approaches the coast, influenced by the bottom conditions or the focusing effects dedicated due to the traits of the location of the source and the propagation path.

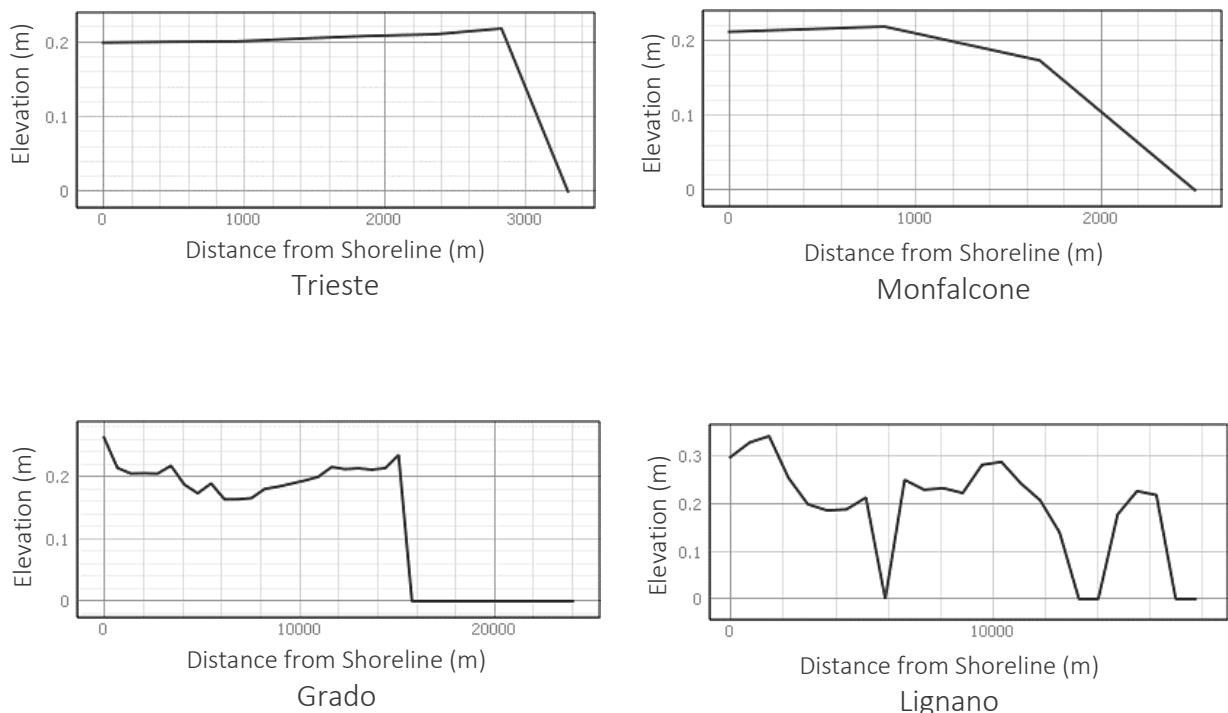


Figure 3.3: The 2D profiles of maximum tsunami amplitude from the coastline to the perpendicular flooded to urban zone. (Author's, 2020).

The behaviour at coastline varies in each of the cities of interest and the highest wave height values occur at the coastline in Lignano and Grado extending for 10 to 20 kilometres in each, as opposed to Trieste and Monfalcone with landfall values of 0.22 m maximum extending for 2 to 3 kilometres.

These values vary depending on the state of sea level conditions, since in many areas of the study areas the sea level is below sea level and a minimum alteration in these conditions is reflected in various affectations, as in the case of Lignano and Grado, coastal towns below sea level.

3.1.2 Runup

Runup is defined as elevation reached by seawater measured relative to some stated datum such as mean sea level, mean low water, sea level at the time of the tsunami attack, etc., and measured ideally at a point that is a local maximum of the horizontal inundation. A Runup of 0.3 m in was obtained for Grado (Figure 3.4), owing to this location has no protection or breakwater either offshore or inland. The estimated runup value for Trieste and Monfalcone is 0.1 m (Figure 3.4).

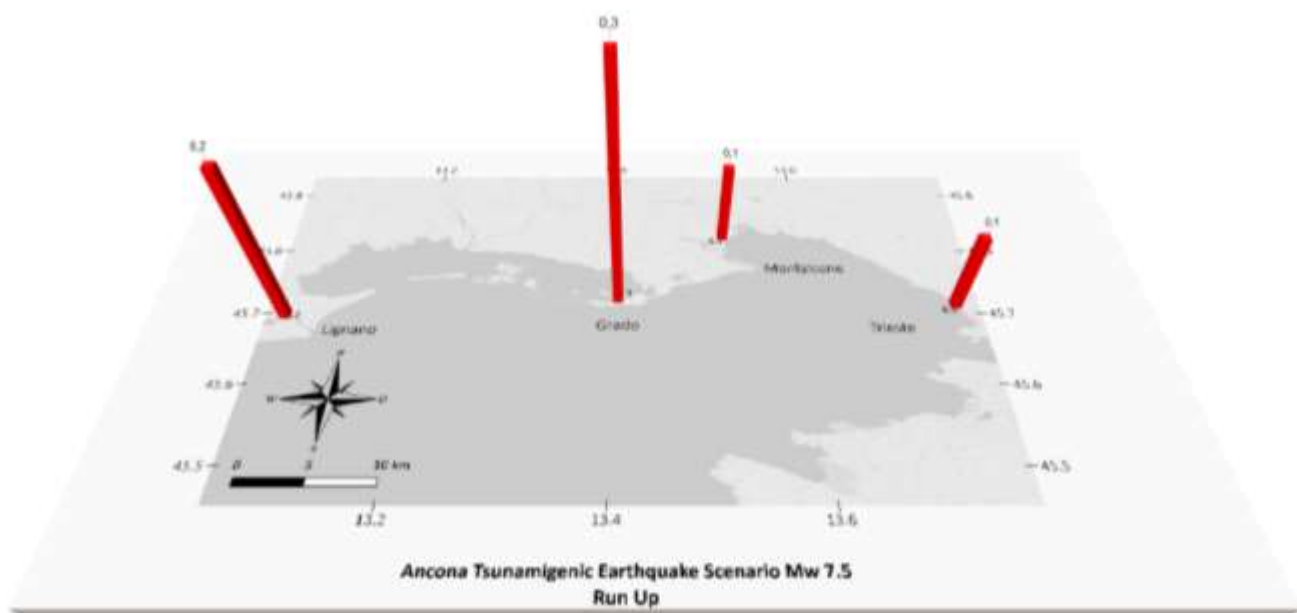


Figure 3.4: Runup at the selected sites. (Author's, 2021)

3.1.3 Tsunami Wave Velocity

The tsunami velocity is mainly managed by the change in water depth as explained previously. It plays important role in the damage caused by a tsunami since the damage and destruction generally happen due to wave impact, erosion and inundation. The maximum tsunami wave velocity vector for the area of interest due to the Ancona scenario is shown in Figure 3.5. The velocity values in the cities of interest range from 0.6 m/s to 2.4 m/s, different from the behaviour in the inner part of the Adriatic Sea, where the propagation velocity did not exceed 0.5 m/s

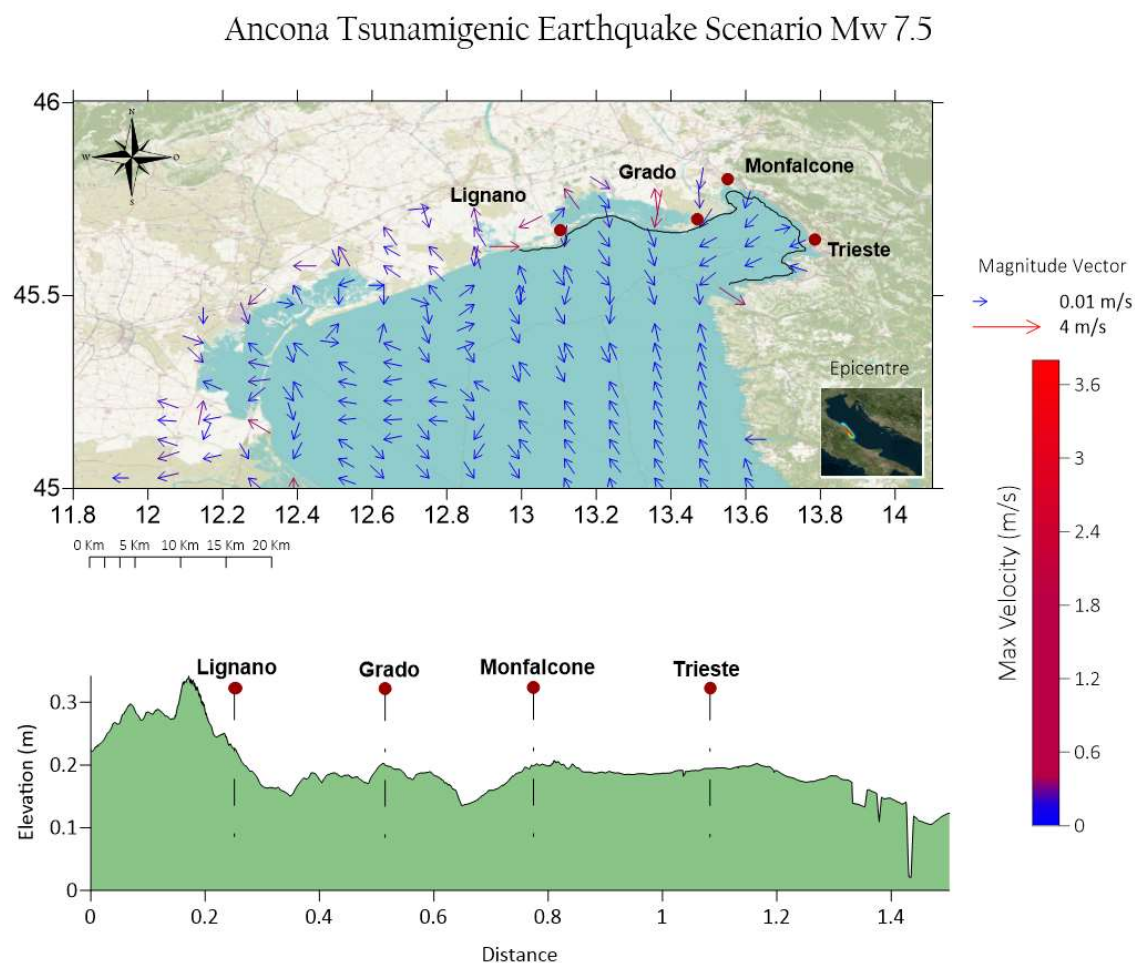
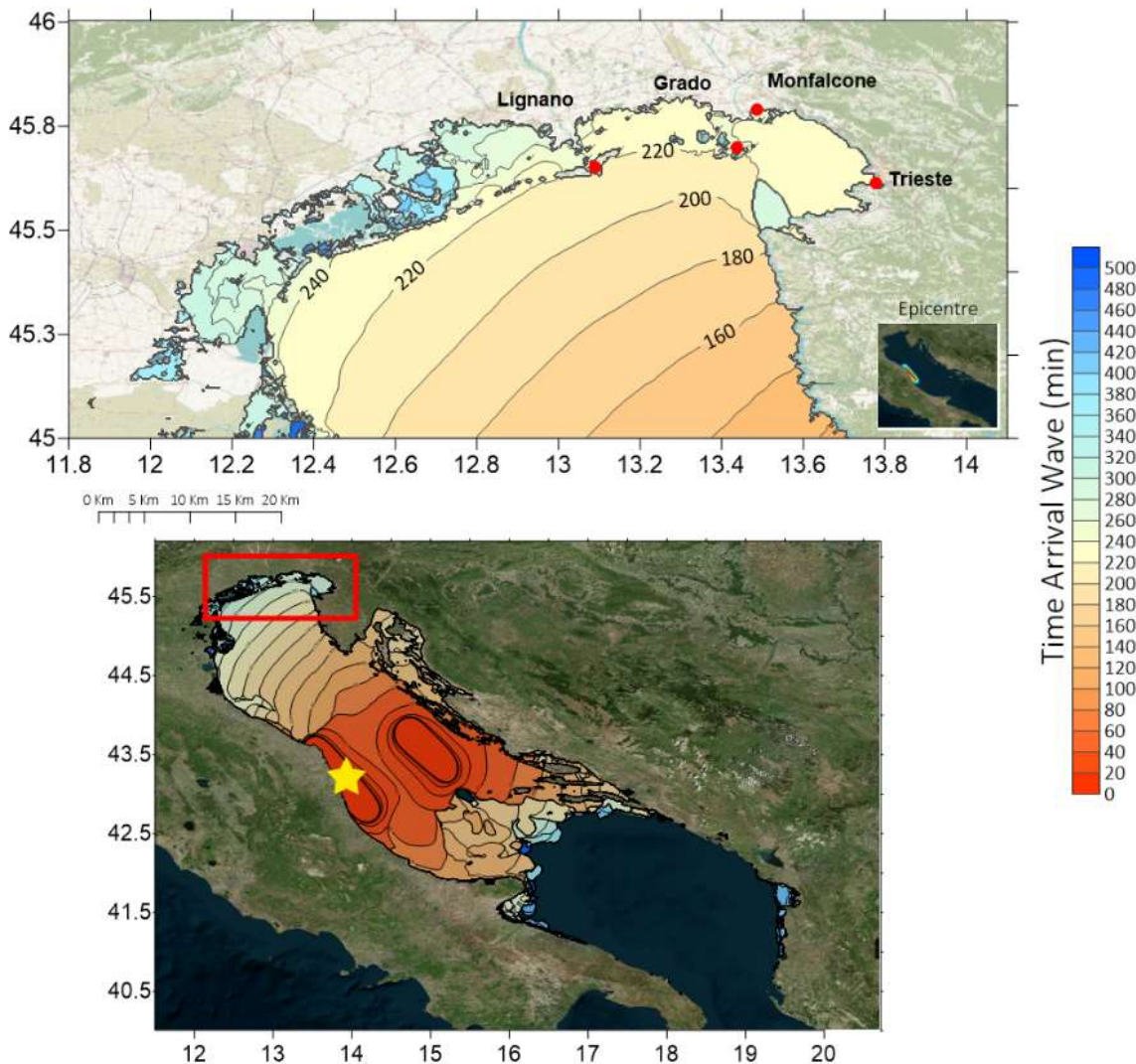


Figure 3.5 Maximum instantaneous tsunami wave speed in the medium study domain.(Author's, 2020)

3.1.4 Arrival Time of First Wave

Ancona Tsunamigenic Earthquake Scenario Mw 7.5



**Figure 3.6: Tsunami travel time in minutes for the Ancona scenario.
(Author's, 2020)**

In the cities of interest, the arrival time of the first wave varies from one location to another. The first tsunami wave to reach the coastal of Lignano and Grado is about 220 minutes from the earthquake's origin time. Whereas, in Trieste and Monfalcone, which are located at the far east end of the Adriatic, i.e., the Gulf of Trieste, the travel time is slightly longer than 240 minutes (Figure 3.6). The slow propagation or long travel time of tsunami waves in north Adriatic is attributed to the shallow bathymetry effect that lowers the speed without considerable dissipation of energy.

3.2 Split – Croatia

The Split scenario is characterized by a geological zone dominated by typical thrust or slip faults. The epicentre takes as reference under the coordinates of the maximum event recorded at 15.21° E, 43.65° N with a magnitude of Mw 6.20, which is our focal site of reference for our Mw 7.5 earthquake proposed for this zone (Figure 3.7).

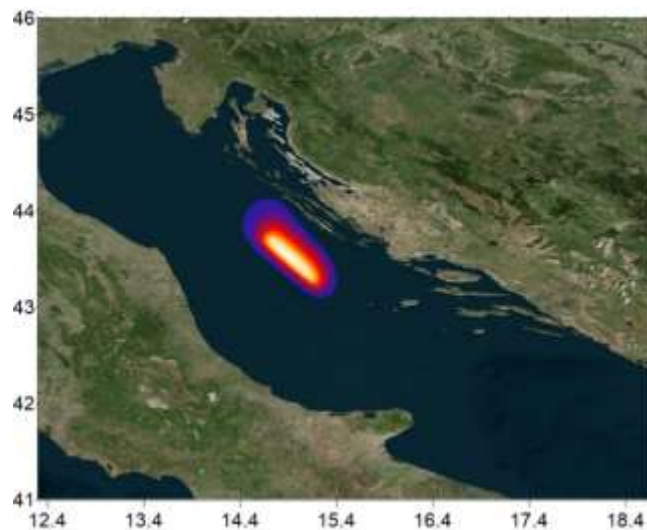


Figure 3.7 Seismic source of the Split Scenario. (Author`s, 2021)

Table 3.2 Different fault parameters for the Split area according to their magnitude. (Author`s, 2020)

Zone	SPLIT (Coastal Croatia)		(Tiberti, 2008)
Mw	7.50	7.00	6.10
L	124	57	16
W	34	20	7
FOCAL DEPTH	10		1.00
SLIP-RAKE	110	110	110
STRIKE	312	312	312
DIP-DELTA	40	40	40

3.2.1 Wave Amplitudes (Water Height)

The sea-level rise resulting from the simulation of the Split scenario on the Croatian coast shows a dissipative effect of the energy due to the geographical location of the source. To the north of this location is the Istrian peninsula in the Croatian jurisdiction, which performs a dissipative function of the wave height impact on the cities of Grado, Monfalcone and Trieste, unlike Lignano which is located further east close to Venice and therefore is not protected and is impacted by sea level rises of 0.25 m which are considerable in comparison to the other sites in the northern Adriatic Sea. The inner part of the Gulf of Trieste receives wave amplitude between 0.08 m almost imperceptible if local conditions at the coastal edge of the tide are considered. In the Monfalcone despite the slight intensity and low sea level height estimated between 0.08 m suffered minor flooding on small plots of land.

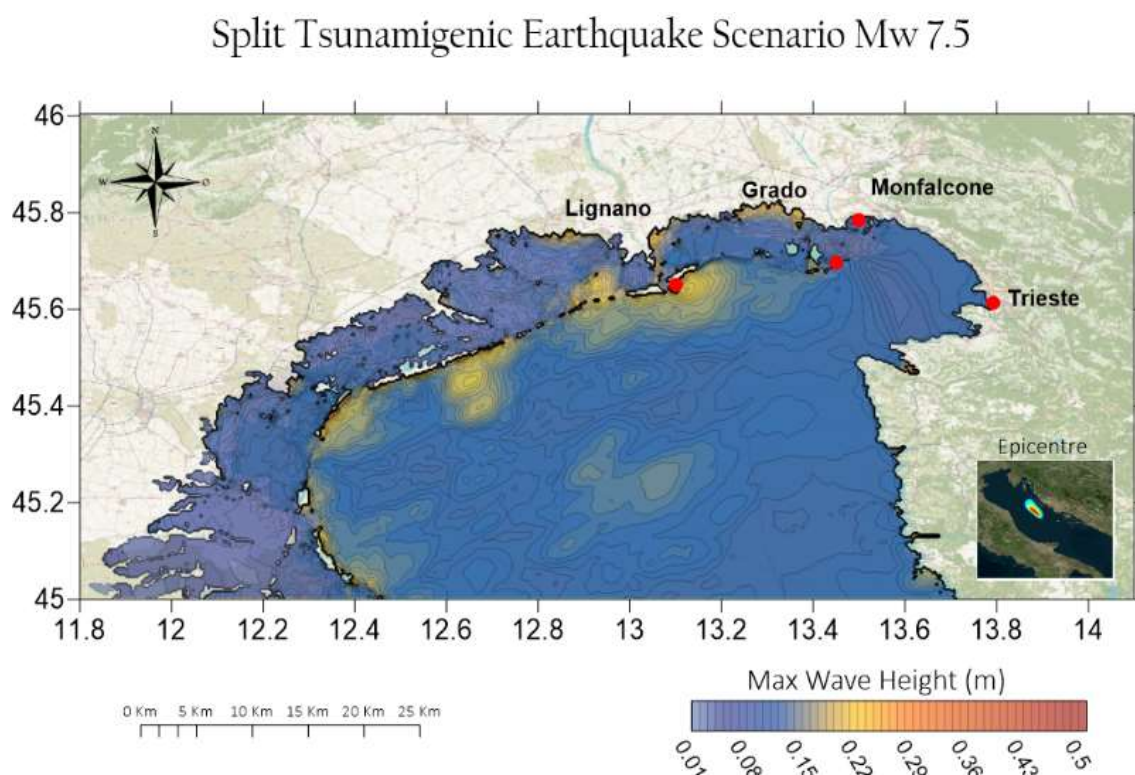


Figure 3.8: Maximum coastal amplitude in the middle domain. (Author's, 2021)

The cities of Lignano and Grado are the most affected in this scenario because the sea level rise level is 0.30 m to 0.22 m respectively, with large tracts of land inundated due to topographic conditions, as this area extends at -0.5 below sea level. Therefore, tsunami inundation is almost inevitable. The onshore inundation behaviour in each city shows a low elevation trend. In the city of Trieste, the value of sea-level rise does not exceed more than 0.10 m at a 2 km inundation on land in areas such as the harbour, almost similar in the city of Monfalcone. The Lignano urban runup extends 10.5 km away on land with a representative level of 0.2 m which behaves with significant variations due to the presence of elevated land, different case in Grado in which the runup was 10 km and did not exceed 0.15 m of which in the hinterland there is land below sea level so that the flooding values increased in the hinterland.

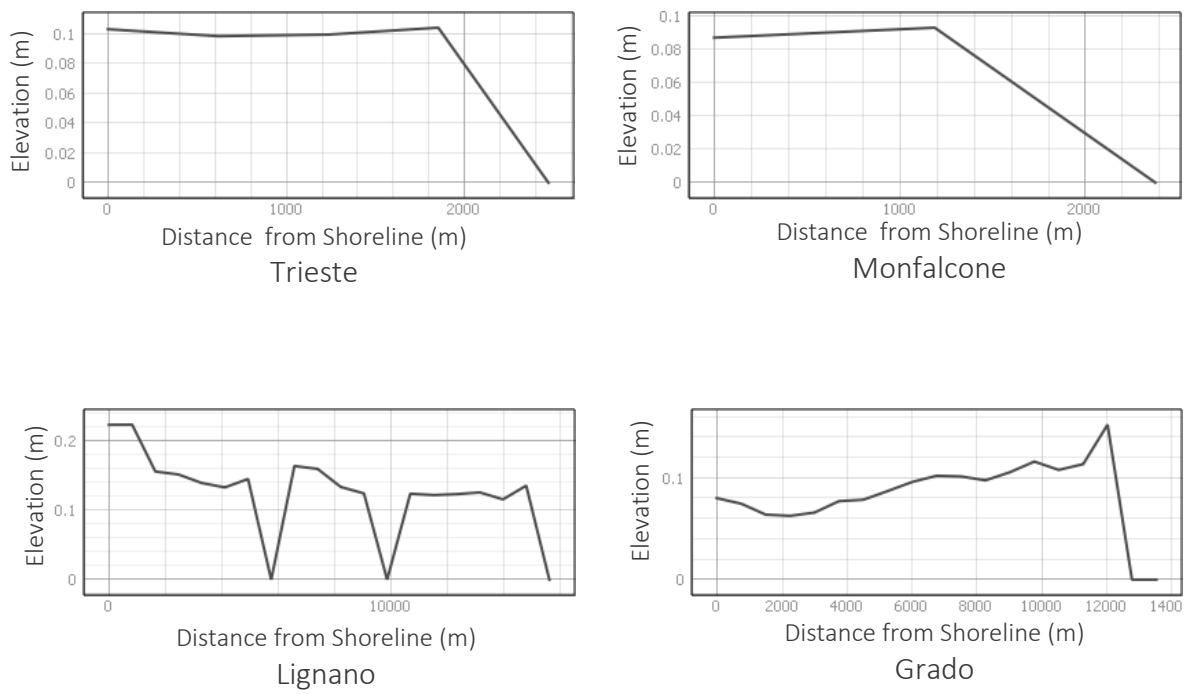


Figure 3.9: The 2D profiles of the maximum tsunami amplitude, perpendicular trace from the coastline to the flooded urban area. (Author's, 2020)

3.2.2 Runup

Due to the irregularity of the bottom that grows upon reaching the coasts of Croatia and having the same conditions in its bathymetry up to the area of interest the Run-up values are like the Ancona scenario (3.1.2), so the elevation from sea level to the arrival at the coast of 0.3 m is still predominant. Followed by Lignano of 0.2 m, Monfalcone and Trieste with the minimum value of 0.1m according to Figure 3.10.

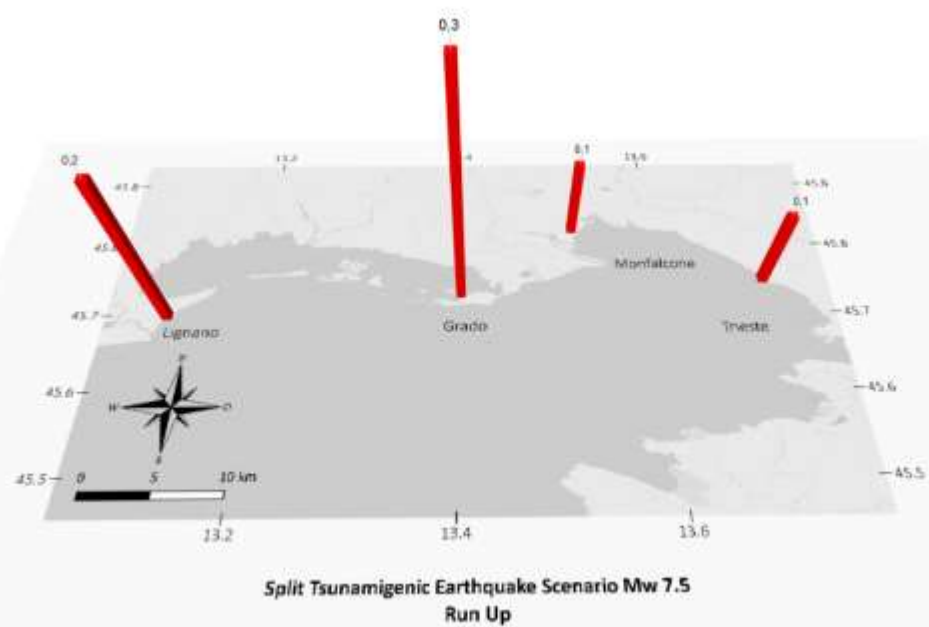


Figure 3.10: Runup at the selected sites. (Author's, 2020)

3.2.3 Tsunami Wave Velocity

The values of maximum instantaneous velocity recorded along the domain grid allow us to visualize values of maximum magnitude ranging from 1.2 m/s to 1.8 m/s with particularity in the coastal edge much more evident in the lagoon of Grado and on the coast of Lignano, originated by the conservation of the variation in the topographic level after overcoming the coastline. The velocity value is consistent in the points of greater intensity with the elevation of the sea level at that point which is higher than the other study localities.

Split Tsnamigenic Earthquake Scenario Mw 7.5

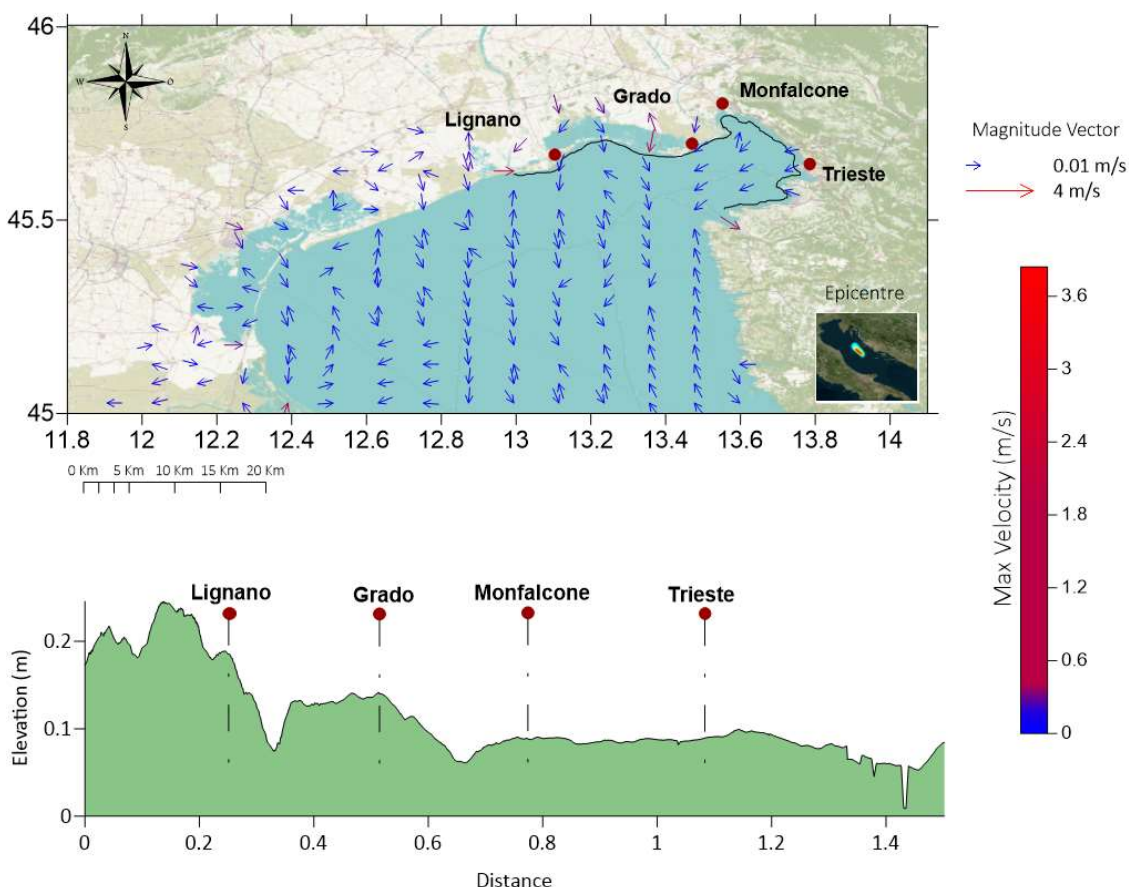
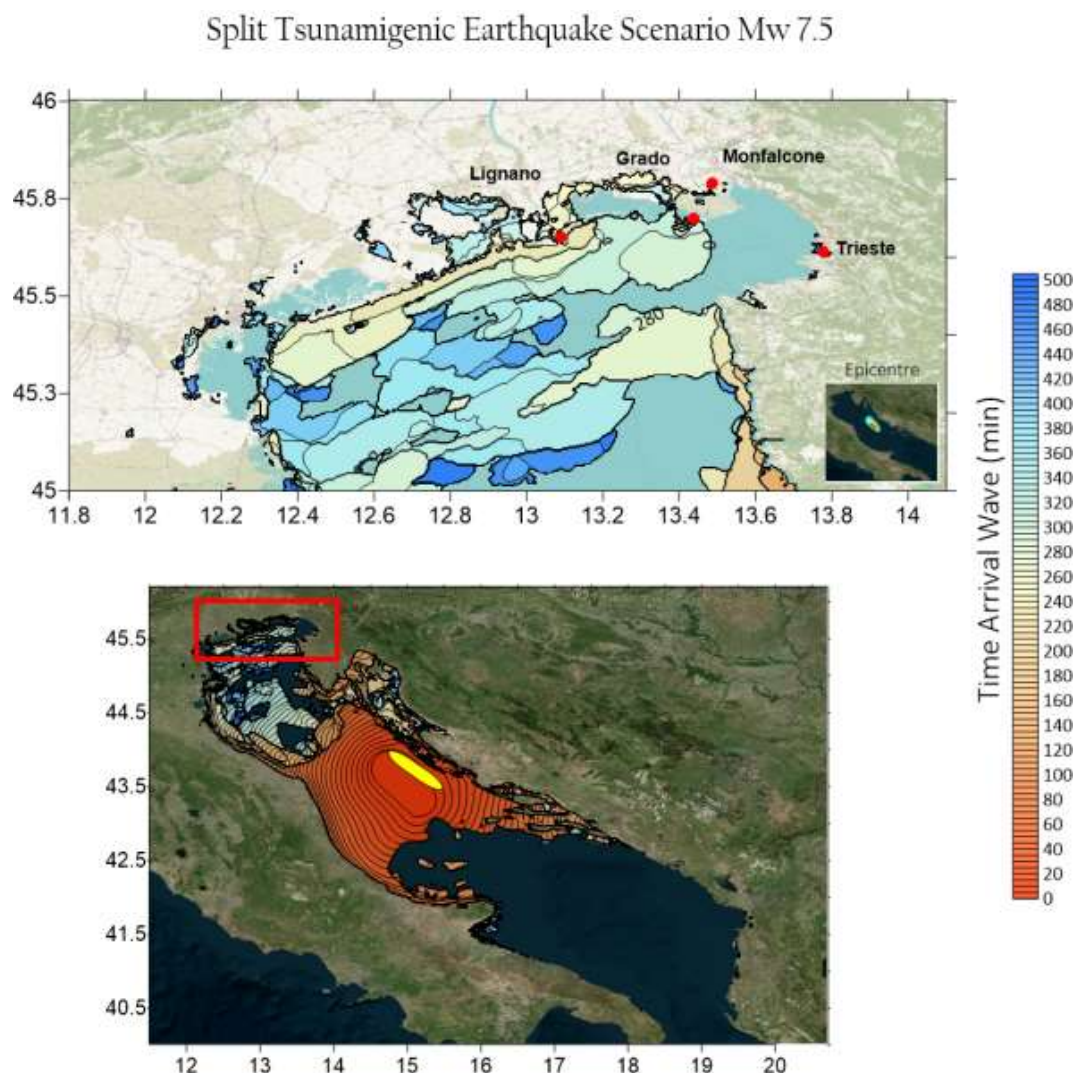


Figure 3.11: Maximum instantaneous tsunami wave speed in the medium study domain.
(Author's, 2020)

In the cities of Monfalcone and Trieste, as well as in the entire northern basin of the Adriatic Sea, it presents low values of approximately 0.12 to 0.15 m/s, the records agree with the literature where the velocity is almost invariable inland and is only affected as it approaches the coast.

3.2.4 Arrival Time of First Wave

The tsunami propagation map for the time allowed to identify the behaviour of the wave, for the Split source there were particularities related to the location of the source. The epicentre generated on the Croatian coasts presents a variable tsunami propagation form due to the resonance effect, which is induced by the shock of the wave on the coast in front of the site of origin, causing a rebound effect on the coast of the central part of the Adriatic Sea basin.



**Figure 3.12: Tsunami travel time in minutes for the Split scenario.
(Author's, 2020)**

The propagation of the wave is highly influenced by the geography for such reason the values of time of arrival are representative 420 to 450 min of this in localities close to the frontal path of a tsunami as Venice, Lignano Ancona.

3.3 Offshore Montenegro

The main scenario occurred on April 16th 1979, of Mw 7.1 of the shallow fault (7-10km) with a direction of 14° which is parallel to the coastline with the dipping fault, the location of the mainshock is 42.04°N and 19.21°E between the cities of Bar and Ulcinj with a release moment of 4.38e19 Nm, with these characteristics was determined the scenario of Montenegro near the city of Budva where the aftershock of the main earthquake was recorded according to records of Mw 6.20 (Benetatos & Kiratzi, 2006).

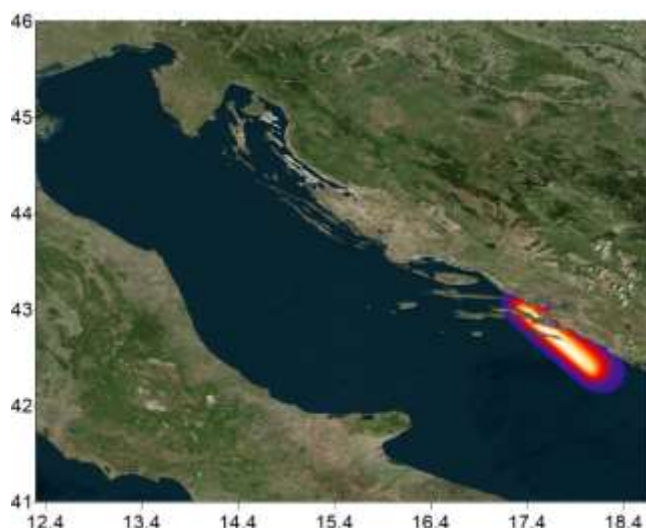


Figure 3.13: Seismic source of the Montenegro Scenario. (Author's, 2020)

Table 3.3: Different fault parameters for the Montenegro area according to their magnitude, (Author's, 2020)

Zone	Montenegro	(Tiberti, 2008)
Mw	7.50	7.00
L	124	57
W	34	20
FOCAL DEPTH	10	10
SLIP-RAKE	82	82
STRIKE	312	312
DIP-DELTA	35	35

3.3.1 Wave Amplitudes (Water Height)

Montenegro Tsunamigenic Earthquake Scenario Mw 7.5

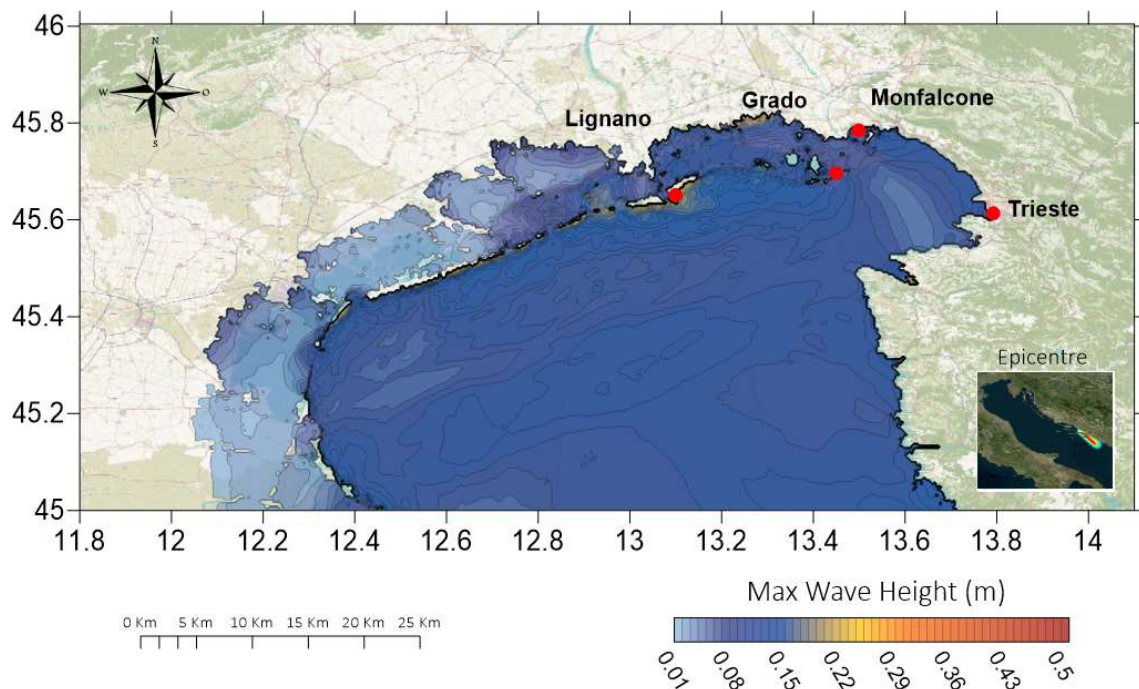


Figure 3.14: Maximum coastal amplitude in the middle domain. (Author's, 2021)

All the coasts of the province of Venice from the city of Chioggia the maximum amplitude were recorded between 0.08 to 0.15 m (medium to dark blue colours) in the whole extension of the beach width up to the urban area, in the case of Lignano and Grado between 0.22 to 0.29m presenting the highest values in the area of interest, all the islands parallel to both cities reach an amplitude of 0.15m remaining kind of a small lake between these localities until reaching the entrance of the basin of Fiume Corno to Fiume Ausa the estimated value 0.25 m approximately.

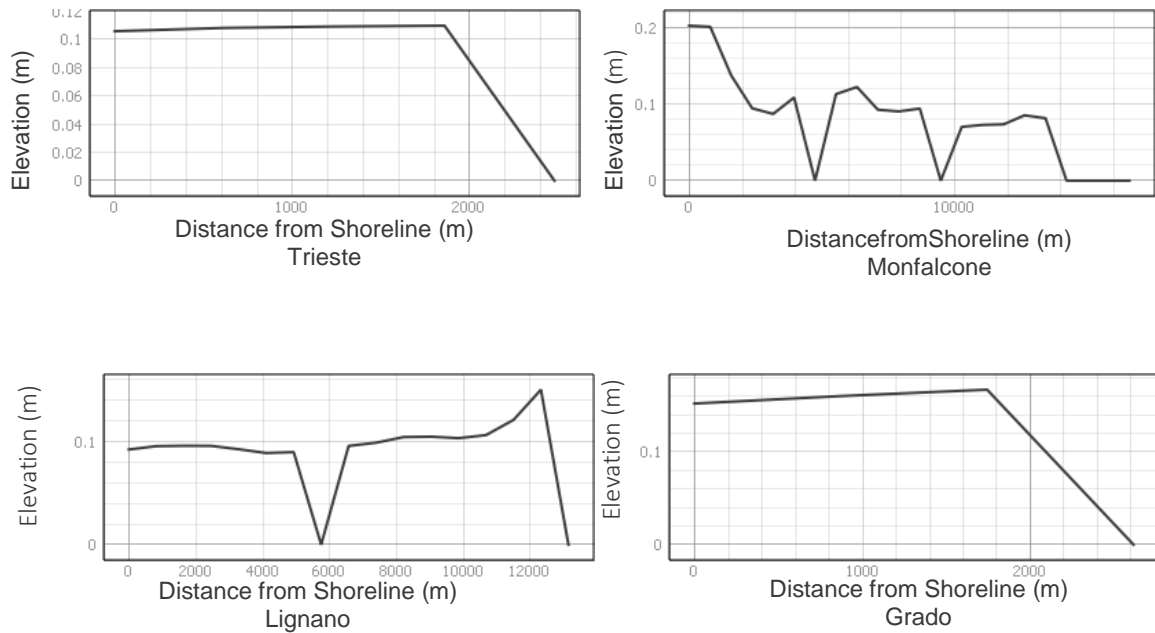


Figure 3.15: The 2d profiles of maximum tsunami amplitude from the coastline to the perpendicular flooded to urban zone. (Author's, 2020)

The elevations predominate 0.1m in the localities of Lignano and Trieste, its behaviour from the coastline to 1000m inland is constant until reaching the top and a decline occurs until reaching 0m.

The effects on sea level on the coasts of each of the cities are little affected due to the remoteness of the focal epicenter of the tsunami, considering its direct exposure Lignano and Grado with elevation 0.20m average are the maximum expression of affectation but its dissipation is very fast so it tends to decrease to 0.10m or 0m.

In the cities of Trieste and Monfalcone are more affected by resonance effect due to their geographical location, the superposition of sea waves make their sea level equal to the Lignano and Grado with the difference of their constant with respect to time because always fed by diffracting waves increasing their period of propagation.

3.3.2 Runup

The height is propagating with greater amplitude to the NW of the Adriatic Sea for its passage of South Adriatic Pit gets the highest amplitude value 0.3 m in Lignano, then dissipates again rising a threshold of 170 m propagating to the NE, decreasing to reach its Grado and Monfalcone of 0.2 m (Figure 3.16).

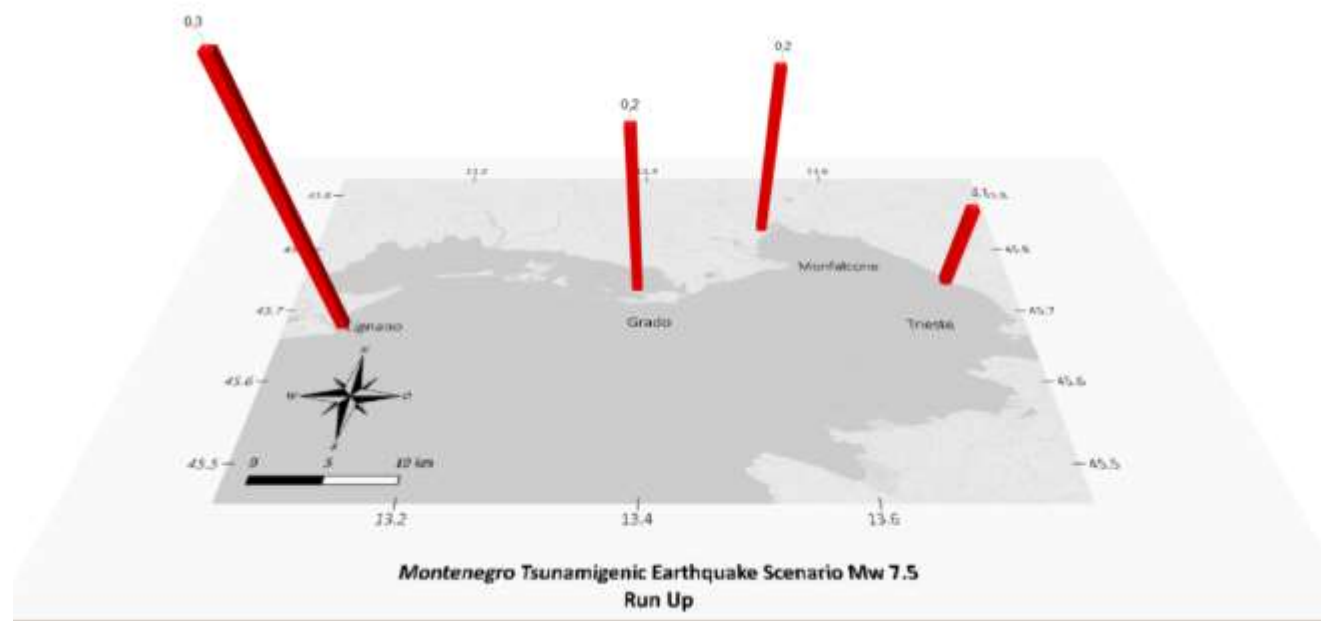


Figure 3.16: Runup at the selected sites. (Author's, 2020)

3.3.3 Tsunami Wave Velocity

The surface velocities presented in Figure 3.17 from Montenegro to Savudrija in Croatia travel parallel to the coast, then change direction drastically towards Monfalcone and Trieste with a velocity of 0.05 m/s.

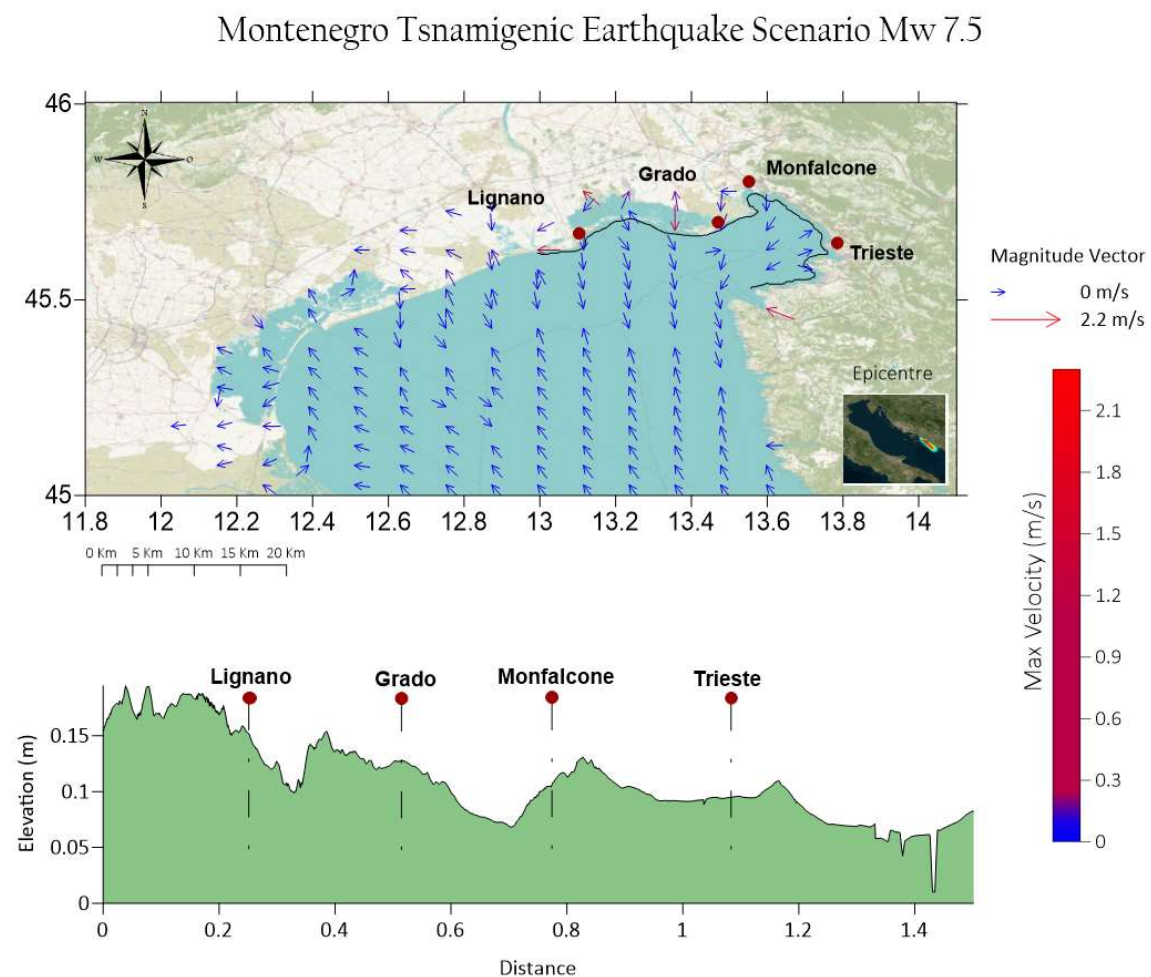


Figure 3.17: Maximum instantaneous tsunami wave speed in the medium study domain.
(Author's, 2020)

Due to the "North Winds" or "Bora Winds" travelling from NE from Trieste to Albania reaching 25 to 30 m/s affects the direction of the velocities caused by the earthquake abruptly changing its direction to the West and increasing Lignano and Grado to 0.15 m/s.

3.3.4 Arrival Time of First Wave

Waves begin to be observed in the last 100 minutes of the simulation due to the location of the epicenter and the bathymetric conditions mentioned in the run-up parameters at 3.3.2 section.

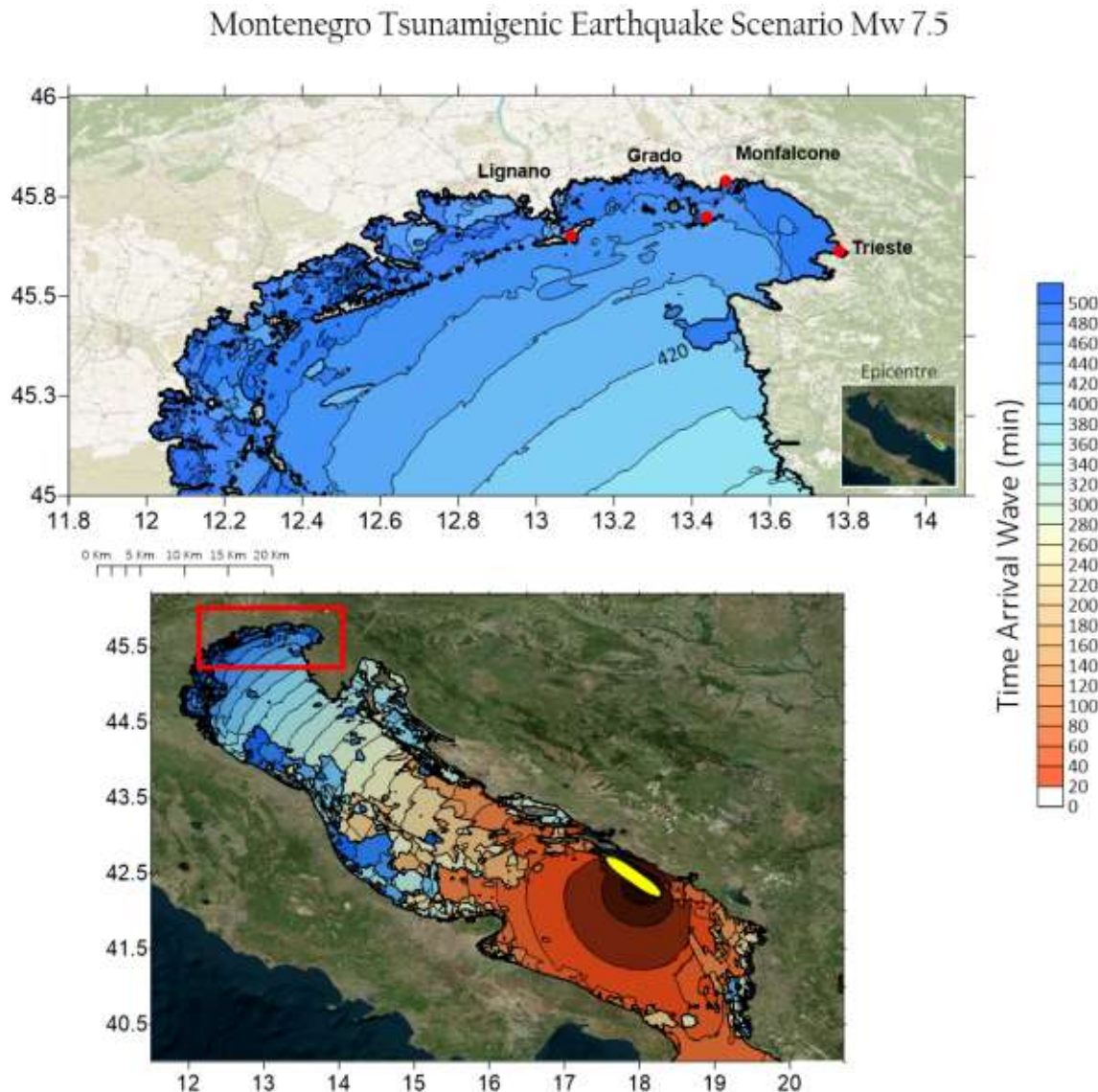


Figure 3.18: Tsunami travel time in minutes for the Montenegro scenario. (Author's, 2020)

The irregularities of the bottom and the friction it causes decreases the propagation energy and increases the travel time of the wave causing the first wave at Trieste of 400, the last minutes 420,440 500 min the cities of Lignano, Grado and finally Monfalcone respectively.

3.4 Time series histories in the zone of interest

According to the area of interest chosen due to its relevant effect on its coasts, the results of maximum amplitude as a function of time were presented according to the record of their respective meters. After the analysis of all the scenarios studied, Split shore Croatia was chosen because it reported important changes in its height from the 200th minute.

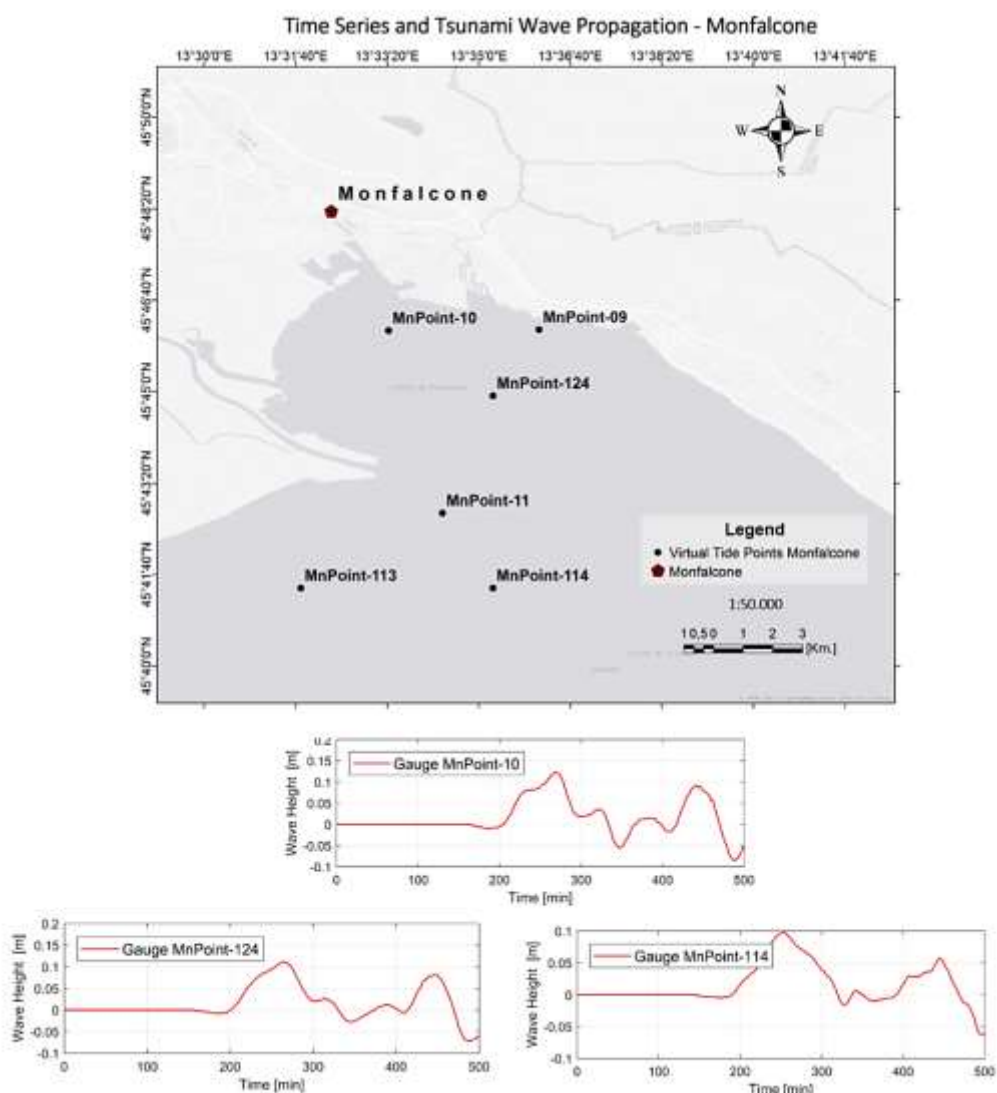


Figure 3.19: Maximum amplitude with respect to the transfer time according to the generated Monfalcone gauges. (Author's, 2020)

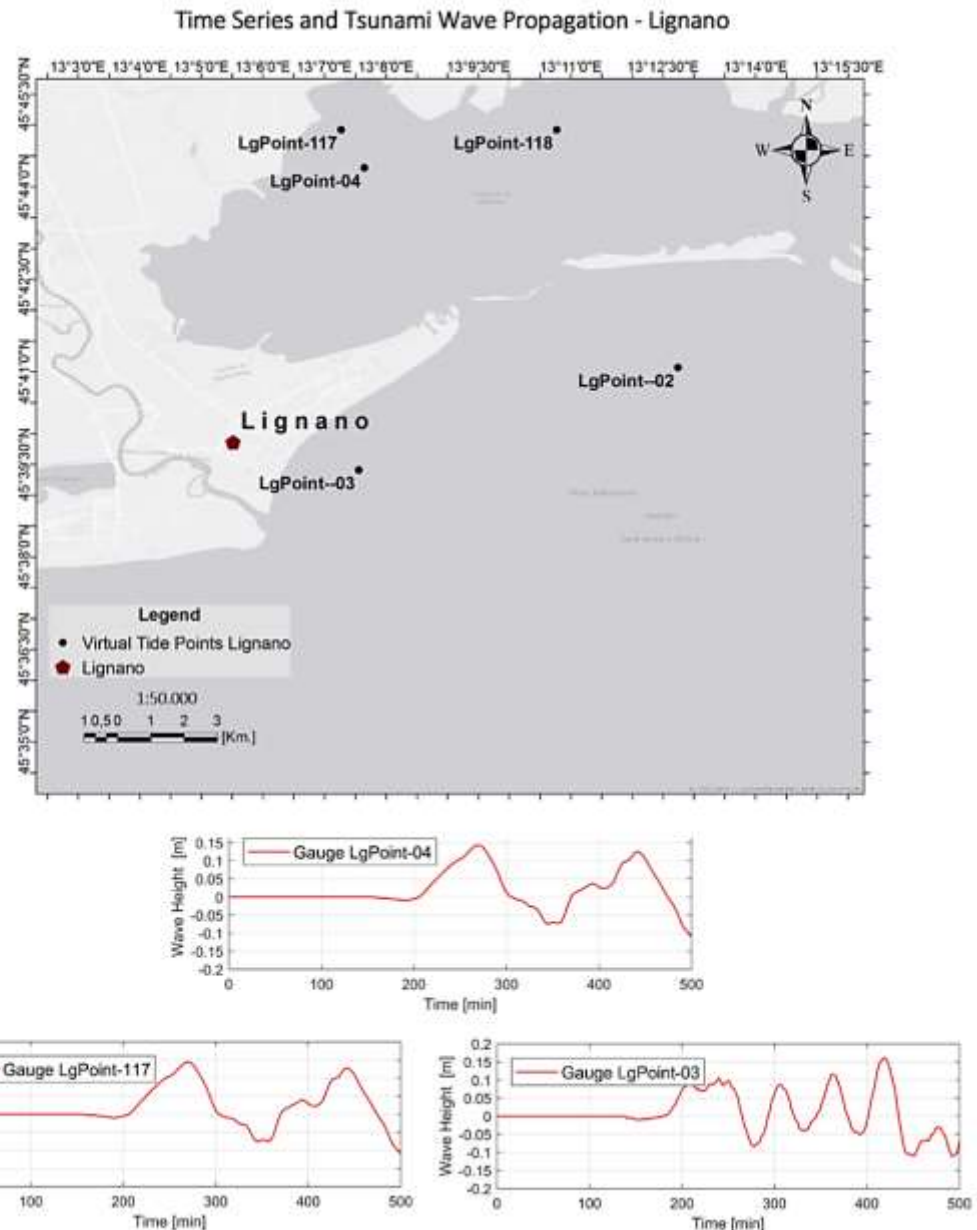


Figure 3.20: Maximum amplitude for the transfer time according to the generated Lignano gauges. (Author's, 2020)

Time Series and Tsunami Wave Propagation - Grado Coastal

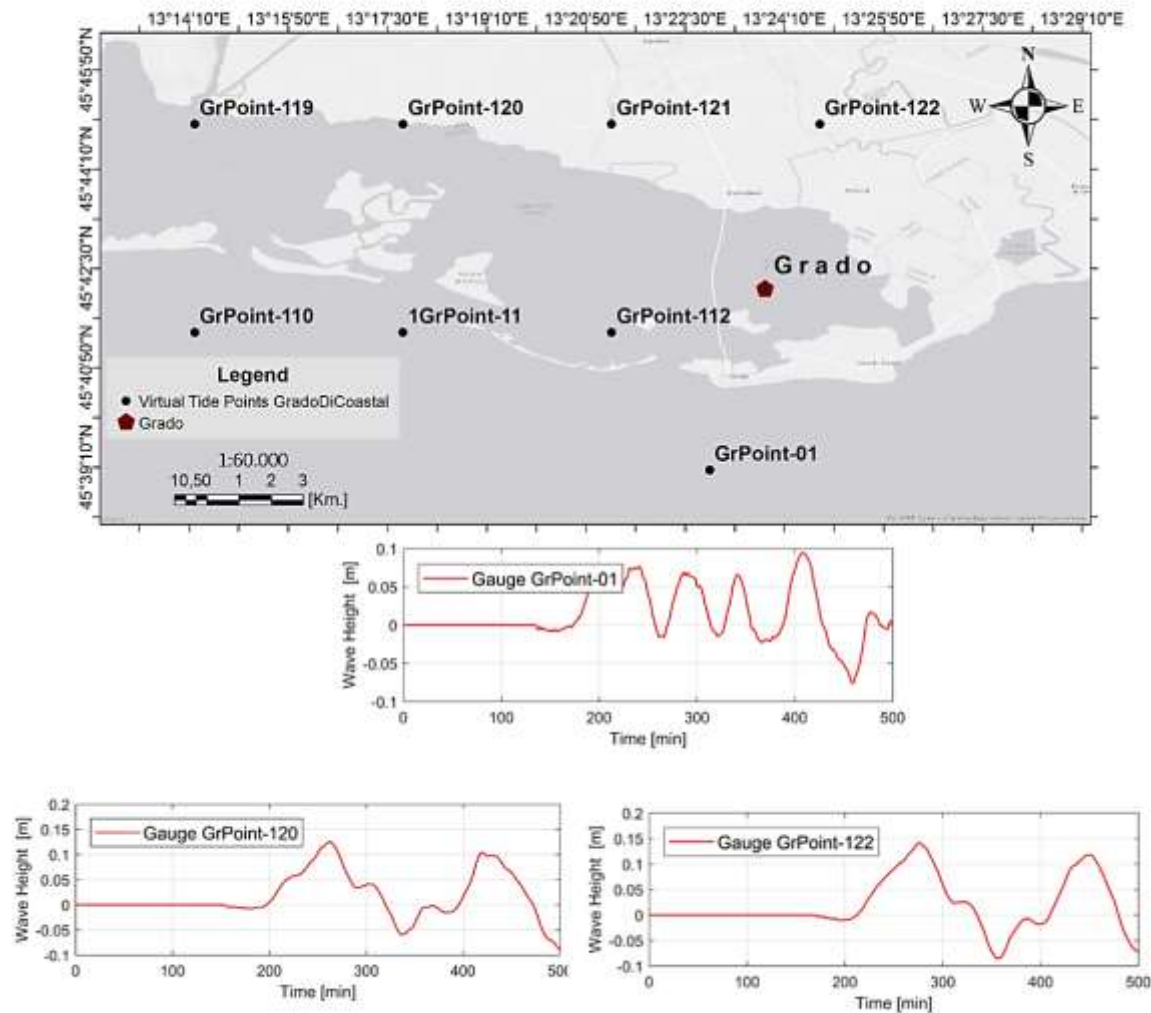


Figure 3.21: Maximum amplitude for the transfer time according to the generated Grado gauges. (Author's, 2020)

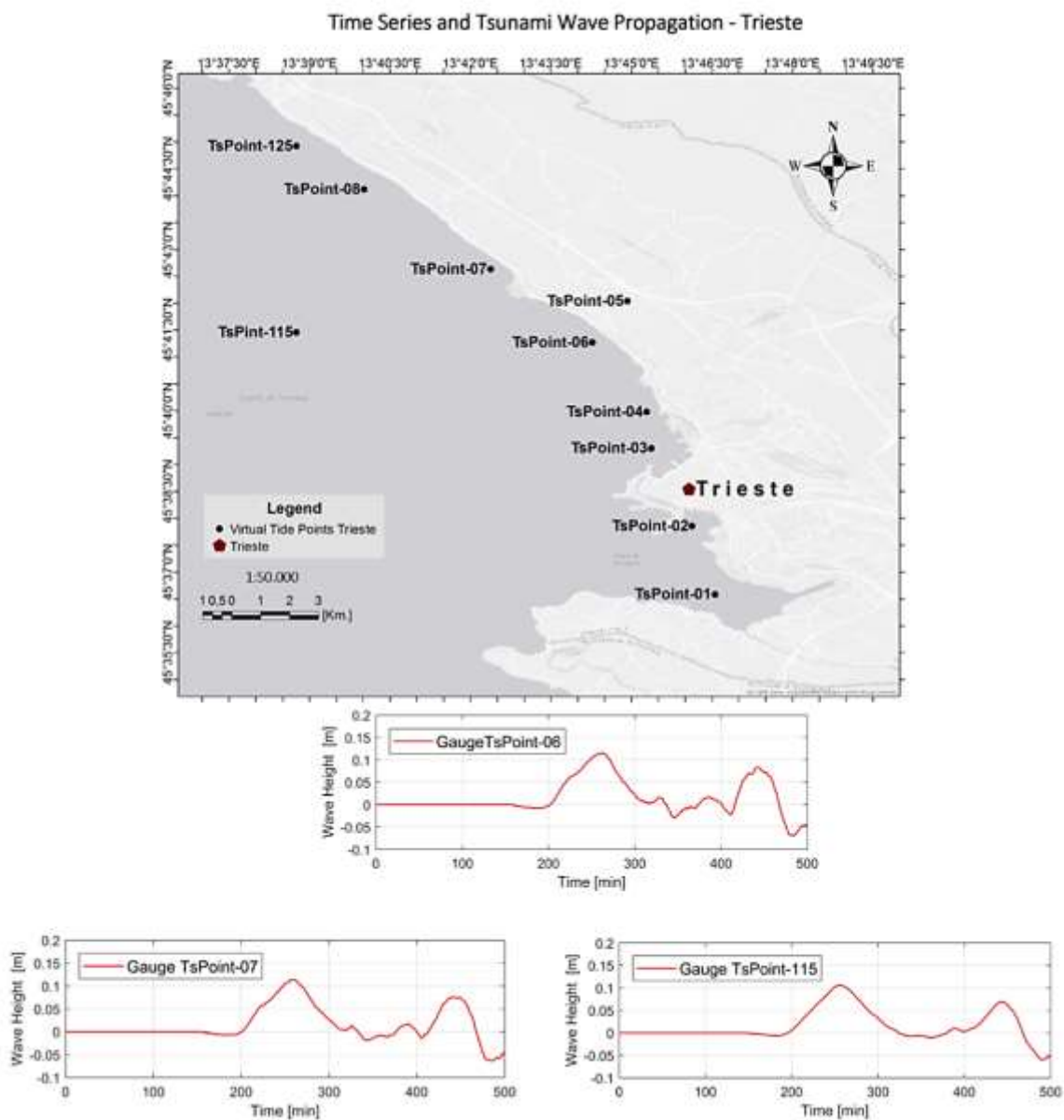


Figure 3.22: Maximum amplitude for the transfer time according to the generated Trieste gauges. (Author's, 2020)

3.5 Validation

To validate the results obtained from the simulation, experimental correlation will be performed using NRMSE (Root Mean Square Error), an important tool that will help determine the accuracy of the tsunamigenic scenario model proposed in the chapter, in this case, the maximum height variable of the zones of interest will be evaluated,

Table 3.4 Error limits allowable for model validation/verification based on OAR-PMEL-135 Standard, (Kurnia, 2017)

Category	Tested Parameter		OAR PMEL-135 Allowable Error	
	NRMSE	MAX	% NRMSE	% MAX
Laboratory Experiments	Water level time history/water level in the selected data segment	Runup or max./min. free surface elevation	15	10

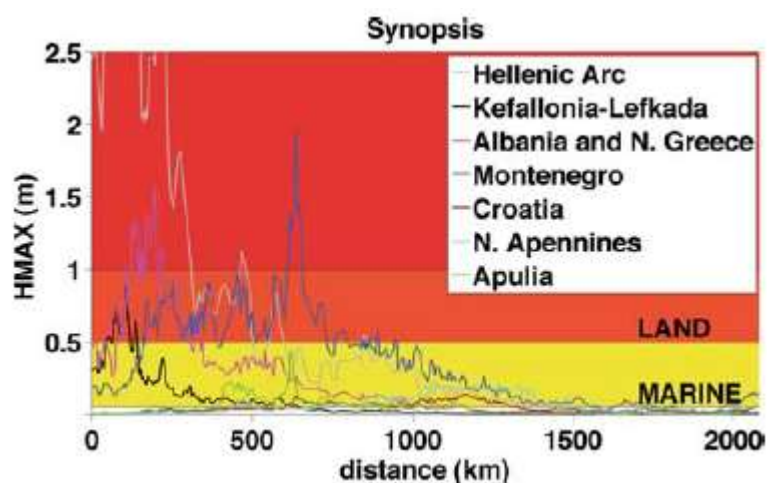


Figure 3.23: Maximum recorded height according to (Tiberti, Lorito, et al., 2008)

$$f(x_i) = \text{Investigación Tiberti}$$

$$y_i = \text{Resultados Nami Dance}$$

$$\sqrt{\frac{1}{n} \times \sum_{i=1}^n (f(x_i) - y_i)^2} \quad (3.1)$$

Table 3.5 : Root mean square error of Hmax, (Author`s, 2020)

	Tiberti	NamiDance	NRMSE	Max
	Ancona			Satisfy
TS	0.2	0.19	0.50%	5.00%
Mn	0.2	0.1917	0.65%	4.15%
Gr	0.25	0.27	1.19%	8.00%
Lg	0.3	0.32	1.56%	6.67%
	Split-Croatia			Satisfy
TS	0.09	0.096	0.30%	6.67%
Mn	0.1	0.092	0.50%	8.00%
Gr	0.12	0.11	0.71%	8.33%
Lg	0.2	0.21	0.87%	5.00%
	Montenegro			Satisfy
TS	0.1	0.105	0.25%	5.00%
Mn	0.1	0.107	0.43%	7.00%
Gr	0.2	0.18	1.09%	10.00%
Lg	0.2	0.208	1.16%	4.00%

3.6 Overview of results

Table 3.6: Summary of simulation results (Author's, 2020)

Source	Ancona				Split				Montenegro				
Interest Cities	Units	Ts	Mn	Gr	Lg	Ts	In	Gr	Lg	Ts	Mn	Gr	Lg
Wave Amplitude	m	0.22	0.22	0.25-0.39	0.25-0.39	0.08	.08	0.22	0.25	0.08	0.08	0.22	0.29
Runup	m	0.1	0.1	0.3	0.2	0.1	0.1	0.3	0.2	0.1	0.2	0.2	0.2
Velocity Wave	m/s	0.04	0.1	2.4	1.8	0.01	.01	1.2	0.6	0.1	0.1	1.2	0.3
Time Arrival	min	240	240	220	220	500	60	380	280	400	500	440	420
Flood Land	m	0.05	0.15	0.2	0.3	0.05	.06	0.03	0.03	0.05	0.05	0.15	0.15

3.7 Flood effects

The effects of inundation vary depending on each of the study zones due to zonal structural conditions which vary depending on the demographic level, these analyses are the basis for future studies of the effects on structures caused by tsunamis. The flooding conditions in the city of Trieste(Figure 3.24) are maximized due to the relevance of the flooding in the city's commercial port located in the south, which compromises several container yards, as well as several naval shipyards in the jurisdictional zone of the port. Within the urban levels with a high number of residences.



Figure 3.24 Flooding of Trieste Commercial Port. (Author's, 2020)



Figure 3.25 Flooding of Trieste Commercial Port south zone and nearby urban area.
(Author's, 2020)

Figure 3.27

En la ciudad de Lignano (Figura 3.26 y Figura 3.27), los niveles de inundación están comprometidos por grandes extensiones de las playas destinadas al turismo, gran parte de los inmuebles, así como edificios destinados a posadas y resorts extendidos desde la línea de playa hasta la última zona de máxima llegada a 500 metros o 1 kilómetro. La capacidad hotelera de Lignano es bastante importante para esta ciudad y el alto grado de exposición a un tsunami hace de gran relevancia el análisis futuro de esta zona.

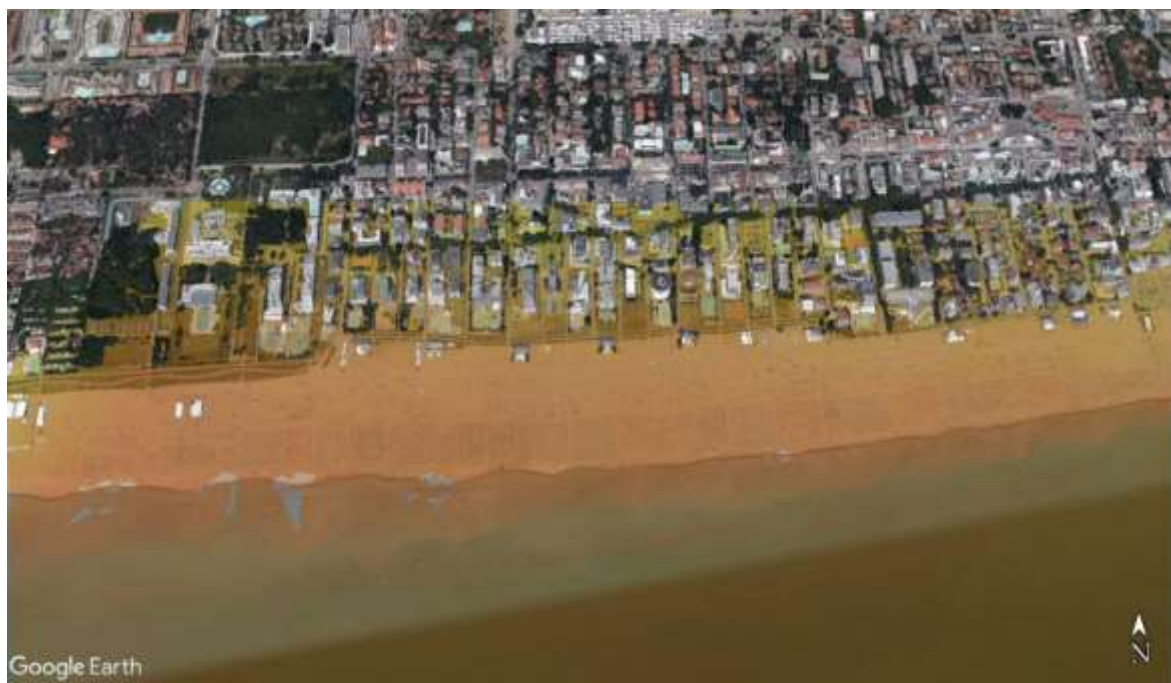


Figure 3.26 Flooding on the beach extension of Lignano. (Author`s, 2020)



Figure 3.27 Oblique view flooding on Lignano beach extension. (Author`s, 2020)

Due to the geographical conditions of Grado(Figure 3.28) very characteristic of inlets or lagoons generated by deltas below sea level, in addition to the level of development of this highly touristic area with several marinas with hundreds of boats, which makes the high level of inundation a great exposure to a tsunami, however the impact indices determined by the Froude level which are less than 1 give an indication that the exposure to the first waves during a tsunami in this area are very few, considering its rapid propagation.



Figure 3.28 Affected area in the city Grado. (Author's, 2020)

Monfalcone (Figure 3.29) has characteristics due to the fact that it is located in an inlet, so the maximum levels of flooding in the outermost areas of the city, in these areas are located large chemical and petrochemical industries, so the exposure to a flood would be complicated to solve considering the machinery and industry involved.



Figure 3.29 Monfalcone affected area. (Author's, 2020)

The effects of flooding are relevant to establish the necessary conditions for a planned development of each of these cities, so the information provided in this introductory report will allow establishing a future study on the risk indexes for the cities.

CHAPTER 4

4 CONCLUSIONS AND RECOMMENDATIONS

4.1 Conclusions

1. Although tsunamigenic earthquakes are not so often in the Adriatic Sea, their impacts along the coastline could be considerable and are required to be evaluated for sake of disaster mitigation and risk assessment. One of the main inputs for tsunami risk evaluation is a hazard, so a detailed tsunami hazard analysis for the coastline of the Adriatic Sea is urgent that help in mitigating the existent and proposed socio-economic activities.
2. In this work, tsunami hazard assessment is carried out for the North-eastern coast of the Adriatic Sea for a set of distant tsunamigenic earthquakes (more than 3 hours). The area of interest comprises the city of Trieste, Monfalcone, Grado, and Lignano. The distant tsunamigenic earthquakes are Ancona, Split, Montenegro scenarios from north to south, respectively.
3. The fault parameters for these scenarios were compiled from DISS interactive geospatial-database and the published works of Tiberti et al. (2008) and Paulatto et al. (2007) needed to generate tsunami source based on Okada's source of a finite rectangular fault model. Bathymetry data of about 400 m and 115 m were extracted from GEBCO 2020 for tsunami propagation and inundation modelling.
4. The simulation duration was tuned for 500 minutes to catch the major part of the wave train in the computational numerical model NamiDance. It seems that the scenario could produce the greatest effects on the coasts of Trieste, Monfalcone, Lignano and Grado Di Coastal is the Split scenario, where a maximum height of 05 m was obtained. Runup of about 0.3 m and a Froude number of 0.65 which corresponds to a subcritical flow, so the effect is moderate. The estimated travel times of the first wave is ranging between 200-300 minutes (Section3.4)
5. An inverse relationship exists between the travel time of the first wave and tsunami waves velocity, because the longer the arrival time, the low velocity of the propagation of the wave. In the case of Ancona, the closest of the scenarios

proposed for the work, Trieste has 0.04 m/s with a time of 240 minutes, a different case occurs in Grado with a maximum speed range of the zone of interest of 2.4 m/s at 220 minutes.

6. In the case of Montenegro and Split, Grado received the maximum velocity of 1.2 m/s and travel time of 440 minutes, both scenarios are distant to the area of interest and the direction of this is perpendicular thus receiving the greatest impact as well as the maximum run-up of 0.3 m.
7. Therefore, Grado and Lignano will be exposed to receive the maximum speeds due to its location, because the easterly winds influence its magnitude reaching the coastline in less time, the opposite happens in Trieste and Monfalcone, due to its morphology of inlet type as well as its abrupt bathymetric changes the arrival time is longer and speed is almost null (0-0.05 m/s).
8. The geographic locations that are located in bays or geological inlets are highly affected by the resonance caused by tsunamis generated by the transfer of sea waves and diffracted by the geographical conditions of the place producing an overlapping effect in their transfer.
9. In the context of development, the degree of impact on the coasts of the cities of Trieste, Monfalcone, Lignano and Grado are highly damaging due to their importance for Italy as axes of tourist, industrial and port development, since they are the most important cities in the productive matrix of Italy. Considering the effects of a tsunami, the development of mitigation measures or plans are the most suitable tools to consider, since this study only analyzed the tsunamigenic sources as origin, and in the global context, the seasonal tidal cycle and climatic conditions should be considered for a more accurate study and thus to avoid a possible affectation of major consequences for these cities.

4.2 Recommendations

1. The projections that can be made based on this project are widely extended due to its importance in cities and its significance at macro scales. Therefore, the following recommendations are made.
2. The compilation of information from historical records of tsunamigenic events should be carried out covering the parameters of fault rupture, characteristics of the tsunami recorded and effects on coasts. In such a way that the estimation of values for the definition of realistic and "maximum credible" scenarios (including parametric tests, can be performed).
3. Obtain bathymetry data files of different source and size resolutions from smallest to largest to establish the domains which, as the global domains change to local ones, require greater precision in the files.
4. To obtain more realistic results, the two-parameter conditions per domain that can be improved are the use of bottom friction by grid and sea level means, as well as atmospheric pressure, which are variables that can be entered in the simulation, if necessary.
5. Prefer to use grid files ASCII version 7 Grid Binary Golden Surfer, as these are best suited for Golden Surfer 18 and earlier versions.
6. Preferably selected scenarios should be geographically located in historical locations, thus avoiding divergence in the form of propagation. Although it does not eliminate the possibility of an epicentre of origin variability.
7. To obtain a better approximation when working with historical seismic data from a tsunami, a considerable amount of data should be gathered to refine the interpretation of the information, as well as to filter it, group it according to its common characteristics and validate it to have a sustained record of the scenario to be generated.
8. The hardware equipment used to carry out the modelling should have high-performance conditions of virtual memory and graphic capacity because the simulations and products obtained will depend on these. A long simulation time-step (dt) and a short simulation time may affect the results of the modelling; in fact, they will provide too coarse values in the time series and/or losing important parts of the time-series (mareograms) which may bias the interpretation of results.

5 BIBLIOGRAPHY

- Altıner, Y., Bačić, Z., Bašić, T., Coticchia, A., Medved, M., ida Mulić, M., & Nurçe, B. (2006). Present-day tectonics in and around the Adria plate inferred from GPS measurements. In *Postcollisional Tectonics and Magmatism in the Mediterranean Region and Asia* (Vol. 409, pp. 43–55). Geological Society of America. [https://doi.org/10.1130/2006.2409\(03\)](https://doi.org/10.1130/2006.2409(03))
- Benetatos, C., & Kiratzi, A. (2006). *Finite-fault slip models for the 15 April 1979 (Mw 7.1) Montenegro earthquake and its strongest aftershock of 24 May 1979 (Mw 6.2)*. 1979(July). <https://doi.org/10.1016/j.tecto.2006.04.009>
- CERC, U. (U. S. A. C. of E. C. E. R. (1984). SHORE PROTECTION MANUAL US Army Corps of Engineers. *Coastal Engineering, I.*
- Clawpack 4.6.3. (2009). *Earthquake sources: Fault slip and the Okada model*.
- Cushman-Roisin, B., Gacic, M., Poulain, P.-M., & Artegiani, A. (2001a). *Physical Oceanography of the Adriatic Sea: Past, Present and Future*. <https://doi.org/10.1007/978-94-015-9819-4>
- Cushman-Roisin, B., Gacic, M., Poulain, P.-M., & Artegiani, A. (2001b). *Physical Oceanography of the Adriatic Sea: Past, Present and Future*. <https://doi.org/10.1007/978-94-015-9819-4>
- de Leeuw, A., Mandic, O., Krijgsman, W., Kuiper, K., & Hrvatović, H. (2012). Paleomagnetic and geochronologic constraints on the geodynamic evolution of the Central Dinarides. *Tectonophysics*, 530–531(2), 286–298. <https://doi.org/10.1016/j.tecto.2012.01.004>
- Dias, F., & Dutykh, D. (2007). Dynamics of Tsunami waves. *NATO Security through Science Series C: Environmental Security*, 201–224. https://doi.org/10.1007/978-1-4020-5656-7_8
- DISS, I. N. di G. e V. (n.d.). *Database of Individual Seismogenic Sources*. <https://doi.org/10.6092/INGV.IT-DISS3.2.1>.
- Euro-Mediterranean Tsunami Catalogue*. (n.d.). Retrieved February 2, 2021, from <https://www.arcgis.com/apps/StorytellingTextLegend/index.html?appid=8329c2ad9b7f43c18562bdddc6c1ad26>
- GEBCO. (2020). *GEBCO data download*. <https://download.gebco.net/>
- Hassan, H. M., Frischknecht, C., ElGabry, M. N., Hussein, H., & ElWazir, M. (2020).

- Tsunami hazard and risk assessment for Alexandria (Egypt) based on the maximum credible earthquake. *Journal of African Earth Sciences*, 162(December 2019). <https://doi.org/10.1016/j.jafrearsci.2019.103735>
- Hollenstein, C., Kahle, H.-G., Geiger, A., Jenny, S., Goes, S., & Giardini, D. (2003). New GPS constraints on the Africa-Eurasia plate boundary zone in southern Italy. *Geophysical Research Letters*, 30(18). <https://doi.org/10.1029/2003GL017554>
- IEEE. (2020). *Try Engineering*. <https://tryengineering.org/es/link/society-of-naval-architects-and-marine-engineers/>
- Iglesias Cerdeira, O. (2015). Generación y propagación de tsunamis en el mar Catalano-Balear Olaia Iglesias Cerdeira Aquesta tesi doctoral està subjecta a la llicència Reconeixement-NoComercial-CompartirIgual 4.0. Espanya de Creative Commons. Esta tesis doctoral està sujeta a la licen. In *TDX (Tesis Doctorals en Xarxa)*. Universitat de Barcelona.
- INPRES, I. N. de P. S. (2013). *Fallas Geológicas*. Inpres. https://www.google.com/search?biw=1366&bih=625&sxsrf=ALeKk01OfEkjcJq5vQHOc-te9DObfV6YA%3A1610041593936&ei=-Uj3X7XMOMXAsAXk-oeADg&q=las+fallas+tectonicas+pdf&oq=las+fallas+tectonicas+pdf&gs_lcp=CgZwc3ktYWIQAzIGCAAQFhAeOgQIABBHOglIAFDX-QJY0YADYN6DA2gAcAJ4A
- Kurnia, D. (2017). Опыт аудита обеспечения качества и безопасности медицинской деятельности в медицинской организации по разделу «Эпидемиологическая безопасность». No Title. *Вестник Росздравнадзора*, 4(June), 9–15.
- Maramai, A., Graziani, L., & Tinti, S. (2007). Investigation on tsunami effects in the central Adriatic Sea during the last century - A contribution. *Natural Hazards and Earth System Science*, 7(1), 15–19. <https://doi.org/10.5194/nhess-7-15-2007>
- METU. (n.d.). *METU - Middle East Technical University | WE CAN CHANGE THE WORLD*. Retrieved January 17, 2021, from <https://www.metu.edu.tr/>
- NCEI Hazard Tsunami Search. (n.d.). Retrieved January 7, 2021, from <https://www.ngdc.noaa.gov/hazel/view/hazards/tsunami/event-search#>
- Necmioglu, O., & Ozel, N. (2014). An Earthquake Source Sensitivity Analysis for Tsunami Propagation in the Eastern Mediterranean. *Oceanography*, 27(2), 76–85. <https://doi.org/10.5670/oceanog.2014.42>
- NTHMP. (2017). Proceedings and Results of the National Tsunami Hazard Mitigation Program 2015 Tsunami Current Modeling Workshop. *NTHMP Publications and Resources*, 194 p.

- Okada, Y. (1985). *Surface deformation due to shear and tensile faults in a half-space*.
- Ozer Sozdinler, C., Necmioglu, O., Bayraktar, H. B., & Ozel, N. (2019). Tectonic Origin Tsunami Scenario Database for the Marmara Region. *Natural Hazards and Earth System Sciences*, 1–15. <https://doi.org/10.5194/nhess-2019-186>
- Palano, M. (2015). On the present-day crustal stress, strain-rate fields and mantle anisotropy pattern of Italy. *Geophysical Journal International*, 200(8), 969–985. <https://doi.org/10.1093/gji/ggu451>
- Pasarić, M., Brizuela, B., Graziani, L., Maramai, A., & Orlić, M. (2012a). Historical tsunamis in the Adriatic Sea. *Natural Hazards*, 61(2), 281–316. <https://doi.org/10.1007/s11069-011-9916-3>
- Pasarić, M., Brizuela, B., Graziani, L., Maramai, A., & Orlić, M. (2012b). Historical tsunamis in the Adriatic Sea. *Natural Hazards*, 61(2), 281–316. <https://doi.org/10.1007/s11069-011-9916-3>
- Paulatto, M., Pinat, T., & Romanelli, F. (2007a). Natural Hazards and Earth System Sciences Tsunami hazard scenarios in the Adriatic Sea domain. In *Hazards Earth Syst. Sci* (Vol. 7).
- Paulatto, M., Pinat, T., & Romanelli, F. (2007b). Tsunami hazard scenarios in the Adriatic Sea domain. *Natural Hazards and Earth System Science*, 7(2), 309–325. <https://doi.org/10.5194/nhess-7-309-2007>
- Plan, M. A., Pol, M. E. D., Nations, U., Programme, E., Programme, M., The, O. F., Adriatic, E., & Area, C. (1994). *MAP Technical Reports Series No . 86 (Issue 86)*.
- Quimiz, L., Rodríguez, D., Sabando, J., Salvador, M., & Sánchez, E. (2019). *Fallas Geológicas en la tierra generadas por sismos*.
- SATREPS Tsunami Proyect, J.-C. (2016). *Guía para la Estimación de Peligro de Tsunami Proyecto de Investigación para el Mejoramiento de Tecnología para desarrollar una Comunidad Resiliente ante los Tsunamis*.
- Stirling, M., Rhoades, D., & Berryman, K. (1998). *Evaluation of Wells and Coppersmith (1994) earthquake and fault relationships in the New Zealand context | EQC Earthquake Commission*.
- Survey, T. I. N. S. N. and the U. S. G. (2012a). Advanced National Seismic System (ANSS), ShakeMap, Italy Region, Maps of ground shaking and intensity for event 744871, Central Mediterranean Sea. *Shakemap Data for 744871*.
- Survey, T. I. N. S. N. and the U. S. G. (2012b). Advanced National Seismic System (ANSS), ShakeMap, Italy Region, Maps of ground shaking and intensity for event

744871, Central Mediterranean Sea. *Shakemap Data for 744871*.

- Tiberti, M. M., Basili, R., Piatanesi, A., Lorito, S., & Valensise, G. (2008). Earthquake-generated tsunamis in the Mediterranean Sea: Scenarios of potential threats to Southern Italy. *Journal of Geophysical Research*, 113(B1), B01301. <https://doi.org/10.1029/2007JB004943>
- Tiberti, M. M., Lorito, S., Basili, R., Piatanesi, A., & Valensise, G. (2008). Scenarios of earthquake-generated tsunamis for the Italian coast of the Adriatic Sea. *Pure and Applied Geophysics*, 165(11–12), 2117–2142. <https://doi.org/10.1007/s00024-008-0417-6>
- Trobèc, A., Busetti, M., Zgur, F., Baradello, L., Babich, A., Cova, A., Gordini, E., Romeo, R., Tomini, I., Poglajen, S., Diviacco, P., & Vrabec, M. (2018). Thickness of marine Holocene sediment in the Gulf of Trieste (northern Adriatic Sea). *Earth System Science Data*, 10(2), 1077–1092. <https://doi.org/10.5194/essd-10-1077-2018>
- IOC-UNESCO | IOC UNESCO. Retrieved January 17, 2021, from <https://ioc.unesco.org/>
- Velioglu, D., Kian, R., Yalciner, A. C., & Zaytsev, A. (2016). Performance assessment of NAMI DANCE in tsunami evolution and currents using a benchmark problem. *Journal of Marine Science and Engineering*, 4(3). <https://doi.org/10.3390/jmse4030049>
- Velioglu Sogut, D., & Yalciner, A. C. (2019). Performance Comparison of NAMI DANCE and FLOW-3D® Models in Tsunami Propagation, Inundation and Currents using NTHMP Benchmark Problems. *Pure and Applied Geophysics*, 176(7), 3115–3153. <https://doi.org/10.1007/s00024-018-1907-9>
- Wells, D. L., & Coppersmith, K. J. (1994). New Empirical Relationships among Magnitude, Rupture Length, Rupture Width, Rupture Area, and Surface Displacement. In *Bulletin of the Seismological Society of America* (Vol. 84, Issue 4).
- Zaytsev, A., Yalciner, A., Chernov, A., & Pelinovsky, E. (2019). *Tsunami Numerical Model Nami Dance GPU User Manual*.

APPENDIX

6 APPENDIX A

Appendix A 6.1: Data from Tsunamigenic Event Logs of the Institute of Volcanology and Geophysics of Italy(DISS Catalogue)

Year	Long	Lat	Mag
2003	3.66	36.84	6.90
2009	5.37	43.63	5.90
365	23.69	35.42	8.40
2003	15.33	43.09	5.50
1996	17.90	42.76	6.00
1962	16.94	43.15	6.10
1962	16.88	43.20	5.90
1915	13.61	41.96	6.70
1030	13.97	41.84	6.40
1805	14.47	41.50	6.60
1732	15.10	41.07	6.60
1857	15.78	40.35	6.50
900	16.24	39.78	6.20
1857	15.60	40.53	6.30
1783	16.19	38.59	6.60
1783	16.02	38.34	6.60
1908	15.60	38.05	7.00
1703	13.26	42.42	6.50
1997	12.84	43.09	6.00
1997	12.93	43.00	5.70
1997	12.93	42.91	5.60
1273	15.97	41.72	6.40
1875	15.64	41.72	6.10
1924	13.10	43.75	5.60
1984	13.95	41.70	5.80
1690	13.70	43.59	5.90
1930	13.26	43.64	5.90
1916	12.74	44.04	5.60
2016	12.66	44.09	5.70
1786	12.52	44.00	5.60
1875	12.46	44.10	5.70
1984	12.57	43.23	6.00
1783	15.82	38.27	5.30
1894	15.76	38.30	5.30
1894	15.93	38.23	5.80
2007	16.05	38.18	6.00
1928	16.02	38.49	6.00

Year	Long	Lat	Mag
1978	15.07	38.26	6.10
1781	12.48	43.58	6.20
1741	12.94	43.38	6.20
1799	13.10	43.16	5.80
1920	10.32	44.18	6.40
2002	14.94	41.69	5.80
2002	14.81	41.70	5.70
1627	15.35	41.71	6.70
1873	13.14	43.05	6.00
2002	13.71	38.37	5.90
2003	11.40	44.25	5.30
1806	12.75	41.73	5.60
1854	12.59	43.04	5.40
1832	12.66	42.97	5.80
1878	12.72	42.86	5.50
1917	12.18	43.48	5.80
1789	12.22	43.51	5.50
1846	10.49	43.52	5.70
1481	10.03	44.22	5.80
1883	13.89	40.74	5.40
2001	10.51	45.63	5.70
1943	13.67	42.93	5.90
1808	7.26	44.84	5.70
1808	7.36	44.87	5.60
1693	15.01	37.15	6.60
1980	15.29	40.80	6.80
1980	15.48	40.68	6.20
1980	15.35	40.85	6.20
1731	15.80	41.29	6.30
1851	15.66	40.98	6.30
1361	15.52	41.29	6.00
1560	16.37	41.28	5.70
1990	15.85	40.68	5.80
1834	9.91	44.37	5.70
1919	11.47	43.96	6.20
1542	11.33	44.01	5.90
1930	15.46	41.03	6.70

Year	Long	Lat	Mag
1570	11.50	44.89	5.50
1505	11.24	44.47	5.50
1456	15.06	41.24	6.90
1781	11.81	44.26	5.80
1456	13.91	42.21	6.00
1456	14.50	41.66	7.00
1950	13.43	42.51	5.70
1767	16.25	39.44	5.80
1835	16.26	39.35	5.90
1688	11.94	44.38	5.80
1695	11.87	45.82	6.60
1929	11.16	44.48	5.60
1802	9.79	45.39	5.70
1693	15.07	37.54	6.00
2012	11.07	44.85	6.00
1776	12.70	46.21	5.90
1794	12.80	46.29	5.80
1836	11.83	45.82	5.50
1976	13.26	46.24	5.70
1976	13.14	46.25	6.50
1976	13.22	46.27	6.00
1976	13.20	46.28	6.10
1936	12.43	46.03	6.10
1873	12.55	46.12	6.40
1887	8.28	43.88	6.60
2009	13.45	42.32	6.30
1893	16.37	41.65	6.00
2012	11.32	44.85	6.10
2008	10.33	44.55	5.40
1349	14.13	41.45	6.50
2005	16.19	38.80	6.80
1117	10.99	45.27	6.70
1624	11.85	44.64	5.80
1638	16.60	39.13	6.80
1511	13.89	46.08	6.80
1998	13.66	46.29	5.70

Appendix A 6.2 Data from Tsunamigenic Event Logs of the Institute of Volcanology and Geophysics of Italy (CFT5Med Catalogue)

Year	Long	Lat	Mag
1065	10.21	45.55	5.1
1087	16.00	41.25	5.6
1117	11.17	45.37	6.8
1120	13.92	41.38	5.8
1125	15.00	41.60	5.6
1125	15.29	37.08	5.8
1160	13.10	41.93	5.2
1161	13.33	41.57	5.1
1169	14.95	37.22	6.4
1170	13.33	41.57	5.6
1184	16.19	39.40	6.7
1222	10.23	45.48	6
1231	13.83	41.49	5.1
1249	10.93	44.65	4.9
1269	13.56	43.56	5.6
1268	12.08	45.74	5.4
1273	15.81	40.64	5.8
1276	12.09	42.72	5.6
1279	11.78	44.03	5.9
1279	12.93	43.11	6.5
1284	12.34	45.44	4.7
1293	10.91	43.93	5.6
1293	14.55	41.31	5.8
1298	12.91	42.57	6.2
1308	12.57	44.06	5.4
1315	13.46	42.32	5.8
1328	13.02	42.86	6.4
1329	15.00	37.75	4.9
1334	10.99	45.44	4.9
1345	11.25	43.78	4.7
1346	11.62	44.84	4.9
1348	13.54	46.58	7.1
1349	13.91	41.58	6.8
1352	15.09	37.50	5.4
1352	12.15	43.49	5.8
1353	12.14	43.57	5.6
1361	15.56	41.21	6
1365	11.34	44.50	5.4
1367	13.87	41.54	5.1
1369	8.61	44.91	4.9
1376	11.55	45.55	4.9
1389	13.20	46.41	4.9
1389	12.36	43.54	6.1
1396	9.27	45.59	5.4
1399	10.92	44.44	5.1

Year	Long	Lat	Mag
1403	12.22	46.15	4.7
1403	13.43	46.09	5.6
1409	10.33	44.80	5.1
1414	10.61	43.93	5.2
1414	11.12	43.27	5.6
1414	16.18	41.88	5.8
1433	11.34	44.50	4.7
1438	10.24	44.84	5.6
1453	11.28	43.79	5.3
1455	11.26	44.42	4.9
1456	14.05	41.17	4.7
1458	12.24	43.46	5.8
1458	12.24	43.46	4.7
1461	13.54	42.31	6.4
1466	15.33	40.77	6.1
1467	11.33	43.32	4.9
1480	13.80	42.90	5.4
1481	10.13	44.28	5.6
1483	12.23	44.16	5.7
1491	11.88	45.41	5
1494	15.55	38.19	5.4
1501	10.84	44.52	6
1504	11.82	43.70	5.1
1504	11.46	45.05	5.3
1505	11.23	44.51	5.6
1509	15.68	38.10	5.6
1509	11.87	44.32	5
1511	13.43	46.20	7
1511	13.73	46.05	6
1527	10.91	43.93	5.4
1536	8.90	44.42	4.7
1542	11.38	44.01	5.9
1542	15.01	37.23	6.8
1545	9.83	44.47	5.3
1547	10.63	44.70	5.1
1554	11.25	43.78	4.9
1560	16.49	41.25	5.6
1561	15.38	40.63	5.6
1561	15.49	40.51	6.5
1564	7.27	44.03	6
1570	11.63	44.82	5.5
1584	11.99	43.86	5.8
1597	11.43	43.99	5.2
1599	13.02	42.73	6
1611	11.36	44.01	5.1

Year	Long	Lat	Mag
1613	14.79	38.12	5.6
1622	14.66	46.18	5.4
1624	11.85	44.64	5.5
1624	14.74	37.27	5.6
1626	16.46	38.85	6
1627	15.34	41.74	6.8
1627	15.38	41.69	5.8
1627	15.33	41.76	6
1627	15.36	41.60	5.8
1628	10.33	44.80	4.9
1628	10.33	44.80	4.7
1633	15.03	37.61	5.8
1638	16.29	39.05	7
1638	16.81	39.28	6.9
1639	13.27	42.64	6.1
1639	13.25	42.65	6.2
1642	9.93	45.28	5.4
1644	7.32	43.99	6
1646	10.32	43.55	4.7
1646	15.94	41.87	6.3
1654	13.68	41.64	6.3
1659	16.25	38.70	6.6
1661	10.86	44.74	4.9
1661	9.98	45.66	5.1
1661	11.90	44.02	6.1
1669	15.03	37.61	5.3
1671	10.87	44.68	5.3
1672	12.58	43.94	5.6
1688	11.94	44.39	5.8
1688	14.56	41.28	7
1690	13.88	46.64	6.5
1690	13.59	43.55	5.4
1691	14.45	46.09	5.4
1693	15.04	37.14	6.2
1693	15.01	37.14	7.4
1694	12.09	43.62	5.1
1694	15.41	40.86	6.8
1695	11.95	45.80	6.5
1695	12.11	42.63	6.2
1697	11.33	43.32	4.9
1697	11.33	43.32	4.9
1697	11.33	43.32	4.7
1697	11.33	43.32	4.7
1697	11.33	43.32	4.7
1700	12.88	46.41	5.7

Year	Long	Lat	Mag
1702	14.78	41.13	4.9
1702	14.99	41.12	6.5
1702	14.78	41.13	4.9
1702	14.78	41.13	4.9
1703	13.07	42.71	6.7
1703	13.10	42.62	6
1703	13.29	42.44	6.7
1706	14.08	42.08	6.8
1708	15.80	39.94	4.7
1717	15.21	38.10	5
1719	13.05	42.88	5.5
1724	11.00	43.19	5.4
1725	11.57	44.21	5.4
1726	13.35	38.12	5.6
1729	11.70	43.77	4.9
1730	13.12	42.75	5.9
1731	15.76	41.27	6.5
1732	15.06	41.06	6.6
1739	14.74	38.10	5.1
1740	10.49	44.08	5.5
1741	13.01	43.43	6.2
1742	10.32	43.55	4.9
1743	12.07	42.62	5
1743	18.05	40.25	6.9
1743	16.37	38.70	5.7
1746	10.45	44.09	5.1
1747	12.75	43.22	5.8
1751	12.74	43.23	6.3
1753	7.18	44.94	5.2
1755	12.96	40.90	5.8
1755	7.99	46.32	5.9
1762	11.51	44.01	5.1
1762	13.59	42.31	6
1767	10.12	44.13	5.4
1767	7.50	45.27	5.1
1767	16.28	39.38	6
1768	11.90	43.94	5.9
1770	11.41	43.70	4.9
1771	11.16	44.14	4.7
1774	10.11	45.56	4.7
1779	11.48	44.45	5.2
1779	11.33	44.46	5.2
1780	11.31	44.57	5.1
1781	11.80	44.25	5.9
1781	12.55	43.58	6.3
1781	11.99	44.27	5.6
1781	9.59	45.50	4.9
1783	15.97	38.30	7

Year	Long	Lat	Mag
1783	15.64	38.18	6.3
1783	16.20	38.58	6.6
1783	16.30	38.77	5.9
1783	16.46	38.79	7
1785	12.96	43.07	5.1
1785	12.79	42.54	5.7
1786	15.02	38.10	6.2
1786	9.60	45.30	5.1
1786	13.37	42.32	5.4
1786	12.56	43.99	5.6
1787	11.62	44.84	4.9
1788	13.02	46.40	5.1
1789	12.22	43.51	5.9
1791	16.27	38.64	6
1791	12.86	42.95	5.5
1794	12.82	46.31	6
1794	14.92	41.11	5.2
1794	12.80	46.30	5.3
1796	11.88	43.55	5.1
1796	13.91	40.75	5.6
1796	11.67	44.62	5.6
1798	11.48	43.35	4.8
1799	13.15	43.22	6.2
1801	11.42	44.47	5.1
1802	9.85	45.42	5.7
1804	11.11	43.45	4.9
1805	14.47	41.50	6.6
1806	12.73	41.72	5.5
1808	7.25	44.84	5.7
1808	7.26	44.82	4.9
1808	7.32	44.85	5.3
1812	11.14	43.66	5.2
1812	12.57	46.03	5.7
1813	11.97	44.25	5.3
1815	13.02	42.83	5.5
1817	6.64	46.25	5.5
1818	15.14	37.60	6.2
1818	7.64	43.81	5.5
1818	14.76	37.21	5.5
1818	14.08	37.81	5.2
1818	10.30	44.70	5.3
1819	7.93	43.86	4.9
1819	14.04	37.94	5.3
1823	14.09	37.99	5.7
1826	15.73	40.52	5.8
1828	13.90	40.75	5.8
1828	9.05	44.82	5.8
1829	12.68	41.76	4.8

Year	Long	Lat	Mag
1831	7.85	43.86	5.5
1831	10.54	44.75	5.5
1831	10.47	44.65	4.7
1832	12.61	42.98	6.3
1832	16.92	39.08	6.6
1832	10.49	44.77	5.5
1834	9.85	44.43	5.8
1834	9.95	44.53	5.2
1834	11.32	44.48	4.9
1835	11.42	43.96	4.7
1835	7.55	44.33	4.9
1835	16.29	39.33	5.8
1836	16.74	39.57	6.2
1836	16.64	39.57	5.1
1836	11.82	45.81	5.6
1836	15.78	40.14	6
1837	10.18	44.18	5.8
1838	12.79	42.76	5
1838	12.91	42.84	5.3
1841	14.08	42.08	5
1843	11.26	44.00	5.1
1846	14.92	37.54	5
1846	10.56	43.47	5.9
1848	15.10	37.54	5.5
1849	11.41	44.10	4.7
1849	9.79	44.45	4.7
1851	15.67	40.95	6.4
1851	15.65	40.99	5.6
1853	15.22	40.82	5.6
1854	16.30	39.26	6.2
1854	12.58	43.04	5.6
1854	7.56	43.79	5.7
1855	7.70	45.84	5.7
1857	15.84	40.35	7
1857	15.99	40.30	5.4
1858	7.31	44.89	4.7
1859	12.10	45.89	5.2
1859	11.35	43.33	4.8
1859	11.35	43.33	4.8
1864	11.28	44.04	4.8
1865	15.16	37.70	5.4
1865	12.31	43.28	5.1
1866	10.80	45.74	4.9
1868	10.80	45.74	4.7
1869	11.33	43.34	4.9
1869	11.12	44.31	5.4
1869	11.11	43.45	4.9

Year	Long	Lat	Mag
1870	16.33	39.22	6.1
1870	12.06	44.13	5.6
1871	10.62	43.30	5.4
1871	11.35	43.42	4.6
1873	13.24	43.09	6
1873	12.38	46.16	6.3
1873	13.78	41.69	5.4
1873	9.95	44.44	5.5
1874	11.57	44.20	5.1
1874	13.83	41.66	5.5
1875	12.55	44.06	5.8
1876	10.79	45.75	4.9
1876	10.79	45.76	4.9
1876	10.79	45.73	4.9
1877	13.35	41.71	5.2
1877	10.81	45.76	4.6
1878	11.54	44.43	5.1
1878	7.36	44.44	4.9
1878	12.68	42.85	5.4
1879	13.04	42.77	5.6
1879	11.59	44.17	5.1
1879	15.15	37.69	5.7
1880	8.06	46.27	5.4
1881	11.35	44.40	5.2
1881	11.48	44.41	5
1881	13.90	40.75	5.4
1881	14.28	42.23	5.6
1882	9.08	44.66	5
1882	14.20	41.56	5.3
1882	10.77	45.71	5
1883	13.87	40.74	5.7
1884	9.77	45.55	4.9
1884	6.62	44.94	5.3
1887	7.99	43.89	6.3
1887	11.22	43.75	4.5
1887	16.22	39.56	5.5
1889	15.16	37.65	5
1891	11.17	45.57	5.9
1892	11.20	45.57	4.9
1893	16.08	41.71	5.4
1894	11.14	45.58	4.8
1894	15.11	37.66	5.7
1894	15.87	38.29	6.1
1894	10.12	45.57	5.1
1895	14.53	46.13	6.2
1895	11.26	43.70	5.4
1895	11.82	44.03	4.6
1897	14.50	46.06	5.3

Year	Long	Lat	Mag
1897	12.38	43.50	5.1
1898	11.77	44.65	4.8
1898	10.26	44.66	5.4
1898	12.99	42.90	5
1898	12.98	42.91	5.3
1899	11.12	43.96	5.1
1899	12.69	41.80	5.1
1901	13.75	41.72	5.2
1901	10.49	45.58	5.7
1904	13.32	42.10	5.6
1904	10.64	44.49	4.9
1904	10.84	44.20	4.9
1904	6.82	44.89	4.8
1905	7.01	46.02	5.7
1905	16.06	38.68	6.7
1907	11.07	45.32	4.9
1907	15.99	38.09	6
1907	11.37	43.49	4.6
1908	13.19	46.47	5.4
1908	15.69	38.17	7
1909	11.33	43.14	5.6
1910	15.42	40.90	5.7
1910	12.93	42.74	4.9
1911	12.08	44.12	5.3
1911	11.82	43.81	4.7
1911	11.34	43.44	5.2
1911	15.15	37.70	5.6
1913	16.24	39.53	5.7
1914	15.13	37.66	5.9
1914	7.36	45.05	5.4
1915	13.65	41.98	7
1915	12.89	43.01	5
1915	12.46	43.08	4.6
1916	12.62	44.01	5.8
1916	12.60	44.02	4.9
1916	12.67	43.96	5.7
1916	13.17	42.65	5.5
1917	12.13	43.47	5.9
1917	12.64	42.59	5.1
1918	9.60	45.78	4.9
1918	11.93	43.92	5.9
1919	11.48	43.96	6.3
1919	11.76	42.82	5.3
1919	12.68	41.54	5.3
1920	10.28	44.19	6.5
1924	13.14	43.74	5.3
1925	14.19	41.72	5.1
1926	14.28	45.76	5.9

Year	Long	Lat	Mag
1927	12.70	41.70	4.9
1928	12.98	46.38	5.8
1928	10.90	44.76	4.7
1929	11.48	44.43	5.2
1929	11.20	44.48	5.3
1929	11.14	44.48	5.4
1929	11.13	44.48	5
1929	11.10	44.49	5.1
1929	11.12	44.48	5.2
1930	11.51	43.99	5
1930	15.34	41.06	6.7
1930	13.27	43.67	5.8
1931	11.76	44.82	4.8
1931	11.37	44.06	4.7
1931	11.49	44.07	4.7
1932	10.73	45.63	5.1
1933	14.09	42.08	6
1935	6.63	44.65	5.3
1936	8.04	45.56	4.7
1936	12.41	46.03	6.2
1937	10.34	44.76	4.8
1938	6.74	44.59	5.3
1939	11.42	44.02	4.7
1940	13.43	38.08	5.3
1941	15.24	38.81	5.4
1943	13.65	42.91	5.8
1945	9.15	44.82	4.9
1945	9.13	44.83	5.2
1947	16.52	38.65	5.7
1948	12.14	43.58	5.1
1948	15.81	41.55	5.5
1948	15.74	41.61	5.3
1948	15.81	41.44	5.5
1951	9.60	45.25	5.4
1952	11.88	43.98	5
1953	10.79	44.79	4.8
1956	11.33	44.21	4.7
1956	11.90	43.94	5
1956	11.88	44.00	4.6
1958	13.48	42.34	5.2
1959	6.71	44.49	5.2
1959	13.04	46.47	5.2
1960	7.98	46.35	5.3
1960	11.39	44.00	5
1961	13.04	42.40	5.1
1962	14.95	41.23	6.1
1962	11.36	43.60	4.7
1963	8.07	43.92	5.4

Year	Long	Lat	Mag
1967	14.41	37.86	5.6
1968	13.00	37.76	5.6
1968	12.99	37.76	6.5
1969	13.79	41.57	5.1
1971	11.85	42.44	5.2
1971	10.34	44.82	5.7
1972	13.36	43.62	4.6
1972	13.30	43.59	5.3
1972	13.28	43.59	5.4
1972	13.51	43.60	4.7
1972	13.33	43.66	5.2
1972	13.51	43.60	4.7
1972	13.51	43.60	5.1
1972	13.42	43.58	5.5
1974	12.93	42.81	5.2
1975	15.64	38.12	5.3
1976	13.06	46.24	6.5
1976	13.18	46.27	5.7
1976	13.11	46.26	6.1
1978	15.98	38.01	5.5
1978	15.02	38.13	5.7
1979	9.55	45.64	4.9
1979	13.08	42.72	5.8
1980	15.28	40.84	6.7
1980	9.76	44.80	5.2
1985	9.68	44.64	4.9
1349	13.13	42.27	6.1
1349	11.93	42.51	6.4
1091	12.48	41.90	5.1
1982	15.77	40.01	5.4
1983	10.27	44.76	5.3
1984	12.51	43.21	5.6
1984	14.06	41.67	5.8
1990	14.98	37.26	5.4
1760	14.40	40.80	4.7
1984	14.08	41.72	5.4
1477	12.70	42.96	4.9
1730	12.58	43.35	5.4
1832	13.11	42.96	4.7
1832	13.12	42.95	4.8
1832	13.07	43.01	5.3
1838	12.88	42.88	5.1
1455	11.18	44.33	5.6
1172	15.55	38.19	5.6

Year	Long	Lat	Mag
1255	15.55	38.19	4.9
1258	13.99	41.76	5.6
1280	14.26	40.86	5
1295	14.00	37.50	5.8
1303	14.03	43.77	5.6
1429	15.55	38.19	4.9
1558	12.19	43.51	5.1
1559	12.09	43.62	5.1
1690	12.24	43.46	4.9
1693	16.11	39.80	5.6
1517	15.21	41.01	5.4
1708	16.01	40.00	5.5
1780	14.98	38.08	5.4
1631	12.86	43.06	5.1
1349	13.97	42.02	6
1721	12.86	43.06	5.1
1793	12.81	43.03	5.4
1693	12.34	43.45	4.9
1699	12.07	42.48	4.7
1725	12.43	43.46	4.9
1731	12.04	43.67	5.4
1737	14.66	40.92	5.1
1738	16.13	38.71	4.9
1740	16.59	38.92	4.9
1741	14.93	41.03	5.4
1743	16.08	39.13	5.1
1744	16.78	39.04	5.7
1748	12.79	43.11	4.7
1761	16.59	38.92	4.9
1778	13.51	43.60	4.7
1209	13.88	42.17	6
1339	11.62	44.84	4.7
1409	11.62	44.84	4.7
1411	11.62	44.84	5.1
1497	9.92	44.25	5.8
1536	10.93	44.37	5.3
1438	12.68	41.79	5.4
1492	12.05	44.22	4.9
1740	12.79	43.11	4.7
1046	11.07	45.83	6
1117	10.45	44.09	5.3
1275	13.91	40.73	5.8
1348	13.10	41.93	5.6
1353	15.65	40.99	6
1377	15.90	38.68	5.4

Year	Long	Lat	Mag
1386	14.26	40.86	5.4
1270	12.14	43.57	5.6
1345	11.25	43.78	4.7
1457	14.26	40.86	4.7
701	12.83	37.58	5.8
1997	13.00	43.04	5.6
1997	12.90	43.11	5.7
1997	12.97	42.95	5.5
725	12.22	44.40	5.6
778	12.24	45.67	5.8
801	12.48	41.90	5.4
847	14.16	41.62	5.6
853	15.55	38.19	5.4
951	16.64	39.57	6
989	15.17	41.01	6.9
1456	13.91	42.19	6.3
1456	14.51	41.53	7.1
1456	14.87	41.18	7.1
1456	15.66	41.09	6.3
911	10.10	35.67	6.2
977	11.07	35.50	6.2
1204	22.21	40.52	6
1250	22.38	38.38	6
1270	19.45	41.32	6.2
1278	19.92	39.62	6
1321	23.32	38.32	6
1359	20.09	41.11	6
1395	22.05	40.80	6
1395	22.95	40.64	5.4
1399	15.23	44.11	4.9
1402	22.33	38.15	6.6
1407	15.23	44.11	4.7
1417	24.00	38.50	5.8
1418	15.56	43.96	5.6
1420	22.95	40.64	6
1421	22.73	37.64	5.2
1421	24.00	38.50	5.6
1422	21.96	36.99	5.8
1428	21.83	36.81	5.8
1444	19.21	41.93	5.8
1456	24.33	40.16	5.4
1462	21.84	38.39	5.8
1469	20.67	38.25	5.8
1481	18.12	42.65	5.4

Appendix A 6.3 Data from tsunamigenic event records published in Paulatto's work in 2007.

Year	Long	Lat	Mag
346	41.24	19.24	6.8
1323	44.3	11.2	4.2
1324	45.2	14.7	6.2
1349	46.22	13.35	6.9
1350	46.5	13.45	6.4
1481	42.6	18.1	6
1511	46.15	13.2	6.8
1511	46.12	13.26	6.5
1511	46.26	13.26	6.2
1520	42.6	18.1	6.7
1624	44.39	44.51	5.5
1624	44.66	11.91	5.5
1627	41.44	15.21	6.8
1627	41.73	15.26	7
1628	41.36	15.21	5.7
1648	41.52	15.56	6.1
1649	41.83	16	6.4

Year	Long	Lat	Mag
1668	42.36	18.06	7.2
1672	44	12.45	5.6
1673	43.56	12.35	5.5
1695	40.53	15.21	4.68
1696	40.9	15.43	7
1721	45.3	14.4	6.2
1731	41.3	15.3	6.6
1732	41.16	15.45	6.6
1733	41.31	15.8	6.2
1744	39.51	18.47	7.3
1745	39.66	19	7
1802	45.3	14	5.5
1803	45.4	14.3	5.5
1821	42.1	15.5	6
1838	45.3	14.6	4.7
1851	40.42	19.24	6.8
1852	40.95	16.65	6.4

Year	Long	Lat	Mag
1866	40.24	19.36	6.6
1866	40.24	19.3	6.3
1866	40.5	19.3	6.1
1866	40.3	19.3	5.6
1869	38.51	20.48	6.4
1871	43.3	10.63	5.5
1876	44.04	12.33	5.8
1877	44.06	12.56	5.2
1878	45	14.9	6
1890	41.75	15.38	5
1891	41.5	15.42	5.6
1893	40.06	19.42	6.6
1920	40.18	20	6.3
1937	43.2	16.4	5.2
1962	43.15	16.94	6.1
1979	42.02	19.07	6.8

Appendix A 6.4 Data from tsunamigenic event records published in Pasarie's work in 2012

Year	Long	Lat	Mag
1511	13.4	46.2	6.5
1520	18.1	42.6	6.74
1627	15.35	41.73	6.7
1667	18.1	42.6	7.39
1672	12.58	43.93	5.6
1731	15.75	41.27	6.3
1743	18.78	39.85	6.9

Year	Long	Lat	Mag
1750	14.4	45.3	5.66
1780	18.5	42.4	5.66
1823	18.2	42.7	5.3
1838	14.5	45.2	5.3
1843	17.7	42.8	5.3
1853	18.6	42.4	5.3
1875	12.55	44.07	5.7

Year	Long	Lat	Mag
1889	15.7	41.83	5.6
1916	12.4	43.58	5.9
1930	12.67	43.97	5.9
1937	16.6	43.19	5.2
1962	16.94	43.15	6.1
1979	19.07	42.02	6.8

Appendix A 6.5 Data from Tsunamigenic Event Logs of California University (Northern California Earthquake Data Center)

Year	Long	Lat	Mag	Year	Long	Lat	Mag	Year	Long	Lat	Mag	Year	Long	Lat	Mag
1962	38.00	20.20	5	1965	44.30	12.10	4.4	1967	42.90	17.70	4.4	1968	37.80	12.90	4.4
1963	40.50	20.10	4.6	1965	39.40	16.10	4.1	1967	36.50	19.40	4.5	1968	37.70	12.80	4.6
1963	43.60	17.00	5.3	1965	40.60	14.90	4.5	1967	38.90	15.00	4.5	1968	37.90	12.80	4.3
1963	40.50	20.10	4.7	1966	40.10	20.30	4.3	1967	45.60	13.90	4	1968	38.10	17.80	5.3
1963	42.20	19.40	4.4	1966	38.60	14.80	4.2	1967	40.60	19.40	4.4	1968	37.90	13.10	4.4
1963	39.30	20.40	4.4	1966	43.50	17.70	5.4	1967	37.90	15.30	4.3	1968	39.60	20.40	4.8
1963	41.80	20.20	4.9	1966	40.30	19.80	4.7	1967	40.70	20.20	4.7	1968	41.30	20.30	4.4
1963	39.00	15.00	4.4	1966	43.30	13.10	4.9	1967	44.30	17.70	4.2	1968	39.80	14.90	4.3
1963	38.50	14.90	4.7	1966	40.90	15.80	4.2	1967	40.80	19.70	4.4	1968	38.54	14.99	4.9
1963	45.60	14.90	4.3	1966	43.20	18.10	4.2	1967	44.30	11.10	4.2	1968	45.10	17.06	5.8
1963	39.60	15.20	4.2	1966	42.00	18.70	5	1967	41.60	14.00	4.5	1968	43.02	17.12	4.3
1963	44.50	11.90	4.9	1966	42.20	18.80	5.2	1967	43.30	16.80	4.3	1968	42.90	18.56	4.2
1963	36.10	18.00	5.3	1966	42.20	18.80	4.9	1967	37.80	14.60	4.8	1968	37.96	14.87	4.8
1963	39.00	20.40	4.3	1966	42.20	18.90	4.2	1967	39.40	20.40	4.6	1968	45.87	11.33	4.6
1963	44.50	11.00	4.1	1966	40.20	19.80	4.8	1967	41.70	20.40	4.3	1968	40.94	19.95	4.5
1963	42.50	13.30	4.2	1966	40.20	19.70	4.7	1967	41.20	20.10	4.7	1968	42.97	17.44	4.3
1964	45.70	14.10	4.6	1966	42.20	18.70	5.6	1967	41.40	20.30	4.5	1968	40.20	15.45	4.2
1964	45.30	18.10	5.88	1966	42.00	18.60	5.6	1967	41.30	20.30	5.4	1968	38.30	20.19	4.5
1964	39.00	14.50	4.3	1966	42.10	18.90	4.5	1967	41.40	20.10	4.4	1968	42.13	19.39	5.3
1964	45.30	18.10	4.6	1966	42.10	18.60	4.8	1967	42.30	13.60	4.6	1968	44.56	18.43	4.7
1964	43.90	16.10	4.7	1966	42.20	18.80	4.5	1967	42.50	13.20	4.6	1968	43.95	11.63	4
1964	43.00	13.00	4.5	1966	41.90	18.70	4.7	1967	41.30	20.30	4.4	1968	39.74	16.81	4.1
1964	44.20	16.40	4.4	1966	41.90	18.70	4.2	1967	41.30	20.20	4.5	1969	38.53	20.14	4.3
1964	37.90	19.80	4.5	1966	42.10	18.90	4.6	1967	42.00	16.50	4.5	1969	39.41	20.25	4.5
1964	44.10	11.10	4.3	1966	40.20	20.30	4.4	1967	41.50	20.40	4.8	1969	44.62	11.98	4.5
1964	39.40	15.40	4.2	1966	42.80	17.60	4.5	1967	41.50	20.40	4.7	1969	38.35	20.10	4.1
1964	43.40	19.70	4.9	1966	44.20	12.10	4.4	1967	44.70	12.20	5.3	1969	39.15	20.22	4.5
1964	44.30	11.60	4.3	1966	42.20	19.10	4.4	1968	42.40	12.80	4	1969	40.04	15.17	4.6
1965	44.20	18.00	5	1966	45.50	16.00	4.9	1968	37.80	13.10	5.1	1969	39.03	15.35	4.8
1965	43.30	17.90	4.4	1966	42.10	18.90	5.1	1968	37.90	13.10	4.7	1969	38.02	20.17	4.5
1965	37.70	20.30	4.5	1967	38.43	15.07	4.3	1968	37.90	13.10	5.1	1969	40.74	19.89	5.5
1965	38.00	20.30	4.5	1967	39.92	20.10	4.4	1968	37.90	13.10	5.4	1969	40.59	19.88	4.6
1965	38.88	17.65	4.6	1967	43.31	17.36	4.2	1968	37.90	13.10	4.6	1969	40.61	19.79	4.3
1965	43.00	13.60	4.1	1967	44.51	16.02	4.5	1968	37.80	12.80	5.3	1969	40.70	19.81	5.1
1965	38.30	20.40	5	1967	38.70	14.80	4	1968	37.70	13.10	4.1	1969	38.25	20.08	4.5
1965	37.40	19.80	4.2	1967	41.60	16.20	4.4	1968	37.80	12.90	4.7	1969	38.84	14.83	4.1
1965	42.90	12.80	4.4	1967	44.20	19.10	4.5	1968	37.60	12.80	4.8	1969	39.63	14.82	4.1
1965	42.90	12.80	4.4	1967	43.70	19.20	4.2	1968	37.80	12.90	4.6	1969	41.57	13.85	4.6
1965	44.00	12.20	4.7	1967	44.20	19.20	4.3	1968	37.90	13.10	5.1	1969	38.39	20.37	4.6
1965	41.70	19.20	4.6	1967	40.70	19.50	4.4	1968	38.00	13.20	4.3	1969	41.29	20.26	4.4
1965	40.20	19.80	4.5	1967	40.80	19.80	4.3	1968	37.80	13.20	5.1	1969	38.04	20.13	4.6

Year	Long	Lat	Mag												
1969	38.24	20.15	4.5	1970	41.10	19.77	5.7	1971	39.29	15.20	4.5	1972	43.60	13.39	4.4
1969	38.48	20.20	4.5	1970	43.24	11.06	5.1	1971	39.68	15.20	4.3	1972	44.05	16.20	4.5
1969	42.26	12.06	4.4	1970	38.07	20.00	4.6	1971	41.89	20.24	4.9	1972	44.03	17.11	4.4
1969	42.29	12.22	4.5	1970	43.29	18.41	5.2	1971	41.20	15.29	4.3	1972	40.33	19.70	5.1
1969	39.67	16.66	4.3	1970	41.45	19.42	4.4	1971	41.14	15.24	4.9	1972	38.28	20.34	6.3
1969	37.56	20.28	5.4	1970	40.72	19.90	4.3	1971	43.94	12.48	4.4	1972	38.47	20.34	4.8
1969	40.55	19.76	4.5	1970	38.03	20.16	5.2	1971	39.63	12.83	4.3	1972	38.25	20.24	4.6
1969	37.95	20.21	4.7	1970	43.78	18.10	4.4	1971	38.20	20.14	4.3	1972	37.97	20.28	4
1969	44.23	11.87	4.1	1970	43.96	15.96	4.6	1971	42.87	13.10	5	1972	38.32	20.22	4.8
1969	42.38	19.43	5	1970	43.01	12.89	4.3	1971	43.06	12.90	4.4	1972	44.49	11.02	4.2
1969	42.22	19.26	4.6	1970	43.95	16.06	5.5	1971	44.54	10.96	4.6	1972	37.54	20.21	4.5
1969	43.99	12.10	4	1970	41.08	19.57	4.1	1971	40.40	15.80	4.9	1972	38.33	20.37	5.3
1969	43.21	12.45	4.6	1970	44.23	15.66	4.5	1972	43.76	13.42	4.5	1972	37.39	20.32	4.3
1969	41.77	20.09	4.9	1970	38.01	20.10	4.4	1972	43.79	13.44	4.8	1972	39.51	20.34	5.3
1969	37.22	20.11	4.6	1970	39.30	20.14	4.7	1972	43.86	13.30	4.3	1972	42.95	13.40	5.6
1969	39.74	20.44	5.1	1970	41.72	13.83	4.4	1972	43.82	13.31	4.8	1972	44.11	13.04	4.6
1969	39.89	15.01	4	1970	44.03	15.78	5	1972	43.94	13.20	4.8	1972	42.74	13.25	4
1969	38.98	14.97	4	1970	38.28	20.25	4.5	1972	43.93	13.21	4.4	1972	38.35	20.20	4.7
1969	44.87	17.29	5.6	1970	37.85	19.94	4.6	1972	43.78	13.31	4.4	1972	38.17	20.17	4.7
1969	44.96	16.96	4.9	1970	38.03	19.89	4.6	1972	43.82	13.42	4.8	1973	38.22	20.17	4.3
1969	44.92	17.23	6.1	1970	38.19	20.06	4.7	1972	43.83	13.35	4.8	1973	38.17	19.55	4.3
1969	44.91	16.99	4.8	1970	44.82	17.23	4.4	1972	43.83	13.29	4.8	1973	38.18	19.87	4.3
1969	45.15	16.76	4.1	1970	44.84	17.33	5	1972	43.24	13.73	4.4	1973	38.28	20.34	4.2
1969	40.69	15.70	4.7	1970	42.13	19.32	4.9	1972	43.74	13.45	4.6	1973	38.26	20.26	4.1
1969	40.67	19.85	4.6	1971	37.58	20.22	4.6	1972	43.85	13.26	4.7	1973	38.43	20.01	4.5
1969	44.86	17.16	5.1	1971	39.92	20.08	4.4	1972	43.75	13.37	4.7	1973	38.38	20.13	4.6
1970	44.75	17.09	4.4	1971	38.74	14.06	4.3	1972	44.01	13.19	4.9	1973	38.32	20.28	4.3
1970	38.76	14.88	4.7	1971	38.70	14.15	4.5	1972	43.81	13.24	4.4	1973	38.25	20.15	4.1
1970	44.31	11.71	4.4	1971	38.77	14.34	4.4	1972	43.84	13.28	4.6	1973	39.97	20.10	4.6
1970	44.31	11.58	4.2	1971	42.49	11.85	4.6	1972	42.04	15.38	4.7	1973	41.80	20.05	4
1970	39.74	16.09	4.4	1971	43.32	12.52	4.7	1972	44.69	18.42	4.9	1973	41.50	19.98	4.7
1970	37.66	20.09	4.4	1971	43.34	12.58	4.2	1972	35.83	14.84	4.6	1973	39.09	16.96	4.7
1970	39.87	19.47	4.5	1971	44.20	16.89	4.8	1972	43.64	15.98	4.9	1973	44.05	12.77	4.2
1970	39.19	15.44	4.4	1971	43.20	12.50	4.2	1972	42.89	17.14	4.6	1973	38.11	19.77	4
1970	41.23	20.01	4.6	1971	42.70	12.17	4.4	1972	43.29	17.65	4.4	1973	45.55	12.01	4
1970	41.47	19.37	4.7	1971	38.71	20.33	4.8	1972	43.66	13.86	4.3	1973	42.38	18.65	4.6
1970	38.45	20.24	4.8	1971	38.03	20.23	4.7	1972	43.79	13.39	4.1	1973	44.08	13.27	5.3
1970	38.68	20.36	5.1	1971	38.03	20.07	4.5	1972	44.30	16.53	4.1	1973	41.64	19.89	4.2
1970	42.83	13.00	4	1971	43.06	13.09	4.5	1972	43.71	13.44	4.9	1973	37.72	19.82	4
1970	44.11	15.95	4.7	1971	43.04	12.97	4.5	1972	43.67	13.47	4.7	1973	44.14	12.69	4
1970	44.67	12.82	4.2	1971	38.98	14.79	4.4	1972	43.71	16.86	5.3	1973	38.80	20.19	4.1
1970	44.15	16.15	4.2	1971	42.50	20.07	4.6	1972	44.04	15.76	4.4	1973	41.75	19.39	4.6
1970	37.94	16.49	4.3	1971	41.91	20.34	4.8	1972	43.84	13.26	4.4	1973	40.82	15.39	4.7

Year	Long	Lat	Mag												
1973	41.73	13.87	4.4	1974	39.74	20.38	4.8	1976	38.64	20.42	4.5	1977	42.69	12.73	4.1
1973	38.90	20.44	5.8	1975	37.88	20.13	4.2	1976	37.99	14.66	4.9	1977	43.21	18.59	4.6
1973	41.68	13.76	4	1975	38.17	15.63	4.9	1976	38.84	14.70	4.9	1977	41.50	20.07	4.7
1973	38.13	20.26	4.2	1975	38.25	15.68	4.1	1976	37.54	20.37	4.9	1977	38.49	20.28	4.6
1973	44.00	11.23	4.2	1975	41.19	19.67	4.6	1976	39.70	18.81	4.6	1977	40.25	19.90	5.1
1973	44.02	13.23	4.4	1975	37.95	19.97	4.5	1976	41.69	19.85	4.6	1977	45.39	12.70	4.7
1973	45.48	18.70	4.8	1975	41.45	19.93	4.2	1976	39.60	18.76	4.7	1977	38.55	15.62	4.7
1973	38.79	14.82	5.1	1975	44.13	11.05	4.6	1976	39.78	18.88	4.7	1977	40.41	12.94	4.5
1973	38.64	20.36	4.6	1975	38.39	15.52	4.4	1976	39.77	18.91	4.5	1977	40.00	15.42	5.6
1973	43.40	12.33	4.1	1975	39.56	19.82	4.6	1976	39.55	18.78	4.3	1977	40.00	15.40	4.4
1974	38.90	14.82	4.3	1975	37.45	14.44	4.5	1976	37.23	20.14	4.2	1978	43.21	17.36	4.3
1974	38.32	19.98	4.7	1975	41.70	15.77	5.2	1976	37.21	20.33	4.3	1978	42.91	15.77	4.4
1974	39.81	14.59	4.6	1975	37.99	20.18	4	1976	42.83	17.19	4.8	1978	42.69	16.17	4.9
1974	38.35	20.22	4.4	1975	43.01	13.87	4.1	1976	37.50	20.08	4.6	1978	41.11	14.89	5
1974	41.85	19.38	4.3	1975	43.67	17.40	4.9	1976	37.21	20.10	4.2	1978	44.13	16.92	4.5
1974	37.15	14.99	4.6	1975	38.67	15.56	4.5	1976	37.44	20.07	4	1978	43.71	13.05	4.1
1974	43.38	17.07	4.7	1975	40.04	19.66	4.5	1976	37.30	20.35	4.8	1978	43.93	16.92	5.1
1974	39.07	20.40	4.2	1975	45.79	15.73	4.4	1976	40.29	19.54	4	1978	37.94	15.80	4.5
1974	38.54	20.42	4.8	1975	41.52	19.30	4.2	1976	38.93	20.17	4.5	1978	38.10	16.03	5.6
1974	44.35	17.71	5.1	1975	41.59	19.31	5.1	1976	41.05	18.91	4.3	1978	43.13	17.82	4.6
1974	39.65	18.66	4	1975	41.47	19.19	4.6	1977	43.55	17.10	5.3	1978	43.64	16.69	4.9
1974	40.12	19.74	4.3	1975	41.47	19.21	4.2	1977	44.04	15.98	4	1978	42.77	12.66	4.3
1974	39.36	15.44	4.7	1975	38.17	20.34	4.6	1977	43.87	15.79	4.3	1978	42.22	13.15	4.3
1974	37.24	19.61	4.3	1975	38.24	15.85	4.1	1977	43.36	18.65	4.7	1978	38.23	15.18	4.1
1974	37.89	19.64	4.1	1975	39.98	20.14	5.2	1977	43.60	12.12	4.7	1978	38.39	15.07	5.7
1974	38.34	19.97	4	1975	44.53	11.86	4.9	1977	41.73	16.40	4.7	1978	38.02	15.58	4.3
1974	38.43	19.78	4.4	1976	45.61	13.11	4.7	1977	37.62	20.07	4.1	1978	44.06	11.01	4.9
1974	40.09	19.70	4.4	1976	38.81	20.39	4.1	1977	37.50	19.88	4.2	1978	38.82	13.87	4.1
1974	39.73	18.85	4.6	1976	38.84	20.28	4.4	1977	44.92	17.39	4.6	1978	43.21	18.72	4.8
1974	43.72	17.58	4.2	1976	44.15	15.72	5.2	1977	44.87	17.37	4	1978	38.31	15.06	4.5
1974	39.70	18.89	4.9	1976	45.75	12.94	5.2	1977	43.18	18.93	4.3	1978	43.17	18.68	4.9
1974	39.73	15.05	4	1976	40.70	19.68	4.9	1977	43.15	16.03	4.7	1978	43.19	18.73	4.8
1974	39.65	18.84	4.3	1976	43.65	12.39	5.3	1977	37.88	14.46	4.9	1978	37.85	20.08	4.1
1974	44.63	18.41	5.1	1976	38.83	16.14	4.5	1977	39.68	18.87	4.3	1978	41.71	20.29	4.7
1974	44.64	18.35	4	1976	43.40	17.49	5.5	1977	40.86	15.24	4	1978	42.65	12.46	4.7
1974	38.96	20.26	4.8	1976	37.84	15.03	4.4	1977	38.44	20.35	4.3	1978	42.58	12.57	4.3
1974	39.93	18.91	4.4	1976	37.56	20.35	6.4	1977	39.25	15.82	4.2	1978	40.12	19.67	4.3
1974	39.71	19.08	4.7	1976	45.46	13.00	4	1977	44.29	11.56	4.5	1978	38.68	15.80	4.3
1974	42.99	12.97	4.9	1976	39.72	20.32	4.6	1977	38.63	14.71	5.3	1978	38.18	20.42	4.1
1974	42.65	13.09	4	1976	37.00	20.32	4	1977	38.57	11.98	4.6	1978	41.86	20.30	5.1
1974	43.06	12.63	4.2	1976	36.73	20.15	4.1	1977	41.56	20.07	4.8	1978	38.02	14.12	4.4
1974	42.80	12.90	4	1976	39.40	20.39	4.6	1977	44.92	17.48	4	1978	39.00	20.23	4.4
1974	38.61	20.41	5	1976	37.40	20.44	4.6	1977	38.85	16.98	5	1978	43.88	16.96	4.3

Year	Long	Lat	Mag												
1978	40.80	16.11	4.3	1979	41.95	19.19	4	1979	42.21	18.77	4	1979	39.07	14.74	4.6
1978	37.34	20.32	4.8	1979	41.83	19.40	4.8	1979	42.98	18.71	4.1	1979	43.53	18.08	5.1
1978	43.62	13.40	4.9	1979	41.84	19.38	4.3	1979	42.24	18.76	4.7	1979	39.66	20.14	4.2
1978	43.73	17.51	4	1979	41.99	19.25	5.2	1979	42.16	18.66	4.1	1979	43.48	18.15	4.7
1978	41.69	19.98	4.6	1979	42.09	18.94	4	1979	42.17	18.77	4.7	1979	40.48	19.27	4.1
1978	41.04	19.65	4.3	1979	41.88	19.31	4.4	1979	42.21	18.77	4.5	1979	43.10	18.87	4.4
1978	40.95	19.67	4.7	1979	41.95	19.36	4.7	1979	42.20	18.74	4.2	1979	41.13	19.90	4.6
1978	43.08	12.83	4.2	1979	41.98	19.17	4.3	1979	41.90	19.02	4.7	1979	39.49	20.08	4.7
1978	44.46	11.99	4.6	1979	41.86	19.40	4.2	1979	43.13	18.88	4.1	1979	40.91	19.98	4
1978	43.38	17.26	4.4	1979	42.52	18.58	4.9	1979	42.32	18.80	4.6	1979	39.99	19.44	4
1978	44.93	11.13	4.1	1979	42.09	18.98	4.2	1979	42.32	18.61	4.8	1979	42.94	18.72	4.4
1978	41.11	13.58	5.6	1979	41.98	19.16	4.1	1979	42.30	18.63	4.8	1979	39.54	20.40	5.4
1979	44.22	15.85	4.1	1979	45.54	14.16	4.3	1979	42.12	18.77	4.8	1979	41.75	19.00	4
1979	38.26	15.01	5.5	1979	41.96	19.11	4.4	1979	42.02	15.22	4.8	1979	39.55	20.36	4.2
1979	38.67	12.86	5.2	1979	41.90	19.14	4	1979	42.29	18.76	4.1	1979	41.07	19.60	4.7
1979	42.81	12.97	4	1979	42.13	19.01	4.8	1979	42.18	18.68	4.8	1979	39.39	20.12	4.5
1979	42.84	13.18	4.4	1979	42.33	19.13	4	1979	42.33	18.60	4.2	1979	39.50	20.02	4
1979	37.80	20.33	4.7	1979	41.98	19.10	4.8	1979	43.16	12.78	4	1979	38.14	20.07	4.3
1979	41.54	20.15	4.5	1979	42.04	18.97	4.6	1979	42.21	18.65	4.5	1979	42.79	13.08	4.1
1979	42.92	12.78	5.1	1979	42.05	18.90	4	1979	42.18	18.71	4.7	1979	41.81	19.07	4.5
1979	38.81	15.85	4.7	1979	41.84	19.79	5	1979	44.53	11.07	4	1979	38.94	20.00	4.1
1979	39.44	15.21	4.5	1979	42.07	19.09	4.6	1979	44.44	11.09	4	1979	39.57	20.19	5.1
1979	41.92	18.98	4.3	1979	41.83	19.41	4.2	1979	43.11	18.84	4.2	1979	43.16	20.01	4.5
1979	41.96	19.02	5.3	1979	41.82	19.12	4.6	1979	44.06	16.63	4.8	1979	41.97	18.83	4.6
1979	41.94	19.09	4.2	1979	41.90	19.10	4.2	1979	43.13	18.82	4.3	1979	40.43	20.16	4.5
1979	42.10	19.21	6.9	1979	41.94	19.20	4.4	1979	42.00	19.08	4.9	1979	44.18	15.74	4.1
1979	41.96	19.16	4.1	1979	41.99	19.15	4.5	1979	41.94	16.72	4.7	1979	43.41	20.03	4.2
1979	41.97	19.35	4.1	1979	41.87	19.24	4.4	1979	42.32	18.74	4	1979	39.26	19.89	4.1
1979	42.33	18.58	4.4	1979	41.78	19.37	4.2	1979	39.23	15.12	4.6	1979	40.84	19.39	4.5
1979	42.07	19.15	4.2	1979	41.99	19.25	4.5	1979	43.54	17.17	4.2	1979	41.30	19.61	4.2
1979	41.96	19.23	4.4	1979	41.84	19.33	4.1	1979	43.17	18.85	4	1979	38.28	11.74	5.4
1979	41.93	19.29	5.1	1979	42.29	18.66	4	1979	42.06	18.96	4.5	1979	43.45	19.91	4.3
1979	42.12	18.97	4.5	1979	42.25	18.76	4.8	1979	42.32	18.53	4.1	1979	38.27	11.60	4.3
1979	41.93	19.33	4.6	1979	42.01	19.23	4.1	1979	42.34	18.55	4.1	1979	42.82	12.94	4.3
1979	41.97	19.11	4.4	1979	42.26	18.77	4.7	1979	43.36	18.79	4.8	1979	42.81	12.97	4.4
1979	42.44	18.63	4.6	1979	42.24	18.84	4	1979	40.99	20.02	4.2	1979	42.26	18.68	4.1
1979	42.71	19.04	4	1979	42.33	18.76	4.9	1979	41.87	19.27	4.2	1979	42.71	12.98	4.1
1979	42.75	19.16	4.5	1979	43.13	18.90	4.1	1979	38.60	16.03	4.6	1979	44.48	11.03	4.1
1979	42.32	18.68	5.7	1979	41.98	19.13	4.7	1979	42.81	13.06	5.9	1979	44.49	11.03	4.1
1979	43.15	18.18	4.6	1979	42.23	18.68	4.2	1979	42.76	12.99	4	1979	41.73	19.30	4.6
1979	41.88	19.23	4.3	1979	43.13	12.86	5.1	1979	42.82	13.02	4.5	1979	42.78	13.11	4
1979	42.53	18.53	4.5	1979	42.26	18.75	6.2	1979	42.79	12.98	4.2	1980	38.36	20.37	4.3
1979	42.08	19.15	4.6	1979	42.21	18.86	5.1	1979	41.96	19.35	4.7	1980	42.15	18.79	4.1

Year	Long	Lat	Mag												
1980	42.31	18.84	4.2	1980	43.03	17.67	4.4	1980	40.85	15.33	5.1	1981	39.44	20.43	4.5
1980	42.35	18.89	4.6	1980	40.75	19.50	4.3	1980	41.29	15.11	4.2	1981	39.28	20.28	4.3
1980	38.62	15.01	4.5	1980	39.72	13.00	4.6	1980	41.02	15.28	4.6	1981	38.49	14.09	4.8
1980	44.34	11.44	4.5	1980	42.73	18.81	4.1	1980	41.14	15.29	4.2	1981	38.43	14.17	4.4
1980	39.30	16.21	4.8	1980	37.68	20.15	4.2	1980	40.74	15.48	4.9	1981	37.87	20.12	4.9
1980	39.32	16.19	4.6	1980	38.19	20.32	4.2	1980	40.86	15.51	4.7	1981	38.27	20.02	4.1
1980	42.82	12.99	5.1	1980	42.77	18.69	4.1	1980	40.91	15.29	4.2	1981	38.27	20.00	4.1
1980	42.82	13.03	4.4	1980	40.91	15.37	6.9	1980	40.82	15.24	4.4	1981	37.91	20.06	4.4
1980	42.81	13.02	4.2	1980	41.11	15.28	4.8	1980	38.89	16.22	4.8	1981	38.02	20.10	4.5
1980	42.81	13.04	4	1980	40.67	15.61	4.8	1980	40.90	15.25	4.4	1981	38.36	19.96	4.5
1980	39.03	16.56	4.2	1980	40.72	15.59	4.7	1981	43.73	16.79	4	1981	38.30	20.04	4.3
1980	39.94	16.13	4.6	1980	41.12	15.87	4.4	1981	39.90	13.57	4.6	1981	38.14	20.02	4.2
1980	38.69	20.32	4.6	1980	40.85	15.35	4.9	1981	37.94	20.05	4.6	1981	37.93	20.15	4.6
1980	42.78	13.06	4.1	1980	40.97	15.37	4.6	1981	40.77	15.76	4.5	1981	37.92	20.06	4.5
1980	42.80	13.04	4	1980	40.80	15.30	4.5	1981	39.77	20.01	4.1	1981	38.43	20.07	4.2
1980	42.77	13.06	4.2	1980	41.54	15.71	4.5	1981	40.88	15.43	4.5	1981	37.89	20.07	5.2
1980	38.71	20.38	4.9	1980	40.96	15.09	4.6	1981	40.95	15.37	5.3	1981	38.32	19.91	4.5
1980	38.69	20.26	4.9	1980	40.83	15.31	4.6	1981	40.85	15.41	4.3	1981	37.57	20.18	4
1980	40.61	13.56	4.3	1980	41.43	15.76	4.4	1981	41.04	15.32	4.1	1981	37.86	20.02	4.4
1980	44.39	17.77	4	1980	40.89	15.26	5.1	1981	40.76	15.46	4.1	1981	37.91	20.04	4.7
1980	39.38	20.01	4.2	1980	40.77	15.36	4.5	1981	40.70	15.42	4	1981	38.07	19.89	4.4
1980	39.08	14.55	4.5	1980	39.04	14.59	4.5	1981	39.55	19.46	4.5	1981	38.25	20.03	4.3
1980	40.46	15.86	4.5	1980	40.90	15.33	4.9	1981	41.05	14.60	4.9	1981	37.96	19.84	4.4
1980	43.01	17.70	4.1	1980	40.98	15.25	4.2	1981	37.04	14.50	4.4	1981	38.35	19.97	4.3
1980	42.85	13.16	4.5	1980	40.91	15.39	4.4	1981	43.24	17.40	4.4	1981	38.09	19.98	4.4
1980	42.15	13.22	4.2	1980	40.87	15.20	4	1981	43.30	17.54	4.3	1981	37.89	19.95	4.1
1980	38.48	14.25	5.7	1980	40.96	15.01	4.5	1981	41.89	19.42	4.2	1981	38.24	19.96	4.3
1980	42.81	13.16	4.2	1980	41.02	15.01	4.3	1981	40.80	15.56	4.1	1981	37.97	19.95	4.2
1980	38.39	14.33	4.9	1980	40.86	15.24	4.4	1981	43.23	18.71	4.5	1981	37.88	20.11	4.6
1980	38.72	14.42	4.2	1980	40.77	15.35	4.3	1981	43.19	18.66	4.3	1981	41.45	19.53	4.4
1980	42.29	13.88	4.6	1980	40.77	15.32	4.7	1981	38.35	14.87	4	1981	38.35	20.08	4.4
1980	40.11	20.42	4.4	1980	40.70	15.47	5.1	1981	41.12	20.07	4	1981	38.68	20.05	4
1980	38.74	20.29	4.7	1980	40.71	15.48	4.4	1981	39.88	20.16	4	1981	38.14	19.87	4.6
1980	42.53	12.79	4	1980	40.65	15.40	5.3	1981	39.60	15.34	4.6	1981	37.94	20.01	4
1980	41.85	13.74	5	1980	41.20	15.30	4.4	1981	44.04	19.04	4	1981	38.30	20.02	4.1
1980	41.88	13.70	4.5	1980	40.69	15.64	4.5	1981	37.91	20.08	4.6	1981	38.18	19.87	4.3
1980	43.11	17.42	5.1	1980	41.08	15.28	4.3	1981	37.95	20.15	4.4	1981	38.05	19.97	4.6
1980	40.77	19.22	4.9	1980	40.88	15.38	4.4	1981	37.89	20.11	4.2	1981	37.58	20.20	4.4
1980	41.46	20.28	4.9	1980	40.97	15.35	4.6	1981	37.87	20.13	4.4	1981	38.08	19.93	4.6
1980	45.15	15.07	4	1980	40.91	15.46	4.5	1981	37.67	12.47	4.9	1981	38.24	19.84	4.7
1980	44.36	18.59	4.4	1980	41.02	15.24	4.7	1981	38.41	20.09	4.2	1981	37.97	19.83	4.4
1980	39.93	14.99	4	1980	41.35	15.13	4.3	1981	37.16	12.60	4.6	1981	38.23	19.57	4.1
1980	41.71	13.20	4.4	1980	40.52	15.73	4.6	1981	38.38	16.47	4.6	1981	38.33	19.90	4.1

Year	Long	Lat	Mag												
1981	37.92	19.90	4.2	1981	38.13	19.91	4.2	1982	41.39	14.95	4.3	1983	38.14	19.79	4.2
1981	38.09	19.84	4.2	1982	42.96	17.36	4.5	1982	41.38	20.04	4	1983	38.16	19.88	4.6
1981	38.24	19.82	4.4	1982	43.77	11.00	4.8	1982	39.31	15.49	4.2	1983	38.03	19.76	4.3
1981	38.16	19.75	4.1	1982	39.34	20.35	4	1982	43.10	19.03	4	1983	38.14	19.78	4.3
1981	38.37	20.07	4.1	1982	37.55	20.38	4.1	1982	37.56	20.26	4.7	1983	38.19	19.76	4.4
1981	38.72	20.17	4	1982	42.21	19.20	4.3	1982	40.90	15.41	4.3	1983	38.15	19.85	4.2
1981	41.15	19.84	4.7	1982	37.81	16.28	4.2	1982	38.54	19.56	4.2	1983	38.03	19.96	4.6
1981	37.91	20.01	4.7	1982	38.53	20.10	4.3	1982	43.07	18.02	4.1	1983	37.80	19.85	4.4
1981	38.33	20.05	4.1	1982	39.89	19.75	4.3	1982	43.18	17.81	4.1	1983	38.35	19.85	4
1981	38.45	20.13	4	1982	40.01	19.83	4	1982	43.17	12.56	4.3	1983	38.11	19.99	4.1
1981	37.88	19.95	4.1	1982	41.84	13.62	4.2	1982	43.16	12.56	4.3	1983	38.30	20.08	4.5
1981	37.91	20.00	4.4	1982	39.92	15.78	5.2	1982	43.12	12.59	4.6	1983	38.15	20.09	4.3
1981	38.11	19.89	4.2	1982	44.48	11.82	4.1	1982	43.16	12.59	4.7	1983	38.22	20.11	5
1981	42.05	18.88	4.4	1982	40.19	19.68	4.3	1982	43.20	12.60	4.3	1983	38.62	19.58	4.4
1981	38.17	19.88	4.1	1982	38.50	15.50	4.9	1982	43.13	12.63	4.6	1983	38.16	19.92	4.4
1981	38.21	20.16	4.2	1982	38.66	20.25	4.9	1982	43.16	12.67	4.4	1983	38.34	19.57	4.3
1981	38.29	20.08	4.1	1982	38.02	19.78	4.1	1982	38.03	14.83	4.4	1983	37.98	19.69	4.3
1981	38.09	19.88	4.4	1982	41.93	19.13	4.5	1982	38.04	14.81	4.1	1983	38.04	19.95	4.4
1981	37.58	20.09	4	1982	41.89	20.00	4.3	1982	42.07	19.20	4.5	1983	37.84	19.96	4.6
1981	44.85	17.31	5.4	1982	43.31	18.79	4.1	1982	40.88	19.59	5.6	1983	38.26	20.16	4.5
1981	38.12	20.06	4.4	1982	42.64	18.86	4.2	1982	40.86	19.52	4.9	1983	38.25	19.60	4.2
1981	42.20	18.92	4.5	1982	42.41	18.64	4.2	1982	40.85	19.44	4.4	1983	37.74	20.05	4.5
1981	42.08	20.19	4.5	1982	38.96	19.99	4	1982	40.77	19.40	4.6	1983	38.10	20.07	4.6
1981	45.86	17.50	4.1	1982	43.44	17.36	4.5	1982	42.76	18.58	4.4	1983	38.17	20.23	5.1
1981	38.87	15.60	4.2	1982	39.77	20.27	4.3	1982	42.83	18.62	4.2	1983	38.06	20.13	4.5
1981	38.09	20.04	4.1	1982	39.67	15.43	4.3	1982	45.61	15.45	4	1983	38.56	20.01	4.1
1981	38.23	20.07	4.2	1982	45.70	14.63	4.3	1983	41.93	19.11	4.5	1983	38.27	19.68	4.1
1981	38.12	20.11	4.3	1982	38.59	14.66	4.3	1983	38.03	20.23	6.1	1983	37.74	19.87	4.6
1981	38.22	20.01	4	1982	43.49	20.10	4.1	1983	37.73	19.87	4.6	1983	38.48	20.03	4.1
1981	38.19	20.02	4.1	1982	37.40	20.34	4.6	1983	37.67	19.82	4.9	1983	37.89	19.96	5.3
1981	40.74	15.76	4.4	1982	38.27	20.07	4.2	1983	37.85	19.43	4.2	1983	39.03	19.82	4.3
1981	40.74	15.91	4.1	1982	44.25	10.88	4.2	1983	38.15	19.89	4.3	1983	38.11	19.88	4.6
1981	36.99	20.44	4.1	1982	40.88	19.75	4.1	1983	38.19	19.94	4.2	1983	38.15	20.03	4.5
1981	41.17	20.11	4.1	1982	38.49	19.57	4	1983	38.08	19.82	4.2	1983	38.20	19.92	4.2
1981	38.85	14.70	4.2	1982	37.23	20.08	4.4	1983	37.96	19.83	4.2	1983	38.22	19.97	4.5
1981	42.54	20.10	4	1982	39.72	20.44	4.9	1983	38.49	19.36	4.1	1983	38.22	19.87	4.3
1981	40.74	15.64	4.9	1982	37.97	19.98	4.6	1983	38.10	20.30	4.9	1983	38.09	20.14	4.3
1981	40.10	19.84	4	1982	38.21	19.97	4.2	1983	38.22	19.80	4.1	1983	38.08	19.77	4.1
1981	43.14	19.59	4	1982	40.81	15.36	4.8	1983	38.16	19.86	4.5	1983	38.51	20.14	4
1981	37.29	20.43	4.8	1982	39.30	20.27	4	1983	38.04	20.16	5.1	1983	38.09	20.11	4.7
1981	43.50	19.91	4.4	1982	39.59	20.40	4.5	1983	37.88	19.93	4.3	1983	38.02	19.97	4.4
1981	40.31	15.92	4.1	1982	39.41	20.36	4	1983	37.87	20.30	4.3	1983	38.88	19.67	4.1
1981	43.06	18.19	4	1982	38.80	20.28	4.8	1983	38.04	19.93	4	1983	37.77	19.99	4.2

Year	Long	Lat	Mag												
1983	37.81	20.02	4.2	1983	38.01	20.10	4.2	1983	38.18	19.94	4.1	1983	38.55	20.17	4.5
1983	37.58	19.66	4.5	1983	37.52	20.40	4	1983	38.14	20.05	4.1	1983	38.41	20.34	4
1983	38.17	19.91	4.8	1983	38.10	20.05	4.2	1983	38.42	20.09	4.6	1983	43.78	18.86	4
1983	38.63	19.96	4.1	1983	37.84	20.17	4.7	1983	36.76	19.83	4.7	1983	37.86	14.59	4.3
1983	38.14	19.95	4.2	1983	37.83	19.92	4	1983	38.07	20.15	4.9	1983	38.18	20.02	4.4
1983	37.78	20.16	4.5	1983	37.89	20.10	5.2	1983	38.28	20.09	4.8	1983	38.48	20.23	4.8
1983	37.96	20.05	4.6	1983	37.85	19.87	4.5	1983	38.20	19.92	4.3	1983	38.53	20.36	4.9
1983	38.06	19.94	4.3	1983	37.81	20.03	4.2	1983	38.19	19.94	4.4	1983	38.47	20.31	4.6
1983	38.19	19.64	4.2	1983	37.86	19.95	4.3	1983	38.20	20.05	5	1983	38.20	20.04	4
1983	38.29	19.46	4	1983	37.82	19.98	4.2	1983	38.18	20.11	4.6	1983	38.51	20.30	4.7
1983	38.11	19.93	4.3	1983	38.13	20.07	4.7	1983	38.62	20.04	4.1	1983	38.43	20.33	4.1
1983	38.12	19.96	4.2	1983	37.41	19.11	4.4	1983	38.04	19.95	4.4	1983	38.49	20.36	5
1983	38.49	19.86	4.2	1983	38.13	20.04	4	1983	38.55	19.86	4.3	1983	38.44	20.28	4.9
1983	38.07	20.02	4.1	1983	40.17	19.59	4.4	1983	38.20	19.95	4.8	1983	38.31	20.20	4.2
1983	38.24	20.16	4.3	1983	38.07	20.12	4.4	1983	38.16	20.11	5	1983	38.43	20.16	4.1
1983	38.12	20.06	4.6	1983	37.93	20.03	4.4	1983	38.48	20.07	4	1983	38.33	20.32	4.2
1983	37.84	19.46	4.4	1983	37.41	19.95	4.2	1983	38.25	20.03	4.9	1983	38.13	20.26	4
1983	38.20	20.35	4.4	1983	37.74	20.04	4.3	1983	38.19	20.14	4.8	1983	38.32	20.30	4.5
1983	37.96	19.73	4	1983	39.72	20.06	4	1983	38.04	20.20	4.9	1983	38.32	20.28	4.7
1983	38.09	19.96	4.2	1983	37.93	19.94	4.2	1983	38.11	20.05	4.3	1983	37.96	19.94	4.1
1983	38.34	19.68	4.1	1983	38.00	20.13	4	1983	38.34	19.94	4.2	1983	38.38	20.04	4.4
1983	38.29	20.02	4.2	1983	38.18	20.07	4.5	1983	38.13	19.58	4	1983	38.47	20.29	4.5
1983	38.13	20.16	4	1983	38.13	20.31	4	1983	38.11	19.63	4.1	1983	37.52	20.30	4.2
1983	38.16	20.01	4.3	1983	38.18	20.11	4.3	1983	38.17	19.92	4.7	1983	39.03	15.56	4
1983	38.11	20.30	5.1	1983	38.62	19.74	4.2	1983	38.52	20.04	4.4	1983	37.76	20.29	4
1983	38.06	19.94	4.4	1983	37.99	20.02	4	1983	38.27	19.99	4.8	1983	38.11	20.20	4.3
1983	37.73	20.07	4.1	1983	37.68	19.90	4	1983	38.16	19.68	4.2	1983	38.42	20.39	4
1983	40.59	15.74	4.4	1983	38.15	20.06	4.7	1983	38.13	19.87	4	1983	37.50	15.15	4.4
1983	38.10	20.20	4.6	1983	38.38	19.74	4.4	1983	38.08	19.89	4	1983	45.86	11.33	5.1
1983	38.03	20.11	4.4	1983	38.18	19.95	4.4	1983	38.30	19.95	4	1983	40.62	15.23	4.4
1983	37.82	19.91	4.7	1983	38.29	20.26	5.8	1983	38.19	20.09	4.8	1983	44.26	15.83	4
1983	38.05	19.94	4.2	1983	38.03	19.82	4.5	1983	37.82	20.03	4	1983	37.70	20.24	4.2
1983	38.56	20.02	4	1983	38.06	19.82	4.5	1983	38.10	20.02	4.5	1983	45.81	13.77	4.1
1983	41.70	19.71	4.4	1983	38.21	19.80	4.1	1983	38.41	19.89	4	1983	39.84	19.80	4.1
1983	38.31	19.70	4.1	1983	38.11	20.08	4.7	1983	38.26	20.12	4.3	1983	39.80	19.85	4.1
1983	38.26	20.10	4.2	1983	38.01	19.78	4.2	1983	37.89	20.03	4.1	1983	41.75	13.85	4.8
1983	38.42	20.04	4.2	1983	38.45	20.04	4.9	1983	37.89	20.29	4.1	1983	37.94	20.21	4.6
1983	38.68	20.05	4.1	1983	38.27	20.04	5	1983	38.24	20.16	4.1	1983	38.29	20.33	4.3
1983	38.71	20.16	4.1	1983	38.15	20.15	4.2	1983	38.52	20.18	4.7	1983	42.68	18.30	4.7
1983	37.95	20.19	4.3	1983	38.61	19.91	4.2	1983	37.84	20.23	4.1	1983	37.71	12.93	4.4
1983	38.07	20.15	4.2	1983	38.15	19.91	4.3	1983	37.98	20.13	4	1983	40.88	15.21	4.3
1983	38.06	20.14	4.3	1983	38.18	20.32	5.3	1983	38.19	19.72	4	1983	40.36	14.92	4.6
1983	38.15	20.38	4.3	1983	38.33	20.00	4	1983	43.75	16.28	4.4	1983	41.81	16.11	4.1

Year	Long	Lat	Mag												
1983	45.47	15.91	4.3	1984	41.77	13.82	4.3	1984	39.69	14.20	4.9	1985	42.28	13.34	4.1
1983	42.35	18.79	4.1	1984	41.78	13.87	4.6	1984	37.66	19.95	4.2	1985	41.15	19.81	4.3
1983	42.26	18.78	4.1	1984	41.74	13.95	4.2	1984	41.78	13.87	4.7	1985	39.85	15.75	4.3
1983	38.66	12.92	5	1984	41.83	13.94	4.8	1984	39.78	16.62	4	1985	39.66	20.18	4
1983	39.53	14.15	4.7	1984	41.72	13.86	4.3	1984	37.32	20.41	4.7	1985	43.99	17.53	4
1983	39.12	15.92	4.5	1984	41.77	13.90	4.6	1984	37.74	15.41	4.4	1985	39.87	13.58	4.9
1983	37.93	20.12	4.8	1984	41.84	13.89	4	1984	45.45	14.22	4	1985	37.90	12.77	4
1983	37.98	19.93	4.8	1984	41.45	14.06	4.1	1984	39.65	15.59	4.9	1985	38.27	12.84	4.6
1983	42.16	18.74	4.5	1984	41.61	13.95	4.1	1984	38.68	20.26	4	1985	43.49	17.50	4.1
1983	41.96	19.07	5.3	1984	42.17	13.57	4.3	1984	41.01	19.93	4.4	1985	44.88	14.92	4
1984	40.13	15.72	4.5	1984	41.93	13.82	4.1	1984	39.77	20.44	4.5	1985	43.90	16.72	4.4
1984	40.23	19.81	4	1984	42.97	17.73	5.1	1984	37.63	20.33	4.1	1985	39.04	20.35	4.2
1984	42.78	18.13	4.7	1984	42.94	17.69	4.7	1984	41.99	19.56	4.3	1985	39.58	18.49	4.1
1984	38.48	20.16	4.7	1984	42.98	17.72	4	1984	42.04	19.68	4.1	1985	42.91	17.62	5
1984	42.04	19.05	4.9	1984	42.94	17.64	4	1984	42.04	19.74	4.8	1985	43.92	16.54	4.1
1984	40.05	19.64	4.2	1984	42.97	17.62	4.2	1984	42.05	19.75	4	1985	42.45	18.52	4.4
1984	38.12	20.09	4.7	1984	41.85	13.85	4	1984	41.98	19.62	4	1985	38.04	16.36	4.3
1984	39.69	15.72	4.2	1984	42.85	18.53	4	1984	42.02	19.78	4.8	1985	41.53	15.63	4.2
1984	42.90	18.64	4.1	1984	43.00	17.74	4.2	1984	39.49	13.28	4.5	1985	37.94	19.86	4.4
1984	42.01	19.09	4.4	1984	42.96	17.72	4.9	1984	37.42	19.90	4.3	1985	42.27	19.91	4.6
1984	42.59	19.13	4	1984	42.75	17.30	4.1	1985	39.35	16.29	4.6	1985	42.30	19.90	4.2
1984	45.87	15.48	4.6	1984	42.95	17.67	4.6	1985	37.45	20.23	4.1	1985	41.70	19.39	5.5
1984	39.03	20.36	4.2	1984	39.94	19.98	4.2	1985	40.76	19.20	5.3	1985	41.65	19.28	4.5
1984	44.57	17.12	4.2	1984	38.53	13.40	4.2	1985	38.53	15.38	4.2	1985	42.32	19.86	4.1
1984	39.42	15.23	5.1	1984	43.17	17.92	4	1985	38.29	20.32	4.6	1985	41.90	20.04	4.4
1984	38.46	14.11	4.1	1984	37.86	20.15	4.5	1985	37.67	19.98	4.6	1985	42.31	19.90	4.5
1984	41.09	19.99	4.4	1984	41.68	13.88	4.2	1985	41.53	20.35	4.6	1985	42.26	19.90	4
1984	44.57	17.17	4.4	1984	44.48	11.04	4	1985	41.63	14.26	4.3	1985	42.29	19.85	4.6
1984	43.37	17.51	4	1984	39.48	16.61	4.4	1985	37.91	20.02	4.8	1985	42.31	19.91	4.2
1984	43.36	17.41	4.1	1984	41.83	13.92	4.2	1985	43.31	17.32	4.5	1985	43.89	12.04	4.5
1984	43.26	12.56	5.2	1984	38.26	20.08	4.2	1985	43.89	16.51	4.5	1985	42.31	19.85	4.2
1984	43.26	12.44	4.1	1984	41.17	19.71	4	1985	39.11	15.79	4.3	1985	42.30	18.75	4.8
1984	43.19	12.50	4.3	1984	41.83	13.95	4.5	1985	40.81	20.35	4.5	1985	42.36	18.85	4.5
1984	43.17	12.65	4.4	1984	39.17	14.78	4	1985	43.00	13.71	4.4	1985	42.29	18.74	5
1984	43.24	12.46	4.6	1984	38.24	19.85	4.2	1985	42.29	19.45	4.2	1985	42.32	18.77	4.1
1984	43.26	12.52	4.6	1984	38.04	20.00	4.2	1985	38.61	20.21	4	1985	43.42	12.16	4
1984	41.77	13.90	5.5	1984	39.64	14.87	4.4	1985	44.01	18.20	4.2	1985	42.30	18.75	4.9
1984	41.69	13.83	4.5	1984	37.76	19.82	4.1	1985	38.22	15.68	4	1985	42.30	19.90	4.5
1984	41.78	13.82	4.1	1984	44.01	17.14	4.2	1985	42.31	13.31	4.1	1985	42.29	19.89	4
1984	41.69	13.76	4.2	1984	44.90	17.34	4.5	1985	38.32	20.20	4.6	1985	41.71	19.33	4
1984	41.82	19.55	4.1	1984	43.95	17.14	4.2	1985	42.25	13.30	4.7	1985	42.23	19.92	4.6
1984	43.22	12.48	4.3	1984	41.38	14.53	4.1	1985	38.34	14.99	4.2	1985	42.21	19.91	4.6
1984	41.83	13.96	5.2	1984	42.93	17.78	4.9	1985	40.00	20.08	4.3	1985	43.52	16.91	4.2

Year	Long	Lat	Mag												
1985	42.27	19.93	4	1986	37.86	20.06	4.1	1987	40.95	15.47	4.6	1987	45.76	11.37	4
1985	42.27	19.91	4.4	1986	44.45	10.77	4.4	1987	38.70	14.78	4.2	1987	39.07	15.55	4.7
1985	37.69	15.07	4.3	1986	41.22	19.51	4.4	1987	36.29	12.70	4.3	1987	38.58	15.36	4.3
1985	42.28	19.95	4.3	1986	41.11	19.48	4.6	1987	37.78	14.76	4.3	1987	42.10	19.06	4.4
1985	37.69	15.18	4.3	1986	36.47	11.36	4.7	1987	40.20	19.82	5.1	1987	39.47	20.01	4.3
1985	42.35	19.87	4.7	1986	40.02	19.58	4.2	1987	38.47	20.29	5.3	1988	39.66	20.26	4.3
1986	42.57	15.33	4.4	1986	40.11	14.15	4.3	1987	44.11	16.40	4.3	1988	40.08	16.01	4.8
1986	42.59	15.32	4.8	1986	44.34	12.00	4.1	1987	44.15	12.20	4.2	1988	41.25	19.63	5.3
1986	42.65	15.41	4.3	1986	43.57	13.66	4.2	1987	44.17	12.19	4.2	1988	41.17	19.66	4.2
1986	39.47	15.34	4.4	1986	41.19	19.56	4.7	1987	38.92	15.71	4.4	1988	40.33	15.48	4.3
1986	42.35	19.89	4.2	1986	37.54	20.27	4.2	1987	41.64	12.61	4.1	1988	39.76	20.15	4.3
1986	40.26	12.73	4.4	1986	37.84	20.19	4.3	1987	44.21	12.14	4.9	1988	44.58	17.67	4.5
1986	42.29	19.93	4.4	1986	40.68	15.66	4.6	1987	43.69	20.44	4.9	1988	42.84	17.63	4.1
1986	42.31	19.87	4.6	1986	42.77	17.96	4.2	1987	44.85	11.11	4.4	1988	42.14	19.11	4.6
1986	42.62	15.37	4.9	1986	37.40	20.40	4.6	1987	39.42	14.96	4.5	1988	40.45	19.07	4.1
1986	42.44	15.19	4.2	1986	37.48	20.17	4.2	1987	42.69	15.26	4.2	1988	39.76	15.34	4.5
1986	41.24	19.49	4.8	1986	37.44	20.36	4.3	1987	43.25	13.94	5.3	1988	40.16	19.67	4.3
1986	42.25	19.99	4.9	1986	38.55	15.77	4.2	1987	43.26	13.85	4.1	1988	42.09	19.21	4.3
1986	43.15	12.94	4.7	1986	39.52	15.56	4.1	1987	43.27	13.90	4.4	1988	42.36	16.52	4.2
1986	42.63	15.33	4.8	1986	37.70	19.98	4.1	1987	43.79	12.23	4.5	1988	40.18	19.89	5
1986	37.87	20.28	4	1986	37.88	20.10	4	1987	43.28	13.87	4.4	1988	42.48	16.64	4.1
1986	37.89	20.05	4.1	1986	44.38	10.87	4.6	1987	42.53	19.39	4.3	1988	42.39	16.59	4.2
1986	38.11	20.21	4.1	1986	42.96	13.21	4.1	1987	43.32	20.06	4.1	1988	38.40	14.76	4.4
1986	41.97	20.29	5	1986	42.89	13.20	4.4	1987	44.74	11.29	4.1	1988	40.11	19.99	4.1
1986	41.95	20.29	4.7	1986	43.16	13.83	4	1987	44.05	11.85	4.3	1988	37.93	20.28	4
1986	41.93	20.27	4.3	1986	39.63	20.23	4.2	1987	37.27	20.05	4.1	1988	39.76	16.93	4.7
1986	43.74	13.20	4.2	1986	43.17	13.85	4.7	1987	38.51	20.41	4	1988	42.37	16.60	5.1
1986	39.83	13.59	4.9	1986	41.93	19.46	4.9	1987	38.53	20.38	4.3	1988	42.21	16.48	4.5
1986	41.90	20.30	4	1986	41.95	19.43	4.3	1987	37.90	15.07	4.8	1988	42.37	16.61	4.1
1986	41.13	20.10	5.1	1986	37.48	20.02	4.3	1987	43.73	20.41	5	1988	37.71	19.97	4.7
1986	39.10	20.33	4	1986	42.91	18.18	4.1	1987	44.10	12.01	4	1988	40.51	19.73	4.1
1986	43.25	18.86	4.1	1986	44.12	16.34	5.3	1987	43.24	13.87	5.1	1988	38.44	20.43	4.5
1986	41.71	14.99	4.4	1986	44.06	16.22	4.5	1987	44.08	13.03	4	1988	38.45	20.37	4.4
1986	45.10	14.77	4.1	1986	36.46	13.51	4.3	1987	37.80	16.01	4.2	1988	38.25	20.44	4.1
1986	39.29	15.37	4.5	1986	44.06	15.23	4.3	1987	43.25	13.89	4.6	1988	37.09	19.88	4.3
1986	39.34	20.33	4.1	1986	38.61	14.93	4.3	1987	37.34	20.39	4.4	1988	38.36	20.42	4.6
1986	37.99	20.21	4.6	1986	44.85	11.42	4.5	1987	35.54	12.95	4	1988	38.41	20.42	4.2
1986	43.68	16.46	4.2	1986	42.96	14.16	4.2	1987	44.18	12.20	4.2	1988	38.27	20.34	4
1986	37.27	20.39	4.5	1986	37.74	20.38	4	1987	37.59	20.42	4.4	1988	39.33	14.19	4.4
1986	42.33	19.97	4.1	1986	45.06	14.80	5	1987	39.65	15.48	4.5	1988	38.27	20.41	4
1986	38.15	19.67	4	1986	39.84	19.87	4.9	1987	44.07	16.36	4.1	1988	40.59	20.30	4.1
1986	36.75	19.85	4	1986	44.09	16.35	4.8	1987	43.42	18.51	4.4	1988	43.70	17.44	5
1986	37.84	20.05	4.2	1987	43.72	16.84	4.8	1987	38.38	20.23	4.2	1988	43.64	17.26	4

Year	Long	Lat	Mag												
1988	43.33	17.78	4.4	1989	45.80	11.21	5.1	1990	45.83	14.62	4	1991	42.12	13.27	4.1
1988	40.41	19.20	4.1	1989	37.80	14.96	4.3	1990	42.72	12.88	4.3	1991	40.56	20.27	4.5
1988	44.08	11.78	4	1989	41.26	19.48	4.1	1990	44.64	17.58	4.7	1991	41.31	20.25	4.5
1988	40.15	19.74	4.7	1989	42.24	15.55	4.6	1990	41.33	20.09	4.1	1991	40.19	13.82	5.5
1988	38.07	20.35	4	1989	42.21	15.59	4.7	1990	43.02	17.81	4.9	1991	40.67	19.59	4
1988	37.44	20.43	4.5	1989	43.62	18.86	4.3	1990	43.02	17.78	4.6	1991	39.26	20.43	4.5
1988	38.03	20.14	4.5	1989	42.87	12.91	4.3	1990	38.81	14.76	4.3	1991	41.15	20.00	4.1
1988	39.74	20.36	4.6	1989	42.88	12.95	4.1	1990	43.02	17.76	4.6	1991	37.97	19.95	4.8
1988	44.74	14.97	4.5	1989	38.13	15.91	4.1	1990	40.13	19.78	4.3	1991	39.29	16.72	4.3
1989	35.63	11.63	5	1989	38.63	15.18	4.4	1990	40.16	19.77	4.2	1991	39.65	19.75	4.1
1989	35.69	11.69	4	1989	43.65	16.87	4.9	1990	38.27	20.41	4.5	1991	39.72	19.68	4.2
1989	35.59	11.69	5	1989	43.66	16.88	4.3	1990	43.37	17.31	4.1	1991	44.11	19.07	4.8
1989	35.37	11.50	4	1989	43.81	12.50	4	1990	40.76	15.92	4.2	1991	40.53	19.58	4
1989	41.69	19.37	4	1989	43.06	12.76	4.7	1990	42.80	12.65	4	1991	40.27	15.95	4.6
1989	35.65	11.63	5.1	1989	41.18	19.86	4	1990	44.13	19.33	4	1991	40.73	15.77	5.1
1989	40.17	19.54	4.3	1990	39.17	16.93	4.5	1990	37.83	19.81	4.5	1991	38.91	20.30	4.1
1989	37.76	19.83	4.1	1990	39.19	16.95	4.1	1990	38.00	20.13	4.4	1991	42.54	13.14	4.1
1989	44.82	14.65	4.2	1990	38.38	20.29	4.1	1990	43.86	20.35	4.2	1991	42.93	18.57	4.3
1989	35.58	11.71	4.4	1990	42.17	15.66	4	1990	40.50	19.56	4.3	1991	35.63	11.66	4.8
1989	44.87	17.34	4	1990	42.15	15.61	4.1	1990	36.23	14.67	4.5	1991	37.98	15.52	4.5
1989	39.93	19.65	4.4	1990	42.20	15.57	4.7	1990	43.85	16.63	5.1	1991	42.16	18.75	4.9
1989	40.18	19.56	4.4	1990	37.89	20.01	4	1990	43.90	16.64	5.1	1991	39.22	16.20	4.2
1989	41.24	19.89	5.1	1990	42.18	15.56	4.4	1990	43.88	16.67	4.2	1991	37.65	15.12	4.5
1989	42.94	18.40	4	1990	38.69	15.25	4.4	1990	43.84	16.62	4.3	1991	41.24	20.22	4.2
1989	42.83	18.73	4.5	1990	42.18	16.45	4.7	1990	43.85	16.56	4	1992	43.21	18.28	4.3
1989	39.69	20.28	4.5	1990	41.22	19.63	4.1	1990	39.96	15.75	4.2	1992	38.36	20.23	4.4
1989	42.95	17.61	4.1	1990	41.26	19.94	4.5	1990	43.88	16.66	4.3	1992	38.35	20.32	5.1
1989	40.59	15.76	4.5	1990	45.88	14.69	4	1990	43.47	17.50	4.2	1992	38.36	20.31	5
1989	39.67	20.01	4.4	1990	38.19	14.93	4.7	1990	43.90	16.55	4.4	1992	38.28	20.27	4.2
1989	38.30	20.44	4	1990	43.42	17.39	5.6	1990	43.85	16.60	4.2	1992	38.36	20.37	4.1
1989	39.68	20.27	4	1990	43.39	17.42	4	1990	35.53	11.54	4.4	1992	38.29	20.31	4.3
1989	39.62	20.17	4	1990	38.20	20.30	4.5	1990	37.30	15.44	5.5	1992	36.62	16.03	4.5
1989	37.65	19.85	4.2	1990	42.14	19.20	4.6	1990	39.35	15.36	5.3	1992	42.45	14.28	4.1
1989	41.94	20.02	4.7	1990	42.13	19.13	5.1	1990	37.28	15.45	4.5	1992	45.46	14.33	4.1
1989	40.81	20.11	4.3	1990	41.01	19.78	4.9	1990	42.86	17.91	4	1992	38.51	20.35	4.5
1989	37.98	20.15	4.1	1990	43.32	19.89	4.3	1990	40.26	19.54	4.3	1992	38.95	17.03	4.1
1989	42.22	15.54	4.1	1990	38.49	20.35	4.3	1990	39.27	19.86	4.3	1992	44.44	11.94	4.3
1989	38.00	20.18	5.1	1990	40.74	15.85	4.6	1990	36.02	11.08	5	1992	37.84	14.62	4.7
1989	37.95	20.10	4.7	1990	40.78	15.77	5.3	1991	43.24	18.99	4	1992	44.48	11.06	4.4
1989	38.07	20.04	4.2	1990	40.75	15.81	5	1991	43.28	19.12	4.3	1992	43.26	17.98	4.3
1989	38.01	20.10	4.3	1990	41.28	20.24	4.1	1991	43.29	19.12	4.4	1992	38.58	14.94	5.4
1989	41.74	12.70	4.1	1990	43.58	12.13	4	1991	42.40	16.71	4.2	1992	43.69	17.65	4
1989	43.16	13.34	4.2	1990	40.68	19.81	5.2	1991	43.84	11.87	4.1	1992	36.70	20.43	4.1

Year	Long	Lat	Mag												
1992	43.27	17.49	4.1	1993	43.12	12.68	4.4	1994	43.57	16.52	4.5	1995	41.10	15.05	4.2
1992	40.11	19.75	4.7	1993	43.12	12.68	4.9	1994	38.79	20.34	4.3	1995	38.05	20.22	4.1
1992	43.67	16.82	4.7	1993	39.26	20.39	4.1	1994	41.20	19.97	4	1995	37.58	13.85	4.2
1992	39.00	20.03	4.3	1993	42.26	19.51	4.1	1994	38.65	20.38	4.1	1995	39.61	17.08	4.1
1992	44.19	11.52	4	1993	37.99	14.22	4.9	1994	39.75	15.46	5.1	1995	43.15	15.16	4.5
1992	44.15	11.46	4.3	1993	43.83	16.96	4.2	1994	45.10	14.74	4	1995	40.13	15.23	4
1992	43.05	12.95	4.2	1993	41.10	20.16	4	1994	42.91	12.57	4.1	1995	45.63	14.24	4.4
1992	43.84	18.81	4.8	1993	38.32	20.27	4	1994	39.53	19.88	4.1	1995	45.62	14.23	4.9
1992	39.14	19.81	5	1993	41.93	15.22	4	1994	37.71	14.12	4.8	1995	37.91	12.07	4.8
1992	38.64	15.07	4.1	1993	39.46	20.43	4.2	1994	37.77	19.81	4.5	1995	40.28	16.05	4.1
1992	42.43	14.30	4.5	1993	39.68	20.07	4.3	1994	43.09	17.10	4.7	1995	39.37	20.25	4.6
1992	39.47	15.46	4.3	1993	43.28	10.93	4.2	1994	42.42	13.22	4.2	1995	45.81	11.05	4.1
1992	42.18	19.37	4.2	1993	39.56	17.13	4.2	1994	42.45	13.26	4.2	1995	42.75	17.41	4.7
1992	38.84	17.89	4.2	1993	42.82	18.65	4.5	1994	43.49	19.21	4.1	1995	42.80	17.54	4
1992	39.16	20.39	4.7	1993	40.17	20.30	4	1994	41.04	20.13	4.2	1995	42.78	17.49	4.2
1992	42.39	19.34	5.1	1993	44.52	17.50	4.2	1994	38.71	20.44	4.8	1995	39.88	13.22	4.2
1992	43.14	19.45	4.3	1993	39.06	16.82	4	1994	38.00	20.15	4	1995	38.18	20.37	4.4
1992	42.44	19.17	4.1	1993	39.97	15.09	4.7	1994	41.98	13.28	4.2	1995	43.50	17.52	4.4
1992	37.81	14.80	4.1	1993	38.57	20.33	4	1994	45.54	15.93	4.2	1995	38.64	14.68	4.1
1992	37.84	14.73	4	1993	43.33	17.42	4.2	1994	43.31	18.45	4.4	1995	42.89	14.24	4
1992	40.43	19.97	4.1	1993	43.79	16.20	4	1994	42.74	18.90	4	1995	37.90	15.41	4
1992	44.13	18.46	4.4	1993	37.79	19.74	4	1994	39.74	15.38	4.8	1995	38.56	12.42	4.4
1992	42.42	19.02	4.7	1993	44.23	12.17	4	1994	45.86	11.20	4.3	1995	39.78	16.48	4.2
1992	41.68	15.80	4.4	1993	44.38	12.14	4.1	1994	43.43	16.95	4.2	1995	42.59	19.82	4
1992	37.91	16.60	4.1	1993	44.86	17.15	4.4	1994	39.36	20.16	4.2	1995	41.37	19.67	4
1992	37.62	20.43	4	1993	44.23	12.23	4.2	1994	43.16	17.83	4.1	1995	44.13	10.76	4.7
1992	43.51	17.02	4	1993	44.22	12.20	4.1	1994	38.56	20.20	4.3	1995	45.37	17.64	4.9
1992	43.04	17.56	4.3	1993	44.21	12.21	4.1	1994	38.63	20.26	4.1	1995	38.23	15.29	4.2
1992	41.87	20.03	4.2	1993	37.99	20.11	4.3	1994	41.92	20.22	4.2	1995	43.15	17.62	4.5
1993	42.28	18.66	4.3	1993	42.60	10.74	4	1995	37.94	19.93	4	1995	42.63	18.16	5.2
1993	37.69	20.37	4.4	1993	38.90	14.86	4.8	1995	41.97	19.50	4.1	1995	41.87	15.89	5.2
1993	43.63	12.28	4.4	1993	45.45	14.34	4.4	1995	37.91	19.96	5	1995	37.87	20.27	4.2
1993	41.58	19.61	4.2	1993	43.88	12.78	4	1995	38.68	20.33	4.1	1995	38.12	20.27	4.7
1993	39.46	20.44	4.2	1993	41.97	19.12	4.6	1995	38.44	12.81	4	1995	38.11	20.30	4.2
1993	39.76	19.69	4	1993	40.16	19.82	5.2	1995	38.81	20.35	4	1995	38.20	20.24	4.2
1993	38.57	14.54	4.2	1993	43.40	17.07	4.1	1995	40.86	15.41	4.1	1995	41.32	15.05	4.2
1993	42.82	17.89	4.1	1993	40.00	19.57	4.1	1995	37.67	15.07	4.5	1995	35.67	11.66	4.6
1993	40.72	15.76	4.2	1993	39.77	15.93	4.4	1995	37.83	20.29	4.5	1995	43.27	17.71	4.1
1993	43.03	17.79	4.2	1994	39.09	15.15	5.8	1995	42.94	17.30	4.3	1995	43.33	14.99	4.2
1993	39.03	15.92	4.4	1994	39.67	15.38	4.1	1995	37.77	15.73	4.1	1995	44.54	17.25	4.6
1993	45.56	15.21	5.1	1994	40.15	17.37	4.1	1995	38.62	20.40	4	1995	38.17	20.43	4.2
1993	42.31	19.40	4.1	1994	43.64	16.48	4.1	1995	38.66	20.35	4.6	1995	42.11	14.97	4.4
1993	38.78	20.41	4.7	1994	42.83	19.00	5	1995	38.60	20.31	4	1995	37.51	20.04	4

Year	Long	Lat	Mag												
1995	37.43	20.19	4	1996	42.89	17.85	4.3	1997	45.22	16.19	4.3	1997	43.08	12.74	4.2
1995	36.49	13.44	4.1	1996	42.93	17.85	4.1	1997	44.79	15.78	4	1997	42.97	12.79	4.2
1995	43.15	13.54	4.1	1996	42.86	17.68	4.2	1997	41.40	14.63	4.6	1997	43.08	12.70	4.4
1995	38.49	20.16	4	1996	42.83	17.81	4.5	1997	36.93	16.03	4.7	1997	43.64	12.14	4.6
1996	43.56	17.29	4.1	1996	42.77	17.87	5.3	1997	37.66	19.92	4.3	1997	43.64	12.12	4.4
1996	43.87	15.54	4.6	1996	42.80	17.91	4.1	1997	41.30	14.56	4.4	1997	43.08	12.79	5.3
1996	40.04	13.12	4.7	1996	37.60	20.43	4.4	1997	43.31	18.90	4.2	1997	42.95	12.90	4.1
1996	43.17	13.61	4.2	1996	45.44	16.22	4.7	1997	42.87	17.64	4.2	1997	42.97	12.88	4.4
1996	37.47	16.27	4	1996	42.76	17.85	4.3	1997	42.77	12.48	4.4	1997	42.90	12.90	4.6
1996	43.15	13.61	4.1	1996	42.85	17.70	4.4	1997	41.05	20.17	5.4	1997	42.93	12.86	4.6
1996	37.83	19.92	5.3	1996	42.84	17.81	4.1	1997	41.06	20.25	4.2	1997	42.96	12.83	4.7
1996	36.36	12.58	4.2	1996	42.87	17.80	4.6	1997	41.10	20.18	4.2	1997	42.93	12.90	4.5
1996	44.51	17.24	4.9	1996	42.32	17.48	4.2	1997	40.25	19.95	4.1	1997	42.92	12.85	4.1
1996	44.50	17.22	4	1996	42.77	17.59	4.1	1997	38.57	16.21	4.2	1997	43.05	12.84	5.5
1996	38.81	15.69	4.8	1996	42.92	17.87	4.3	1997	41.26	19.82	4.5	1997	43.01	12.78	4.6
1996	38.06	19.90	4	1996	42.75	17.45	4	1997	41.43	19.75	4	1997	42.96	12.97	4.2
1996	44.34	15.40	4	1996	42.69	17.58	4	1997	41.32	19.84	4	1997	43.01	12.85	4.8
1996	44.34	15.38	4.7	1996	42.59	17.50	4.4	1997	43.04	12.83	4.7	1997	42.98	12.86	4.2
1996	43.94	15.48	4.3	1996	42.85	17.71	4.4	1997	38.34	16.35	4.3	1997	42.93	12.75	4
1996	40.76	15.49	4.7	1996	42.93	17.90	4.1	1997	43.01	12.84	4.2	1997	42.98	12.79	4.3
1996	40.72	15.47	4.4	1996	42.84	17.81	4.3	1997	43.05	12.88	5.7	1997	42.90	12.90	5.3
1996	40.73	20.32	4	1996	42.87	17.82	5.5	1997	42.97	12.80	4.2	1997	43.01	12.75	4.4
1996	36.20	12.88	4.1	1996	42.93	17.62	4.2	1997	43.02	12.84	4.2	1997	42.86	13.06	4
1996	39.70	16.65	4.6	1996	42.84	17.80	4.5	1997	43.03	12.70	4.2	1997	42.90	12.95	4.3
1996	38.32	20.39	4.7	1996	42.70	17.88	4	1997	42.55	13.38	4.4	1997	42.86	12.87	4
1996	39.34	15.47	4.1	1996	42.79	17.87	4.2	1997	42.82	12.80	4	1997	42.86	12.97	4.6
1996	38.19	20.34	4.4	1996	42.86	17.86	4.1	1997	42.93	12.84	4	1997	42.92	12.92	4.6
1996	42.96	14.00	4.5	1996	41.93	20.27	4.1	1997	43.04	12.78	4.7	1997	42.97	12.88	4
1996	38.79	14.61	4	1996	38.65	15.85	4.1	1997	43.08	12.81	6	1997	42.87	12.91	4
1996	44.96	11.32	4.1	1996	44.79	10.78	5.3	1997	43.16	12.75	5.3	1997	42.90	13.00	4.5
1996	37.42	20.28	4	1996	44.75	10.74	4.7	1997	43.06	12.70	4.2	1997	42.93	13.00	4.1
1996	37.79	14.95	4	1996	42.81	17.82	4.6	1997	43.03	12.94	4.7	1997	42.89	12.92	4.9
1996	43.97	15.41	4.3	1996	42.60	13.28	4.7	1997	43.01	12.85	4.1	1997	42.68	13.10	4.1
1996	43.95	15.41	4	1996	42.73	13.52	4	1997	43.07	12.85	4.6	1997	42.86	12.88	4
1996	40.88	19.51	4.2	1996	41.84	15.20	4.4	1997	43.08	12.88	4	1997	42.82	12.91	4
1996	42.80	17.94	6	1996	37.48	20.15	4.5	1997	43.03	12.73	4	1997	42.96	12.89	5.5
1996	42.83	17.85	4.9	1996	39.91	19.91	4.3	1997	43.09	12.78	4.2	1997	42.68	13.06	4.2
1996	42.80	17.81	4.2	1996	41.43	19.82	4	1997	43.03	12.77	4.1	1997	42.94	12.75	4.5
1996	42.65	17.87	4.4	1996	37.81	13.84	4.7	1997	43.04	12.72	4.2	1997	42.87	12.85	4
1996	42.81	17.85	4.4	1996	40.04	13.02	4.9	1997	43.07	12.69	4.2	1997	42.97	12.84	4.4
1996	42.83	17.92	4.4	1997	42.84	17.89	4	1997	43.13	12.77	4.8	1997	42.92	12.92	4.2
1996	42.87	17.76	4.6	1997	40.96	19.67	4.8	1997	43.02	12.83	4.5	1997	42.93	12.86	4.7
1996	42.90	17.81	4.5	1997	40.82	19.67	4.8	1997	43.06	12.77	4.5	1997	42.96	12.89	4.3

Year	Long	Lat	Mag												
1997	42.87	12.96	4	1998	44.85	10.79	4.8	1998	41.93	20.39	5.3	1999	36.64	15.27	4.1
1997	42.93	12.89	4.5	1998	44.68	17.68	4.6	1998	37.69	20.26	4.2	1999	37.36	20.39	4.1
1997	42.91	12.92	4.7	1998	43.36	17.63	4.5	1998	37.90	20.36	4.2	1999	39.83	15.20	4.8
1997	42.98	12.89	4.5	1998	44.04	12.25	4	1998	37.51	20.36	4.2	1999	38.38	15.75	4.1
1997	43.02	12.85	4.8	1998	45.59	14.20	5.2	1998	38.06	20.35	4	1999	44.82	17.41	4.1
1997	42.88	12.97	4.5	1998	43.11	18.18	4.6	1998	37.72	20.38	4.7	1999	43.10	18.95	4
1997	42.89	12.91	4.5	1998	42.96	12.88	4.7	1998	37.90	20.27	4.4	1999	38.22	15.04	4.2
1997	42.92	12.87	4	1998	42.95	12.83	4.5	1998	37.72	20.39	4.6	1999	42.67	13.19	4.7
1997	42.97	12.81	4.5	1998	43.03	12.89	4.1	1998	37.95	20.25	4.2	1999	43.10	18.96	4
1997	43.09	12.83	4.3	1998	42.94	12.92	4.1	1998	37.90	20.36	4.7	1999	38.84	14.65	4.8
1997	42.84	13.01	4.6	1998	42.93	12.95	4	1998	44.25	20.07	4.2	1999	37.77	19.98	4.7
1997	41.76	12.77	4.5	1998	43.26	12.97	5.4	1998	40.36	13.73	4.4	1999	43.51	17.73	4.1
1997	42.90	12.94	4.6	1998	43.16	12.70	5.2	1998	39.75	15.32	4	1999	40.27	19.76	4.8
1997	42.89	12.93	4.1	1998	43.23	12.67	4.4	1998	38.19	20.43	4.6	1999	41.55	19.38	4.7
1997	42.90	12.95	5	1998	43.21	12.77	4	1998	38.06	20.31	4	1999	42.85	13.14	4.1
1997	42.91	12.85	4.2	1998	43.19	12.72	4.7	1998	39.68	13.40	4.6	1999	39.37	15.60	4.2
1997	39.34	20.23	4.8	1998	37.91	20.28	4.5	1998	37.87	20.17	4.2	1999	38.21	20.37	4.1
1997	43.31	20.35	4.7	1998	38.34	20.34	4.2	1998	45.72	11.39	4.1	1999	40.96	20.37	4
1997	43.05	12.79	4.1	1998	40.99	20.00	4.2	1998	37.86	19.76	4	1999	38.77	14.23	4.1
1997	40.97	19.73	4.1	1998	39.83	19.83	4.2	1998	37.85	19.66	4	1999	38.29	11.86	4.9
1997	42.95	12.90	4.1	1998	43.44	18.14	4.3	1998	44.23	20.05	4	2000	44.30	11.99	4.1
1997	37.27	20.44	4.1	1998	39.25	15.11	5.5	1999	39.07	17.79	4.2	2000	38.27	11.80	4.4
1997	37.46	20.32	4.5	1998	38.28	12.60	4.3	1999	44.02	11.92	4.8	2000	39.06	17.10	4.1
1997	40.33	20.25	4	1998	43.21	12.68	4.4	1999	36.19	10.78	4.1	2000	39.81	15.49	4.2
1997	43.99	16.54	4.2	1998	43.18	12.76	4.5	1999	38.17	15.06	4.5	2000	43.47	17.26	4
1997	40.15	14.82	4	1998	45.72	10.84	4.2	1999	39.36	20.39	4.3	2000	44.30	11.69	4.2
1997	39.48	20.09	4.4	1998	43.17	12.75	4.2	1999	37.72	19.94	4.2	2000	45.06	13.32	4
1997	42.88	12.95	4.6	1998	38.46	12.86	4.1	1999	38.14	20.19	4.2	2000	41.93	12.92	4.7
1997	42.87	12.98	4.1	1998	38.43	12.67	4.7	1999	41.48	19.60	4	2000	45.15	14.84	4
1997	42.88	12.90	4.1	1998	38.36	12.57	4	1999	37.38	20.23	4.3	2000	42.63	16.23	4.1
1997	36.02	19.66	5.3	1998	38.39	12.62	4.2	1999	44.18	20.07	5.4	2000	39.10	13.78	4.5
1997	37.51	20.38	4.2	1998	38.43	12.67	4.5	1999	44.19	20.10	4.6	2000	39.50	15.84	4.6
1997	38.92	13.86	4.4	1998	42.97	12.75	4.2	1999	45.53	15.92	4.1	2000	42.84	11.69	4.5
1997	37.72	15.07	4.2	1998	43.09	12.60	4	1999	38.79	14.14	4.2	2000	44.30	11.99	4
1997	42.87	12.99	4.5	1998	39.32	17.56	4.1	1999	40.41	19.40	4.4	2000	44.35	11.95	4.1
1998	42.78	12.92	4	1998	42.41	12.98	4.8	1999	38.02	20.18	4.1	2000	39.43	20.43	4.5
1998	38.40	12.89	4.9	1998	42.53	19.05	4	1999	45.68	17.47	4.2	2000	39.23	15.16	4.4
1998	38.83	14.53	4.1	1998	37.30	19.57	4.1	1999	43.27	17.63	4	2000	37.83	19.71	4.3
1998	42.37	16.30	4.4	1998	40.04	15.98	5.9	1999	41.18	19.66	4	2000	38.02	19.57	4
1998	39.87	19.70	4.1	1998	38.46	13.61	4.9	1999	45.35	12.25	4.1	2000	44.80	17.40	4
1998	45.56	14.58	4	1998	41.80	15.92	4.5	1999	44.29	10.90	4.7	2000	44.34	11.99	4
1998	43.03	12.80	4.6	1998	41.73	15.82	4	1999	44.29	10.94	4.4	2000	44.24	12.02	4.5
1998	41.87	15.78	4.4	1998	44.21	20.08	5.5	1999	44.27	10.93	4.4	2000	44.03	13.27	4.2

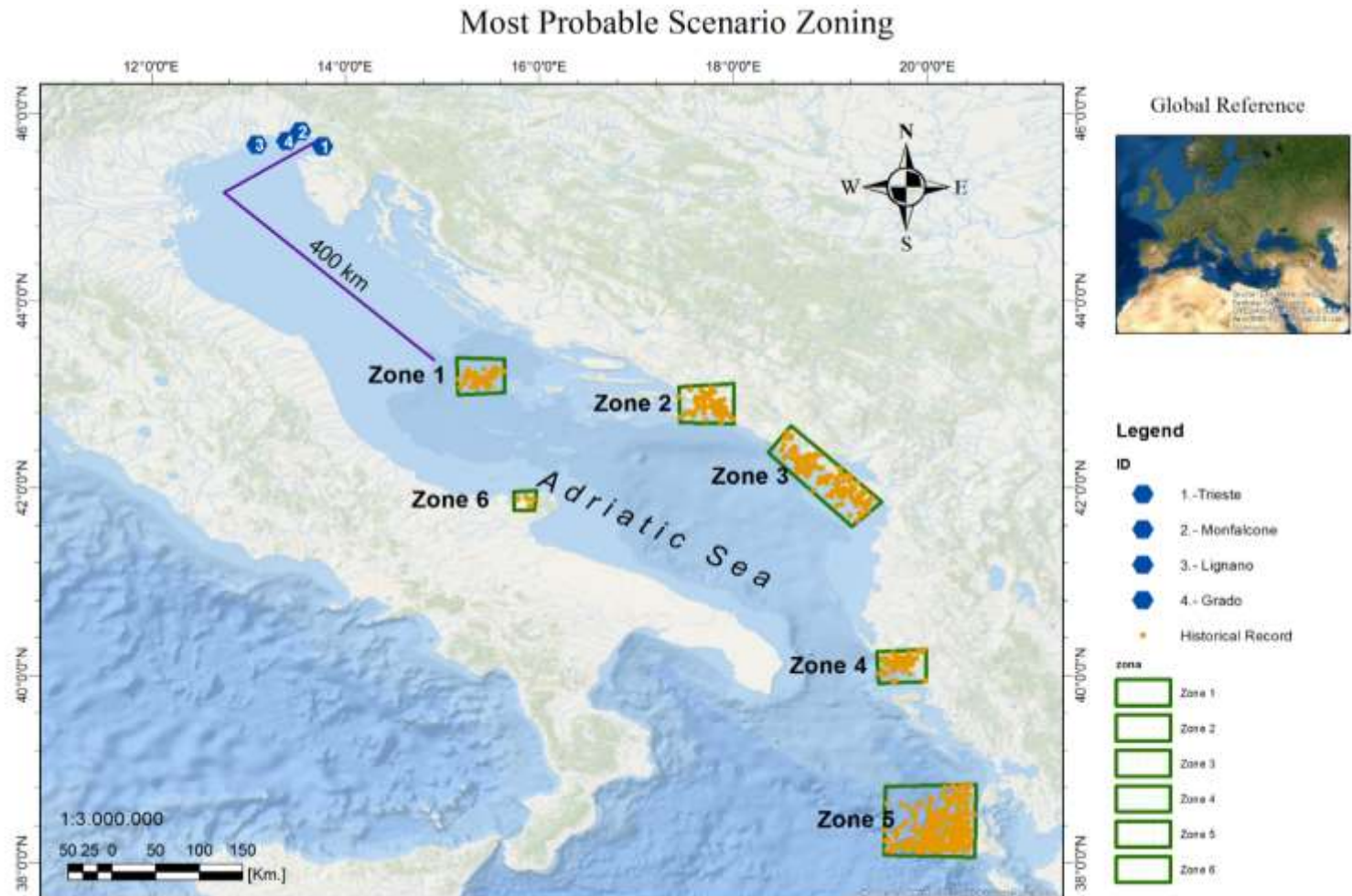
Year	Long	Lat	Mag												
2000	44.14	11.97	4.5	2001	39.31	20.22	4.1	2002	40.02	15.25	4	2002	38.38	13.72	4.1
2000	44.34	11.96	4.6	2001	44.18	20.37	4.2	2002	42.41	19.82	4.3	2002	37.87	19.97	5.2
2000	44.35	11.99	4.5	2001	43.91	16.77	4	2002	45.63	14.23	4.6	2002	39.03	20.22	4.8
2000	44.31	11.96	4.1	2001	38.10	20.23	4.8	2002	44.44	10.80	4.6	2003	44.98	14.65	4.6
2000	44.36	11.96	4	2001	37.97	20.04	4.1	2002	44.47	10.75	4.2	2003	37.81	20.12	4
2000	44.35	11.97	4.2	2001	37.74	20.13	4.4	2002	41.29	20.29	4.3	2003	41.39	20.36	4
2000	44.04	12.04	4.2	2001	37.51	20.17	4	2002	38.38	13.70	6	2003	43.88	11.96	4.7
2000	44.32	11.94	4.2	2001	40.08	20.41	5.1	2002	38.38	13.67	4.2	2003	43.89	11.95	4.6
2000	44.34	11.96	4.7	2001	40.58	19.45	4.5	2002	38.40	13.67	4	2003	43.88	11.95	4.7
2000	44.32	11.91	4.8	2001	37.72	15.10	4.1	2002	37.63	19.98	4.4	2003	43.90	11.93	4.4
2000	44.32	12.00	4.7	2001	38.96	15.53	5.2	2002	38.47	13.70	4	2003	43.21	16.01	4.5
2000	44.32	12.00	5.1	2001	37.46	16.34	4.8	2002	38.46	13.74	4.5	2003	41.66	14.75	4.1
2000	44.31	11.95	4.1	2001	43.26	18.98	4	2002	43.36	17.61	4.4	2003	41.29	20.17	4.1
2000	44.36	11.87	4.3	2001	38.47	20.35	4.5	2002	38.44	13.70	5.3	2003	40.41	19.71	4.1
2000	44.34	11.91	4.6	2001	41.95	15.29	4.2	2002	38.47	13.71	4.6	2003	43.15	15.34	5
2000	44.35	11.96	4.5	2001	38.12	20.30	4	2002	40.04	20.37	4.7	2003	43.18	15.49	4
2000	37.69	19.79	4.2	2001	38.33	14.69	4.3	2002	40.00	20.44	4.6	2003	43.11	15.43	4.1
2000	39.07	19.97	4.3	2001	37.80	20.26	4.5	2002	39.18	13.65	4.2	2003	43.11	15.46	5.5
2000	43.06	12.52	4.4	2001	37.96	20.12	4.4	2002	42.61	17.16	4.7	2003	43.26	15.43	4
2000	42.57	16.83	4.4	2001	38.53	14.99	4.6	2002	40.01	19.51	4.3	2003	43.24	15.63	4.4
2000	44.76	10.80	4.8	2001	39.39	15.28	4.1	2002	37.42	14.78	4	2003	43.17	15.43	4.3
2000	43.30	12.48	4.8	2001	37.77	13.96	4.9	2002	37.79	15.20	4.1	2003	43.28	15.54	4.2
2000	43.82	12.99	4	2001	43.60	12.07	5.1	2002	37.72	15.09	4.4	2003	43.17	15.53	4.6
2000	41.94	12.93	4.4	2001	43.59	12.03	4	2002	37.84	15.17	4.4	2003	43.20	15.55	4
2000	39.41	15.23	4.1	2001	44.97	11.22	4.4	2002	37.80	15.16	4.8	2003	43.15	15.38	4
2000	43.98	12.34	4.6	2001	39.99	20.28	4.2	2002	37.79	15.19	4.2	2003	43.13	15.47	4.6
2000	43.34	17.71	4.3	2001	39.70	15.10	4	2002	37.92	15.18	4.3	2003	43.12	15.23	4.8
2000	37.74	19.80	4	2001	36.69	20.41	4.1	2002	37.67	15.27	4.5	2003	43.20	15.33	4
2000	42.72	20.30	4.2	2001	41.95	13.04	4.3	2002	37.69	15.56	4.1	2003	43.17	15.37	4
2000	43.26	12.99	4.9	2001	44.96	15.11	4.5	2002	41.79	14.87	5.9	2003	43.17	15.50	4.1
2000	44.69	10.88	4.2	2002	43.90	12.11	4.2	2002	41.74	14.73	4	2003	43.17	15.45	4
2000	44.27	10.80	4.5	2002	36.38	10.92	4.5	2002	41.75	14.82	4	2003	43.20	15.23	4
2000	43.60	16.25	4.1	2002	41.31	19.83	4	2002	41.73	14.88	5.8	2003	43.15	15.43	4.6
2000	43.51	17.79	4.2	2002	43.76	12.05	4.5	2002	41.75	14.76	4.7	2003	43.25	15.27	4.1
2000	38.21	20.29	4.2	2002	39.13	15.28	4	2002	41.87	14.83	4.8	2003	43.20	15.28	4.1
2000	38.17	20.21	4	2002	42.43	19.77	4.4	2002	44.58	12.17	5	2003	43.13	15.39	4.1
2000	44.22	15.98	4.4	2002	42.39	19.79	4.1	2002	41.80	14.74	4.7	2003	43.25	15.57	4
2000	41.86	19.78	4.8	2002	43.07	17.78	4	2002	41.84	14.72	4.2	2003	43.16	15.26	4.5
2000	42.65	12.66	4.3	2002	39.70	16.84	5.3	2002	41.66	14.77	4.8	2003	43.26	15.54	4.5
2000	38.08	20.30	4.4	2002	39.66	16.86	4	2002	41.78	14.64	4	2003	43.14	15.38	4.2
2000	36.85	20.20	4.1	2002	40.69	15.58	4.4	2002	39.93	19.66	4.8	2003	43.25	15.57	4.9
2001	38.95	14.75	4.6	2002	44.14	11.57	4.1	2002	38.72	14.84	4.5	2003	43.19	15.49	4.1
2001	39.07	14.63	4.3	2002	35.37	10.97	4	2002	41.67	14.86	4.4	2003	43.15	15.40	4.1

Year	Long	Lat	Mag												
2003	43.14	15.44	4.2	2004	40.11	19.81	4.3	2005	42.39	19.91	4.5	2006	43.96	11.80	4.3
2003	43.22	15.50	4.3	2004	43.14	13.43	4.2	2005	39.78	19.88	4.1	2006	39.57	17.14	4.5
2003	43.17	15.42	4.1	2004	40.72	15.44	4.4	2005	39.63	14.94	4.4	2006	35.81	20.15	4.6
2003	38.23	20.26	4.3	2004	39.77	15.23	4.8	2005	39.57	16.93	4.1	2006	42.72	17.72	4
2003	41.65	14.80	4.1	2004	38.48	19.88	4.4	2005	45.57	14.25	4.4	2006	40.04	19.75	4.4
2003	43.22	15.51	4.5	2004	41.80	20.13	4.3	2005	39.10	20.02	4	2006	39.80	19.97	4.4
2003	43.91	16.98	4.6	2004	43.73	16.86	4.2	2005	42.72	18.95	4.6	2006	40.23	19.31	4.7
2003	39.55	20.39	4.5	2004	40.67	20.38	5	2005	40.58	19.62	4.4	2006	40.06	19.78	4.5
2003	45.88	15.16	4	2004	38.51	14.81	5.5	2005	36.15	11.53	4.2	2006	44.01	20.17	4.6
2003	43.12	15.37	4.2	2004	43.41	17.45	5	2005	42.68	17.37	4.5	2006	37.65	14.95	4.1
2003	41.66	14.83	4.6	2004	38.54	14.63	4.1	2005	44.21	12.12	4.8	2006	36.87	20.34	5.2
2003	37.70	19.73	4.3	2004	41.91	16.17	4.5	2005	44.23	12.10	4	2006	41.80	15.90	4.7
2003	37.65	19.55	4.1	2004	41.16	20.00	4.2	2005	40.02	12.69	5	2006	37.63	16.52	4.2
2003	43.07	15.31	5	2004	38.38	13.67	4.3	2005	40.83	20.24	4.1	2006	38.95	15.27	4
2003	35.86	14.77	4.1	2004	41.25	19.57	4.5	2005	40.72	13.55	4	2006	40.27	19.96	4.8
2003	43.02	17.70	4.9	2004	38.56	15.46	4.2	2005	38.88	15.50	4.5	2006	41.12	20.04	4.5
2003	38.73	20.40	4.2	2004	40.70	15.68	4.3	2005	41.47	12.53	4.8	2006	40.15	19.78	4.1
2003	38.48	20.35	4.1	2004	45.33	14.58	4.5	2005	38.24	20.35	4	2006	39.71	16.62	4.6
2003	38.59	19.80	4	2004	40.32	12.95	4.5	2005	38.92	20.10	4.1	2006	37.70	20.05	4
2003	38.83	20.44	4.2	2004	39.05	13.91	4.3	2005	38.97	20.14	4	2006	40.16	19.74	4.8
2003	43.03	17.68	4.1	2004	43.00	17.77	4.3	2005	38.18	20.25	4.5	2006	41.89	15.34	4
2003	44.33	11.45	5.3	2004	43.86	16.54	4.1	2005	38.10	20.25	4.8	2006	40.18	19.75	4.8
2003	44.27	11.40	4.2	2004	38.49	15.64	4.2	2005	38.04	20.24	4.8	2006	40.11	19.59	4.6
2003	38.08	20.04	4.4	2004	40.96	19.57	4.3	2005	38.09	20.25	4	2006	40.16	19.75	4.4
2003	37.21	16.94	4	2004	43.17	15.36	5.3	2005	38.18	20.28	4	2006	40.11	19.70	4.4
2003	43.33	19.95	4.1	2004	43.07	15.74	4.5	2005	43.16	18.20	5.1	2006	44.68	18.46	4.1
2003	40.39	14.33	4.6	2004	43.22	15.34	4.1	2005	43.40	16.52	4	2006	42.06	19.29	4.4
2003	38.27	20.34	5.2	2004	43.23	15.28	4.1	2005	38.13	20.22	4.1	2006	38.06	20.34	5
2003	38.30	20.39	4.4	2004	43.07	15.36	4.4	2005	36.32	11.49	4	2006	40.23	19.65	4.1
2003	41.41	20.05	4.4	2004	43.07	15.47	4.3	2005	39.12	17.21	4.2	2006	40.14	19.68	4.4
2003	41.94	19.22	4.7	2004	43.09	15.50	4.8	2005	42.74	12.76	4.3	2006	40.11	19.58	4.3
2003	44.16	12.18	4.8	2004	43.08	15.46	4.5	2006	37.84	19.99	4	2006	40.59	16.16	4.2
2003	36.21	19.10	4.4	2004	39.94	19.67	4.2	2006	37.72	20.11	4	2006	42.07	15.75	4.9
2003	38.24	20.31	4.2	2004	39.76	19.65	4.1	2006	43.41	17.46	4.2	2006	39.70	15.17	4.4
2003	40.34	15.62	4	2004	42.79	13.79	4.7	2006	38.12	20.39	4	2006	42.30	19.80	5
2003	40.11	19.66	4.4	2004	43.07	15.19	4.3	2006	40.13	19.74	4.3	2006	43.65	13.00	4.3
2003	41.64	14.85	4.4	2005	38.82	15.20	4.1	2006	38.16	15.20	4.6	2006	38.65	15.39	5.8
2003	39.02	15.35	4	2005	37.54	20.16	5.7	2006	42.20	19.42	4.4	2006	45.76	15.65	4.2
2004	37.17	20.20	4	2005	39.66	16.88	4.1	2006	37.74	19.90	5	2006	36.38	19.23	4.4
2004	38.23	20.27	4	2005	43.16	15.43	4.2	2006	44.04	20.12	4.8	2006	39.75	13.75	5
2004	40.14	19.61	4	2005	36.10	10.91	4.7	2006	44.26	11.01	4	2006	35.91	18.26	5
2004	40.16	19.86	4.3	2005	36.23	10.87	4.9	2006	44.03	20.16	4.2	2006	35.97	12.94	4.8
2004	44.48	12.58	4.3	2005	38.64	15.49	4.4	2006	43.40	13.49	4.1	2006	36.26	15.76	4.7

Year	Long	Lat	Mag												
2006	41.94	16.20	4.7	2007	38.22	15.17	4.1	2008	38.87	14.82	4	2009	42.51	13.31	4.1
2006	41.92	20.07	4.4	2007	43.13	17.82	4	2008	38.67	20.20	4.4	2009	42.25	13.49	4.1
2006	41.92	20.08	4.2	2007	38.25	20.33	5.1	2008	38.82	20.26	4.1	2009	42.23	13.48	4.3
2006	41.94	20.01	4	2007	41.81	19.79	4.5	2008	42.58	18.56	4.2	2009	43.43	17.27	4.6
2006	37.78	14.91	4.1	2007	41.35	19.47	4.9	2008	39.14	17.50	4.2	2009	42.45	13.36	4.7
2007	43.52	17.66	4.4	2007	39.89	15.38	4.1	2008	37.54	13.69	4.2	2009	42.41	13.39	4.1
2007	45.11	14.93	4.9	2007	43.11	15.13	4.1	2008	37.66	14.96	4	2009	42.34	13.38	4.3
2007	37.91	20.25	4.2	2007	37.92	20.24	4.6	2008	39.21	15.44	5.3	2009	41.39	18.87	4.2
2007	40.11	19.64	4.3	2007	43.23	17.83	4.5	2008	39.33	15.55	4	2009	41.63	13.67	4.2
2007	42.79	13.18	4.2	2007	41.67	14.69	4	2009	38.34	20.23	4	2009	41.90	19.12	5.1
2007	35.37	15.92	4.2	2007	42.41	13.07	4.3	2009	38.51	20.42	4.8	2009	38.60	14.07	4.8
2007	39.99	15.56	4.3	2007	40.67	19.50	4.1	2009	41.11	19.47	4.2	2009	41.41	20.31	4.4
2007	40.04	19.54	4.3	2007	44.07	18.20	4.5	2009	41.21	19.50	4.2	2009	44.11	11.21	4.6
2007	38.20	20.30	4.2	2007	40.01	15.79	4.7	2009	36.59	12.82	4	2009	38.67	14.87	4.3
2007	38.34	20.42	5.7	2007	39.61	15.09	4	2009	40.31	19.64	4.5	2009	41.24	19.47	4.3
2007	38.22	20.30	4.6	2008	38.06	20.26	4.5	2009	42.15	16.57	4	2009	39.96	20.00	4.4
2007	38.35	20.44	4.2	2008	43.88	20.43	4.5	2009	42.04	13.92	4	2009	43.41	13.39	4.7
2007	38.25	20.37	4.3	2008	41.58	13.78	4.6	2009	42.36	13.35	4.4	2009	37.66	17.93	4.1
2007	38.32	20.38	4	2008	37.52	17.99	4	2009	43.79	18.45	4.1	2009	37.78	14.59	4.4
2007	39.26	17.04	4.1	2008	42.40	19.80	4.1	2009	44.24	12.00	4.8	2009	37.51	20.36	5.3
2007	38.32	20.39	4.1	2008	44.05	11.23	4.6	2009	42.33	13.37	4.2	2009	41.48	19.92	4.3
2007	38.36	20.41	4.2	2008	44.05	11.20	4.6	2009	42.33	13.33	6.3	2009	39.66	15.28	4.8
2007	38.26	20.30	4.2	2008	41.90	15.86	4.3	2009	42.41	13.22	4.8	2009	37.42	20.40	4.6
2007	38.27	20.34	4	2008	40.68	20.21	4.1	2009	42.37	13.34	4.2	2009	37.36	20.24	4.7
2007	38.34	20.41	4.2	2008	42.73	18.00	4.6	2009	42.37	13.34	5.1	2009	37.35	20.28	4.1
2007	38.33	20.31	4.1	2008	42.31	19.87	4.3	2009	42.34	13.39	4.6	2009	43.01	12.28	4.3
2007	37.89	20.26	4.5	2008	41.95	20.13	4.4	2009	42.35	13.35	4	2009	37.72	14.98	4.3
2007	36.93	12.91	4	2008	39.16	16.53	4.2	2009	42.36	13.37	4.3	2009	37.78	14.94	4.3
2007	41.17	19.90	5.2	2008	45.30	18.38	4	2009	42.36	13.33	4.4	2010	39.81	15.43	4
2007	38.30	20.37	4.5	2008	41.38	19.66	4	2009	42.40	13.32	4.1	2010	43.12	13.41	4.1
2007	38.16	20.30	4	2008	40.57	14.88	4.4	2009	42.35	13.29	4.1	2010	43.13	13.44	4.1
2007	38.20	20.37	4.3	2008	41.35	19.63	4	2009	42.45	13.36	5.1	2010	42.31	19.34	4.5
2007	38.97	15.91	4	2008	38.53	13.70	4.2	2009	42.34	13.39	5	2010	37.78	15.15	4.2
2007	41.05	19.98	4.6	2008	38.02	20.12	5	2009	42.28	13.46	5.5	2010	42.37	16.60	4.3
2007	39.27	20.26	5.4	2008	38.10	20.17	4	2009	42.38	13.38	4.5	2010	43.78	16.96	4.1
2007	39.29	20.28	4.4	2008	41.78	20.22	4	2009	42.31	13.47	4.1	2010	41.17	20.03	4.9
2007	39.28	20.24	4	2008	39.19	17.22	4	2009	42.51	13.36	4.1	2010	38.42	14.92	4.5
2007	38.80	15.20	5.2	2008	38.35	20.39	4.2	2009	42.48	13.34	5.4	2010	37.24	19.95	5.5
2007	38.30	20.41	4.1	2008	41.16	20.25	4	2009	42.34	13.44	4.4	2010	42.85	12.66	4.3
2007	39.03	17.16	4.2	2008	41.10	20.23	4.8	2009	42.45	13.42	4.2	2010	41.49	15.63	4.4
2007	37.48	19.83	4.2	2008	41.25	20.28	4.1	2009	42.51	13.37	4	2010	37.24	20.35	4
2007	39.36	20.22	4.8	2008	38.96	15.47	4.3	2009	42.50	13.36	5.1	2010	44.14	12.37	4.1
2007	39.30	20.25	4.4	2008	38.43	20.41	4.1	2009	42.53	13.29	4	2010	38.87	16.66	4.1

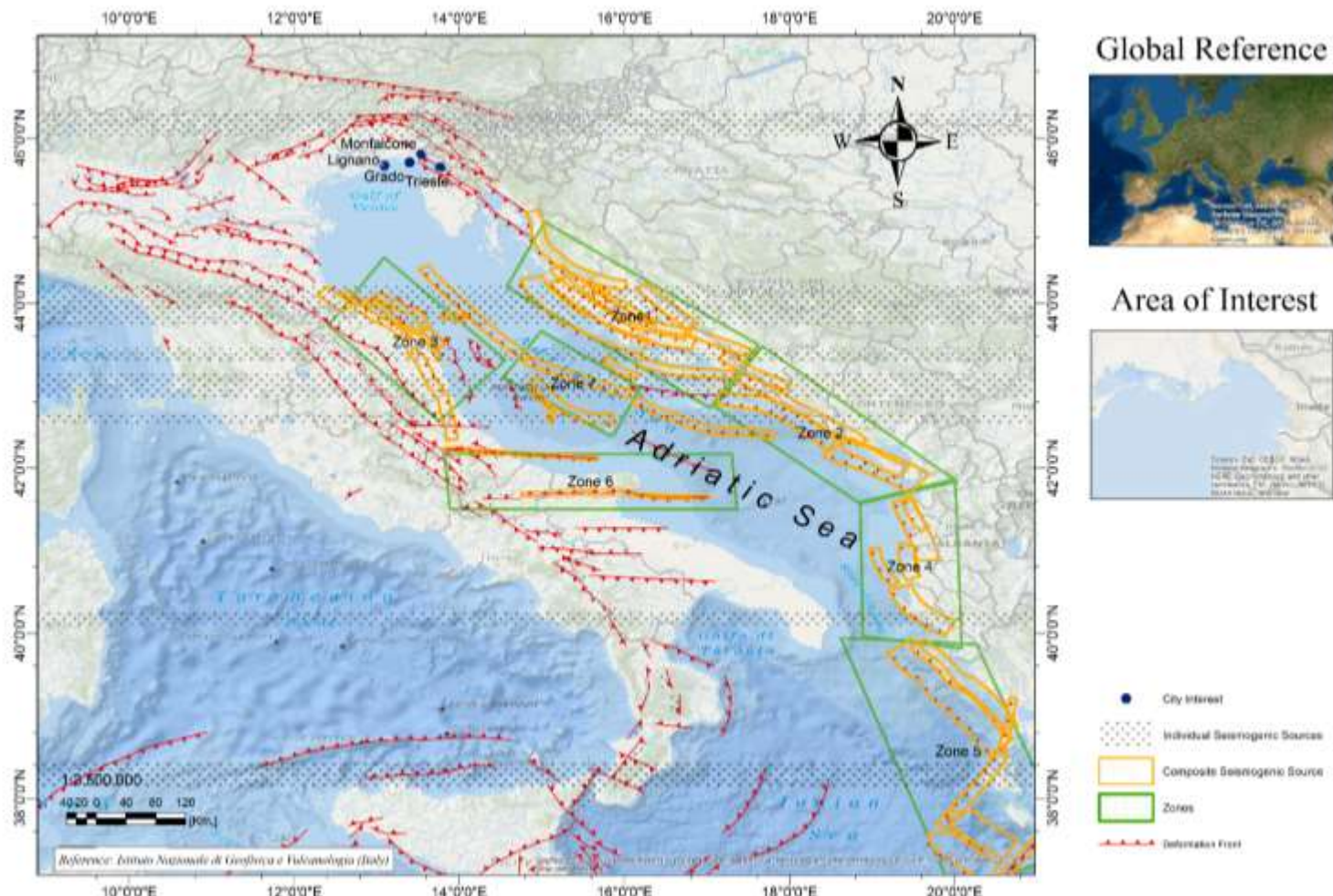
Year	Long	Lat	Mag												
2010	40.04	13.25	5.2	2011	37.21	19.92	5.1	2012	44.84	11.37	4.3	2012	44.43	12.35	4.6
2010	41.91	20.06	4.2	2011	37.31	20.09	4.6	2012	44.88	11.55	4.3	2012	44.88	10.89	4.4
2010	43.13	18.74	4.3	2011	37.13	20.06	4	2012	44.89	11.26	4.3	2012	37.47	16.74	4.7
2010	38.09	20.36	4	2011	43.46	17.57	4.2	2012	44.86	11.10	4.9	2012	38.44	15.14	4.7
2010	37.28	20.22	5	2011	39.84	15.27	4.3	2012	44.92	11.13	4.6	2012	40.60	13.60	4
2010	43.15	18.88	4.1	2011	42.54	18.61	4.6	2012	44.85	11.35	4.6	2012	44.17	17.88	4.5
2011	43.17	18.70	4	2011	38.30	20.30	4.1	2012	44.88	11.11	4.2	2012	44.24	17.85	4.2
2011	43.15	18.73	4.4	2011	39.95	14.80	4.5	2012	44.84	11.17	4	2012	43.99	16.80	4.3
2011	43.88	17.11	4	2011	38.13	20.42	4.2	2012	44.85	11.09	5.8	2012	41.77	16.27	4.1
2011	40.44	19.52	4.1	2011	42.89	17.87	4.3	2012	44.88	11.08	4.3	2012	38.55	13.60	4.4
2011	37.83	19.95	4.1	2011	36.14	12.77	4.7	2012	44.85	11.11	4.7	2012	39.59	15.34	4.2
2011	38.51	20.41	4.6	2011	41.81	19.27	4	2012	44.86	11.06	4.2	2012	38.25	15.71	4.6
2011	35.82	14.88	4.1	2012	45.54	10.97	4.1	2012	44.89	10.96	4.7	2012	36.43	13.09	4
2011	44.81	17.28	4.2	2012	42.48	19.21	4.4	2012	44.89	11.01	5.5	2012	41.17	14.95	4.6
2011	45.00	15.03	4.2	2012	38.46	13.48	4.4	2012	44.87	10.95	4.8	2012	38.46	14.85	4.4
2011	39.21	14.96	4.7	2012	42.81	13.20	4.7	2012	44.87	10.96	5.1	2012	44.10	17.08	4.4
2011	40.72	19.86	4.5	2012	41.79	19.35	4.7	2012	44.88	11.08	4.5	2012	39.76	15.55	4.9
2011	43.80	16.45	4.6	2012	38.58	15.02	4.4	2012	44.87	11.03	4.3	2012	39.88	16.01	5.3
2011	38.06	14.76	4.3	2012	39.70	20.29	4	2012	44.93	10.94	4.3	2012	42.54	19.07	4.4
2011	43.92	11.86	4.5	2012	38.29	13.30	4.4	2012	44.88	10.87	4.2	2012	38.27	15.84	4.4
2011	43.92	11.85	4.6	2012	44.90	11.26	4	2012	44.89	10.98	4.3	2012	42.55	19.02	4.5
2011	45.00	11.29	5	2012	44.89	11.23	6.1	2012	44.90	10.94	5.2	2012	42.40	20.07	4.1
								2012	44.93	10.98	4.2	2012	41.11	19.77	4.1

7 APPENDIX B

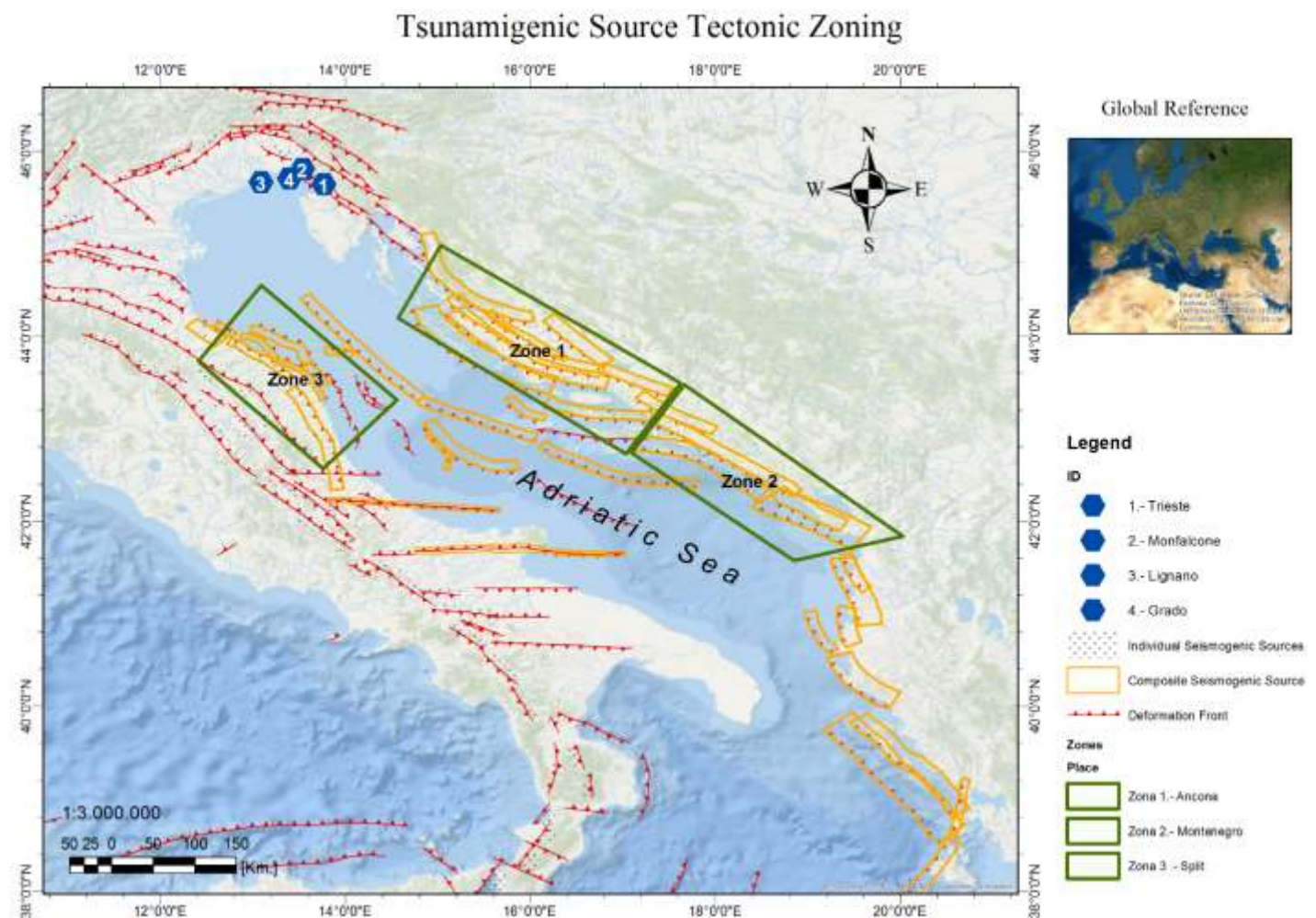


Appendix B 7.1: Probabilistic Zoning Map of the Adriatic Sea. (Author's, 2020)

Tectonic Composition in the Adriatic Sea



Appendix B 7.2: Tectonic Composition in the Adriatic Sea Zoning. (Author's, 2020)

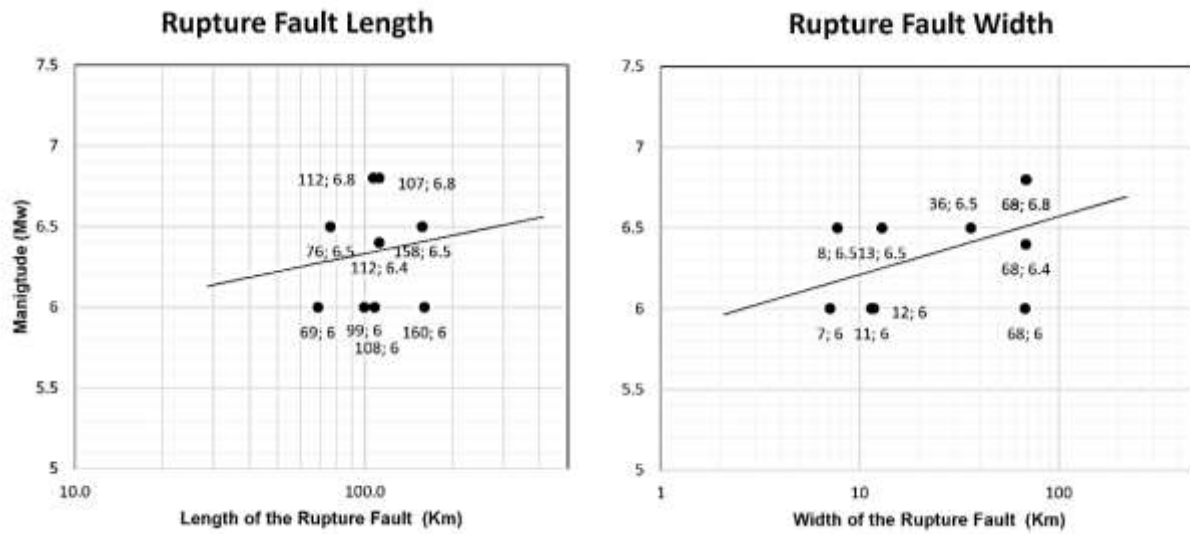


Appendix B 7.3: Tsunamigenic Source Tectonic Zoning. (Author's, 2020)

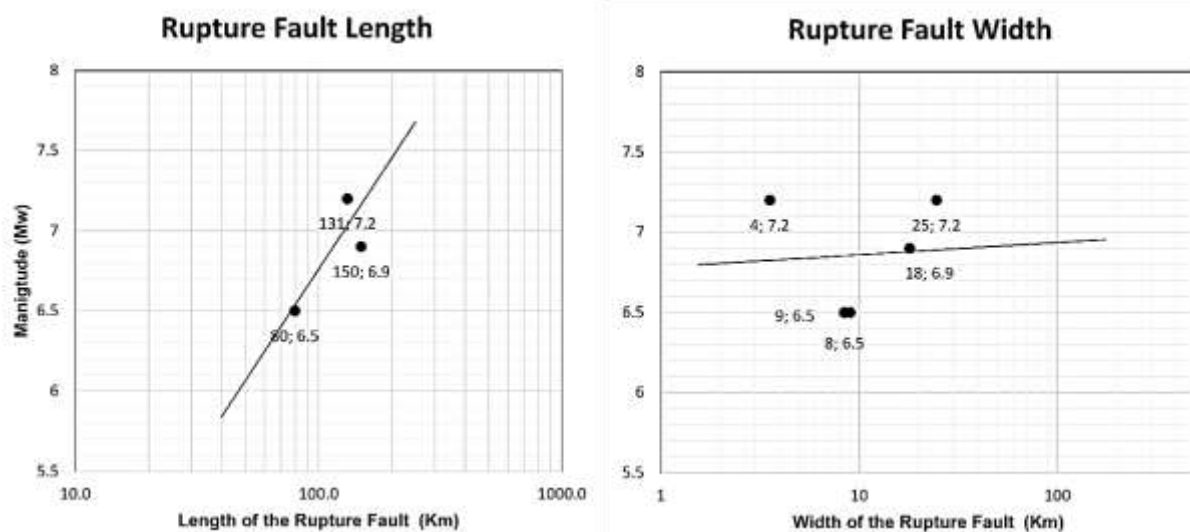
8 APPENDIX C

8.1 Empirical relationships Well & Coppersmith

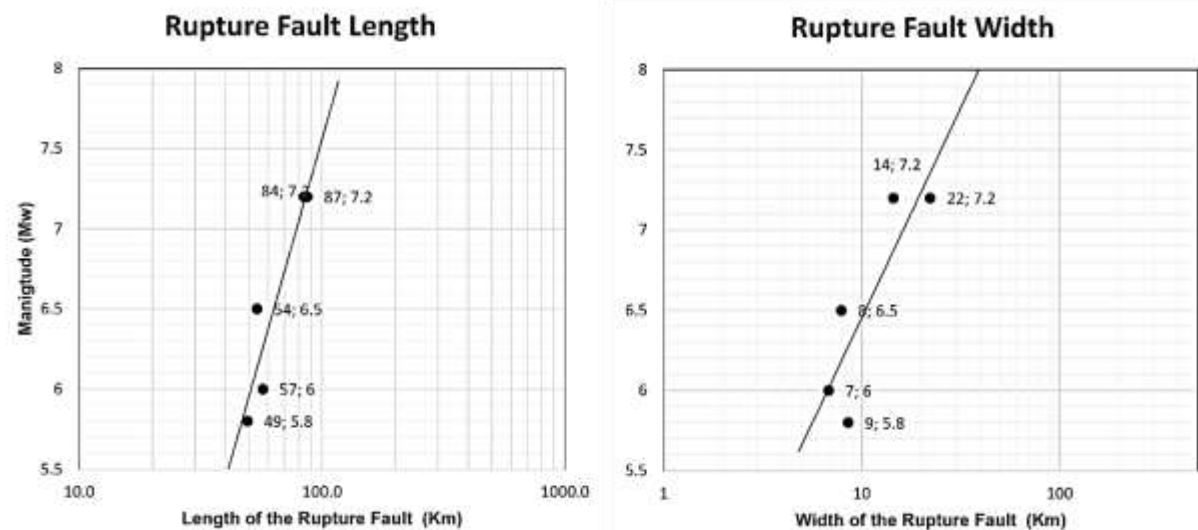
Empirical relationships between fault rupture width, fault rupture length and displacement.



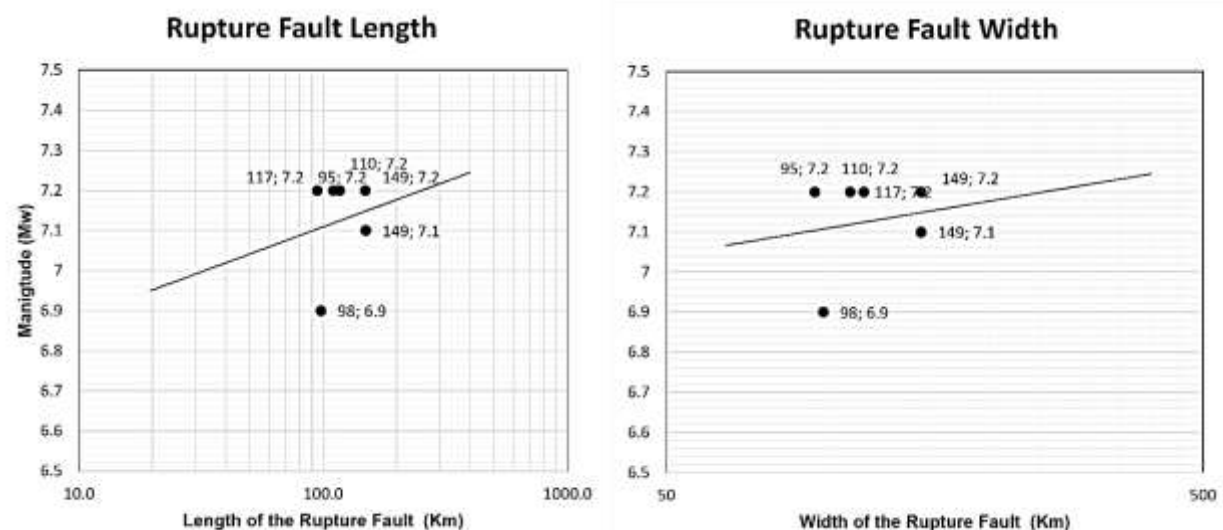
Appendix C 8.1 Zone 1: Croatia Coast, (Author`s, 2020)



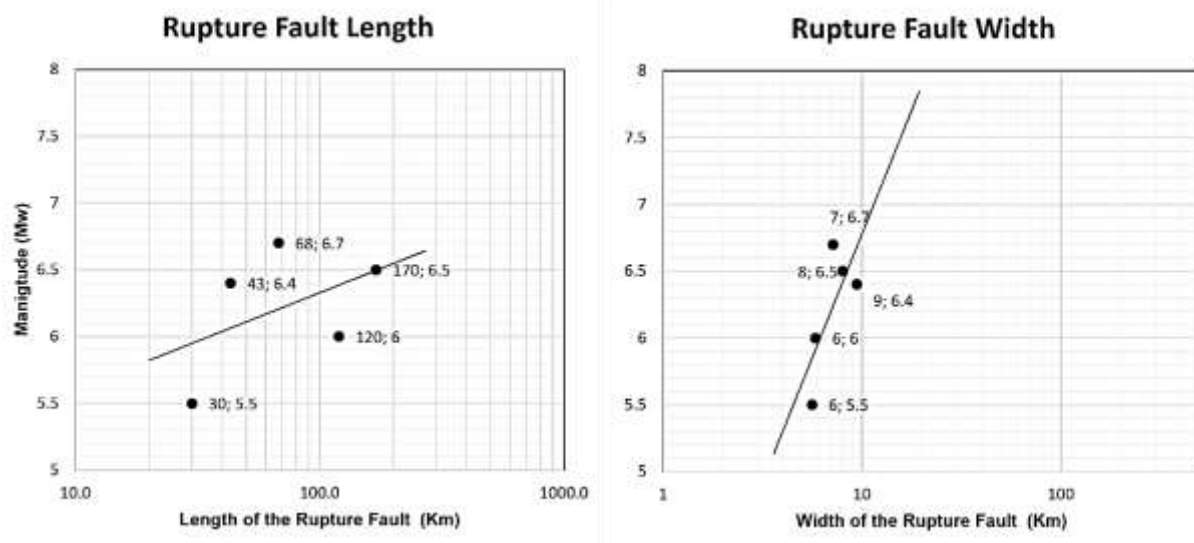
Appendix C 8.2 Zone 2: Albanide, (Author`s, 2020)



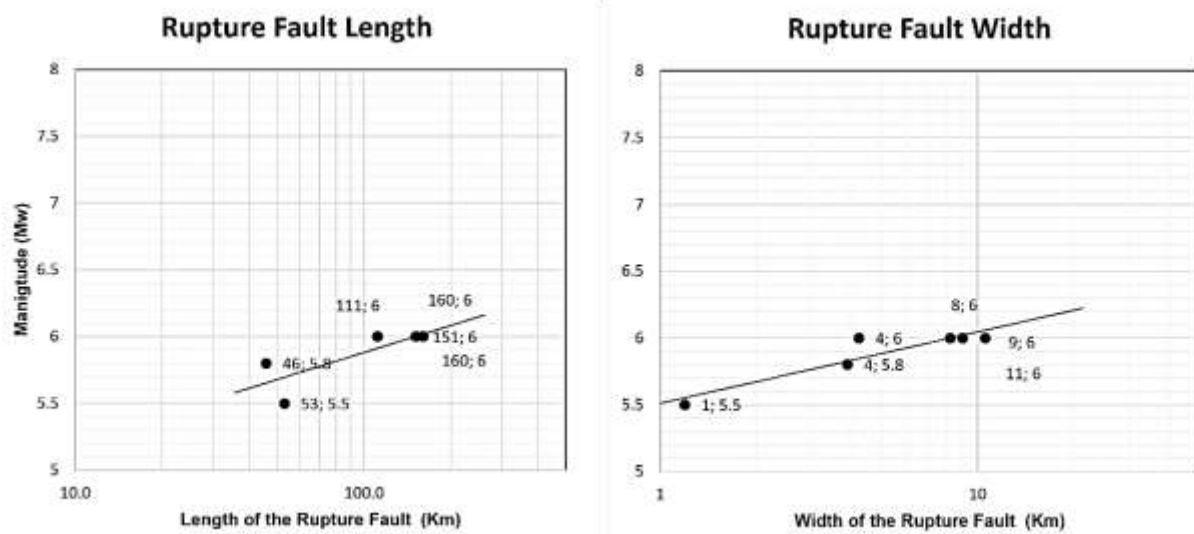
Appendix C 8.3 Zone 3: Offshore Ancona



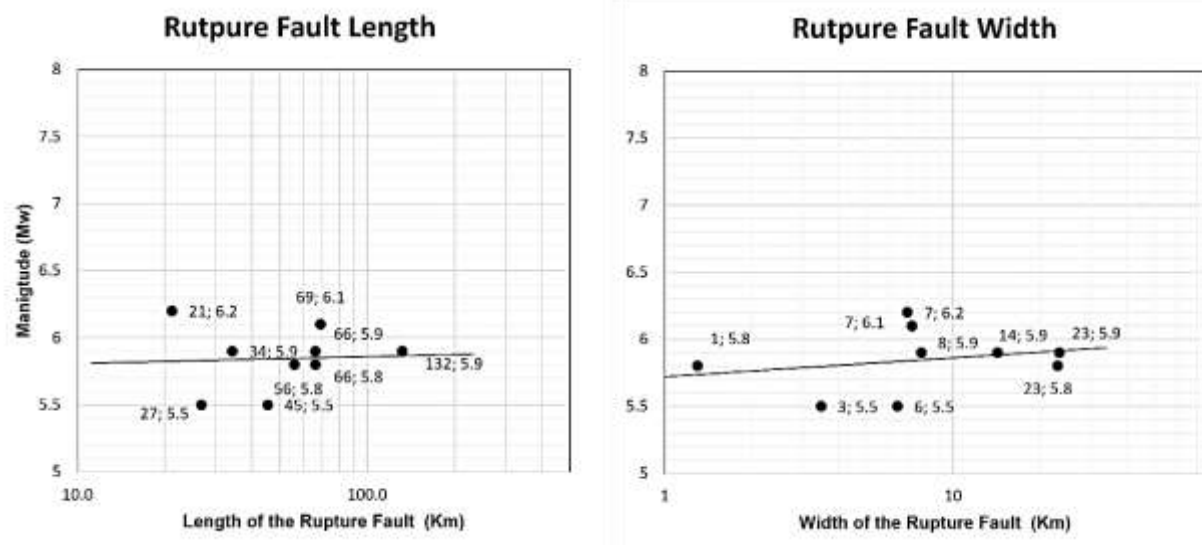
Appendix C 8.4 Zone 4: Kefallonia, (Author's, 2020)



Appendix C 8.5 Zone 5: Gargano Promontory, (Author`s, 2020)



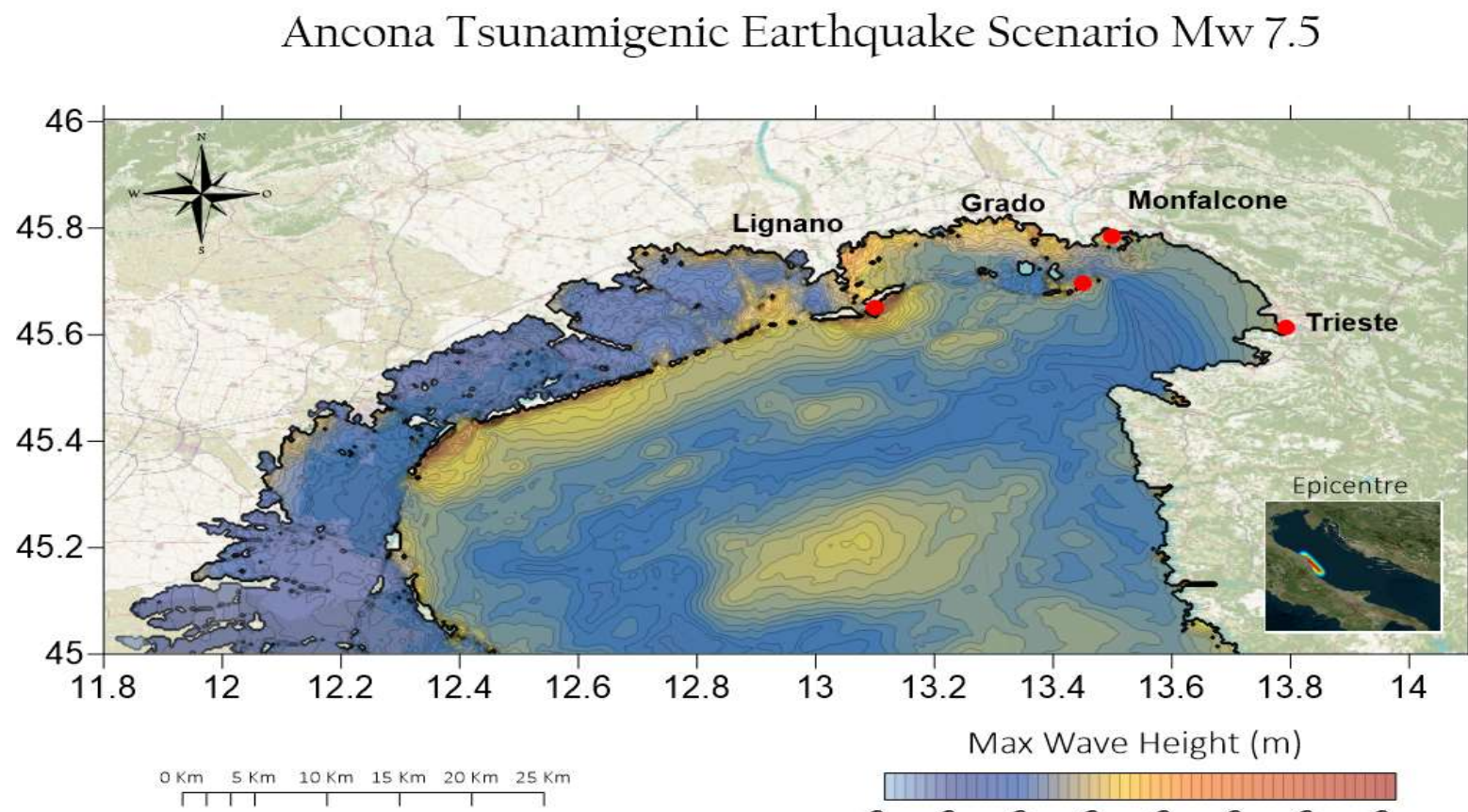
Appendix C 8.6 Zone 6: Apulia, (Author`s, 2020)



Appendix C 8.7: Zone 7: Jabuka Island. (Author's, 2020)

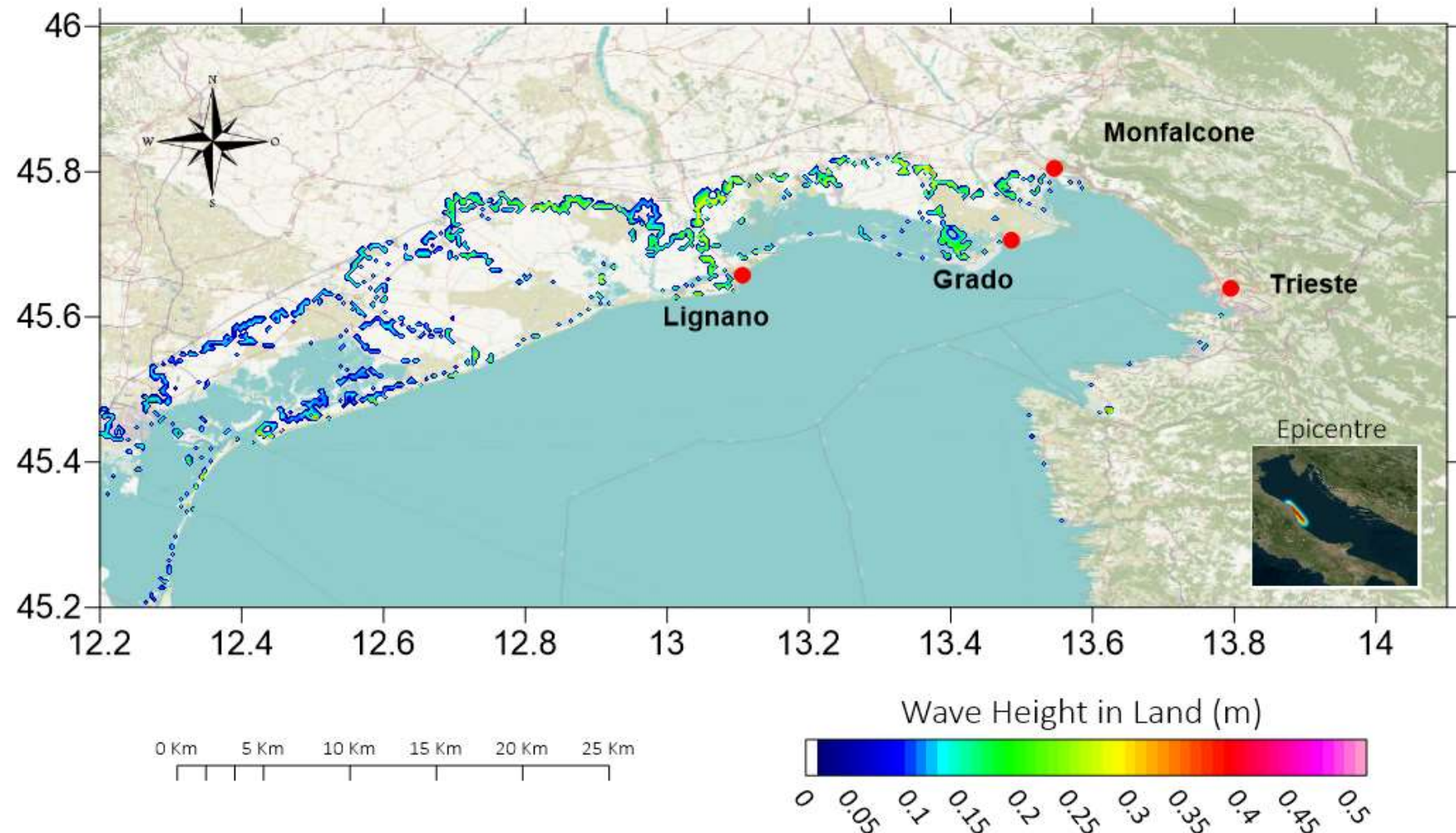
9 APPENDIX D

9.1 Ancona maps



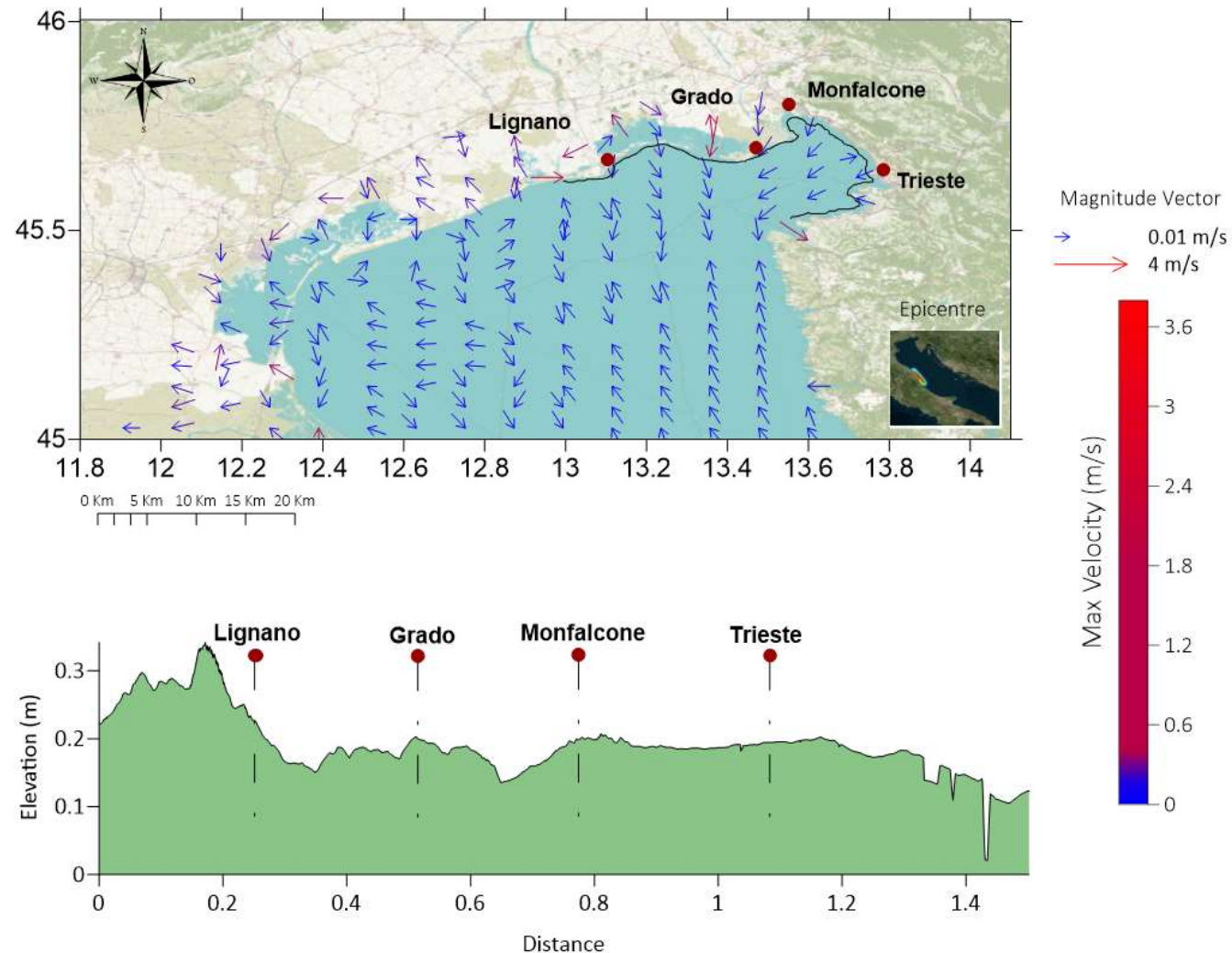
Appendix D 9.1.1: Maximum coastal amplitude in the middle domain during simulation. (Author's, 2020)

Ancona Tsunamigenic Earthquake Scenario Mw 7.5



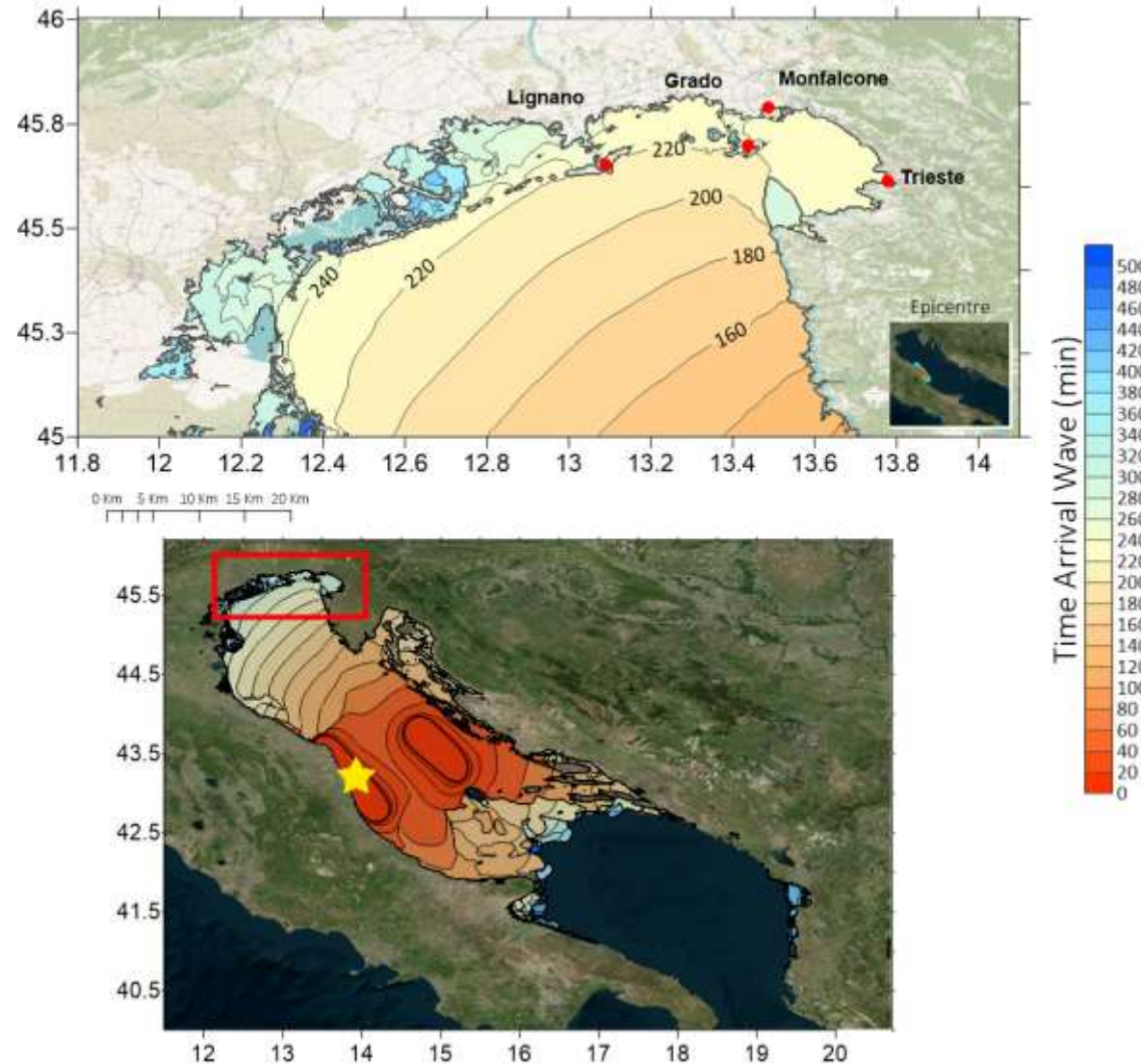
Appendix D 9.1.2: The maximum depth of flow on land during the simulation. (Author's, 2020)

Ancona Tsunamigenic Earthquake Scenario Mw 7.5



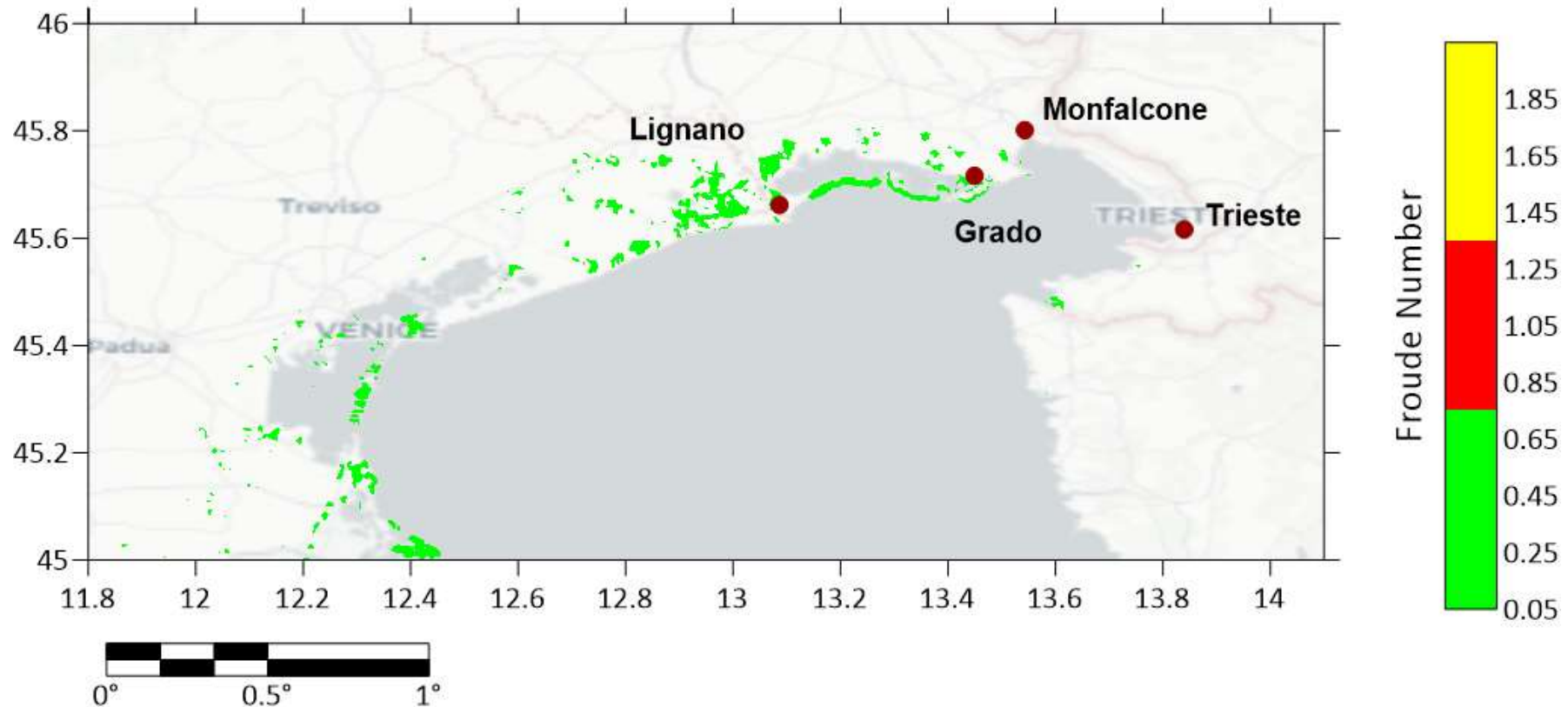
Appendix D 9.1.3: Maximum instantaneous tsunami wave speed in the medium study domain during the simulation. (Author's, 2020)

Ancona Tsunamigenic Earthquake Scenario Mw 7.5



Appendix D 9.1.4: Tsunami travel time in minutes for the Ancona scenario.
(Author's, 2020)

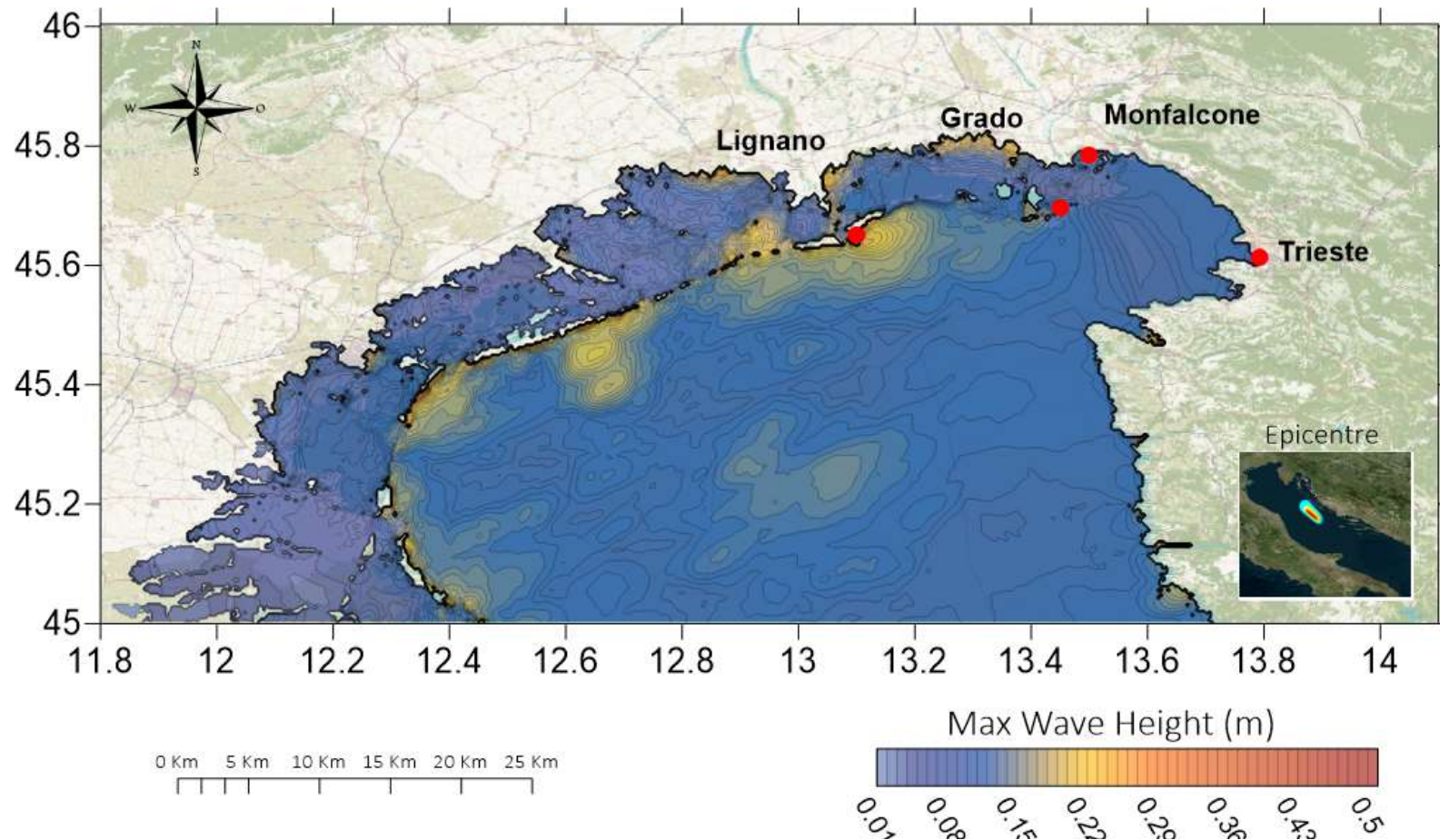
Ancona Tsunamigenic Earthquake Scenario Mw 7.5



Appendix D 9.1.5: Maximum number of Froude in relation to the maximum level of amplitude m (sea elevation).(Author's, 2020)

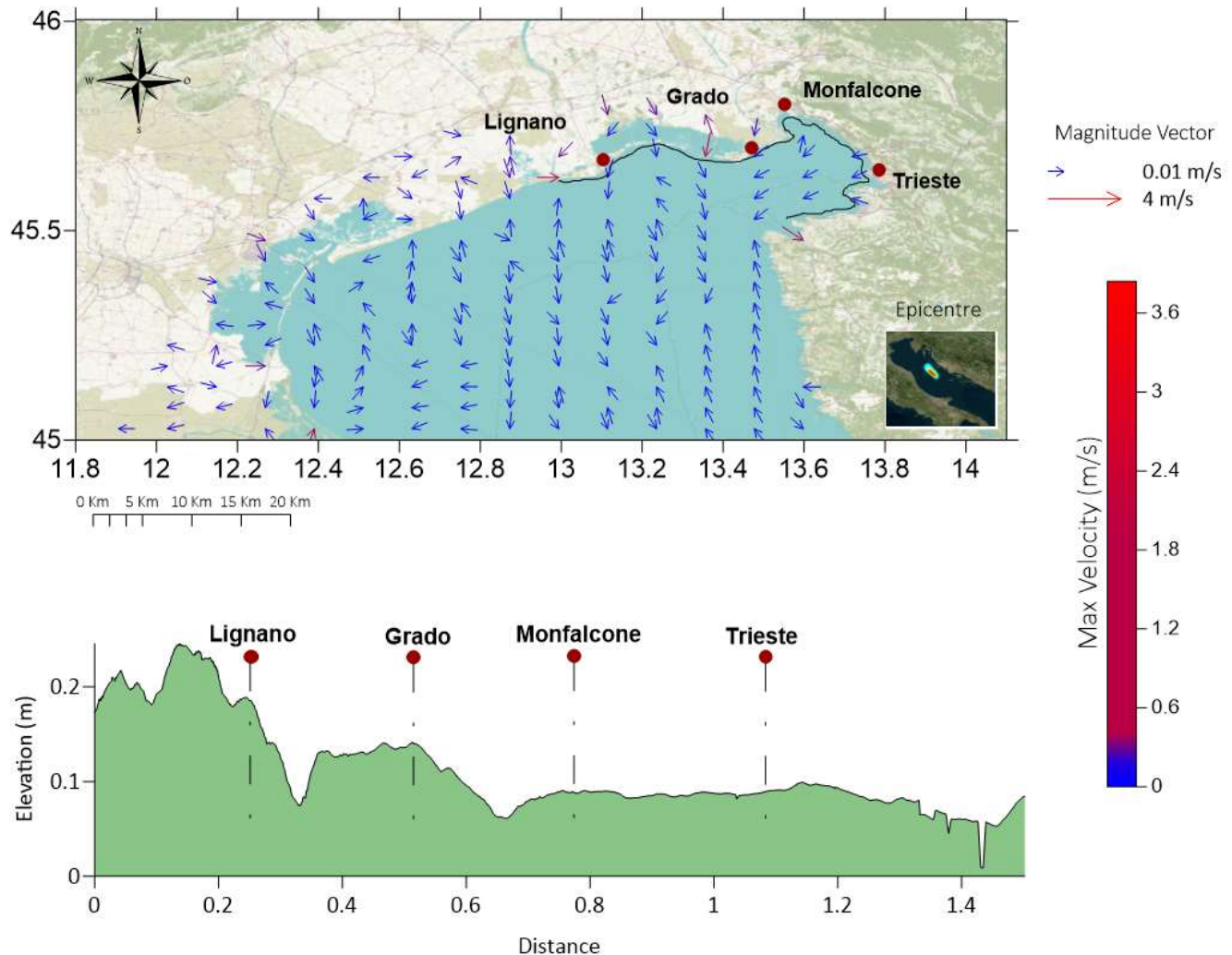
9.2 Split Maps

Split Tsunamigenic Earthquake Scenario Mw 7.5



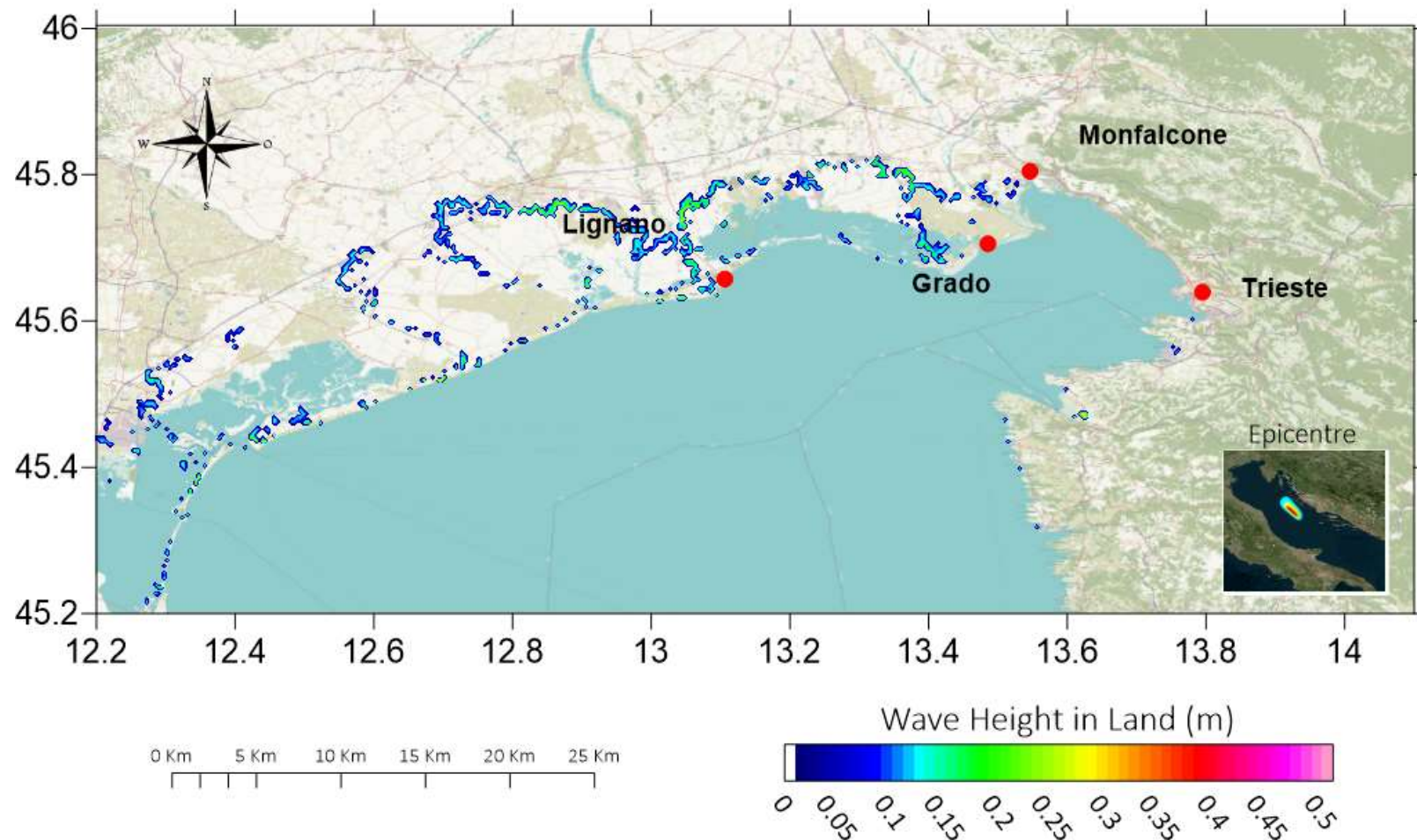
Appendix D 9.1.1: Maximum coastal amplitude in the middle domain during simulation. (Author's, 2020)

Split Tsunamigenic Earthquake Scenario Mw 7.5



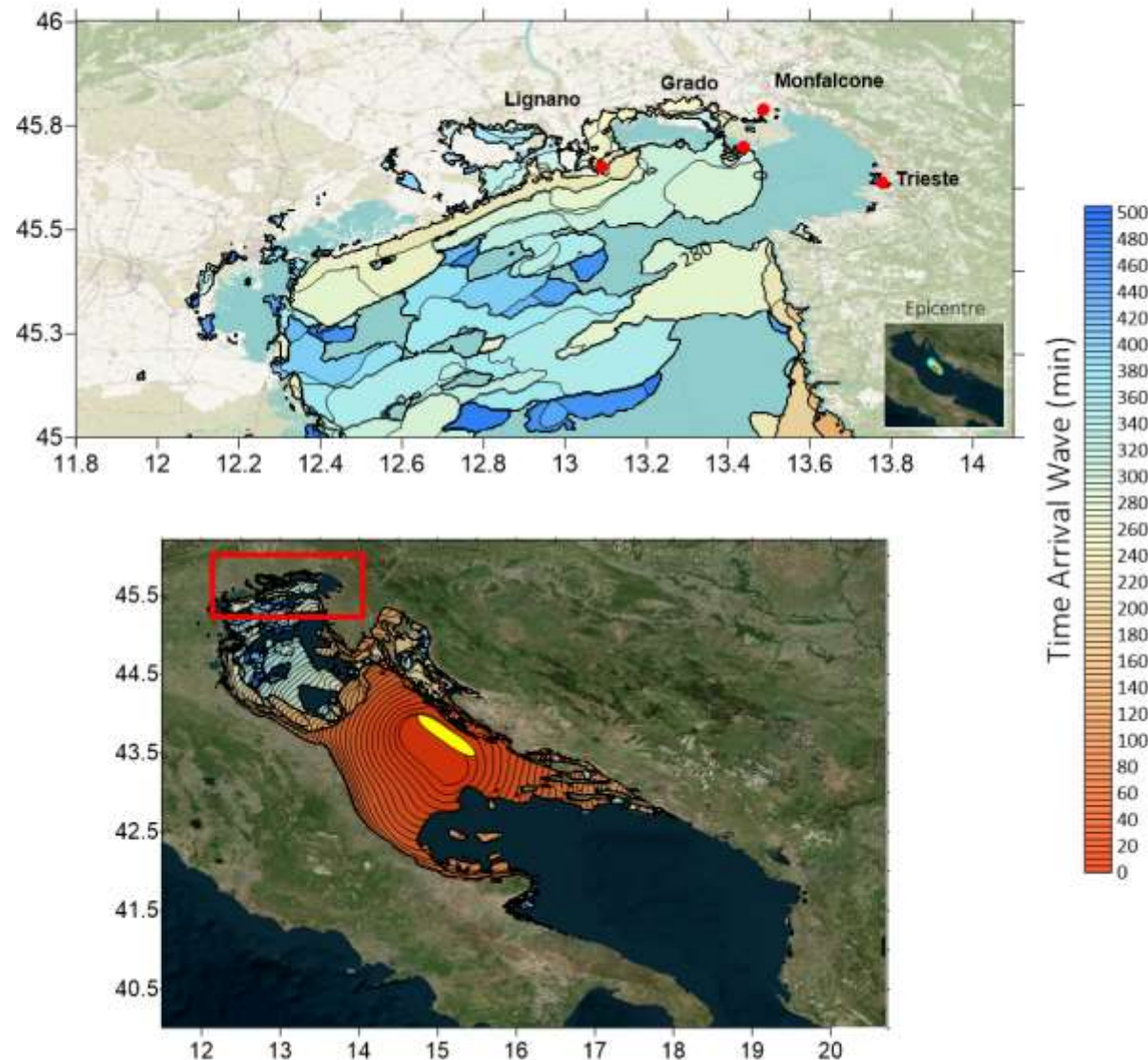
Appendix D 9.2.2: Maximum instantaneous tsunami wave speed in the medium study domain during the simulation. (Author's, 2020)

Split Tsunamigenic Earthquake Scenario Mw 7.5



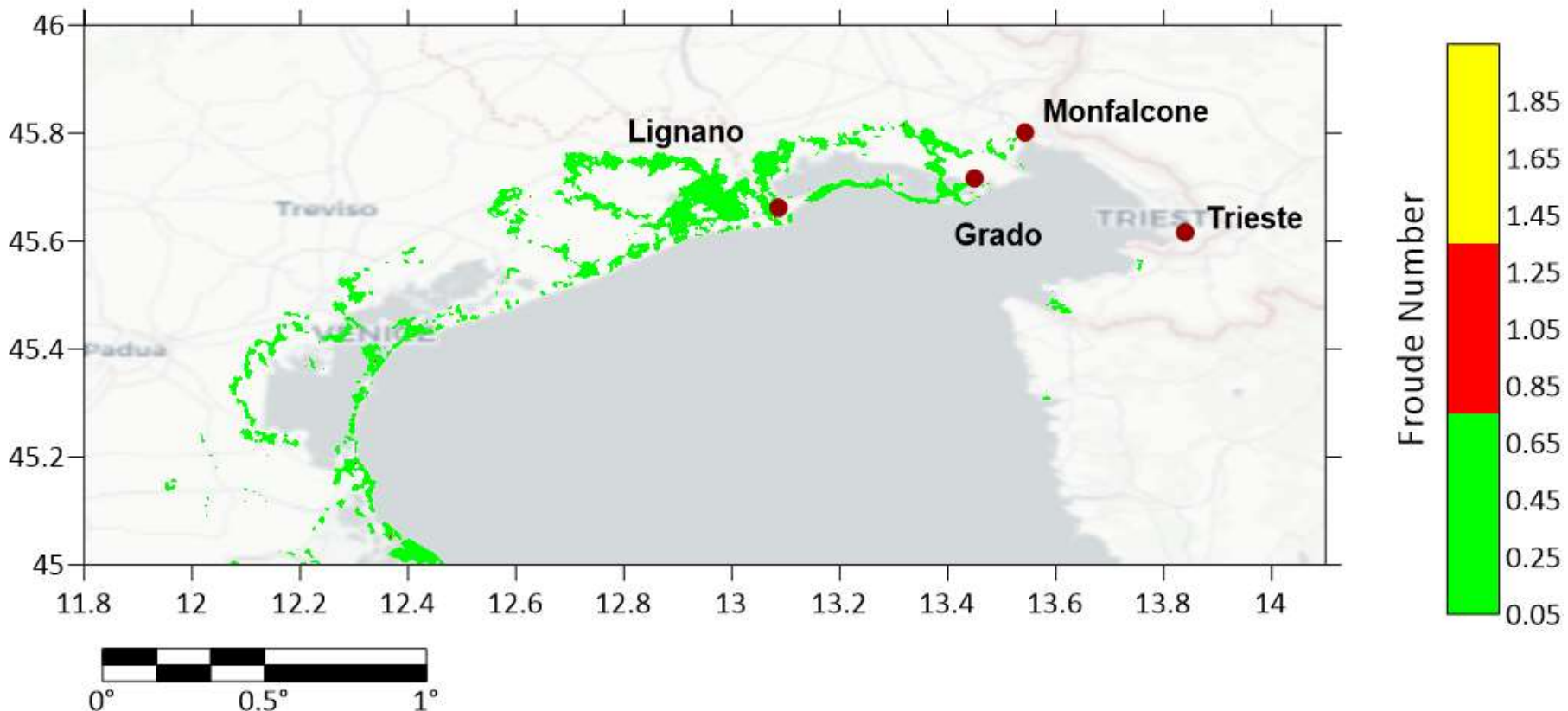
Appendix D 9.2.3: The maximum depth of flow on land during the simulation. (Author's, 2020)

Split Tsunamigenic Earthquake Scenario Mw 7.5



Appendix D 9.2.4: Tsunami travel time in minutes for the Split scenario. (Author's, 2020)

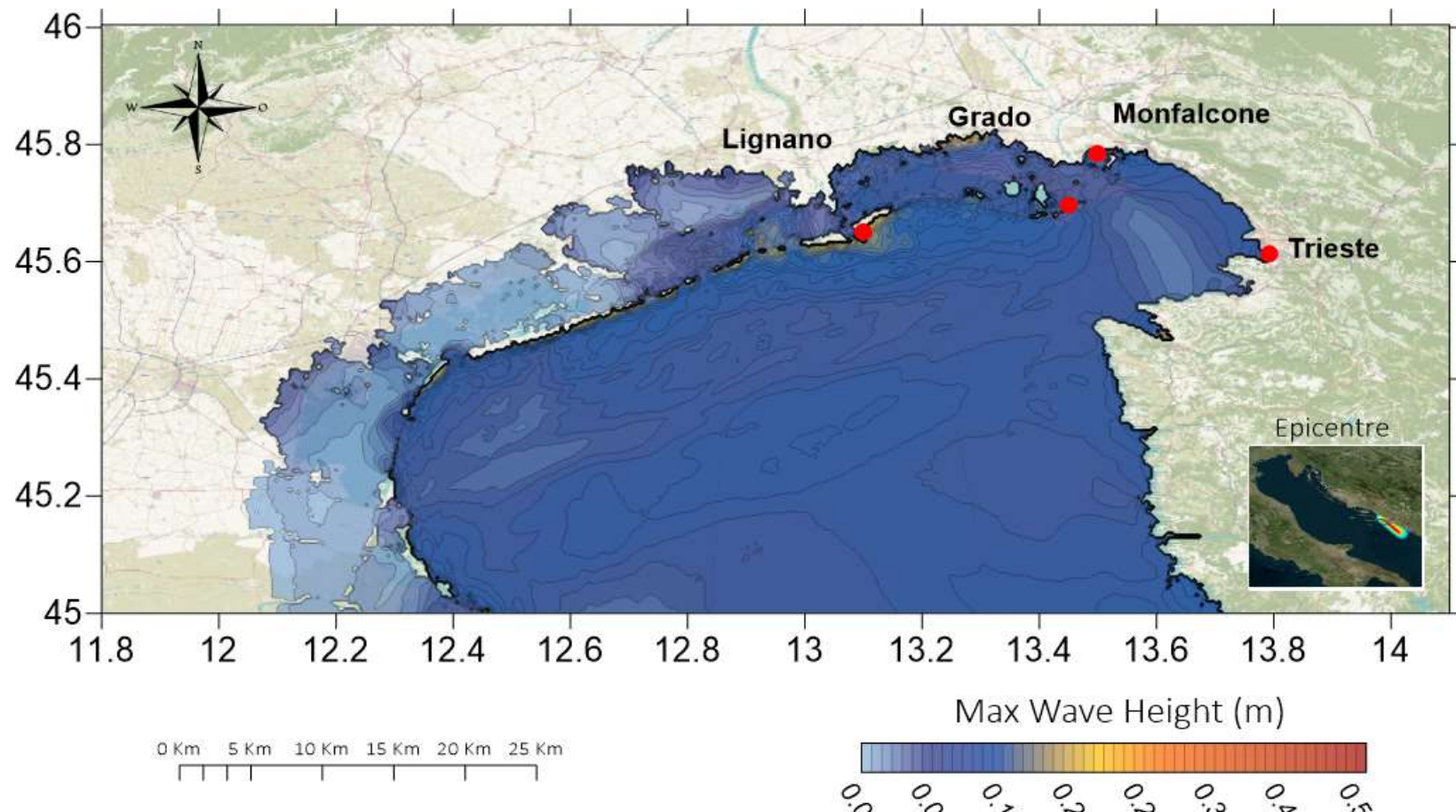
Split Tsunamigenic Earthquake Scenario Mw 7.5



Appendix D 9.2.5: Maximum number of Froude in relation to the maximum level of amplitude m (sea elevation). (Author's, 2020)

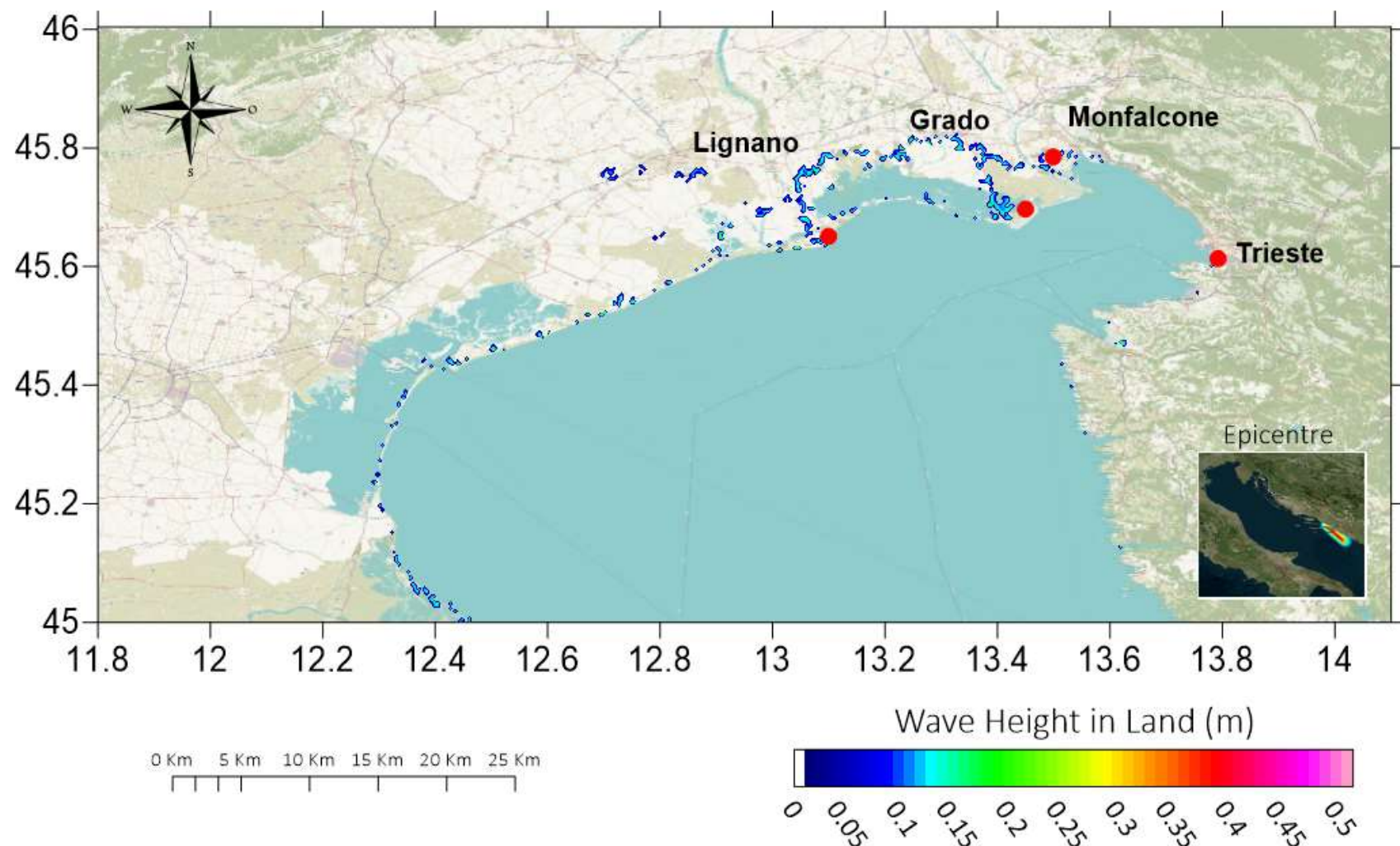
9.3 Montenegro Maps

Montenegro Tsunamigenic Earthquake Scenario Mw 7.5



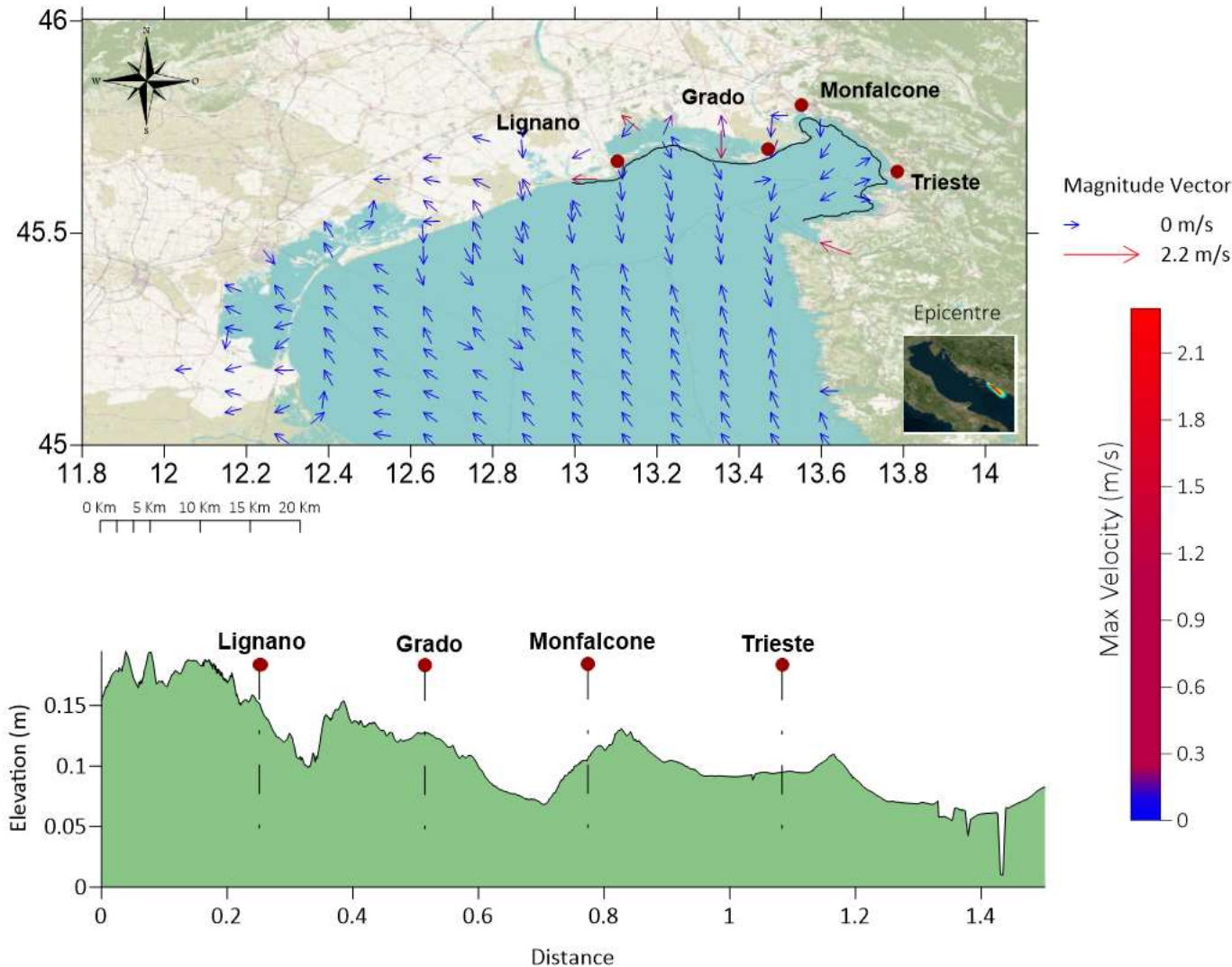
Appendix D 9.2.1: Maximum coastal amplitude in the middle domain during simulation. (Author's, 2020)

Montenegro Tsunamigenic Earthquake Scenario Mw 7.5



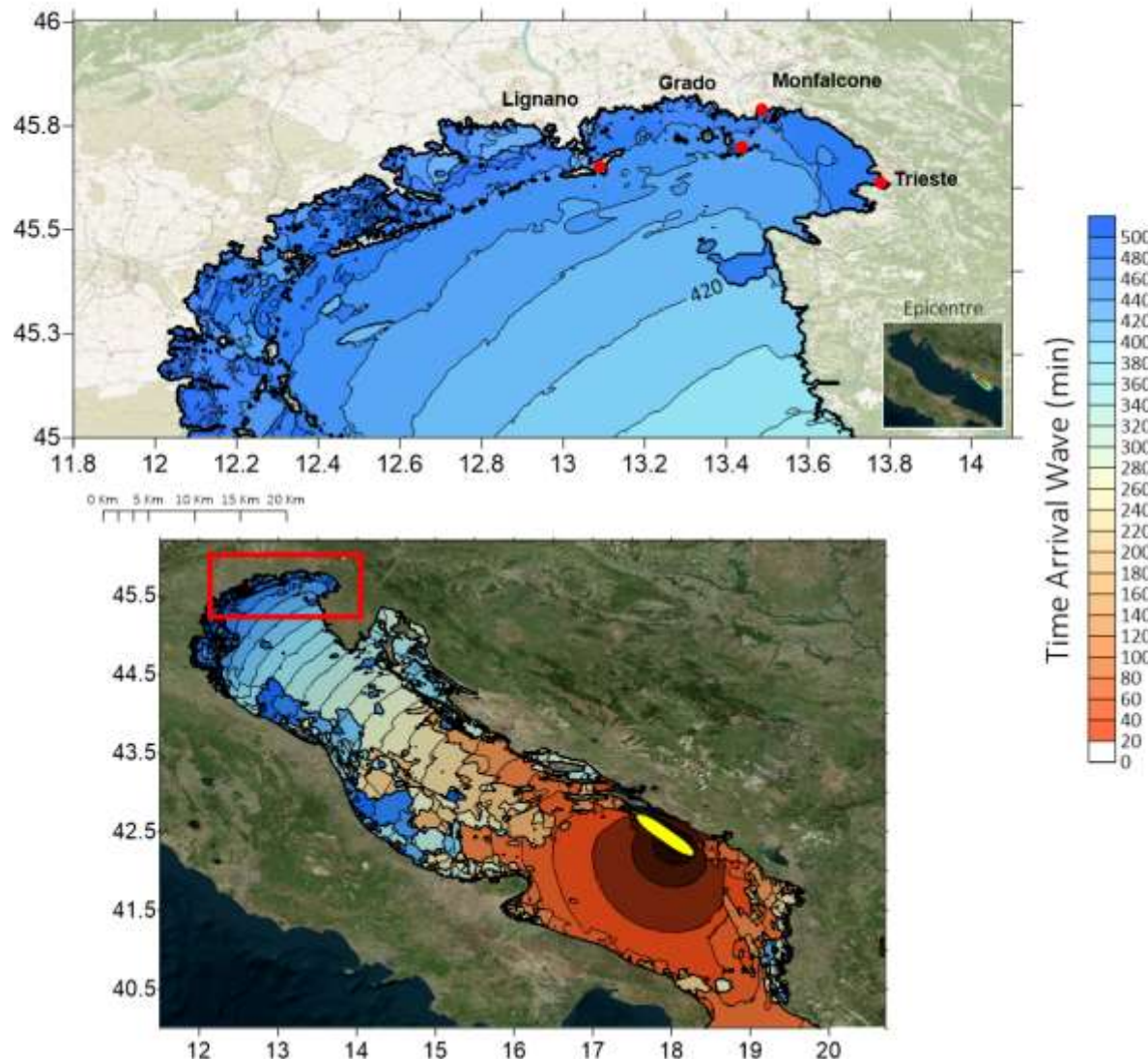
Appendix D 9.3.2: The maximum depth of flow on land during the simulation. (Author's, 2020)

Montenegro Tsunamigenic Earthquake Scenario Mw 7.5



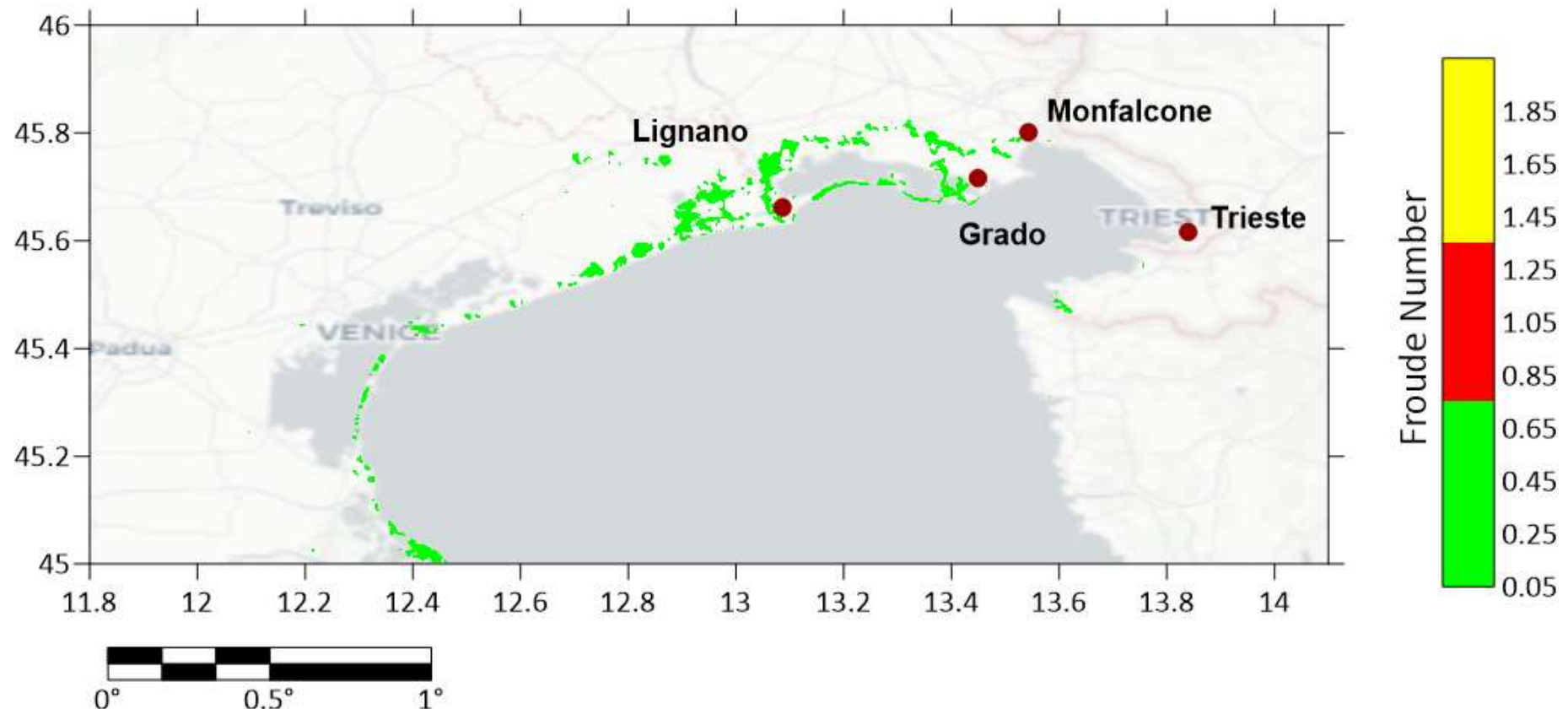
Appendix D 9.3.3: Maximum instantaneous tsunami wave speed in the medium study domain during the simulation. (Author's, 2020)

Montenegro Tsunamigenic Earthquake Scenario Mw 7.5



**Appendix D 9.3.4: Tsunami travel time in minutes for the Montenegro scenario.
(Author's, 2020)**

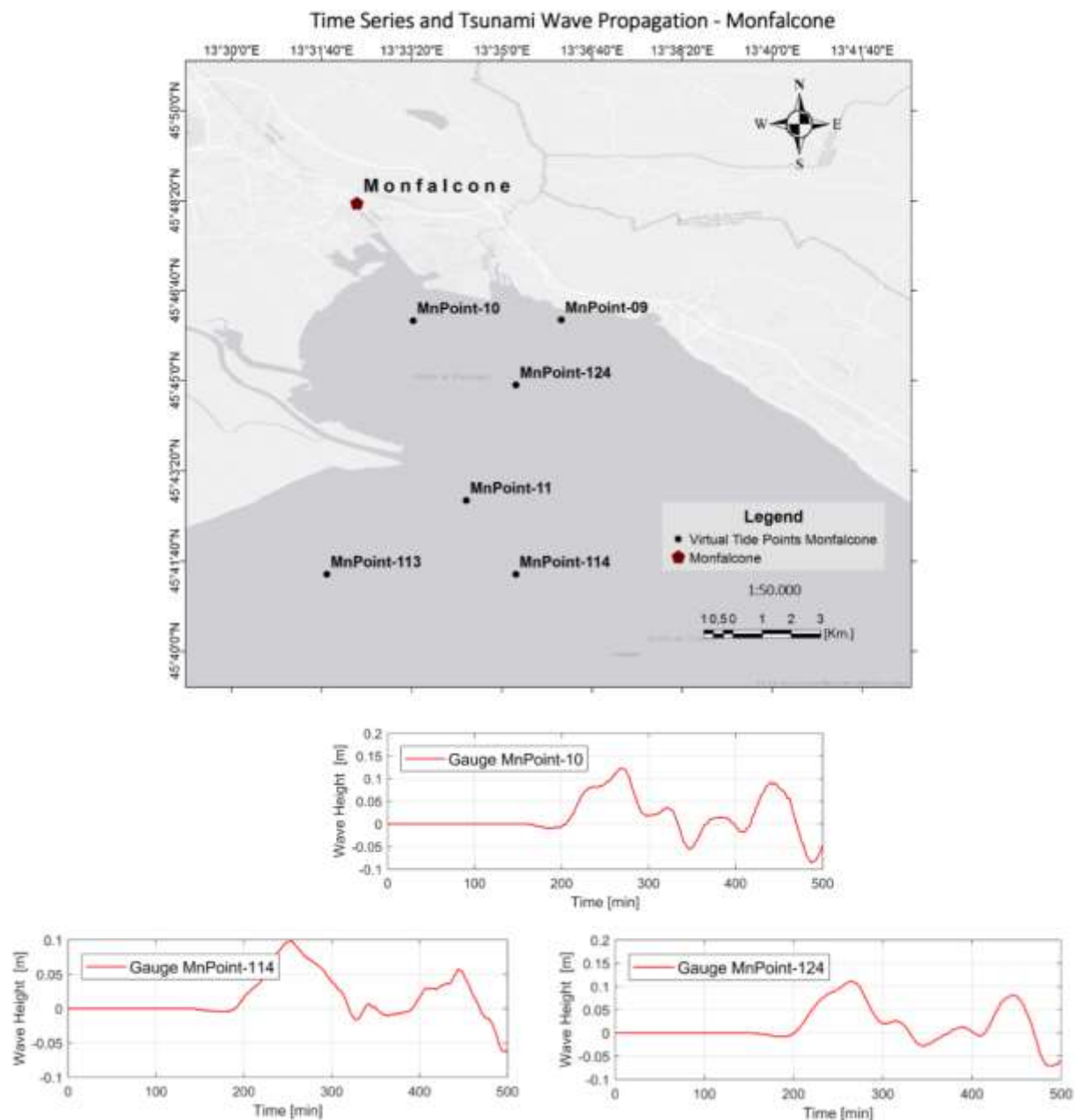
Montenegro Tsunamigenic Earthquake Scenario Mw 7.5



Appendix D 9.3.5: Maximum number of Froude in relation to the maximum level of amplitude m (sea elevation) . (Author's, 2020)

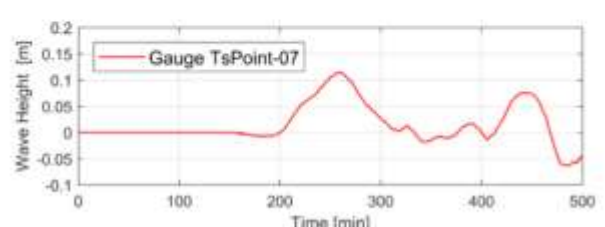
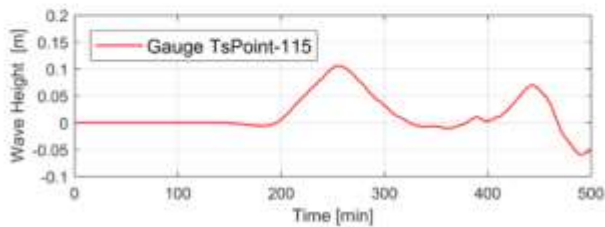
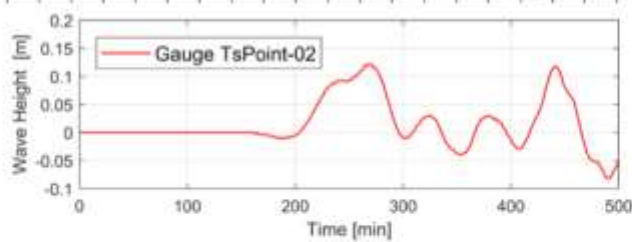
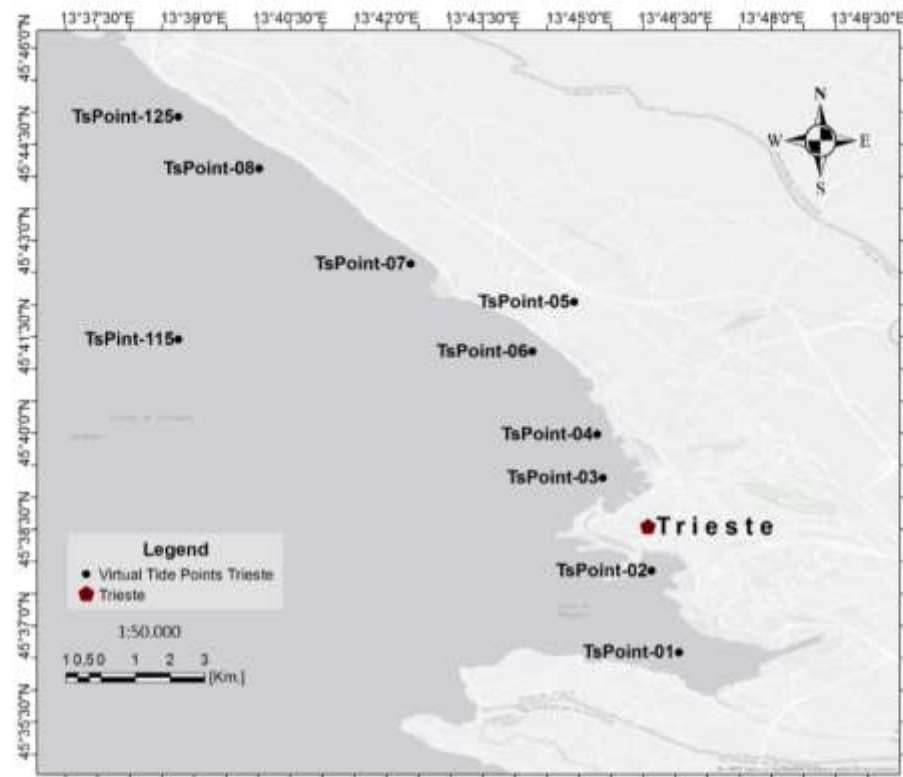
10 APPENDIX E

10.1 Ancona - Maximum Amplitude History



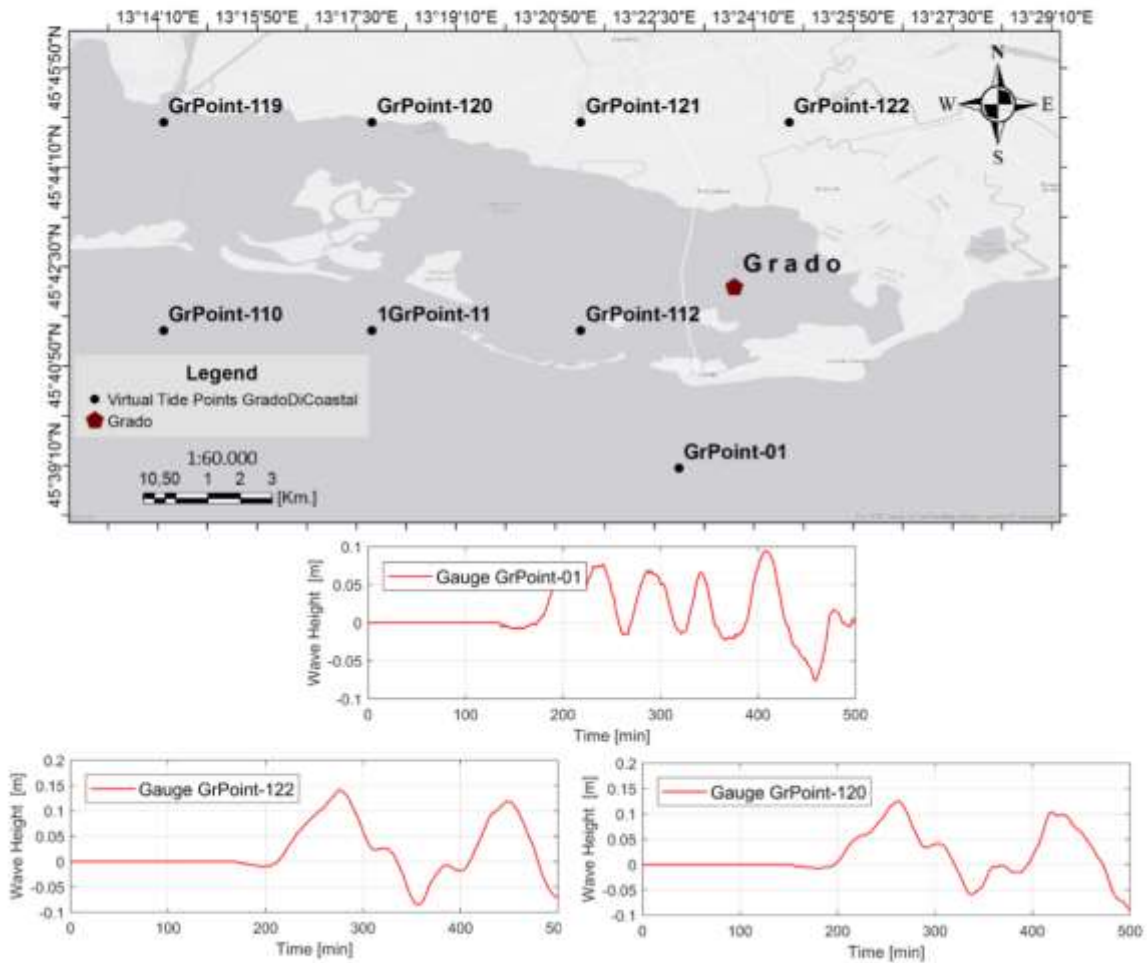
Appendix E 10.1.1: History of maximum sea level amplitude in relation to propagation time.
Ancona. (Author's, 2020)

Time Series and Tsunami Wave Propagation - Trieste



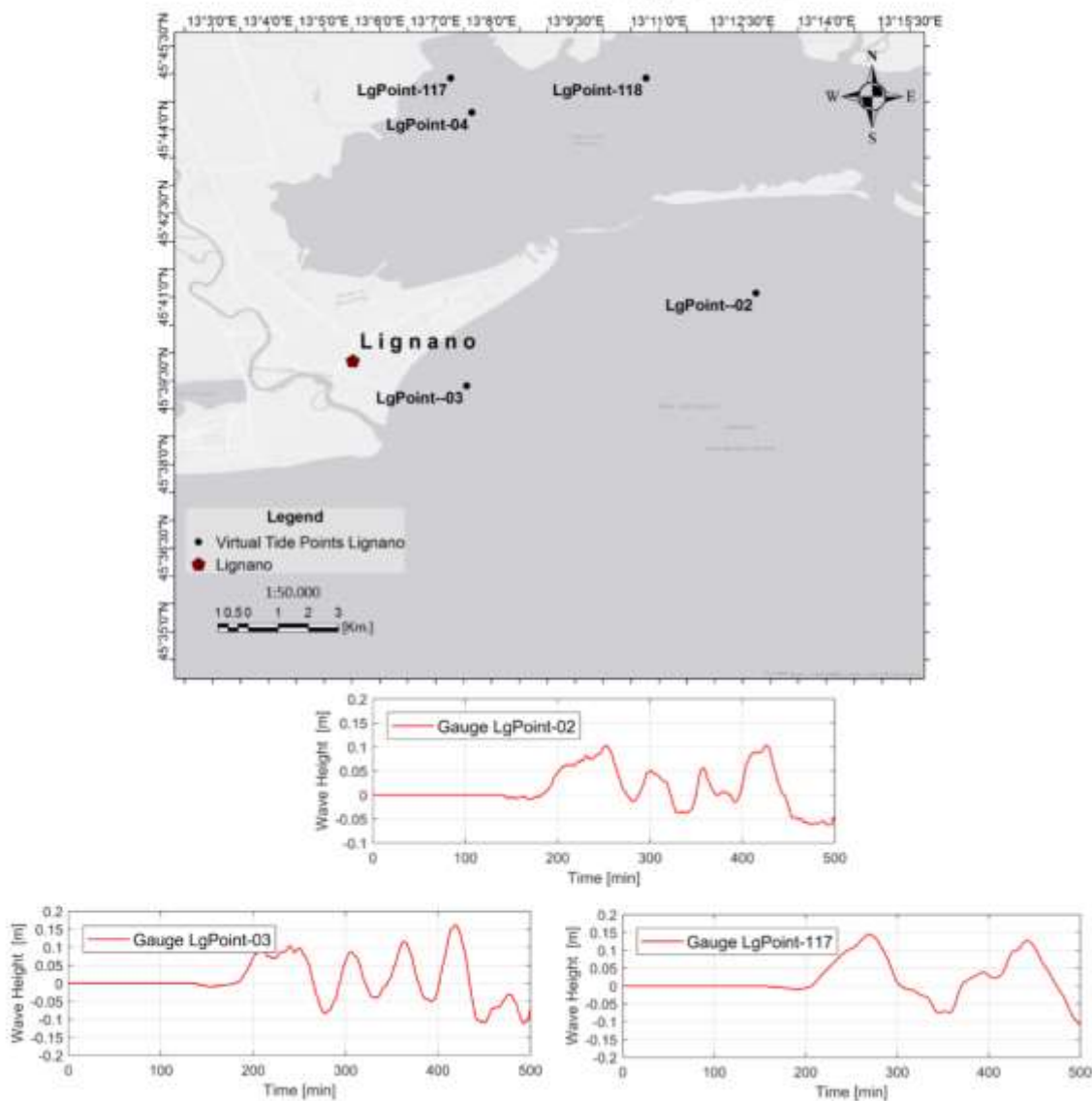
**Appendix E 10.1.1 History of maximum sea level amplitude in relation to propagation time.
Ancona-Trieste. (Author's, 2020)**

Time Series and Tsunami Wave Propagation - Grado Coastal



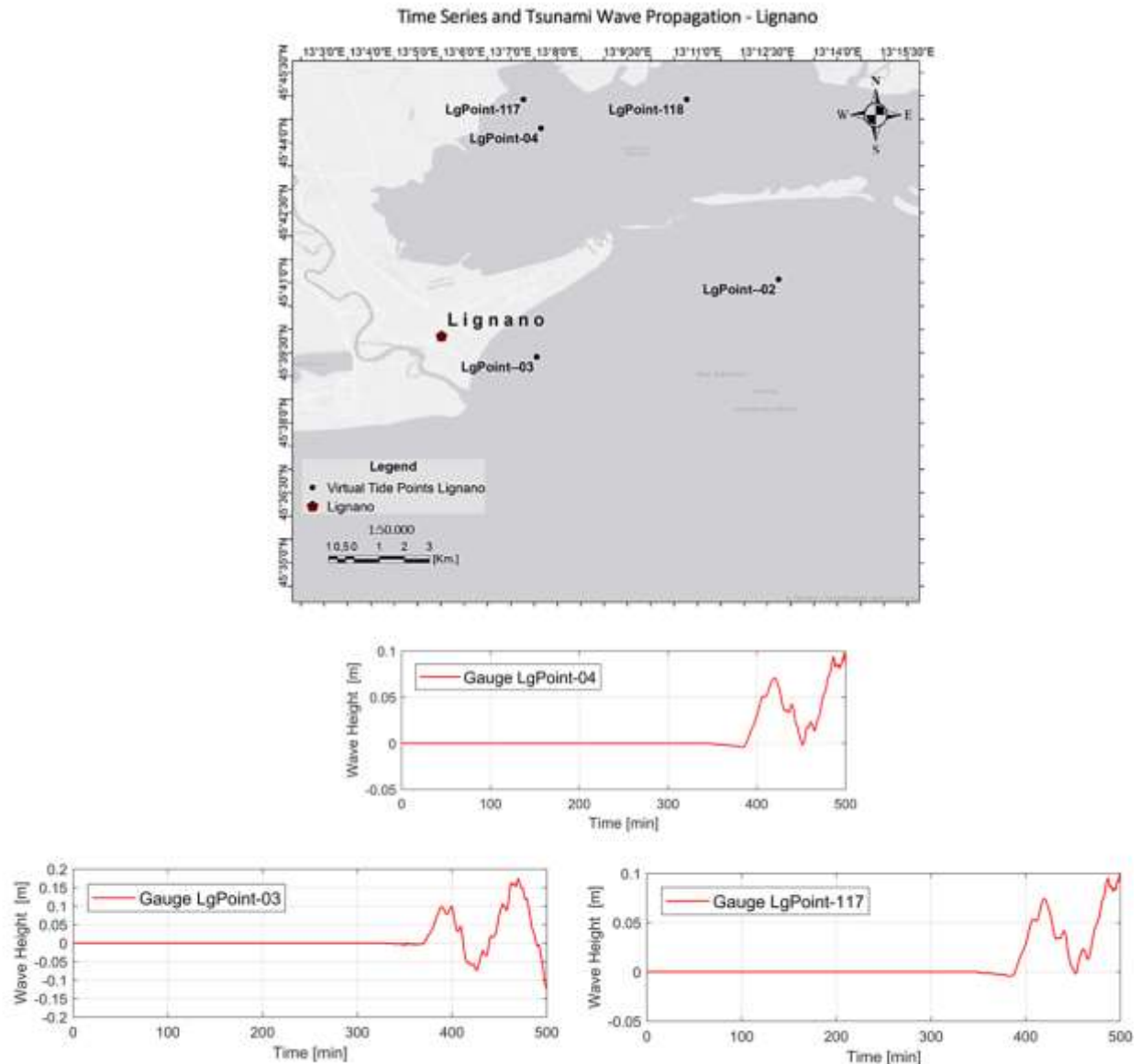
Appendix E 10.1.2: History of maximum sea level amplitude in relation to propagation time. Ancona-Grado. (Author's, 2020)

Time Series and Tsunami Wave Propagation - Lignano



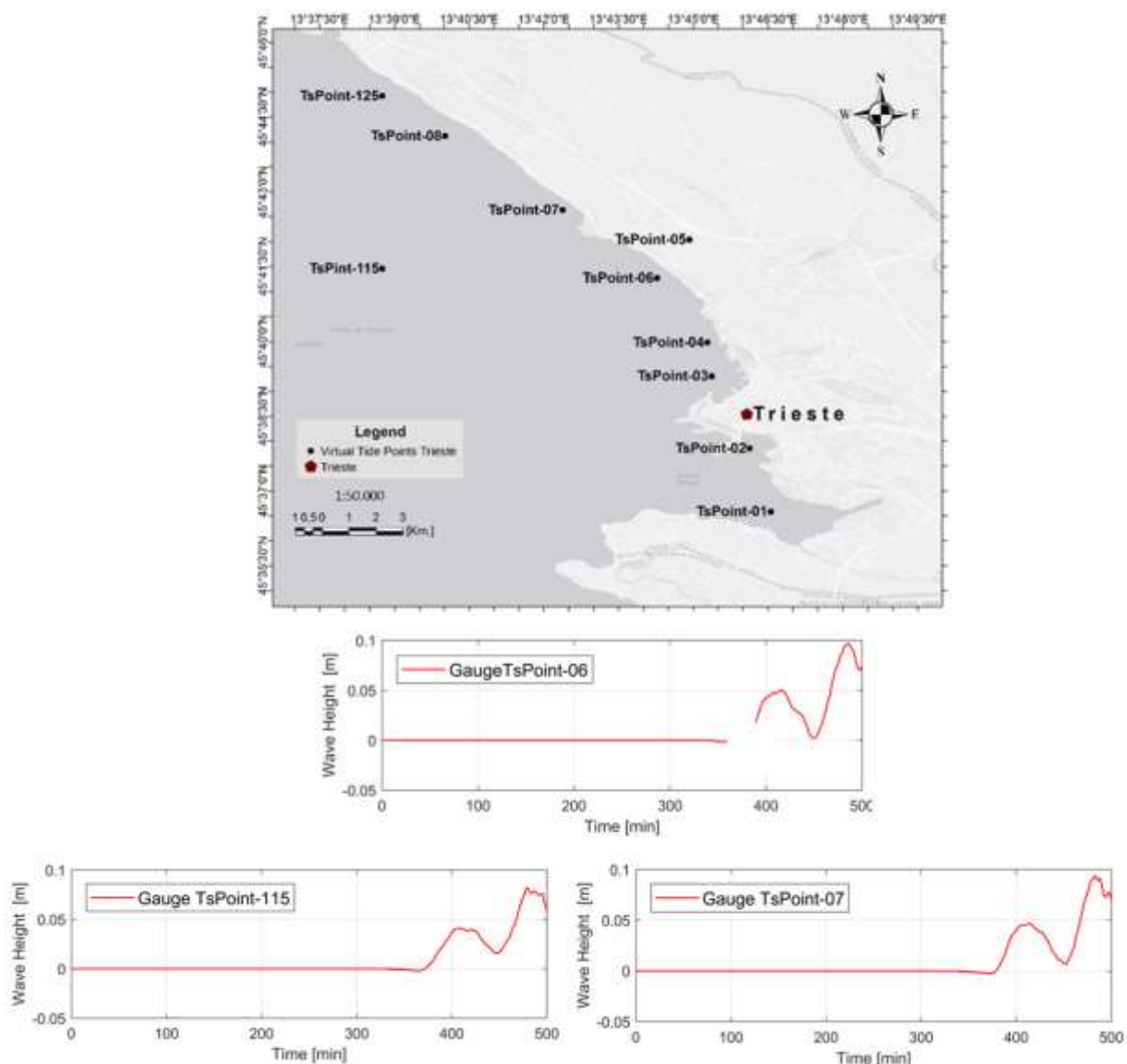
Appendix E 10.1.3 :History of maximum sea level amplitude in relation to propagation time.Ancona-Lignano. (Author`s, 2020)

10.2 Montenegro - Maximum Amplitude History



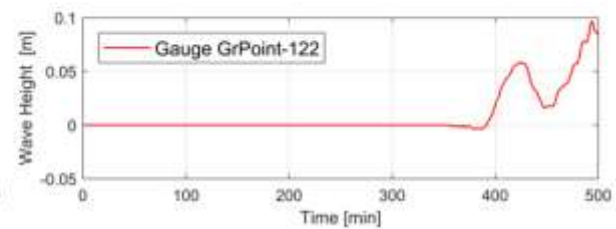
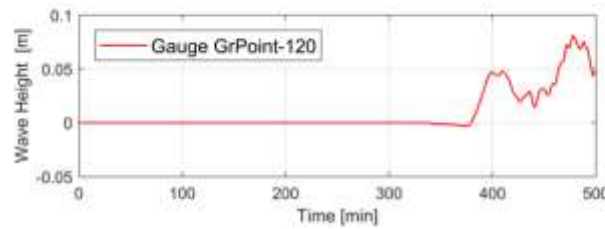
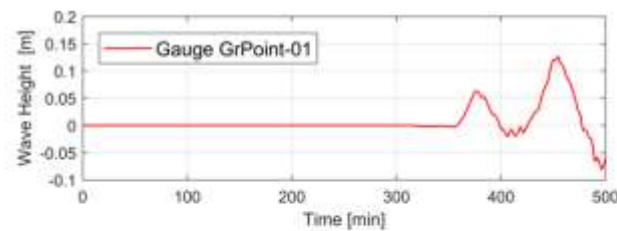
Appendix E 10.2.1:History of maximum sea level amplitude in relation to propagation time. Monfalcone - Lignano. (Author's, 2020)

Time Series and Tsunami Wave Propagation - Trieste



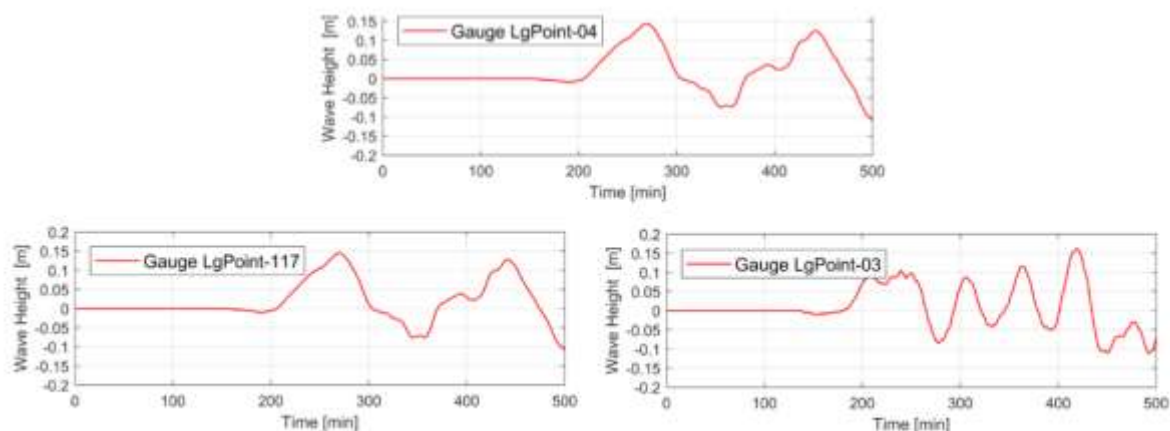
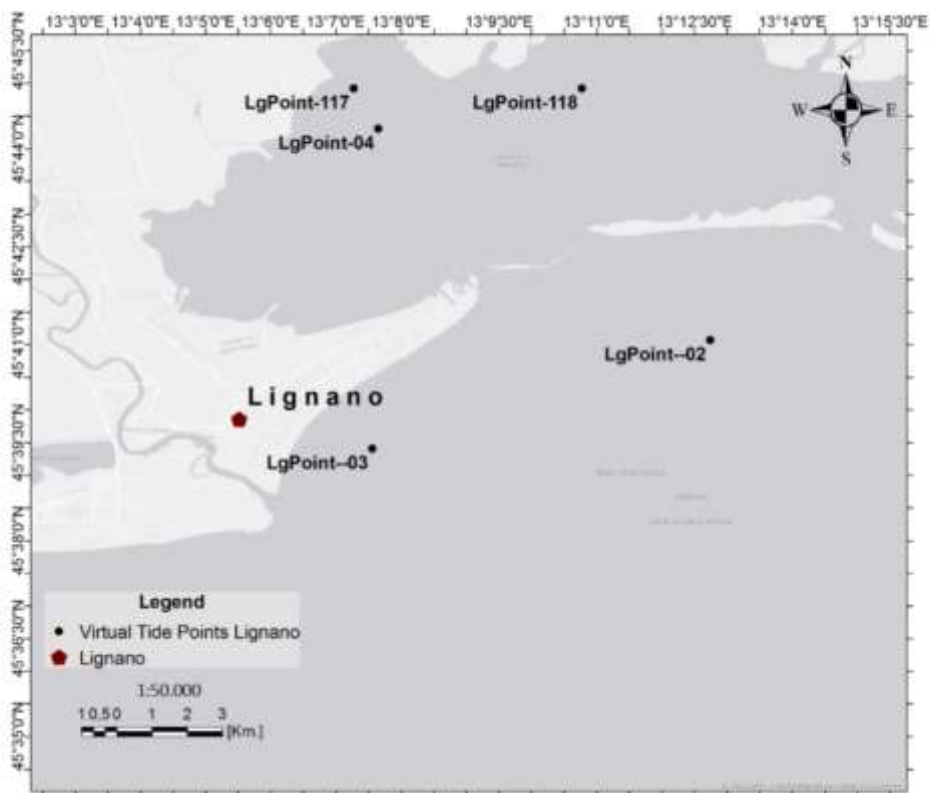
Appendix E 10.2.2: History of maximum sea level amplitude in relation to propagation time. Montenegro - Trieste. (Author's, 2020)

Time Series and Tsunami Wave Propagation - Grado Coastal



Appendix E 10.2.3: History of maximum sea level amplitude in relation to propagation time. Montenegro - Grado. (Author's, 2020)

Time Series and Tsunami Wave Propagation - Lignano



Appendix E 10.2.4: History of maximum sea level amplitude in relation to propagation time. Montenegro - Lignano. (Author's, 2020)